Quantifying the Resilience Enhancement of an Active Distribution System through Multi-Microgrid

by Dillip Kumar Mishra

Thesis submitted in fulfilment of the requirements for the degree of

Doctor of Philosophy

under the supervision of Li Li, Jiangfeng Zhang and Md. Jahangir Hossain

University of Technology Sydney
Faculty of Engineering and Information Technology

November 2022

CERTIFICATE OF ORIGINAL AUTHORSHIP

I, Dillip Kumar Mishra, declare that this thesis is submitted in fulfilment of the requirements for the award of Doctor of Philosophy (Ph.D.) in the School of Electrical and Data Engineering, Faculty of Engineering and Information and Technology at the University of Technology Sydney.

This thesis is wholly my own work unless otherwise referenced or acknowledged. In addition, I certify that all information sources and literature used are indicated in the thesis.

This document has not been submitted for qualifications at any other academic institution.

This research is supported by the Australian Government Research Training Program.

Production Note:
Signature removed prior to publication.

Signature of Student:

Date: 24/11/2022

Dedication

To my beloved parents and family.

Acknowledgment

I would like to express my deepest admiration to my supervisor Dr. Li Li who has the posture and the matter of a genius: he incessantly and conclusively delivered a thirst for adventure in reference to research. I appreciate his patience and thank him for the time he spent advising me and evaluating my work. His help can never be forgotten.

I am also obliged to Dr. Jiangfeng Zhang and Dr. Md. Jahangir Hossain for their constructive remark and unwavering assist throughout the journey.

A debt of appreciation is also matured to my colleagues, Dr. Mojtaba Jabbari Ghadi and Dr. Ali Azizivahed, and Jiatong Wang, for helping us in the direction of modeling and framework.

Finally, none of this would be made possible without the endless love and unconditional support of my wife and family.

Table of Contents

List of figures

Figure numbers and captions **Page no.**

List of Tables

Nomenclature

ADS	Active distribution system
ACE	Area control error
BD	Benders-decomposition
BES	Battery energy storage
CL	Critical load
CUSUM	Cumulative-sum
DAD	Defender-attacker-defender
DOE	Department of Energy
DER	Distributed energy resource
DG	Diesel generator
DSO	Distribution system operator
ENS	Energy not supplied
EDNS	Expected demand not served
IIDG	Inverter-interfaced distributed generator
LFC	Load frequency control
LOLP	Loss of load probability
LP	Linear programming
MC	Monte Carlo
MG	Microgrid
MILP	Mixed-integer linear program
MIP	Mixed integer programming
MINP	Mixed-integer non-linear program
MPC	Model predictive control
MMC	Markov–Monte Carlo
MMG	Multi-microgrid
MSU	Mobile storage unit
NB	Naïve Bayes
OPF	Optimal power flow
PSR	Power system resilience
R&D	Research and development
RERs	Renewable energy sources
SCC	Short circuit capacity
SG	Smart grid
SOC	State of charge

TE	Transactive energy
TL	Tie-line
VSI	Voltage stability index
WRAP	Withstand- Recover- Adapt- Prevent
Chapter 3	
N_{br}	Number of branches
λ_i	Failure rate of branch *i* (*f* /km yr)
L_i	Length of a branch *i* (km)
P_j	Demand power of the j^{th} load
t_{rpr}	Fault repair time (hours)
t_{swc}	Switching time (hours)
Ω_i	Set of buses located at upstream of branch *i*
P_{DG}	Diesel generation power
P_{load}	Active power load
P_{loss}	Network power loss
P_0	Total load in the system
P_{min}	Active load in the system after the event
Chapter 4	
B	Index of energy storage units
D	Index of DG units
H	Index of MSU units
L	Index of loads
M	Index of number of loads pick up by DGs for each scenario
N	Index of disaster scenario considered
R	Index of renewable DG units
C_b	Operation cost of battery, b
C_d	Unit generation cost of DGs, d
C_h	Transportation cost of MSU m per kM
C_l	Load shedding cost of load, l
C_r	Unit generation cost of renewable generation unit, *r*
D_h	Distance travelled by MSU in kMs
E_b^{min}, E_b^{max}	Minimum/maximum energy stored in battery b
$E_{b,t}$	Battery SOC at time instant *t*

P_b	Active power generation by battery b
$P_{CL,k}^{j}$	Critical load of k^{th} load point restored after j^{th} extreme event
P_g	Power output of cost of the generator, g after the event
$P_{l,c}$	Load curtailment, l after the event
P_{LD}	Load demand
P_d	Active power generation by DG d
P_d^{min}/P_d^{max}	Minimum/maximum active power by DG d
P_l	Load curtailment, l after the event
$P_{LD,l}$	Total load demand at load point l
P_r	Active power generation by PV
$P_{b,t}^{ch}(P_{b,t}^{ch,max})$	Charging power (limit)
$P_{b,t}^{dis}(P_{b,t}^{dis,max})$	Discharging power (limit)
R_U , R_D	Ramp-up/down rates of DG units
$\Re_{\mathrm{W}}$ and $\Re_{\mathrm{R}}$	Withstand and Recover index, respectively
$\Re_{\mathrm{A}}$ and $\Re_{\mathrm{P}}$	Adapt and Prevent index, respectively
P_{CLi}	Critical power available after the addition of MG in kW
P_{CL0}	Critical active power available at the end of the event
$P_{CL,j}^{R}$	Critical active power available after restoration step j
$E_{th,j}^{i}$	Thevenin voltage of bus j at the t^{th} stage
$Z_{th,j}^{i}$	Thevenin impedance of bus j at the t^{th} stage
t_{ds}	Disturbance start time
$S_{L,j}^{i}$	Apparent power magnitude of bus i at the j^{th} stage
$\emptyset_j^i$	Power factor angle of bus i at the j^{th} stage
$S_{sc,min,j}^{i}$	Minimal short circuit capacity.
t_{rs}	Restoration start time
t_{rsT}	Restoration start time for traditional system
t_{reT}	Restoration end time for traditional system
Δt	Timeslot duration
$\delta_{b,t}^{i,ch}$ / $\delta_{b,t}^{i,dis}$	Charge/discharge binary indicators of BESs
t_{ds}	Disturbance start time
t_{de}	Disturbance end time
Ψ_i and $P_{lost,i}$	Total outage duration and power lost in i^{th} failure

Chapter 5	
$\mathcal{P}_W$	Wind electric power output
ρ	Air density
$\mathcal{A}_s$	Blade swept-area of wind turbine
$\mathcal{C}_p$	Power coefficient
$\mathbb{W}_s$	Wind speed
$\mathbb{W}_{rated}$& $\mathbb{W}_{cut-in}$	Rated, and cut-in wind speed
$\mathbb{W}_{cut-out}$	Cut-out wind speed
$\mathcal{P}_{PV}$	PV output
$\mathcal{P}_{rated}$	Rated wind power
η	PV array conversion efficiency
$\emptyset$	Solar insolation
$\mathcal{A}_m$	Area of measurement
θ_A	Ambient temperature
$\mathcal{P}_{EV}$	Total charging power at the station
$\mathcal{N}_{con}$	Numbers of connected EVs at the charging station
$\mathcal{P}_{EV\_inv}$	Average charging power at each charging point
$\mathcal{N}_{plug\_out}$	Number of disconnected EVs
$k\Delta t$	Averaged charging time
$\mathcal{W}_{vol}$	Energy density
σ_r, ϱ_m, & l	Tensile stress, material density, and circular path radium
ω_m , $\mathcal{K}_F$, & $\mathcal{V}$	Spinning angular speed , flywheel shape, and flywheel volume
ω_{FH}, $\mathcal{I}$, & σ_{r_Max}	Angular velocity , inertia , and maximum tensile stress
$x, u, y,$ & $\mathcal{W}$	State, control input, output and disturbance variables
$A, B, C,$ & D	State, input, output and feedthrough matrices
$\mathcal{P}_d$, $\mathcal{P}_{PV}$, & $\mathcal{P}_W$	Diesel generator, solar, and wind power
$\mathcal{P}_{EV}$ & $\mathcal{P}_{FESS}$	Electric vehicle and FESS power
$\mathcal{P}_{BESS}$, & $\mathcal{P}_L$	BESS power and load dynamics
Δu_d & Δu_{EV}	Control input to the diesel generator and EV, respectively
$\mathcal{T}_{ij}$	Synchronizing coefficient
$\mathcal{D}$	Equivalent damping constant
$\mathcal{M}$	Equivalent inertia constant
$\Delta\mathcal{P}_{tie}^{i}$	Tie-line power flow exchange
$\mathcal{N}$	The number of areas that are interconnected in the system

$\mathbb{O}$	Area capacity factor
β	Frequency bias parameter
Δf	Change in frequency
$\mathcal{M}_{actual}$	Actual value
$\mathcal{M}_{mea}$	Measured value
$\mathfrak{P}_{C}$	Cyber-attack signal
$\mathcal{X}_{a}$	Random cyber-attack pattern
$\mathcal{K}_{a}$	Scaling attack constant
$\mathcal{S}_{k}$	Sample value of the signal at k^{th} time
$\mathcal{D}$	Load deviation
$\mathcal{G}$ & $\mathfrak{D}$	Statistics and drift parameter
$\mathcal{H}$	Threshold value
$\mathcal{K}_{p}, \mathcal{K}_{p}$, & $\mathcal{K}_{d}$	Proportional gain, integral gain, and derivative gain
K_{e} & K_{ce}	Scaling parameters
e_{max}	Maximum error
Chapter 6	
N	Number of MGs
$\mathcal{C}_{i}$	Total cost of $MG\ i$
$\mathbb{P}_{\mathcal{W},i,t}$	Energy generation from wind in i^{th} MG at time t
$\mathfrak{C}_{t}^{P}$	Pool prices
$\mathfrak{C}_{ij}^{\mathfrak{S}}$	Reference price
$\mathfrak{C}_{t}^{\mathcal{B}}$	Bilateral price
$\mathfrak{C}_{ij,t}^{\mathcal{B}}$	Transaction price
$\mathfrak{C}_{G,t}^{pur}$, & $\mathfrak{C}_{G}^{sell}$	Buying and selling price
T^{on}, T^{mid}, T^{off}	On-, mid-, and off-peak time
$\mathcal{C}_{ij,t}$	Total energy cost
a_{ij}	Power loss
$\mathcal{C}_{\mathbb{B}_{MO},t}$	Market operator benefit
$\mathbb{P}_{\mathcal{PV},i,t}$	Energy generation from PV in i^{th} MG at time t
$\mathbb{P}_{E,i,t}$	Energy trading quantity in i^{th} MG at time t
$\mathbb{P}_{B,i,t}$	Charging /discharging rates for battery storage in i^{th} MG at time t (positive is charging, negative is discharging)
$\mathbb{P}_{LD,i,t}$	Load demand in i^{th} MG at time t
$M_{ij,t}$	Energy trading quantity

$\mathcal{A}_{\mathcal{PV},i}$	Size of the PV panel in i^{th} MG
$\eta_{\mathcal{PV}}$	Efficiency of the PV panel
$\mathfrak{S}_{\mathcal{PV},t}$	Solar radiation at time t
$\mathbb{P}_{\mathcal{W}\mathbb{R},j,max}$	Rated wind power in i^{th} MG at time t
$\mathcal{W}_{s,t}$,$\mathcal{W}_{\mathbb{R},i}$ $\mathcal{W}_{\mathbb{CI}_i}$, and $\mathcal{W}_{\mathbb{CO},i}$	Predicated, rated, cut-in, and cut-out wind speeds in i^{th} MG at time t, respectively.
$SOC_{j,t}$	Battery state-of-charge for MG j at time t
SOC_i^{min} & SOC_i^{max}	Battery minimum and maximum SOC for MG i, respectively
$\mathbb{E}_{\mathcal{B},j}^{c}$	Battery capacity for MG i
$\overline{\mathbb{P}}_{\mathcal{B},j}$	Maximum battery charging/discharging power of MG j
Δt	Time interval
$\eta_{\mathcal{B},c}$ and $\eta_{\mathcal{B},d}$	Charging and discharging efficiency, respectively
$\mathcal{P}_{i,t}^{inj}$	Active power injection/production at i^{th} node at time t
$\mathbb{S}_{i,j,t}^{inj}$	Apparent power between nodes i & j at time t
$\mathbb{S}_{i,j}^{max}$	Maximum apparent power
$\mathcal{V}_{i,t}/\emptyset_{i,t}$	Voltage/phase angle at i^{th} node at time t
$\mathcal{V}_t^{min}/\mathcal{V}_t^{max}$	Minimum/maximum voltage magnitude
$\mathbb{P}_{LD,i}$	Demand profile of MG
$\mathbb{P}_{LD,i}^{actual}$	Actual demand
$\mathbb{P}_{LD,i}^{nc}$	Non-critical load
$\mathfrak{B}$ & $1-\mathfrak{B}$	Percentage of non-critical and critical load, respectively.
$\mathfrak{R}$	Resiliency
$\mathbb{K}_{pu}$, & $\mathbb{K}_{pr}$	Public and private key
$\mathcal{U}$ and $\mathbb{X}$	Plaintext and ciphertext
f	Homomorphic function
$\mathbb{b}$	Balance
$\mathbb{R}$	Energy trading
$\mathbb{Z}_{\mathbb{i}}$	Modulus
$\mathbb{L}$ and $\mathbb{G}$	Lowest common multiple and greatest common factor, respectively

List of Publications

Published

Journals:

1. **D. K. Mishra**, et al, "A review on resilience studies in active distribution systems", *Renewable and Sustainable Energy Reviews*, Vol-135, 110201, 2021 (**IF: 16.799,** Q1)

2. **D. K. Mishra**, et al, "Resilient control based frequency regulation scheme of isolated microgrids considering cyber attack and parameter uncertainties", *Applied Energy*, Vol-306, 118054, 2022 (**IF: 11.446,** Q1).

3. **D. K. Mishra**, et al, "Active distribution system resilience quantification and enhancement through multi-microgrid and mobile energy storage", *Applied Energy*, Vol-311, 118665, 2022 (**IF: 11.446,** Q1).

4. **D. K. Mishra**, et al, "Significance of SMES Devices for Power System Frequency Regulation Scheme considering Distributed Energy Resources in a Deregulated Environment", *Energies*, Vol-15, Issue-5, pp-1766, 2022 **(IF: 3.252,** Q2**)**

Conference:

5. **D. K. Mishra**, et al. "Proposing a Framework for Resilient Active Distribution Systems using Withstand, Respond, Adapt, and Prevent Element", *2019 29th Australasian Universities Power Engineering Conference (AUPEC),* 2019.

6. **D. K. Mishra**, et al, "A Resilience Quantification Framework and Enhancement Scheme for Active Distribution Networks", *2021 IEEE PES General Meeting Poster Session*, 2021.

7. **D. K. Mishra**, et al, "A Resilient Multi-Microgrid based Transactive Energy Framework for Future Energy Markets", *2022 IEEE PES General Meeting Student Poster Session & Competition,* 2022.

Research Showcase:

8. **D. K. Mishra**, et al, "Quantification and Enhancement of Resilience through Multi-Microgrids", *Three Minutes Thesis Competition, School of Electrical and Data Engineering HDR Online Showcase Competition, University of Technology Sydney*, 2020.

9. **D. K. Mishra**, et al, "A Novel Approach to Quantify the Resilience of Active Distribution Networks", *The Next Generation Technology Project | Showcase and Awards 2021*, *Electrical Energy Society of Australia*, Australia, 2021.

10. **D. K. Mishra**, et al, "A Blockchain-enabled Transactive Energy Framework for Future Energy Markets", *IEEE NSW Chapter, UNITE* 2022

Submitted

1. **D. K. Mishra**, et al, "Resilience-Driven Scheme in Multiple Microgrids with Transactive Energy System using Blockchain Technology", *IEEE Transactions on Industrial Informatics,* 2022 (**IF: 11.648**).

2. **D. K. Mishra**, et al, "A Detailed Review on Power System Resilience Enhancement Pillars: Smartening, Hardening, Distributing, and Building", *Renewable and Sustainable Energy Reviews,* 2022 (**IF: 16.799**).

Collaboration research outcome

Published

1. **D. K. Mishra**, et al, "A review on solid-state transformer: A breakthrough technology for future smart distribution grids", *International Journal of Electrical Power and Energy Systems*, Vol-133, 107255, 2021, (**IF: 5.659**).

2. M. J. Ghadi, A. Azzizavahad, **D. K. Mishra**, L. Li, J. Zhang, "Application of small-scale compressed air energy storage in the daily operation of an active distribution system", *Energy,* Vol-231, 120961, 2021 **(IF: 8.857).**
3. S. R. Das, P. K. Ray, A. Mohanty **D. K. Mishra**, "An Advanced Wavelet Transform based Shunt Hybrid Active Filter in PV Integrated Power Distribution System for Power Quality Enhancement", *IET Energy Systems Integration*, Vol-2, Issue-4, pp 331-343, 2020.
4. S. Pati, P. Sahoo, A. K. Barisal, and **D.K. Mishra**, "Frequency Regulation of a Multi-area Renewable Power System Incorporating with Energy Storage Technologies", *Advance in Systems, Control and Automations, Part of the Lecture Notes in Electrical Engineering Book Series, Springer*, Vol-708, pp. 83-92, 2021.
5. A. K. Mishra , P. K. Ray, R. K. Mallick, S. R. Das, A. Mohanty, **D. K. Mishra**, "PSO-GWO Optimized Fractional Order PID Based Hybrid Shunt Active Power Filter for Power Quality Improvements", *IEEE Access*, Vol-8, pp. 74497- 512, 2020 **(IF: 3.367)**.
6. **D. K. Mishra**, et al, "Effect of Superconducting Magnetic Energy Storage on Two Agent Deregulated Power System Under Open Market", *Materials Today: Proceedings, Elsevier*, Vol-21, Part 4, pp. 1919-29, 2020.

Submitted:

7. J. Wang, **D. K. Mishra,** L. Li, and J. Zhang, "Demand Side Management for Industrial Users in Peer-to-Peer Energy Trading Market Based on Two-Level Multi-agent Reinforcement Learning", *IEEE Transactions on Energy Markets, Policy and Regulation*, 2022.

Abstract

Unfavorable events (e.g., natural disasters or man-made attacks) that occur on the mainland can affect the reliability/resiliency of power system networks. Such events may cause load demand–generation imbalance, total power outage, and partial power outage, thereby damaging the electrical infrastructure and incurring a high economic loss. A power outage is defined as a loss of load connectivity or absence of electrical connection between the generation or distribution stations and the consumer end. The utility grid plays a significant role in the power flow from generating station to the prosumer end. However, during a highly disruptive event, a utility grid may be unable to supply power to end-users because of component failure. To solve this problem, a power system at the local stage must manage the needs of local load demand.

The evolution of the technology that governs the utility grids are causing severe issues in disruptive events, thereby necessitating the concept of resilience. The increased frequency of disasters results in increased power system failures and recovery costs, making the system unreliable and non-resilient. Hence, the formation of microgrids (MGs) and multi-MGs (MMGs) can prevent total power outages and support the social economy and flexible energy management scheme. Besides, deploying MMGs with renewable energy sources is ideal because of affordability, decarbonization, supply security, and resiliency. On the other hand, concerning the series of outage events and long-term events, mobile services such as crews and mobile energy storage devices are crucial, which can quickly recover the critical load according to the priority, thereby reducing the impacts on the system.

Furthermore, the increasing frequency of extreme events has increased power outages worldwide, including in Australia. Thus, a resilient infrastructure must be constructed to reduce power system damages and benefit the social and economic impacts. Considering the above concerns, this thesis contributes to the modern power distribution system resiliency study with four manifolds: (a) significance of distributed energy resources on resilience, (b) resilience quantification framework in the wake of extreme events, (c) resilient control-based multi-microgrid scheme against threats, and (d) novel resilient energy market framework considering the microgrid outage conditions. Each technical chapter verifies its framework using various scenario studies, and enhancement of resilience is also illustrated. Finally, this thesis offers an approach to the resilient power distribution system considering sustainability, energy security, and energy equity.

Keywords:

Keywords: Active distribution system; Multi-microgrid; Transactive energy; Resilience; Withstand - Recover - Adapt- Respond (WRAP).

Active distribution system (ADS): ADSs are the distribution networks of power system which plays a key role to control the parameter of distributed generations (DGs) like generators (renewable or non-renewable based sources), loads, and storages (fixed and mobile). Besides, it coordinates the power flow (active and reactive) and controls the voltage and fault levels.

Multi-microgrid (MMG): It is an interconnection of a microgrid in a single platform through a tie switch. It is also called coupled microgrid, networked microgrid, and interconnected microgrid. To improve reliability and resiliency, the contribution of MMGs is significantly high.

Transactive Energy (TE):

Defined by, Gridwise council, " a system of economic and control mechanisms that allows the dynamic balance of supply and demand across the entire electrical infrastructure using value as a key operational parameter".

The smart grid evolved as an emerging technology in the power system in which the energy trading services can take place and the prosumer plays a major role in buying and selling the power. This technology is called TE, where prosumers trade energy economically. In the TE framework, two major factors are considered, control and economic operation.

Resilience: The word resilience originates from the Latin word *resilio*, which means to "spring back." However, the dictionary meaning indicates that this term refers to the capability to recover immediately from disruptive events. Moreover, resilience could be hypothesized to refer to high-impact, low-possibility events. The main idea behind resilience theory is not merely to battle all-natural disasters but also to have immediate recovery operational measures. For low-probability and extreme events, the post-disruption stage is considered vital.

Withstand - Recover - Adapt- Respond (WRAP):

- Withstand refers to the ability or the resistance of the system against high-disruptive events.
- Recover is relevant to the rapidity of the system, which can be measured after the event hits the network.
- Adapt related to the interdependencies and resourcefulness, which are mainly focusing on the extensibility of the system during the events.
- Respond makes reference to predictability, which relates to reliable forecasting and precise decision-making to battle against extreme events.

CHAPTER 1

INTRODUCTION

1.1. Background study

The research on power system resilience is getting considerable attention in the research community due to the increase in natural disasters and cyber-attacks across the globe, and the power system must be reconfigured to a resilient infrastructure with the help of the new generation of technologies. The electric power system is considered the backbone of modern society. Thus, its operation should be safe, reliable, and efficient to maintain stability in terms of social and economic aspects [1, 2]. Although component failures occur due to atmospheric conditions or their haphazard nature, power systems are planned and designed on the basis of N-1 security criteria to address power system vulnerability [3]. However, the frequency of extreme events has been increasing over the decades, thereby increasing power outages; this phenomenon indicates that the design is poorly equipped for extreme eventualities of a bulk power system and level of severity [4, 5]. Therefore, preparing for unexpected events should be prioritized. Resilient power systems can continuously supply electricity even after the occurrence of natural disasters [6]. Understanding resilient power systems, specifically in terms of their risk, safety, and reliability, is a major task [7]. Several smart technologies have been used to enhance grid reliability and resilience in previous decades, for example, smart grid, microgrid (MG), and multi-microgrid (MMG). Resilient power systems mainly provide a reliable power supply to consumers during and after disrupted events [8]. Moreover, the increasing frequency of disruptive extreme can result in the loss of non-robust electricity infrastructures and components directly related to critical economic losses, information technology-related services, water supply, medical services, and security. Obviously, these services cannot be executed without electricity. Hence, several aspects must be considered in the design of electrical infrastructures, and the existing system must be renovated and transformed into a robust one to withstand a large range of possible events.

In the new global economy, the modern power system has become essential owing to its reliable and efficient operation. Considering a huge investment is required to build an electrical infrastructure, the recovery cost is extremely high if this infrastructure collapses, which will directly impact the economy [9, 10]. These philosophies can suitably deal with the acknowledged disruptive events in an entire power system infrastructure. Power system networks are designed under the N-1 security criteria to address unpredictable events. However, the increasing frequency of natural disasters and cyber-physical attacks has led to remarkable challenges to the electricity structure in the modern era [4]. This situation indicates a need to understand the various characteristics of the power outage in different environments. Over the past decade, the majority of the studies on power outages have emphasized the analysis of reliability and sustainability. To understand the reliability concept, two important factors that should be considered are adequacy and security [11]. Adequacy refers to the uninterrupted power supply that will continuously provide *light on* facilities to end-users. Security is the capability to withstand unexpected disruptions, such as sudden power loss caused by component failure and bad weather. Furthermore, the continuous exploration of enhancing a sustainable, safe, and robust power system has resulted in the continuous development of complex and large-scale power system networks [12]. The normal operation of a power system becomes abnormal due to unpredictable and turbulent conditions. Thus, system design may need extremely high safety provisions considering natural disasters and uncontrollable faults. However, only minimal attention has been provided to the concepts of robust systems in early planning stages that consider all probable failure modes. Consequently, increasing attention has been given to resilience study to withstand system complexities and unpredictable failure modes.

The word resilience originates from the Latin "*resilio*", which means to “spring back” [13]. The dictionary meaning indicates that this term refers to the capability to immediately recover from disruptive events. It identifies that extensive planning and operating level is taken to decrease the susceptibility to unexpected events. Although various definitions of “resilience” have been suggested, Holing et al. defined it as the perseverance of systems and their capability to resist, perturb, and uphold identical interactions among people and state variables [14]. The theories of resilience have enlightened significantly in various domains such as finance, engineering, socio-ecological, safety, and infrastructure [15, 16].

In the power system context, resilience is related to the capability to continuously maintain power supply even after highly disruptive events, such as a hurricane, tornadoes, tsunamis, earthquakes, and cyber-physical attacks [17]. Over the past decade, most studies on power systems have emphasized reliability and resiliency. Therefore, the current study aims to investigate the key issues of reliability and resiliency. Such essential factors as robust structures, cost-efficiency, reliable power supply, and smart networks can reconfigure a power system to be resilient and supply power to prosumers without any interruptions. For the first time, the UK Energy Research Center and Power Systems Engineering Research Center defined resilience and distinguished it from reliability [18]. Furthermore, the UK Cabinet Office stated that resilience includes reliability and encompasses resistance, severance, restoration, and action [19]. In 2018, the US Federal Energy Regulatory Commission defined resilience in terms of the bulk power system as "The capability to endure and curtail the degree of enormity and/or period of disruptive actions, which comprises the three main factors such as absorb, adapt and recover from extreme events, and other severe technical faults" [20].

The electric power system is considered as the backbone of modern society. Thus, its operation should be safe, reliable, and efficient to maintain stability in terms of social and economic aspects [21, 22]. Although component failures occur due to atmospheric conditions or their haphazard nature, power systems are planned and designed on the basis of N-1 security criteria to address power system vulnerability [17, 23]. However, the frequency of natural disasters and man-made attacks has been increasing over the decades, thereby increasing power outages; this phenomenon indicates that the design is poorly equipped for extreme eventualities of a bulk power system and level of severity. Therefore, preparing for unexpected events should be prioritized. Resilient power systems can continuously supply electricity even after the occurrence of natural disasters. Understanding resilient power systems, specifically in terms of their risk, safety, and reliability, is a major task [24, 25]. In previous decades, several smart technologies have been used to enhance grid reliability and resilience, for example, smart grid, microgrid, and multi-microgrid. Resilient power systems mainly provide a reliable power supply to consumers during and after disrupted events [26].

Table 1.1 Major power outages [27]

Year	Customers affected (million)	Location	Cause
2010	15	Chile	Earthquake
	0.25	Washington DC, USA	Storm
	30000 homes	Northern Ireland	Winter weather
2011	3.2	Texas, USA	cold weather
	53	Brazil	System failure
	9	Chile	Equipment failure
2012	400	India	System failure
	20	Istanbul, Turkey	System failure
	8	USA	High winds
2013	0.5	Canada	System failure
	1.5	Turkey	Substation failure
	0.25	Queensland, Australia	Cyclone
2014	100	Bangladesh	Grid failure
	100	Egypt	System failure
	20	South Africa	Technical difficulty
2015	140	Pakistan	Technical fault at a power station
	70	Turkey	Grid failure
	0.23	Ukraine	Cyberattack
2016	10	Kenya	Monkey entered a power station
	1.7	Australia	Tornados
	3.5	Puerto Rico	Severe weather
2017	1	USA	Wind storm
	6.68	Taiwan	Equipment failure
	1.8	UK	Storm
2018	10	Brazil	Transmission line failure
	2.95	Japan	Damage to the coal-fired thermal power station
	0.6	BC, Canada	Wind storm
2019	32	Venezuela	Generation-load imbalance
	48	Argentina, Uruguay and Paraguay	Operative error
	100	Java Island	System failure
2020	6.8	Kalimantan, Indonesia	Thunderstorm
	4.3	Texas, USA	Tornados
	10	Mumbai, India	Technical difficulties
2021	200	Pakistan	Frequency drop
	10	Jordan	electrical line interruption
	0.52	Melbourne, Australia	Wind storm
2022	140	Bangladesh	Grid failure
	1.1	Ontario, Canada	Peak winds
	1.5	Kyrgyzstan	Grid failure

Moreover, the increasing frequency of disruptive extreme can result in the loss of non-robust electricity infrastructures and components directly related to critical economic losses, information technology-related services, water supply, medical services, and security. Evidently, these services cannot be executed without electricity. Hence, several aspects must be considered in the design of electrical infrastructures, and the existing system must be renovated and transformed into a robust one to withstand a large range of possible events. Table 1.1. present the number of people affected by power outages from 2010 to 2022 across different countries. Fig. 1.1 illustrates the people affected in Australia due to power outages. Fig. 1. shows the various events from 2010-2022 that caused these power outages. As can be seen, the major percentage of power outages is caused by equipment failures and natural disasters.

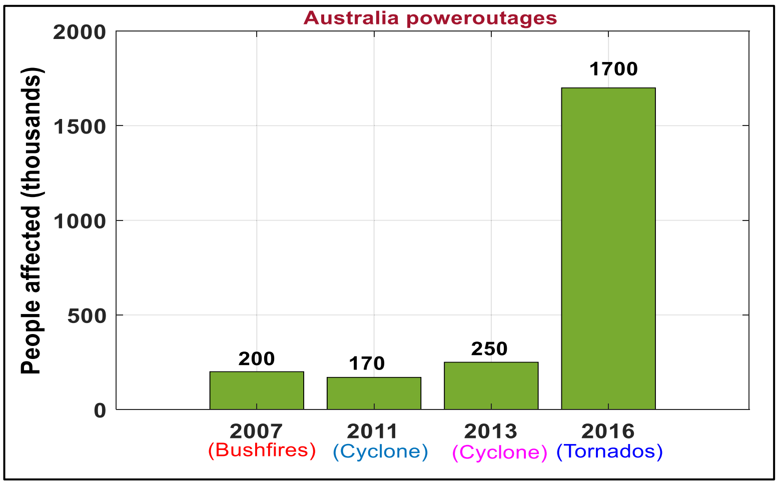

Fig. 1.1 Major power outages across Australia (*Source Ausgrid*)

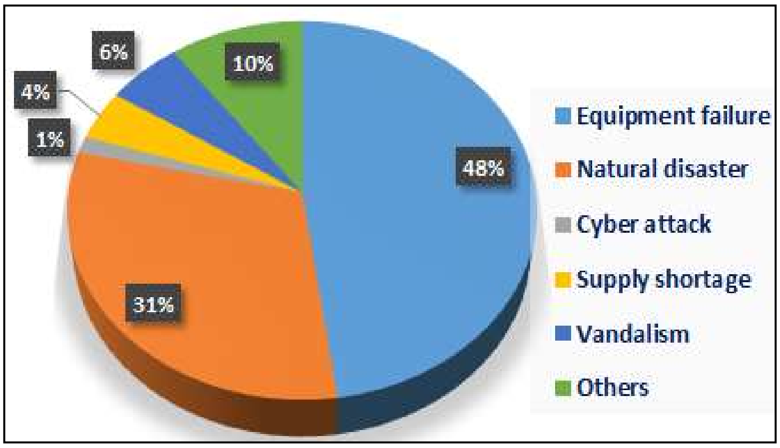

Fig. 1.2 Causes of power outages [17]

On the other hand, the world has observed the stunning transformations of electrical infrastructures in terms of reliability, sustainability, and resiliency over the past few decades. This perception led to the "*light on*" facility system design that already possesses reliable and sustainable grids and is now aiming at reaching a resilient one [28]. While a reliable grid pertains to the "*light on*" phenomenon during normal operating conditions, a sustainable grid refers to meeting the necessities of current scenarios without conceding the capability of the future energy market to meet the specific requirements. Besides, a resilient grid refers to the notion of keeping the light on during and after highly disruptive natural events. Noteworthy, such changes should happen in both aspects of the planning and operation of the grid to reach a network that has the ability to maintain the continuity of supply after severe events.

1.2. Motivation

Over the past few decades, the frequency of disasters has been increasing. Due to that, electric infrastructure has been affected significantly, directly impacting human life and the social economy. Therefore, there is a need for breakthrough technologies that can be incorporated into the power system, which can predominantly anticipate any extreme events and could be the key strategy of the power system resilience. Although the resilience study is not new, standard quantification indices and enhancement techniques still need more attention. The following are the challenges that need to be addressed to improve the resiliency of active distribution systems (ADSs).

- Severe power outages caused by high-disruptive events (shown in Table 1.1, Figs. 1.1, and 1.2)
- Millions of customers affected due to blackouts.
- Very high restoration cost of the power system due to extreme events.
- Dependence on customer requests for fault/outage detection.
- Optimization-based crew scheduling.
- Improper utilization of distributed energy resources and tie-switches.
- Lack of training and awareness.
- Lack of mobility resources, e.g., mobile energy storage, mobile substation, etc.
- Energy market model considering extreme events and cyber-threat issues.

1.3. Research aims and objectives

1.3.1 Research hypothesis

The power system resilience could be hypothesized to refer to high-impact, low-possibility events. The main idea behind resilience theory is not merely to battle all-natural disasters but also to have immediate recovery operational measures. For low-probability and extreme events, the post-disruption stage is considered vital.

1.3.2 Research aims

This research is focused on the quantification of ADS resiliency with the following aims.

Aim 1: To establish a new framework as an approach to assess how active distribution systems are functioning in the context of resilience.

Aim 2: To develop novel resilience evaluation indices through reconfiguration planning and operation towards the enhancement of active distribution system resiliency.

1.3.3 Research objectives

The following objectives have been accomplished with the above aims:

Objective 1: Investigate a new modeling approach to the active distribution system considering the resilience factor against extreme operating conditions.

Objective 2: Propose and validate a novel resilience quantification and enhancement framework through MMG and mobile storage units.

Objective 3: Design and implement a resilient frequency control-based isolated MGs scheme in ADS considering extreme operating conditions.

Objective 4: Develop a resilient energy market model concerning extreme event consideration and cyber-threat issues.

The abovementioned research objectives are achieved in this thesis and are presented in Chapters 3, 4, 5, and 6, respectively. The summary of the contribution of each chapter is also discussed in Section 1.4.

1.3.4 Research significance and innovation

This research can contribute to a better understanding of the major attributes of the resiliency of the ADSs. With the development of the resilience evaluation index, the study can lead to future research on resiliency for power system engineers who are willing to pay attention to the measurement of resiliency. Further, additional studies support the formation of MMGs during the events; this may permit putting into practice a resilience-enhancing strategy in ADSs. More importantly, this study can help the power system engineers diversely: (a) a resilience quantification framework can help to measure the resilience indices, (b) a cyber-resilient control-based ADS framework can support the power system due to grid failure, which will run in an isolated mode, and (c) a novel transactive energy framework can promote the prosumers to participate in the energy market, which is resilient against cyber-attacks.

The above studies are the signification of a resilient system framework which is dealing with minimizing the power system damages and thefts, increasing human lives comfortability (by reducing the power interruption), and finally, the economic benefits to the society (applicable for both prosumers and consumers).

1.4. Contributions and thesis organization

1.4.1. Key contributions

The key contribution of this thesis is outlined as follows.

- In the first attempt, a renewable-based interconnected ADS is designed using the IEEE 33-bus test system. Four MGs are considered in the proposed test system, and each MG comprises solar energy and storage units. The proposed model has been simulated with a different scenario, such as a traditional system (no renewable energy), with PV and storage units and optimal allocation of PV units. In addition, two different operating conditions are demonstrated, with and without considering the emergency loads. In this study, an existing resilience index as energy-not-supplied (ENS) is measured under single and double phase to ground fault conditions, which signifies the network's capability and the number of customers affected. It is reported that better placement of MG units reduces the ENS, which is certainly called high resilience. As far as the emergency load is concerned, it is vital when the system faces extreme events that can lead to power outages and eventually affects human lives. Thus to evade the power system failure, it needs to be resilient, and ENS should be low, which has been demonstrated in Chapter 3.

- In the second attempt, a novel resilience quantification framework is developed, where four major attributes of resilience are defined with their evaluation indices. These attributes have a significant value because when a system experiences an extreme event, it is critical that the system must have a withstanding capability, speed recovery, adaptability in nature, and preventive actions for future events. With this consideration, a framework called WRAP is developed, which is a combination of withstand (W), recover (R), adapt (A), and prevent (P) elements from quantifying the resiliency of the system against extreme events. Further, resilience enhancement techniques are employed through MMG placement and mobile energy storage units. The IEEE 33-bus test system is considered with single and multiple fault cases to validate the proposed framework. Each study has been categorized into four types of scenarios according to resource availability. Moreover, in an emergency situation, mobile energy storage plays a key role in supporting the critical load and enhancing the load restoration against extreme events. The various case studies demonstrated that better reconfiguration planning in terms of resource allocation, availability of mobility services, and placement could significantly enhance the resilience characteristics of ADS, as seen in Chapter 4. Further, the proposed framework has been compared and reported using historical data to reduce the impact on the economy substantially.
- In the third attempt, a resilient-control-based isolated MG is designed. In the last few decades, the penetration of renewable energies has been increasing, which is more challenging as it deals with uncertainties. On the other hand, cyber-attacks are also increasing, which needs more attention. With these two considerations, Chapter 5 presents a resilient-control-based frequency regulation scheme of isolated MGs against cyber-attacks and uncertainties. As noted, the frequency is a very sensitive parameter of the power system; if it deviates from the rigid limits, it could face a power system collapse or blackout. Thus, controlling the system's frequency during the transient condition or any extreme events is vital. In this study, different control methodologies such as conventional PID and fuzzy logic-based PID controllers are employed and compared in light of frequency regulation against unfavourable events and

uncertainties. Finally, the proposed model is validated through a real-time simulation platform, such as OPAL-RT.

- In the fourth attempt, a novel resilient energy market model concept is discussed, combining the control principle and economic operation. Nowadays, the developed countries utilize an energy market to deal with supply shortages and an energy-economic model for the prosumers and customers; the framework is otherwise called transactive energy (TE). However, a better pricing mechanism is always a major concern, which is proposed in Chapter 6. On the other hand, the increase in extreme events also affects the energy market, which can be collapsed, incurring a high economic loss. To address the extreme event challenges in the energy market, this chapter considers the outage condition, and a restoration approach is also presented. Indeed, the TE structure needs a digital platform to do the trading activities, where plenty of transactions are carried out, which increases the vulnerability of the system. Eventually, cyberpunk can disrupt trading activities in the TE model, which leads to a security collapse. To secure it, a recent breakthrough technology such as Blockchain is used in this study. Further, the proposed model has been validated through various case studies, with and without TE and with Blockchain-enabled TE. Two extreme event conditions are employed: MG outage and cyber-attacks. With these two considerations, the proposed method shows a better defensive capability and, finally, shows that a significant amount of energy costs have been saved compared to the traditional system, and a secure platform is ensured.

1.4.2. Thesis organization

The thesis is organized as follows. Chapters 1 and 2 review the background study, literature, and concepts related to resiliency of ADSs. In addition, the research challenges, questions, gaps, and theoretical framework are discussed. Chapter 3 studies the importance of distributed energy resources for the resiliency of the ADSs. The incorporation of renewables and storage units into the ADS and their placement are vital, which is demonstrated in this chapter. Chapter 4 proposes a novel resilience quantification and enhancement framework which is validated under various operating conditions. The importance of building a resilient system is also discussed through the “Prevent” element of the WRAP framework, and it is seen that the outage cost can be saved significantly. Chapter 5 presents a resilient frequency regulation scheme of isolated MG against cyber-attacks and uncertainties. Further, a novel TE model is developed under the concept of resilience in Chapter 6, where a cyber-attack-based event is applied, and the Blockchain has been implemented to defend it. Finally, the conclusions and future works of this thesis are discussed in Chapter 7.

References

[1] M. Panteli, C. Pickering, S. Wilkinson, R. Dawson, and P. Mancarella, "Power system resilience to extreme weather: fragility modeling, probabilistic impact assessment, and adaptation measures," *IEEE Transactions on Power Systems,* vol. 32, no. 5, pp. 3747-3757, 2016.

[2] Y. Wang, C. Chen, J. Wang, and R. Baldick, "Research on resilience of power systems under natural disasters—A review," *IEEE Transactions on Power Systems,* vol. 31, no. 2, pp. 1604-1613, 2015.

[3] S. C. Madathil *et al.*, "Resilient off-grid microgrids: Capacity planning and N-1 security," *IEEE Transactions on Smart Grid,* vol. 9, no. 6, pp. 6511-6521, 2017.

[4] F. H. Jufri, V. Widiputra, and J. Jung, "State-of-the-art review on power grid resilience to extreme weather events: Definitions, frameworks, quantitative assessment methodologies, and enhancement strategies," *Applied Energy,* vol. 239, pp. 1049-1065, 2019.

[5] J. Wang and H. Gharavi, "Power Grid Resilience [Scanning the Issue]," *Proceedings of the IEEE,* vol. 105, no. 7, pp. 1199-1201, 2017.

[6] N. Malla, S. Poudel, N. R. Karki, and N. Gyawali, "Resilience of electrical power delivery system in response to natural disasters," in *2017 7th International Conference on Power Systems (ICPS)*, 2017, pp. 806-811: IEEE.

[7] R. Arghandeh, A. Von Meier, L. Mehrmanesh, and L. Mili, "On the definition of cyber-physical resilience in power systems," *Renewable and Sustainable Energy Reviews,* vol. 58, pp. 1060-1069, 2016.

[8] S. Chanda and A. K. Srivastava, "Defining and enabling resiliency of electric distribution systems with multiple microgrids," *IEEE Transactions on Smart Grid,* vol. 7, no. 6, pp. 2859-2868, 2016.

[9] P. Dehghanian, B. Zhang, T. Dokic, and M. Kezunovic, "Predictive risk analytics for weather-resilient operation of electric power systems," *IEEE Transactions on Sustainable Energy,* vol. 10, no. 1, pp. 3-15, 2018.

[10] S. M. Amin, "Electricity infrastructure security: Toward reliable, resilient and secure cyber-physical power and energy systems," in *IEEE PES General Meeting*, 2010, pp. 1-5: IEEE.

[11] A. M. Rei, A. L. Da Silva, J. L. Jardim, and J. Mello, "Static and dynamic aspects in bulk power system reliability evaluations," *IEEE Transactions on Power Systems,* vol. 15, no. 1, pp. 189-195, 2000.

[12] P. Dehghanian, S. Aslan, and P. Dehghanian, "Maintaining electric system safety through an enhanced network resilience," *IEEE Transactions on Industry Applications,* vol. 54, no. 5, pp. 4927-4937, 2018.

[13] D. E. Alexander, "Resilience and disaster risk reduction: an etymological journey," *Natural hazards and earth system sciences,* vol. 13, no. 11, pp. 2707-2716, 2013.

[14] C. S. Holling, "Resilience and stability of ecological systems," *Annual review of ecology and systematics,* vol. 4, no. 1, pp. 1-23, 1973.

[15] C. Folke, "Resilience: The emergence of a perspective for social–ecological systems analyses,"

Global environmental change, vol. 16, no. 3, pp. 253-267, 2006.
[16] L. Seeliger and I. Turok, "Towards sustainable cities: extending resilience with insights from vulnerability and transition theory," *Sustainability,* vol. 5, no. 5, pp. 2108-2128, 2013.
[17] Z. Bie, Y. Lin, G. Li, and F. Li, "Battling the extreme: A study on the power system resilience," *Proceedings of the IEEE,* vol. 105, no. 7, pp. 1253-1266, 2017.
[18] M. Panteli and P. Mancarella, "The grid: Stronger bigger smarter?: Presenting a conceptual framework of power system resilience," *IEEE Power Energy Mag,* vol. 13, no. 3, pp. 58-66, 2015.
[19] D. Sage, P. Fussey, and A. Dainty, "Securing and scaling resilient futures: neoliberalization, infrastructure, and topologies of power," *Environment and Planning D: Society and Space,* vol. 33, no. 3, pp. 494-511, 2015.
[20] S. Shetty, G. Kamdem, B. Krishnappa, and D. Nikol, "Cyber Resilience Metrics for Bulk Power System," *Risk Analysis Journal,* 2018.
[21] M. J. Ghadi, S. Ghavidel, A. Rajabi, A. Azizivahed, L. Li, and J. Zhang, "A review on economic and technical operation of active distribution systems," *Renewable and Sustainable Energy Reviews,* vol. 104, pp. 38-53, 2019.
[22] M. J. Ghadi, A. Rajabi, S. Ghavidel, A. Azizivahed, L. Li, and J. Zhang, "From active distribution systems to decentralized microgrids: A review on regulations and planning approaches based on operational factors," *Applied Energy,* vol. 253, p. 113543, 2019.
[23] H. Ghoreishi, H. Afrakhte, and M. J. Ghadi, "Optimal placement of tie points and sectionalizers in radial distribution network in presence of DGs considering load significance," in *Smart Grid Conference (SGC), 2013*, 2013, pp. 160-165: IEEE.
[24] M. Panteli, D. N. Trakas, P. Mancarella, and N. D. Hatziargyriou, "Boosting the power grid resilience to extreme weather events using defensive islanding," *IEEE Transactions on Smart Grid,* vol. 7, no. 6, pp. 2913-2922, 2016.
[25] D. T. Ton and W. P. Wang, "A more resilient grid: The US department of energy joins with stakeholders in an R&D plan," *IEEE Power and Energy Magazine,* vol. 13, no. 3, pp. 26-34, 2015.
[26] A. Gholami, T. Shekari, M. H. Amirioun, F. Aminifar, M. H. Amini, and A. Sargolzaei, "Toward a consensus on the definition and taxonomy of power system resilience," *IEEE Access,* vol. 6, pp. 32035-32053, 2018.
[27] "List of major power outages," in *List of major power outages*, ed. Wikipedia: https://en.wikipedia.org/wiki/List_of_major_power_outages, 2018.
[28] S. Leonori, A. Martino, F. M. F. Mascioli, and A. Rizzi, "ANFIS Microgrid Energy Management System Synthesis by Hyperplane Clustering Supported by Neurofuzzy Min–Max Classifier," *IEEE Transactions on Emerging Topics in Computational Intelligence,* vol. 3, no. 3, pp. 193-204, 2019.

CHAPTER 2

LITERATURE REVIEW

Over the past few decades, natural disasters and other unforeseen events have been increasing, which increases the frequent power outage across the globe. In addition, the power systems are designed with reliability principles, *i.e*., security and adequacy. With these principles, the power system can only cope with high-probability and low-impact events, mostly known failures. Moreover, power system infrastructure is unremarkably affected and can be restored within a reasonable time with less impact on society and the economy. However, catastrophic events increased in the past few decades, highlighting the concern for reliability principles [1]. The evidence includes major catastrophic events, such as Hurricane Sandy and Katrina, Japan earthquake, Ukraine cyber-physical attack, and other major events reported in [2-4]. These events affected millions of people and caused energy infrastructure damages, significantly impacting lives and the economy. Thus, to ensure a reduced impact on the economy against power system damage and energy security, the distribution system should be resilient in dealing with four major attributes: withstand, recover, adapt, and prevent (WRAP) [4].

In the power system context, resilience deals with low-probability and high-impact (HILP) events. Hence, to minimize the consequence of HILP events, the migration/ modernization of the power system is necessary [5]. However, extreme events, such as natural disasters or cyber-attacks, are mostly affecting the distribution system. Therefore, the power system planner should emphasize distribution system modernization, where the integration of distributed energy resources (DERs) is vital. Over the past few decades, the utilization of DER has increased remarkably; it has achieved a milestone for microgrid (MG) and smart grid technology. With these technologies, the distribution system can rapidly restore the load (according to priority) after a HILP event, thereby enhancing the distribution system's resiliency [6, 7]. As far as HILP event is concerned, the concepts of reliability and resilience are vital. The detailed discussion about reliability and resilience and its comparison are as follows.

2.1. Resilience concept

2.1.1. Reliability and resiliency

In the power system domain, reliability and resilience are two important factors that must be considered while designing a new structure or renovating an existing one. These two terms are often considered the same, but they differ in terms of probability and effect. Although extensive research has been conducted on these issues, considerable uncertainty remains related to their relationship. The main distinguishing characteristic between reliability and resiliency is high-probability and low-impact, and low-probability, and high-impact events, respectively, as shown in Fig. 2.1, and other key characteristics are highlighted in Table 2.1.

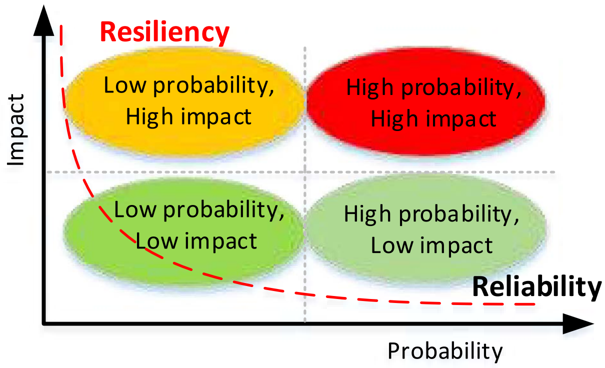

Fig. 2.1 Reliability versus resiliency (*Source: Author*)

Fig. 2.2 Resilient system (*Source: Author*)

Table 2.1 Reliability versus resiliency characteristics

Factor ↓ Key →	**Reliability**	**Resiliency**
Probability of faults	High	Low
Impacts of events	Low	High
Process or system	Static	Dynamic
Objective of concerns	Consumer interruption time	Consumer interruption time and infrastructure recovery time
Restoration time	Low	High
Number of faults	High	Low
Levels of events predictability	High	Low
Targeted loads for restoration	All connected loads	Critical loads
Duration of outages	Short duration	Long duration
Scenario	Controllable fault, overload, short circuit, maintenance	Hurricane, earthquake, Tsunami, tornado, ice-storm, cyber-physical attack
Level of predictability	Predictable	Un-predictable
Needed devices for compensation	Using Flexible alternating current transmission system (FACTS), filter, solid-state transformer, load forecasting, smart grid	Robust design, mobile diesel generator (DG), MG formation, repair crews, black start capabilities, tree trimming, underground cables
Performance evaluation indices	System average interruption duration index (SAIDI), system average interruption frequency index (SAIFI), customer average interruption duration index (CAIDI), customer average interruption frequency index (CAIFI), energy-not-supplied (ENS)	Need to be addressed

Despite some studies that have been conducted with a minimal scientific understanding of the definition of resilience, the significance of this concept is broadly similar to reliability. Therefore, the term resilience can refer to withstanding any extreme event, responding immediately to restore and adapt to unexpected events, and finally preventing future occurrences. The four factors of resilience are illustrated in Fig. 2.2.

Note that resilience has a close relationship with other concepts, such as vulnerability and robustness. The term vulnerability is defined by Holmgren et al. as "*the collection of properties of an infrastructure system that may weaken or limit its ability to maintain its intended function, or provide its intended services when exposed to threats and hazards that originate both within and outside of the system's boundaries*" [8]. The term robustness refers to the system that maintains or holds its system infrastructure (distribution system) unharmed against extreme events and threats [9]. Both factors measure resilience; for example, a more vulnerable system can be called less resilient, while a robust (increased robustness) system can be treated as a better resilient system. Indeed, in this thesis, various factors are considered to measure resilience in different steps, such as withstand, recover, adapt, and prevent. Withstand factor is likely considered as the system's robustness; for example, if the system has a better withstanding capability, the system is more robust, and vice versa.

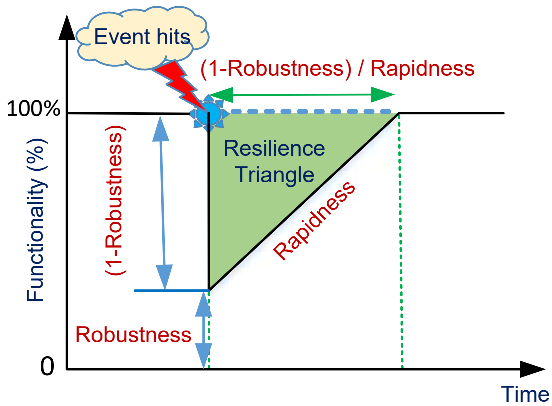

Fig. 2.3 Resilience triangle [11]

2.1.2. Resilience characteristics

Notably, research studies focusing specifically on the resilience curve are evidently lacking. Researchers draw an extensive range of sources and describe the different ways in which the resilience state can be obtained. Several studies have reported the resilience triangle, in which two different states are presented [10-12] and shown in Fig. 2.3. Furthermore, a systematic understanding of each stage of the resiliency operation and resilience trapezoid is studied in [11, 13, 14]. The resilience trapezoid is the detailed analysis of the resilience state during disruptive events through Phases I, II, and III. In Phase-I, the event hits the network, and the state goes into a disruptive phase. Emergency coordination is needed to survive the load demand in Phase II. Lastly, restorative action can take place in Phase III to reach the normal operation state.

In Fig. 2.3 and Fig. 2.4, the authors of [11] present the two expressions in terms of robustness and rapidness. Robustness can be defined as permeable capability by measuring the least percentage of functionality. Rapidness refers to the capability to attain prioritized objectives in a given time frame to encompass threats and evade further disturbance. Thus, the resilience performance level can be estimated as a function of robustness and rapidness [11]. To enhance the resilience characteristics, corrective planning-operational measures are key areas that can facilitate the shifting of the resilience level with a short restoration time to reach a normal operating condition, as shown in Fig. 2.5.

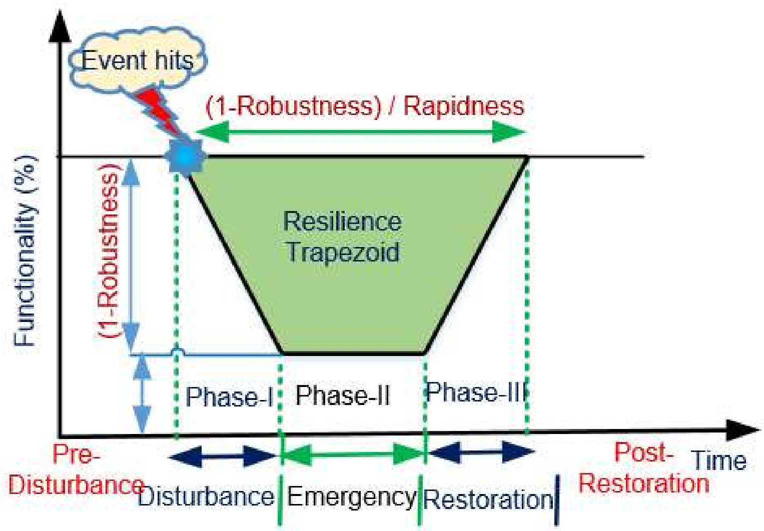

Fig. 2.4 Resilience trapezoid [11]

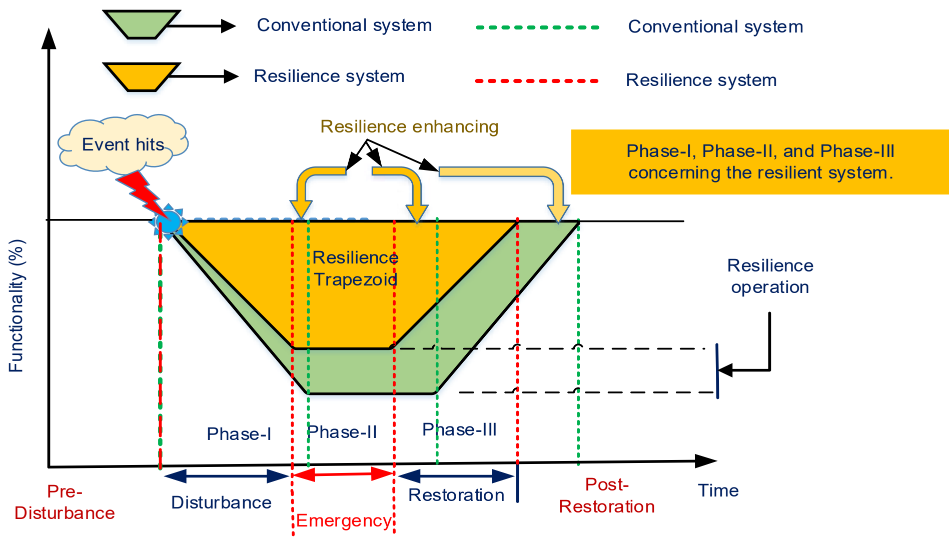

Fig. 2.5 Resilience performance curve (*Source: Author*)

Moreover, the significance of Fig. 2.5 can be explained as the area of the trapezoid is inversely proportional to the resilience level of the system, which can further be treated as the resilience enhancing characteristics. Besides, the resilient system denotes the time required for emergency coordination and restoration is relatively less, and a low disturbance effect should be there. As far as the resiliency of the system is concerned, the system should restore as quickly as possible to minimize the recovery cost and reduce its vulnerability of the system. With these objectives, the performance level is presented in the resilience performance curve.

2.1.3. Resilience study in various contexts

This section generally reports concerns with the overall vision of resilience in various contexts. Numerous studies have explored the factors influencing resilience [10, 15-18]. The probabilistic resilience study with different weather conditions is proposed in [16]. The application of artificial neural networks in the resilience analysis evolved to match load shedding in response to the failure probability with their load profiles is discussed in [17]. Substantial analysis and discussion of resilience metrics are presented in [15], which focus on endurance and recovery time. Subsequently, Ref. [18] proposes several resilience metrics considering past threat experiences and the future probability of threats for a complex power system network.

Several possible solutions related to the resilience metrics are discussed in [19-21]. Moreover, Ref. [20] analyzes the resilience metric estimation of a dynamic power system considering energy storage devices, renewable energy sources, and demand-side management. The strategy of enhancing resiliency is presented in [21], which discusses the association between disaster organization members and critical infrastructure that is crucial in a power system. On the other hand, Ref. [19] reports the major limitations of the preliminary analysis considering the sustainability of low-income households. A clear understanding of the hardening measure and guiding principle for the migration of present distribution systems (DSs) to MGs is presented in [22]. Retrospectively, the hardening and operational measures toward the distribution resiliency scheme are discussed in [23]. Meanwhile, Refs. [24] and [25] report the major power outages and their consequences worldwide and identify the improved strategy of DS resiliency against storms. Moreover, Refs. [26-28] investigate the differential study and remedial action in response to floods, storms, earthquakes, and other weather-related catastrophes. A future projected plan is outlined to indicate the subtle distinctions between reliable DSs and resilient grids. The benefits of each research and development practice are also discussed in [29].

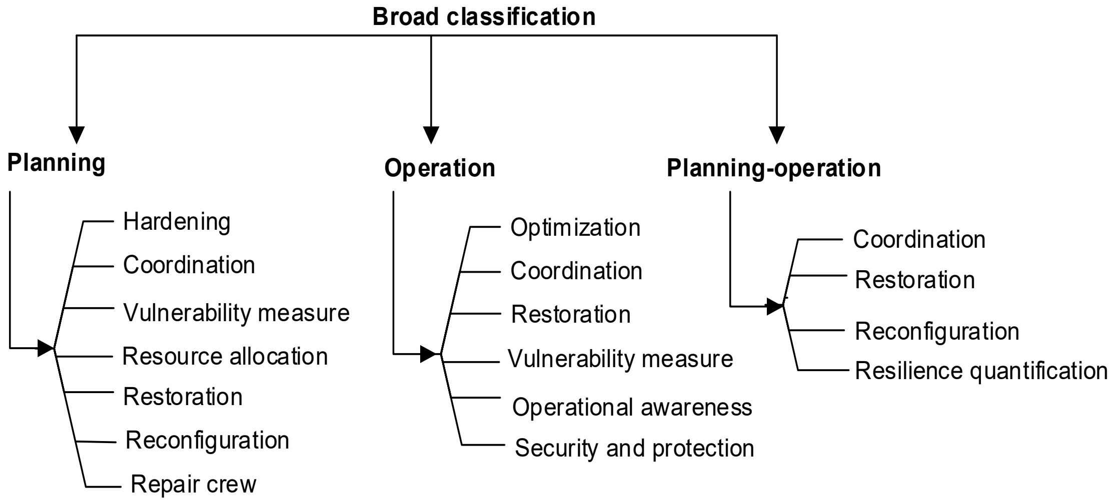

Fig. 2.6 Broad classification of a power distribution system in the resilience context

Moreover, Ref. [30] identifies major contributing factors for the defensive planning of DSs to enhance grid resiliency. A broad perspective is outlined in [31], which holds the view of cyber-physical attainment in the power system (PS) resilience context to address natural disasters. Energy regulators and infrastructure planning bodies are examined in [32, 33] to understand the climate adaptation strategy on resiliency. A recent study by [34] involves various classifications of resilience in the power system context. The study related to the planning-operational measure of active distribution system (ADS) in the resilience context is classified through various means, as depicted in Fig. 2.6. In fact, this figure shows the proposed structure of Section 2.2. The summary of this section is illustrated in Table 2.2.

Table 2.2: An overview of the resilience-dependent factors

Category	Areas of study (overview)	Contributions	Year	Ref.
Hardening overview	Hardening measure	A brief discussion of hardening measures for the metamorphosis of present DSs to future MGs	2007	[22]
	Hardening guidelines	A detailed discussion of distribution system resiliency in contrast with protection, hardening, guidelines, and innovations.	2010	[23]
	Hardening operation	The key area of distribution resiliency toward hardening, and operational	2014	[35]

		measures.		
	Hardening enhancement strategy	A brief discussion of enhancement strategy by hardening and smartening power systems for improved resiliency characteristics.	2017	[36]
Blackout study	Blackout summary	A concise summary of blackouts against natural catastrophic events that lead to power outages.	2014	[24]
	Outages and impacts	Reporting major power outages worldwide and their impact on pole structure and also discussing robust pole structures to enhance potential actions in response to future storms.	2007	[25]
Weather-related study	Protection against flood	Reporting a flood-related study and remedial action from the perspective of substation protection.	2011	[26]
	Protection against storm	Listing various weather- and storm-related blackouts worldwide, their causes, and the corresponding remedial actions.	2012	[27]
	Protection against earthquakes	Outlining the study of power system resilience against earthquakes using a two-phase stochastic method.	2015	[28]
	Climate adaptation strategy	Providing an overview of the key function of microgrids and examining the resiliency among energy regulators and infrastructure planning bodies.	2017	[32]
Future projection	Grid transformation	Future development plan report toward reliable DSs to sustainable and resilient grids and the need for research and development.	2015	[29]
	Defensive planning of DSs	Presenting comprehensive planning to improve the resiliency of power systems against highly disruptive scenarios.	2015	[30]
Cyber-physical based study	DERs withstand against extreme events	Key concepts of PS resilience in terms of cyber-physical attainment to address unfavorable events and leveraging by DERs.	2016	[31]
Resilience framework and taxonomies	Energy infrastructure	Outlining the modeling framework of energy infrastructure regarding resilience outlook.	2019	[33]
	Classification	General understanding of resilience and its classification in the context of the power system.	2018	[34]
	Framework	Optimization framework for resilient distribution system.	2022	[37]

2.2. Active distribution system

Council on Large Electric Systems (CIGRE) introduced the concept of the active distribution network (ADN) in 2008. ADN is the combination of DERs, suchlike generators, loads, and storage, where control action can take place through the distribution system operators (DSO) [38]. However, in 2012, the understanding of ADN has extended to the ADS [39] because of the increase in penetration of DERs. Further, the definition and structure of ADS have been developed by IEEE and CIRED, presented in [40, 41].

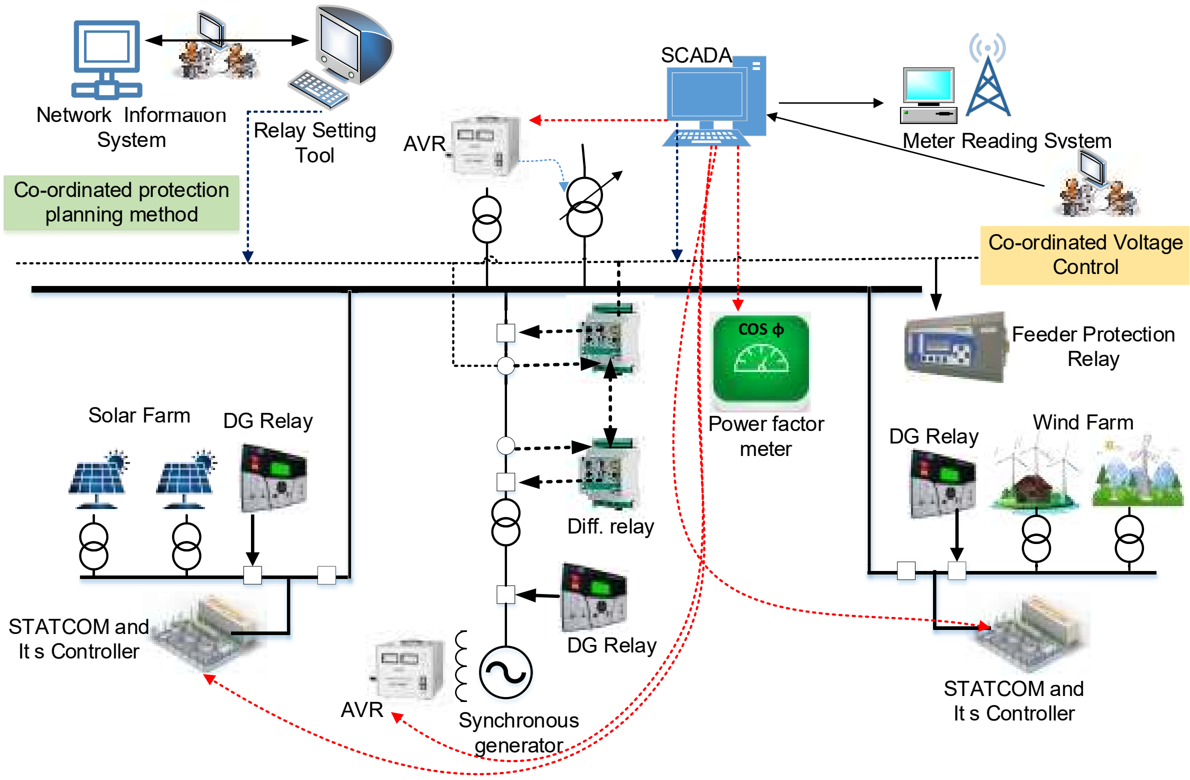

Fig. 2.7 Active distribution network (*Source: Author*)

Over the past few years, there has been a huge transition from conventional distribution networks to ADNs, which implies that the integration of DERs is monitored actively in a coordinated way to enhance DERs utilization. Besides, ADSs are not only considered as simply distribution grids but also a combined system comprising DERs, load demand, storage, and active networks, as shown in Fig. 2.7.

As far as ADS is concerned, MG/multi-microgrid (MMG) is part of this, which greatly enhances the resilience characteristics by proper utilization of DERs and other ancillary devices. The short description of MG and MMG are as follows.

A. Microgrid

Microgrids are projected as future power networks that offer clean and cost-effective power to the prosumer. In a microgrid, power-sharing between sellers and buyers is a point-to-point system combined as an isolated energy system, as shown in Fig. 2.8. These isolated power sources have been combined to cater to the energy need of standalone communities referred to as a microgrid. If there is a surplus of energy generation, then microgrids become self-sufficient and work independently. Therefore a microgrid is essentially a small power system consisting of several isolated power generating stations [42]. Microgrid configuration needs adequate control and management, which provides many more advantages to the beneficiaries, such as more reliability, flexibility, and better power quality combined with less generation cost. Furthermore, surplus energy is generated from the microgrid, which shows the energy involved is not equal to the energy consumed by the individuals, and thus the remaining energy will be sold to a utility company, and similarly when there is a shortage of energy can be bought from the utility company. However, when the generated energy from homes is delivered with the help of alternating current (AC) lines, it will destabilize the power systems. Further, this problem will be overcome by storing the generated power in local storage systems. This method also has many limitations as storage of energy for a 24 hours consumption will require some large-sized batteries [43].

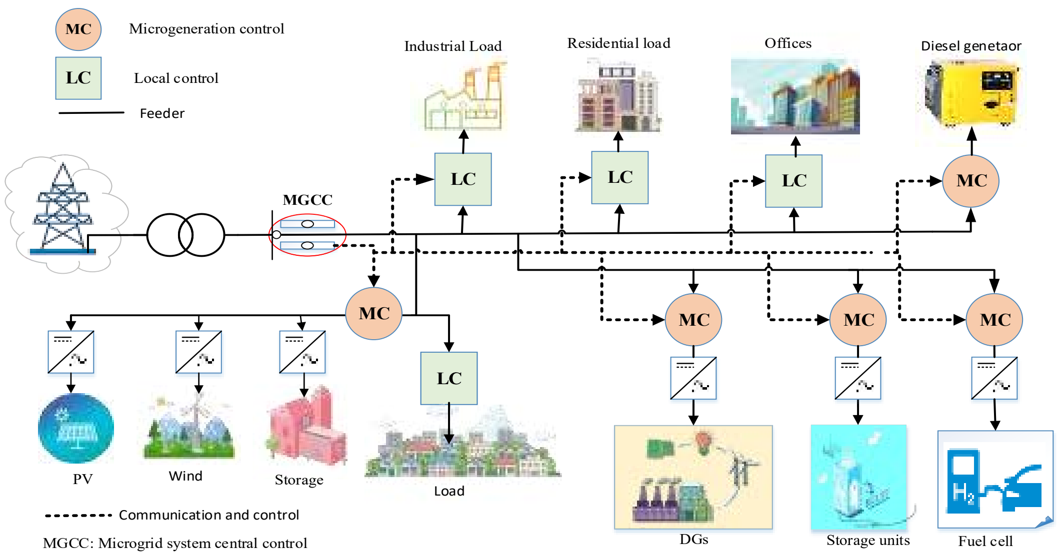

Fig. 2.8 Microgrid structure (*Source: Author*)

B. Multi-microgrid

MMGs are occasionally called interconnected microgrids, and networked microgrids (shown in Fig. 2.9) can be stated as a couple of microgrids organized in extensional closeness with a corresponding energy management system for collaborative support and power exchange. Recent years have seen an increasing number of published studies on MMG. In [44], a self-governing operation of coupled microgrids with AC common bus was pioneered. For smart distributions, coupled microgrids through utility feeders in [45] and direct current (DC) link-based robust interconnected microgrids [46] were addressed. Furthermore, standalone island-based microgrids were presented, in which the focus was on a coordinated dispatch scheme for power balance with different disruptive events [47]. The application of MMGs to enhance the automated control of the distribution system under blackouts was demonstrated in [48], in which microgrids were considered to meet the demand of the external loads through least switch operations. The self-healing strategy of networked microgrids with an economic dispatch plan was presented in [49], in which the surplus energies in each unit were accumulated to satisfy the power demands. Despite enabling energy restoration, MMGs can also contribute to international frequency regulation through supplementary control loops [50].

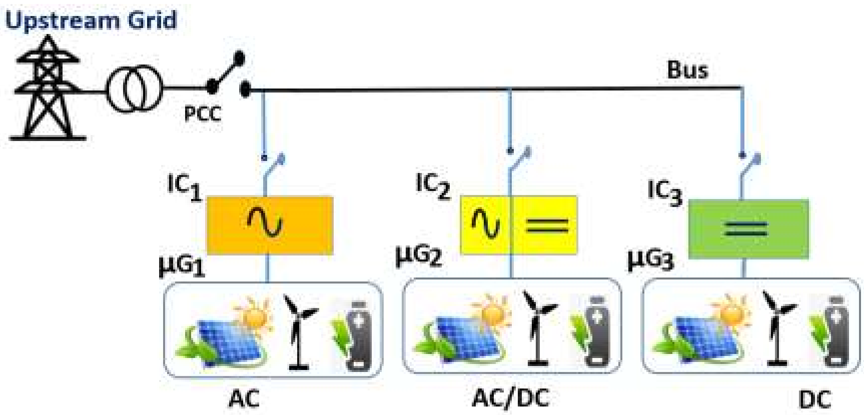

Fig. 2.9 Schematic layout of the multi-microgrid (*Source: Author*)

In-depth analysis and discussion of the communication between coupled microgrids and distribution system operators were presented by [51, 52]. The preceding studies presented provide evidence that the coordination of networked microgrids is a large time-scale operation. However, microgrids cannot provide the exact feasible solution for a reliable power system owing to practical constraints. Thus, rapid power exchange during transient stability operation of interconnected microgrids can be suggested. Resilient infrastructure is necessary to maintain the dynamic stability of MMGs, although this concept has recently been a challenge.

The most important distinguishing feature of MMGs is the rapid power-sharing capabilities between the interconnected distributed generators. However, a standalone microgrid can also be attained in tandem through voltage or frequency control in a centralized or decentralized manner [53, 54]. More recent attention focused on the extension of a single microgrid to MMGs to avert standalone failure and reduce communication overhead [55, 56]. A resilient MMG is also a current trend of research.

2.2.1. Resilience-based ADS planning approaches

Before the occurrence of unfavorable events, such as natural disasters and man-made attacks, some planning actions must be implemented in accordance with weather scenarios to prepare for and minimize the consequences of forthcoming catastrophes [57]. The step includes hardening, resource allocation, coordination, reconfiguration, restoration, and repair crew planning schemes for disastrous hazards and responses. Pre-planning strategy in ADS is significantly beneficial in minimizing the adverse effects of catastrophes [58, 59], enhancing the effectiveness of network recovery, reducing the restoration cost, and improving the resilience of ADS. The summary of ADS planning methods is presented in Table 2.3.

A. Distribution system hardening

Hardening measures refer to physically improving electric infrastructure to minimize its vulnerability to interruptions. Among all the steps, hardening DS is one of the supreme effective plans to decrease the susceptibility of PS [60]. Hardening DS is generally implemented through undergrounding or strengthening the structure materials, such as poles, substations, and distribution lines. However, the hardening is expensive. Therefore, numerous studies have been conducted to make cost-effective hardening decisions. Meanwhile, Ref. [61] proposes the Benders–decomposition (BD) model with the worst-case interdiction study, which provides the hardening decision. The defender–attacker–defender (DAD) technique is introduced in [62] and used to withstand the critical infrastructure against man-made attacks, which shows that the DS component is susceptible to the attack until and unless hardened or protected. The modeling of the optimal and hardening-based MMG structures of DSs with reference to N–k events is explained in [63], where the BD method is used. The objective is to reduce the hardening cost of DSs. In [64], the reconfiguration planning and DER islanding mode are demonstrated through a tri-level DAD model. Through the DAD model, cost-effective hardening decisions with respect to the majority of dreadful attacks are presented. Thereafter, the DSO, in addition to considering the uncertainties of renewable energies like wind [65, 66], solar [67], etc., will execute all desirable remedial schedules to recover the DS after the attack happens. Zhang et al., demonstrates the defense strategies of hardening against typhoon disasters [68]. Overall, the preceding studies have revealed that hardening planning must be undertaken to minimize the power system damage.

B. Resilience-based coordination of MGs

Coordination is one of the significant components of the DS planning stage. The main objective of this type of planning is to organize or manage the system through the improvement of control units (i.e., centralized or decentralized), improved fault detection, energy scheduling, power reserve, and interconnected MGs. A wide range of studies has described coordination planning as follows. A single and double bus partition-based DC MG is studied in [69], where authors mainly focus on components (for instance, during the drop-outs due to solar/wind sources) survivability through controlling the range of loads. In addition, energy exchange cost is considered as the objective function for minimization through a neighborhood optimization algorithm, while this resilience enhancement scheme shows the self-sustainability of DSs. In [70, 71], a distinct test network is studied through centralized and decentralized MMG structure considering flexibility, reliability, and resiliency. The purpose of the current study is to reduce the overall cost of DSs using a decentralized algorithm with a proper energy management strategy. A dynamic MG structure has been proposed in [72], which examines the self-healing strategy during unfavorable events considering DERs and random load change. One of the main concerns of the dynamic MGs is reliability maximization. Therefore, the power disturbance can be minimized even during and after the fault. Active multi-loop control with the design principle of MG has also been established to show the critical area of DSs, like optimal fault isolation, energy balance, and power quality improvement [73]. An appropriate energy management scheduling of DSs can reduce costs and improve resiliency through dual-mode the property, such as stand-alone and grid-connected mode; this concept has been examined and tested through an analytical model presented in [74]. Recent trends in DS planning have led to the proliferation of MG formation to withstand disruptive events and immediate restoration of facilities regarding critical load restoration [75]. The power reserve is one of the most intense requirements during disastrous events to manage power failure. In [76], a mixed-integer linear programming (MILP) method is employed to maintain the power balance in DSs. Thus, the coordination planning scheme particularly involves an energy management strategy during extreme events.

C. Vulnerability measures

The term vulnerability is related to instability or risk. System vulnerability can be defined as a system's inability to cope with a disturbing situation, restrict the impact, and restore and stabilize after the event [77]. Vulnerability depends on weather conditions, which often differ from one region to another, and the most critical events are identified as wind storms, lightning, and ice storm [78]. Moreover, the vulnerability analysis of PS using reliability and the hazard-based scheme is introduced on account of high voltage levels [79]. The consequence of extreme wind events in the DS is investigated with reliability indicators in [80].

In [81], different system conditions are analyzed, apart from weather-related conditions, and measured in the reliability indices. A comparative analysis has been performed considering the risk studies from different states using quantitative reliability indexes. The key purpose of [81] is to provide an optimal allocation of manpower and system components in ADS, which could be preferred for DS planning as preparedness and security measures based on weather forecasts. A sequential attack scenario-based study is proposed to identify the vulnerable nodes and point out the priority of removal for the robust system design, reduce the complexity of the network, and minimize power outages [82]. In [83], the DAD model is employed to improve grid survivability with the objective of minimal load shedding. Column–constraint generation-based algorithm is applied to provide the optimal solution for the protection planning of ADSs, which significantly enhances system resilience against terrorist attacks. In [84], a bi-level mathematical formulation is developed to identify the vulnerable components, where multiple attacks are applied with less computation time used, and consequently, the results show improved reliability and resiliency response.

D. Resource allocation

During and after a catastrophic event, DS resources are generally restricted and difficult to supply because of the affected transportation link. Hence, the functioning of the system recovery action relies on available resources with good quality and surplus quantity [85]. Thus, pre-event resource allocation significantly affects the pro-activeness of system recovery and is a crucial phase in disaster promptness in DS. Several types of resource allocation are reviewed in [86], where three optimization paradigms are likewise discussed (e.g., tactical method and short- and long-term strategic frameworks). The framework in [86] can support the power system components to detect and dispatch mobile units and effectively recover from power outages. In [87], the triangulation model is applied to find the key issues influencing resource accessibility in post-event reconfiguration states. Moreover, various factors, such as rules, policy, regulations, and transfer, have been deliberated, which immensely influence the practicability and exertion of resource allocation. A combined simulation optimization method is explained in [88], which schedules an energy restoration network. Thereafter, the simulation-based model is introduced to assist emergency loads during high-disruptive events. This model also enables the disaster response-based system to maximize operational capacity [89]. Furthermore, a planning procedure using a proactive network decision enabling tool considering the unit commitment problem has been demonstrated to reduce the overall cost [90]. This solution can facilitate the reduction of the outage time, minimize the service interruption cost, and maximize the critical load supply in response to disasters or man-made attacks. Additionally, demand response units can perform a significant role in such situations, which have attracted less attention in this regard [91-94].

E. Restoration planning

Restoration planning is a crucial phase of a resilient power system. This phase is enacted when disaster hits the network (i.e., post-disruption stage), and a major blackout occurs, thereby resulting in damage to the distribution network. Therefore, immediate restorative actions should be planned by using resource allocation in ADS. The allocated resources are used to restore emergency loads not supplied in the DS promptly. However, a part of load restoration is served directly through allocated uninterrupted power supply facilities by DGs, MGs, and charging stations for recovery [95]. The critical issue of DS restoration has been investigated in numerous studies, particularly on identifying the restoration order of loads after a system blackout [37, 96, 97]. In [88], a power restoration planning scheme is pioneered through an integrated simulation approach, which aims to reduce the workforce cost and minimize customer interruption time. Workforce planning is related to the “right” repair crews in the “right” moment and “right” location to achieve the organizational goals [98].

A slow coherency theory is developed in [99] to minimize the power outage by the use of black-start capabilities of island operation to reduce transient oscillation. A black-start restoration model is presented in [100]. In [101], a novel key area in the restoration framework is defined through mixed-integer programming (MIP) to minimize load curtailment and maximize the functional capacity. Recent studies have examined the restoration planning methods in the form of transportable storage units with MG scheduling, specifically to respond to eventualities, reduce the interruption cost, and maximize the reliability of DSs [102].

F. Reconfiguration planning

In ADS, expansion planning extensively focuses on the efficiency, reliability, and financial sustainability of power transfer to prosumers [103-105]. However, such a focus has predominantly been on the claim of disastrous events. Hence, reconfiguration planning related to resilience in response to natural disasters and man-made attacks has been considered an emerging research trend. Besides, the enhancement of resilience against disasters has become a key economic factor in reducing damage to power systems, reducing recovery costs and providing reliable power supply to the end-users, which is crucial for distribution planning. Several approaches are used to reconfigure DS in terms of new installation of power system components, such as energy storage units, on-site DG units, smart transformers, fault protection devices, and integration of renewable energies [106]. MMG formation is also part of the reconfiguration phase. In [107], an energy storage-based grid reconfiguration of ADS is proposed, with voltage magnitude deviance as an objective function through the BD model. Moreover, Ref. [107] concludes that infrastructure deployment and grid reinforcement should be developed for optimal operation. In [108], a two-phase reconfiguration planning framework is established through MMG formation to achieve a resilient structure. Moreover, the research mentioned above has shown that resilience quantification can benefit planning engineers to validate control actions, relate various reconfiguration techniques, and improve effective control actions to evade blackout in response to extreme weather conditions. A probabilistic framework for ADSs to achieve a resilience structure based on on-site generation premises, such as solar and wind generation, is demonstrated in [109]. Its objective is to enhance grid survivability against unfavorable events and accelerate the restoration period.

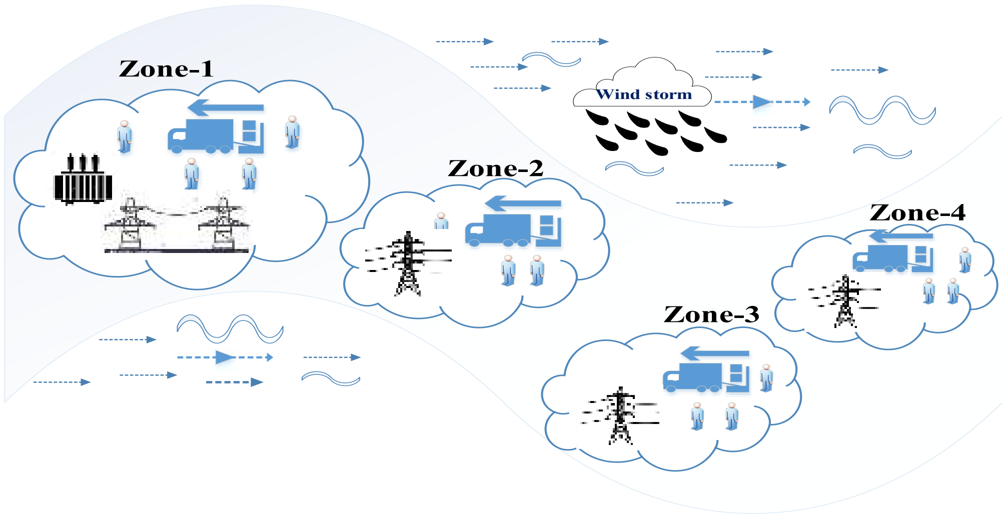

Fig. 2.10. Repair crew allocation (*Source: Author*)

G. Repair crew planning

Repair crew planning in ADS can enhance system reliability during and after disastrous events. Various factors are considered in crew planning, such as immediate crew actions, decreasing failure rates, and specific protective measures [110]. For the planning stage, the deployment of the repair crew needs particular modeling of the maintenance practice in ADSs. For maintenance endeavors, DS is divided into various regions or control zones, with each allocated to a repair crew [111], as shown in Fig. 2.10.

The repair crew resources include individuals, tools, spare parts, and trucks, which are important for the restoration of ADS. After an event, the crew starts the repair process in the order of maintenance received from control centers or distribution operators, and it can be done either manually (customer call) or automatically identifying the system failures.

Therefore, the repair process in each zone is a queuing process. Hence, the input is the sequence of element faults, which cause power disruptions that should be addressed by the crew. The output result is power restoration. This process depends on the quantitative and qualitative terms of the logistical resources from a system performance perspective. Such logistical resources are restricted and must be sensibly coordinated to follow the step of element failures to attain reasonable outage times. Traditionally, the repair process of ADS is not modeled. However, several studies have modeled the repair process with various procedures. In [112], a queuing theory-based repair model and stochastic point method are established to reduce outage time and maximize reliability. A synthetic model to optimally dispatch the crew in ADS is investigated in [113]. Short- and long-term tactical models have been demonstrated to give the optimal placement of crew during catastrophes [86].

Table 2.3: Resilience-based planning methods of ADSs

Area of study	**Contribution**	**Techniques/ Model**	**Objective function**	**Year**	**Ref**
Vulnerability measure	Addressing the plan on hardening measures and improving grid security in relation to the identification of vulnerable components through the IEEE reliability test system.	Interdiction algorithm	Cost minimization	2004	[84]
	Optimal solution with a sensible time toward the enhancement of grid survivability during unfavorable events.	DAD model	Grid disruption minimization	2014	[83]
	Building a sequential attacking model and its resilience analysis in response to various attack scenarios.	Sequential attack procedure	Power outage minimization	2014	[82]
	Demonstrating a vulnerability analysis to help operators make decisions, which enhances distribution reliability, security, and flexibility.	Considering various weather scenarios	Reliability maximization	2012	[81]
Hardening planning	Modeling of optimal hardening structure and MMG formation scheme of DSs on account of N–k events.	BD method with the iterative relaxation process	Hardening cost minimization	2017	[63]
	Reporting the enhancement scheme of DSs through reconfiguration planning and DER islanding with a tri-level DAD model.	DAD model	Load curtailment minimization	2018	[64]
	Introduceing a novel defense strategy for distribution system against typhoons.	Decision dependent theory	Resilience improvement	2022	[68]
Coordination planning	Introducing single and double bus partitioning-based DC microgrids to enhance the unit's survivability, self-sustainability, and control.	Neighborhood optimization	Energy exchange cost minimization	2014	[69]
	Contrasting a case study of centralized and de-centralized control-based MMGs to show adaptability, suitability, reliability, and resiliency of the grid.	Decentralized algorithm	Overall cost minimization	2015	[70]

	Outlining a brief discussion of a centralized and decentralized model of two neighboring MGs and measuring the stability of MMGs.	Centralized and decentralized approach	Load curtailment minimization	2015	[71]
	Proposing a dynamic microgrid structure to enable the self-adequacy during extreme events considering stochastic load and DERs.	MC method	Reliability maximization	2016	[72]
	Demonstrating the design principle and active multi-loop control of MG for good fault isolation, energy balance, and power quality management.	Analytical models	Power extract (peak power) maximization	2016	[73]
	Energy management scheduling of grid-connected and stand-alone modes, which points out the operation costs and resiliency.	Load shedding and ramp down techniques	Energy exchange cost minimization	2018	[74]
	Aiming to manage the power shortage during the events with the incorporation of power reserve facilities.	MILP		2019	[76]
	Formulating the MG formation plan to quickly restore the critical load against extreme disruptions.	MILP	Load pickup maximization	2018	[75]
Reconfiguration planning	Developed a two-phase reconfiguration planning model for MMGs to achieve a cost-effective and resilient structure.	Pre-location theory	Load pickup maximization	2016	[108]
	Establishing a probabilistic model of DS considering the integration of solar and wind energies to improve survivability and reduce the restoration period.	Moment-based design	Total cost minimization	2018	[109]
	Proposing grid reconfiguration planning of ADS by means of energy storage devices and aiming to reduce the cost and voltage deviation.	BD model	Total cost and energy storage install cost minimization	2018	[107]
Restoration planning	Introducing workforce planning for outage management to minimize the cost and consumer interruption time.	Integer programming	Workforces cost minimization	2012	[88]
	Defining a key area of the load restoration model to maximize the functional capacity of critical infrastructures.	MIP	Load curtailment minimization	2014	[101]
	Distinguishing the overall system cost and reliability between transportable storage systems and fixed storage units in MMGs.	MILP	Overall cost minimization	2019	[102]
	Addressing the minimization strategy of blackout using black-start capabilities in response to eventualities.	Cone programming	Restoration path optimization	2022	[100]

Repair crew planning	Demonstrating short- and long-term tactical models for the optimal dispatch of repair crew into the location before and during events.	Goal programming	Damage cost minimization	1998	[86]
	The optimal designing of crew actions regarding failed units and the aims for reliability measures.	Queuing theory	Reliability maximization	2008	[112]
	Introducing a synthetic model for optimal dispatch of crews in ADS for service restoration.	Synthetic model	Unserved energy minimization	2019	[113]
Resource allocation planning	Introducing a simulation-based model to support critical loads in optimal DSs during catastrophic events.	Disaster-response network-enabled environment	Operational capacity maximization	2014	[89]
	Defining a proactive decision-enabling tool for the efficient restoration of DSs to minimize the overall cost incorporating with unit commitment challenge.	Stochastic linear-programming	Restoration cost minimization	2015	[90]

2.2.2. Resilience-based ADS operation

During unfavorable events, such as natural disasters or man-made attacks, operational activities should withstand and optimally coordinate system operation with minimal vulnerability and the lowest restoration time. To obtain an improved understanding of the operational activities against catastrophes, various methods have been described, such as optimal operation, coordinated operation, restoration, vulnerability measures, operational awareness, and software-defined actions. Moreover, in the case of operational activities during the events in the DS, these actions can extensively improve the resilience characteristics, which further re-establish the power system for the prosumers. The operational activities of the ADS operation considering the resilience are discussed as follows, and the summary of this section is presented in Table 2.4.

A. Optimal operation

The optimal operation of DS significantly impacts the overall cost, which is in the form of operational cost minimization during the events. Optimal operation preferably manages the load demand and generation balance to meet the continuity of the supply for the prosumers and particularly for emergency loads. Moreover, this operation includes unit commitment, generation scheduling, optimal dispatch, and optimization algorithms. A large and growing body of research has investigated this area. In [114], a scheduling model of MG to ascertain self-sustainability during the events through a feasible islanding method is demonstrated. In recent years, a proactive scheduling and stochastic programming-based optimal power flow (OPF) model has been established through a load curtailment minimization approach during events [115, 116].

Moreover, this model considers renewable sources to highlight socio-economic benefits. In [117], a proactive operation scheme has been developed through a Markov process to minimize the probability of failure against extreme events. In this regard, MG-based studies have been presented, which mainly focus on operation cost minimization through a hierarchical control scheme [118], graph theory [119], linear programming (LP) [120], and robust optimization [121] in response to various catastrophes. The optimal operation method by means of a voltage and frequency minimization model is also demonstrated to improve system stability and resiliency [122].

B. Coordinated operation

In the case of operational actions, the coordination activity plays a key role in managing the power system operation through centralized/decentralized control practice, grid-connected/stand-alone mode [123], single-/multi-agent approach, and the integration of renewable energy sources (RESs) [124]. In [49, 125-127], the decentralized control-based operation is established to minimize the operation cost of interconnected MGs. The same primitive cost minimization technique is applied using mixed-integer bi-level programming, considering the MMG structure [128], a consensus algorithm for self-healing operation [129], MIP for proper coordination between MGs [130], and robust optimization for islanding feasibility and proactive operation in [131, 132], respectively. To ensure the power supply to the critical or emergency loads, a priority load maximization model is introduced in [133-136] through an agent and linear programming methods by means of MG and MMGs. To extend the service continuity to emergency and non-emergency loads, load curtailment minimization techniques are pioneered through a Markov–Monte Carlo (MMC) model [137], and a fuzzy logic control technique [138] considering the MMG formation. Furthermore, a recovery model is established to minimize the power outage duration in response to highly disruptive events [139]. A probability model is formulated in [140] through the Naïve Bayes technique for the maximization of forecast probability by means of MG energy management strategy. In spite of all these methods, the coordinated operation is also concerned with power system stability, which is discussed in [141], and demonstrates the multi-agent-based DSs through active energy-sharing units. A reliability assessment concerning various outage management schemes is generalized in [142]. Note that these operational activities can enhance resilience characteristics through proper coordination.

C. Restoration operation

The resilient operation, particularly during the restoration period, is essential to minimize power outages during highly disruptive events. Several extensive cross-sectional studies of therapeutic actions have been conducted for rapid and optimal system recovery. In the restoration phase, the maximization of a list of priority loads is a major concern, which is formulated through different algorithms, such as mixed-integer non-linear programming (MINP) [143-145] and the linearized distribution flow model [146, 147]. The list of priority loads considers the optimal switching operation and MMG formation against natural disasters. Furthermore, the list of priority loads is used to stabilize dynamic performances with different fault scenarios during restoration [148].

An optimal dispatching model considering the storage units and DERs is introduced in [149], which mainly focuses on the maximization of restored energy through MINP. A defensive islanding procedure has been adopted to restore DS and immediately minimize load shedding [142]. In [150], crew member deployment with on-site generation unit dispatching schemes for service restoration is presented. To estimate the accessibility of MG for recovery considering RESs, dispatchable DERs are reported in [151]. The energy cost should be minimized during the restoration phase. Therefore, Ref. [152] established an optimization model to maximize the energy capacity in response to extreme weather conditions.

D. Vulnerability measure

Power system failure means that an electric infrastructure sustained considerable damage, which directly impacts the socio-economic life of people. Thus, the vulnerability of the component and system must be analyzed to cope with any eventuality. Various studies have investigated the vulnerability analysis to detect the infirmity of DSs, and then the improvement of survivability and resilience are also presented [153-155]. In [156], the graph-theory-based model is used to measure the vulnerability of interdependent electric infrastructure. A machine learning algorithm is applied to predict the power outage and components' state for vulnerability measure evaluation in [153-155]. An outline of fundamental methods to assess the vulnerability in the power system is recently discussed in [157].

E. Operational awareness

Given the practical constraints of modern DSs, DSOs have to cope with various challenges to sustain reliable supply. Hence, establishing and updating a necessary situation awareness (SA) is a strategic factor in maintaining this reliability, although it is a complex process because of the various factors that regulate its formation in the energy control center. Therefore, operational awareness is definitely needed to support human operators. In [158], the Markov model is used to minimize the probability of man-made errors by enabling executive decisions in response to power outages. Similarly, advanced visualization procedures are applied in [159] to minimize the probability of failure using relevant alertness of power outages. The main concern of [158, 159] is to maintain system reliability through operational awareness activities.

F. Security and protection

The continually increasing installation of protection devices in DSs has prompted particular phase tripping orders at the distribution phase [160]. Accurate phase preference denotes the capability of protective relays to detect faulty phase(s). Conversely, many control algorithms have been developed to improve the efficiency, reliability, and resiliency of the system. Therefore, the components and the entire system should be protected during the operation to significantly reduce outage duration and enhance DS resilience in response to catastrophes. In [161-163], a software-based network is discussed to maximize reliability and reduce the communication cost after considering the software enabling technology to reach a better and more secure control of DSs' operation. Moreover, an inverter interfaced-based algorithm is introduced and integrated with DERs to minimize fault current during the operation [164].

Furthermore, security against intentional attacks and redundancy have been programmed in [165] through the geometric progression rule to minimize the probability of destroying DSs. Moreover, a decision model also plays a vital role in the security and protection of DSs during the operation. Only Refs. [166, 167] have endeavored to study the protection by employing a decision model to minimize the investment and operation costs against disruptive events. On the other hand, the digital revolution in the energy sector has resulted in many advanced technologies and an exponential increase in transactive energy mechanisms, where the internet of things (IoT) and Blockchain concept are pivotal, which could help improve the distribution system resilience. A few recent studies have demonstrated the role of the internet and Blockchain in resiliency, which can be seen in [168-171].

Table 2.4: Operational study of ADSs

Areas of study	Contributions	Techniques /Model	Objective function	Year	Ref
Optimal operation of DSs	Introducing a scheduling model of hybrid MGs to ensure survivability during events by means of feasible islanding	–	Minimization of overall cost during events	2017	[114]
	Formulating the OPF during catastrophic events to reduce the adverse effects of flooding on DSs.	Proactive scheduling	Load curtailment minimization	2018	[115]
	Presenting proactive operation schemes of DSs to minimize load failure because of highly disruptive events.	Markov process and MINP	Probability of failure	2017	[117]
	Modelling and analysis of DC-MG to provide improved energy management capability and economic operation of DSs compared with AC-MG.	Hierarchical control scheme	Operation cost minimization	2014	[118]
	Identifying the socioeconomic benefits of MMGs through a developed mathematical model incorporated with RESs and electric vechicle (EVs) in DSs	Stochastic programming	Minimization of load curtailment	2016	[116]
	Utilizing graph theory-based methods for the optimal operation of MGs considering microturbine and energy storage systems (ESSs) and addressing the energy management strategy to operate DS in normal and self-healing modes	Graph theory	Minimization of operation cost	2017	[119]
	Modelling and analysis of MG considering electric springs to enhance the stability of DSs against intermittent renewable sources	–	Minimization of changes in voltage and frequency	2018	[122]
	Developing an optimal energy management framework to minimize operational cost in the presence of ESSs	LP	Minimization of operation cost	2018	[120]
	Describing the imperative formulation of MG for optimal programming in response to islanding modes against extreme events	Robust optimization	Minimization of operation	2019	[121]
Coordinated operation	Decentralizing controlled operation of MMGs through coordinated actions	Decentralized bi-level technique	Minimization of operation cost	2016	[125]
	Reporting distributive MMGs to realize resilient autonomous power DSs using the independent operation of MGs.	Agent algorithm	Maximization of priority load	2011	[134]

	Investigating the optimal and self-healing operation of MMGs via energy management techniques in a decentralized manner	-	Minimization of operation cost	2016	[49]
	Establishing a robust distributed regulation scheme to manage power flow considering ststic synchronous compensator (STATCOM) and ESSs	Distributed control scheme	Stability enhancement	2016	[127]
	Modelling of decentralized DSs, which comprise a non-linear assumption, capacity extension, N-1 security, and long-term operation	Decompositio n algorithm	Minimization of operational and installation costs	2017	[126]
	Pioneering a three-phase MG recovery model after disruptive events to balance the DSs	Linear relaxation	Minimization of outage duration	2018	[139]
	Comprehensive architecture of MMGs for reliability assessment with various outage management tactics	Monte carlo (MC) model		2018	[142]
	Designing a paradigm for examining the resilience indices of the power grid integration with MMGs in the wake of extreme events	Multi model (MM) MC	Minimization of load curtailment	2017	[137]
	Designing disruption as an event of intentional attacks on MMGs by taking the interconnection of electrical structures and natural gas into account	Mixed-integer bi-level linear programing	Minimization of operation cost	2015	[128]
	Focusing on the energy management strategy of MG on the basis of renewable energy prediction and battery state of charge (SOC).	naive bayes (NB) model	Maximization of forecast probability	2016	[140]
	Proposing a dynamic formation of MGs to maintain power supply of emergency loads after an inevitable accident	MILP	Maximization of priority load	2016	[129]
	Proposing a generalized framework of outage management practices in MMGs for appropriate coordination among MGs through model predictive control and DSO	MILP	Minimization of the overall cost	2016	[130]
	Developing a metamorphic framework of MMGs for optimal operation and autonomous strategy to coordinated self-healing operation through an established cybernetic system and a control algorithm	Consensus algorithm	Minimization of operation cost	2016	[129]
	Introducing a fuzzy logic control (FLC)-based model of MG considering ESS units, which follows the management commands for proper scheduling and operation in normal and non-normal conditions.	FLC	Minimization of load curtailment	2017	[138]
	Highlighting the benefits of MMGs for load restoration and coordination mechanism in consideration of intermittent loads and DERs	MILP	Maximization of priority load	2017	[135]
	Establishing an effective management strategy for MGs to withstand intense windstorms to protect vulnerable components	LP model	Maximization of priority load	2018	[136]
	Pioneering regulated multi-agent-based DSs to stabilize frequency and voltage deviation through proportional active energy sharing units	Stochastic programing	Minimization of changes in voltage and frequency	2018	[141]
	Offering deterministic techniques in response to fragility curves to achieve the proactive operation of DSs	Robust optimization	Minimization of operation cost	2019	[132]

	Presenting a scheduling model of MGs that took the islanding feasibility and survivability of emergency loads into account	Robust optimization	Minimization of operation cost	2019	[131]
Restoration operation of DSs	Proposing a comprehensive mathematical model for load restoration by means of optimal switching operation in ADS	MINP	Maximization of priority load	2016	[143]
	Providing a detailed mathematical formulation of MMGs to restore critical loads during natural disasters	Linearized distribution low	Maximization of priority load	2017	[146]
	Modelling of a resilient MG operation taking account of a master–slave-based DER application.	MINP	Maximization of priority load	2017	[144]
	Establishing dynamic MGs to provided uninterrupted supply to critical loads immediately after events hit the network	MINP	Maximization of priority load	2016	[145]
	Formulating an optimal dispatchable model considering DERs, and control switches.	MINP	Maximization of restored energy	2018	[149]
	Providing an integrated solution on the basis of a decision-making tool to improve situational alertness and survivability	Generalized linear model	Maximization of priority load	2017	[147]
	Developing an enhancement strategy of DSs through defensive islanding to address severe wind contingencies	Defensive islanding-algorithm	Minimization of load shedding	2016	[172]
	Exemplifying the repair crew and restoration operations of DSs after unfavorable events through multiple-vehicle and on-site generation to reduce recovery times	Randomized adaptive vehicle decomposition	Minimization of total outage	2012	[150]
	Describing a service restoration scheme incorporated with RESs, dispatchable DERs and ESSs and introduced a continuous operating time to estimate the accessibility of MG with limited source	MM	Minimization of load curtailment	2016	[151]
	Measuring the stability and dynamic performances of MGs in the process of restoration with regard to different fault states	LP model	Maximization of priority load	2018	[148]
	Pioneering an optimization model of MGs to maximize energy capacity during an emergency in response to disruptive events	MM	Minimization of energy cost	2018	[152]
Vulnerability measure	Discussing two models, namely, network and functional, as interfaces to various DSs and performance evaluations correspondingly for measuring the vulnerability of bulk interdependent electrical infrastructures	Graph theory	-	2010	[156]
	Presenting a predictive model of DSs to determine component states for vulnerability measures through the machine learning algorithm to address extreme incidents	Machine learning method	Outage prediction	2017	[153]
	Proposing an outage prediction paradigm through machine learning technique to identify vulnerable components against forthcoming hurricanes	Machine learning method	Outage prediction	2017	[154]
	Performing a vulnerability comparison analysis of two models to measure the effectiveness of DS operation under man-made attacks	Topological and betweenness basis models	Measuring power grid vulnerability with different	2014	[155]

			attack intensity		
Operational awareness study	Providing a brief description of SA, man-made errors, operational decision enabling, and the MM for proactive SA in response to power system outages	MM	Minimizing the probability of man-made errors	2013	[158]
	Presenting a brief synopsis of relevant alertness of power outages and its main sources to provide operators with an efficient provision in maintaining system reliability	Advanced visualization procedures	Minimization of probability of failure data	2013	[159]
Security and protection	Maximizing software-based programming to enable the networks to identify and respond to failures and obstruction during the run period of MG operations.	Software-based network	Maximization of reliability	2017	[161]
	Presenting a software-enabled architecture for MG operations to utilize global perceptibility, programmability and enhanced controllability for security implications	Software-based network	Maximization of reliability	2016	[162]
	Presenting fast-powered reinforcement models between MMGs through a software-enabled algorithm to improve efficiency, reliability, flexibility, and resiliency	Software-based network	Minimization of communication cost	2018	[163]
	Formulating a new control algorithm for a fault protection	Inverter interface DER model	Minimization of fault current	2018	[164]
	Providing optimal solutions for resource allocation in view of redundancy and security against intentional threats	Geometric progression rule	Minimization of destruction probability	2015	[165]
	Designing a two-level stochastic model for DSs in response to hardening decisions against catastrophic consequences	Progressive hedging optimization	Minimization investment cost	2016	[173]
	Formulating a resiliency-cut index to ensure survivability of emergency loads after events hit the network	Robust optimization	Minimization of operation cost	2018	[167]
	Demonstrating the digital revolution in the energy sector to improve the security and resilience.	column-and-constraint generation	Security enhancement	2021	[169]
	Presenting a blockchain-enabled energy system considering the distribution system resilience	-	Security and resilience improvement	2021, 2022	[168, 170]

2.2.3. Resilience-based ADS planning and operation

The distribution system planning-operation is an increasingly complex and information-intensive procedure. Thus, seeking perceptibility across the continuum of power supply has expanded over intermittencies, updated technology expenses, price signals, response sensitivities, and socioeconomic impact. However, deployment and allocation of novel breakthrough technologies suffer from many issues that differ by means of technology and critical function in the power delivery system. The electricity power supply has been continuously and highly reliable for the last few decades because of enhanced expansion planning and the uninterrupted power supply of DSs across the globe. In the event of natural disasters or other unfavorable occurrences, the operation of power systems may fail to achieve desired reliability. Hence, planning-operation schemes should consider several possible adverse events that demand a more resilient electric infrastructure.

During these events, the planning-operation phases play crucial roles in disaster concerns, which require simultaneous resource and crew allocation, restoration, and coordinated planning-operation schemes to make some decisions about the optimal operation of the power system. It also facilitates the reduction of restoration time after low-power system damages. The study of these schemes is described as follows, and the summary of this section is presented in Table 2.5.

A. Coordination

In the resilience planning-operation procedures of DSs, coordination, which is also called energy management, plays a vital role. Changes experienced in energy management methods of DSs over the past decade have become unprecedented, thereby enhancing the resiliency of power systems. Various models have been employed to coordinate some components of the power systems in the planning-operational phases. In [174], a scenario decomposition-based algorithm is introduced to minimize power outage considering transportable on-site generation facilities in pursuance to installation and proper allocation before and during events. Moreover, the preparedness index is a major concern in the study of resilience against eventualities in enhancing the performance of DSs and minimizing load curtailment. Given these objectives, Ref. [175] established a linear approximation model to maximize the preparedness index through MMG in response to hurricane events. To maximize load pickup, Ref. [144] proposed a master-slave operation of DERs and crew routing. By contrast, Ref. [176] suggested a DER dispatch. However, MMG formation has been regarded recently as one of the key survival factors to resiliency, which is discussed in [173].

B. Restoration

In the restoration phase, planning can be implemented by properly allocating storage units and crew members, identifying vulnerable components and mobile generation units, and using islanding mode [177-179]. These methods can restore the system immediately. Conversely, the same units are used in the operational phase during events to recover the system from low distribution system damage with minimal recovery time. Numerous studies have intended to explain the restoration planning-operation of DSs in view of resilience. In [180], a sectionalized MMG for the optimal operation of DSs is proposed to minimize costs during outages. The importance of sectionalized MMG is that it can cope with highly disruptive events and is capable of isolating the section individually when DSO predicts the consequences. To further discuss this concept, Ref. [181] proposed a deterministic and stochastic model to spring the DS back to normal operation after events. In [155], a network partitioning method is introduced to maintain the continuity of electricity supply in the context of planning-operational movements. To maximize restored energy during events, a mathematical formulation has been developed through MINP, as presented in [182].

C. Reconfiguration

Reconfiguration is an increasingly important area in DS resilience because reconfiguration planning and rapid operation should be conducted during events to immediately address the outage. The majority of the current studies on reconfiguration particularly focus on minimizing the overall and life cycle costs. To enable the optimal operation of DSs during events, thermal stability and reliability are major factors that should be assessed, in which DSs should be designed and operated accordingly [183]. Apart from the aspects mentioned above, enhanced voltage profile, low power loss, and load adjusting should also be considered, as described in [184]; it introduced a power electronic-based module that re-establishes performance using a soft-open point framework. Note that the geometric progression rule is applied to minimize the destruction probability of DSs and address issues in redundancy and security against intentional threats [165].

D. Resilience quantification

To measure the performance of the DSs, resilience quantification plays a crucial role in decision-making in the cases of load switching, DER allocation, and crew position. Accordingly, Ref. [185, 186] concentrates on the distinctive metrics of resilience in the perspective of system design, extreme weather, and repair crew, which aims at maximization of sensitivity. In [187], a quantitative model for resilience estimation and preventive measures is developed in the face of windstorms. This model mainly aims to minimize the probability of failure. Furthermore, a multi-criteria-based decision-making model is pioneered through the graph and pre-location theory to reduce switching operations and maximize load operation [108]. One of the most significant discussions in the study on resilience quantification is that various quantifications can introduce a new resilience index, which can further improve reliability and resiliency characteristics.

Table 2.5: Planning-operational method of ADSs

Area of study	Contributions	Techniques /Model	Objective function	Year	Ref.
Coordination	Establishing an optimal planning strategy for an emergency load restoration using transportable on-site generation facilities in accordance with pre-positioning and practical constraints to reduce outage during emergency operations	Scenario decomposition algorithm	Minimization of power outage	2018	[174]
	Presenting a multi-objective oriented architecture to enhance the effective preparedness of MMGs and cope with forthcoming hurricanes	Linear approximation model	Maximization of the preparedness index	2019	[175]
	Proposing a novel load restoration scheme of the MG to improve the reliability and resiliency of DSs through master-slave DERs during natural disasters	Mixed integer second order cone method	Maximization of critical load pickup	2017	[144]
	Proposing a co-optimization model for crew routing, system reconfiguration, and DER dispatch to enrich the DSs from outage under disruptive events	MILP	Maximization of load pickup	2018	[176]
	Enhancing strategy of MMG formation for survival in extreme events in terms of critical service restoration.	MILP	Minimization of MG scale	2018	[173]
Restoration	Proposing the extensive structure of a distribution system via two modes of operation in relation to sectionalized MMGs for optimal restoration of an outage	Rolling-horizon algorithm	Minimization of operation cost and maximization of profit	2015	[180]
	Designing a deterministic and stochastic model of DSs on account of component failure during events and spring back to normal operation	Probabilistic and deterministic approach	Minimization of overall cost	2018	[181]
	Using network partition-based techniques for survival after a power disruption in terms of planning-operational movements	Network partition method	Minimization of restoration time	2018	[188]
	Developing a successive service restoration model of DSs and MGs using DERs as well as formulating a mathematical power flow model	MINP	Maximization of total restored energy	2018	[182]
	Introducing mobile resource based ancillary services of distribution system for resilience enhancement.	Mixed-integer quadratic programming	Resilience improvement	2022	[177]

Reconfiguration	Addressing the thermal stability and reliability measure of wind-based plants with FACTS functionality in MGs to provide optimal operation and better assessment of DSs.	Coffin–manson model	Minimization of overall cost	2017	[183]
	Developing a network reconfiguration planning scheme with power electronic modules to enhance voltage profile, lessen power loss and adjust load during operation	Soft-open-points paradigm	Optimization of the life cycle cost	2016	[184]
	Providing optimal solutions for resource allocation in view of redundancy and security against intentional threats	Geometric progression rule	Minimization of destruction probability	2015	[165]
Resilience quantification	Proposing new resilience metrics with corresponding estimation approach considering the system design, catastrophe, and repair crews	Dynamic bayesian networks	Maximization of sensitivity	2018	[185]
	Introducing a quantitative model to estimate DS resilience and approach to preventive measures against windstorms.	Degradation model	Minimization of failure of probability	2019	[187]
	Introducing resilience quantification techniques against extreme events	Monte Carlo	Resilience improvement	2022	[186]

2.3. Challenges and key issues

Over the past few decades, power system engineers have been successfully established as reliable power systems. However, presently, attention is increasing towards the resilient power system, which is a significant challenge to the energy sector as natural disasters and cyber-attacks are increasing. The followings are the main challenging areas which are needed to be addressed.

- The integration of DERs, automatic reclosures, and ancillary devices are increasing the complexity of the network, which is affecting the recovery process.
- After catastrophic events, improper crew scheduling can significantly affects the system recovery.
- Reconfiguration operations during the events with their inconvenient connectivity status can lead to total or partial damage to the system.
- Inaccurate disaster prediction can be a cause of immense economic loss and take more time to restore.

The abovementioned problems are to be addressed with the following **research questions**.

- What are the major attributes with their resilience evaluation indices to define the resiliency of an active distribution system?

- How can maneuvering the crews take place to minimize the consequence of events?
- How should resilience evaluation indices be involved in active distribution systems performance and be incorporated within a resilience evaluation framework as a means to have a quantitative assessment?
- What are the decision-making tools to give the quantifiable formation on account of resiliency?
- What is the required information to solve the resiliency problem under extreme operating conditions?

The following key issues are identified as the research gaps which could be addressed in this study:

- The resilience in ADS with all these four factors (withstand, respond, adapt, and prevent) has never been investigated in power system resilience.
- The resilience evaluation indices have not been established yet to show the resiliency of the system.
- The enhancement of ADS resilience through MMG is still to be explored, considering extreme events.
- Several energy market studies have been performed to show the cost-effectiveness of the system; however, a resiliency study is yet to be developed to secure the transactive energy platform.

Based on the literature review, a research gap has been identified, and with that aim, a novel framework for resilience quantification and enhancement method of ADS is proposed, discussed as follows.

2.4. Research methodology

This section presents the research methodology in detail. It starts with a basic concept of the research and literature review on account of resilience. Thereafter, the effect of events on MMGs will be investigated through the simulation results. System development and system reconfiguration will likewise be performed. Lastly, the proposed system will be validated using Hardware-in-Loop (e.g., OPAL-RT), and the results will be compared with the existing system. Finally, the flow of the research methodology is presented.

In the current era of green energy, solar power (photovoltaic (PV)) and wind power-based renewable power generation systems are widely used worldwide because of their broad range of applications. With green energy, the resiliency of the system will be enhanced by the formation of MG and MMG. The current study proposes a novel technique in which the interconnection of a green microgrid, called MMG, is developed. Further, a WRAP model is established to measure the resiliency of MMG. Finally, the proposed study will run through the real-time simulator, i.e., OPAL-RT, for the validation of simulation results. The detailed framework and proposed concepts are discussed as follows.

2.4.1. WRAP model

In the restructured power systems, power producers are migrating from bulk units to small-scale ones (e.g., microgrids and multi-microgrids). This type of structure helps to provide excellent energy management capabilities, improves the reliability of response to disruptive events, and enhances resilience characteristics.

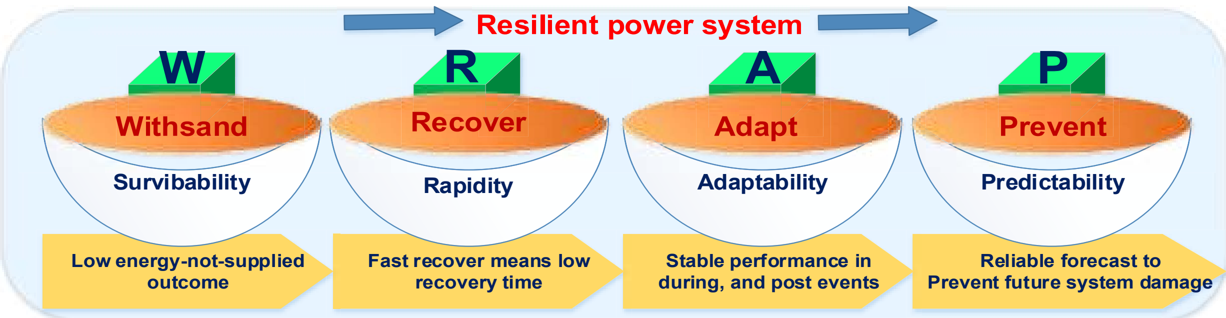

Fig. 2.11 WRAP flow diagram (*Source: Author*)

As an illustration, microgrids are used to enhance the automated control of distribution systems under blackouts [48] and to meet the demands of external loads through the least switch operations. The self-healing strategy of networked microgrids with an economic dispatch plan was presented in [49], in which the surplus energies in each unit were accumulated to satisfy the power demands. Aside from energy restoration, microgrids can also contribute to international frequency regulation through supplementary control loops [56]. Refs. [52, 55] presented an in-depth analysis and discussion of the communication between coupled microgrids and distribution system operators. Increasing attention has been focused on the extension of a single microgrid to interconnected microgrids to avert standalone failure and reduce communication overhead [109, 114]. In addition, a resilient power system is a current research trend. The WRAP elements need to be considered to enhance the severity of resilience, and a robust electrical infrastructure must be constructed to solve the issue of resilient characteristics. WRAP can lessen the vulnerability of power systems while maintaining their stability. The concept of the WRAP flow diagram is depicted in Fig. 2.11. The proposed WRAP model is a novel approach for the quantification of resilience, where each factor, such as withstand, recover, adapt, and prevent, has a significant meaning. These four attributes have never been investigated in a single framework as means of resilience measure.

A. Withstand

Withstand is concerned with the system's preparedness, reinforcement, and robustness against extreme events that are not considered in the traditional system design. Different risks, events, and hazards are estimated in terms of reliability. In addition, training and mandated maintenance programs must be conducted to improve the survivability and sustainability of the power system. Survivability indicates that power systems should withstand disruptive natural events with minimal damage, whereas sustainability refers to the continuity of energy supply to the end-users during and after the occurrence of extreme events [172, 189]. Moreover, skilled engineers should offer a series of intelligence exchange programs regarding technological advancement and new protective measure schemes to improve resiliency. Some research studies have consistently shown that these factors emphasize the improvement of power system resiliency.

To measure the withstand element, the system’s redundancy, prevention, and key maintenance operation should be assessed. Moreover, to measure the significance of this element, “energy not supplied” [190] can be taken as a resilience evaluation index, which indicates the volume of energy to customers lost due to faults or failures on the network. The power system should be designed to cope with disruptive natural events and/or manmade attacks, which consequently minimizes the resilience evaluation index (e.g., energy not supplied) and enhances reliability and resiliency.

B. Recover

Power system recovery has been attracting increasing attention because of the significant dependence of all social and communication networks on electricity, so a delay in electric power system recovery may lead to immense economic losses. Therefore, the recovery stage is concerned with the rapid restoration of a system. Various mechanisms, such as reserve scheduling, black start, crew member deployment, on-site generation units, and island operations, are used to recover the power system [113]. During the black start, the grid can restore the operation without relying on superficial networks to recover from total or partial load curtailment. More crew member deployment is a good solution to decrease the restoration time and is also important for vulnerable components [99]. In the past decades, on-site generation facilities have significantly increased to restore the distribution network and provide load supply during emergencies.

In this phase, two attributes are considered: rapidity and vulnerability. Rapidity refers to the speed of recovery, while vulnerability signifies the weak units of the system. Moreover, the resilience evaluation indices of this phase are time and cost of recovery; the effectiveness of the system is verified when the system is restored within a short time at a low cost.

C. Adapt

To adapt the distribution system to recognize the stabilized performance during and after an event, one of the most significant schemes, i.e., reconfiguration planning, must be taken into account. Besides, numerous factors should be considered in customizing the power system network, including restructuring, policy change, smooth functionality units, emerging hazard assessments, and periodic reviews [101]. These factors can reconcile the system against unfavorable events. Today, power system reconfiguration is important due to the increasing number of disasters and man-made attacks. Small-scale power systems are now preferred over large-scale ones because microgrids, which is an example of the former, can reduce the total outage of the mainstream grid by means of self-healing mode. In addition, the enhancement of resilience indices has become a key economic factor that can reduce power system damage and recovery cost and provide a reliable power supply to the end-users, which is crucial for distribution planning [191]. Several components can be installed to reconfigure distribution systems, including energy storage units, on-site distributed generation units, smart transformers, and fault protection devices. Furthermore, the integration of renewable energy sources and multiple microgrid formations are also parts of the reconfiguration phase.

Interdependency and resourcefulness are taken as the attributes of the adapt phase. However, the most distinct element of this phase is the controller (centralized/decentralized), involving a minimization technique that can smoothly tune and mitigate the transients of the power system [192]. In addition, the frequency and voltage deviations can also play a crucial role during the events, and they have to be stabilized by controlling the renewable sources and flexible alternating current devices. More importantly, this phase signifies the stability of the system during the events and eventually enhances its resilience.

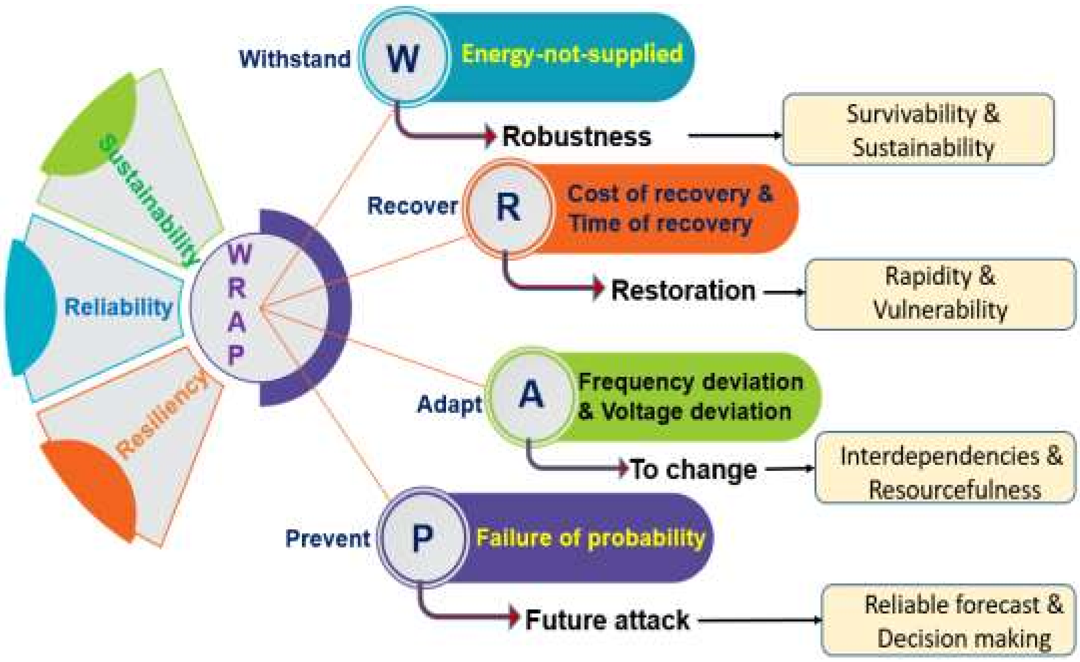

Fig. 2.12 WRAP outline

D. Prevent

To prevent power system disruption, several measures, such as reliable forecasting, review of previous power outages, interventions, utilization of good quality components, and preparations for future attack scenarios, are considered [158]. In addition, many different factors, such as identifying vulnerable units, arranging protective units, decision-making tools, and risk reduction methods, should be considered to precisely predict approaching events and prevent power system damages caused by disasters [153].

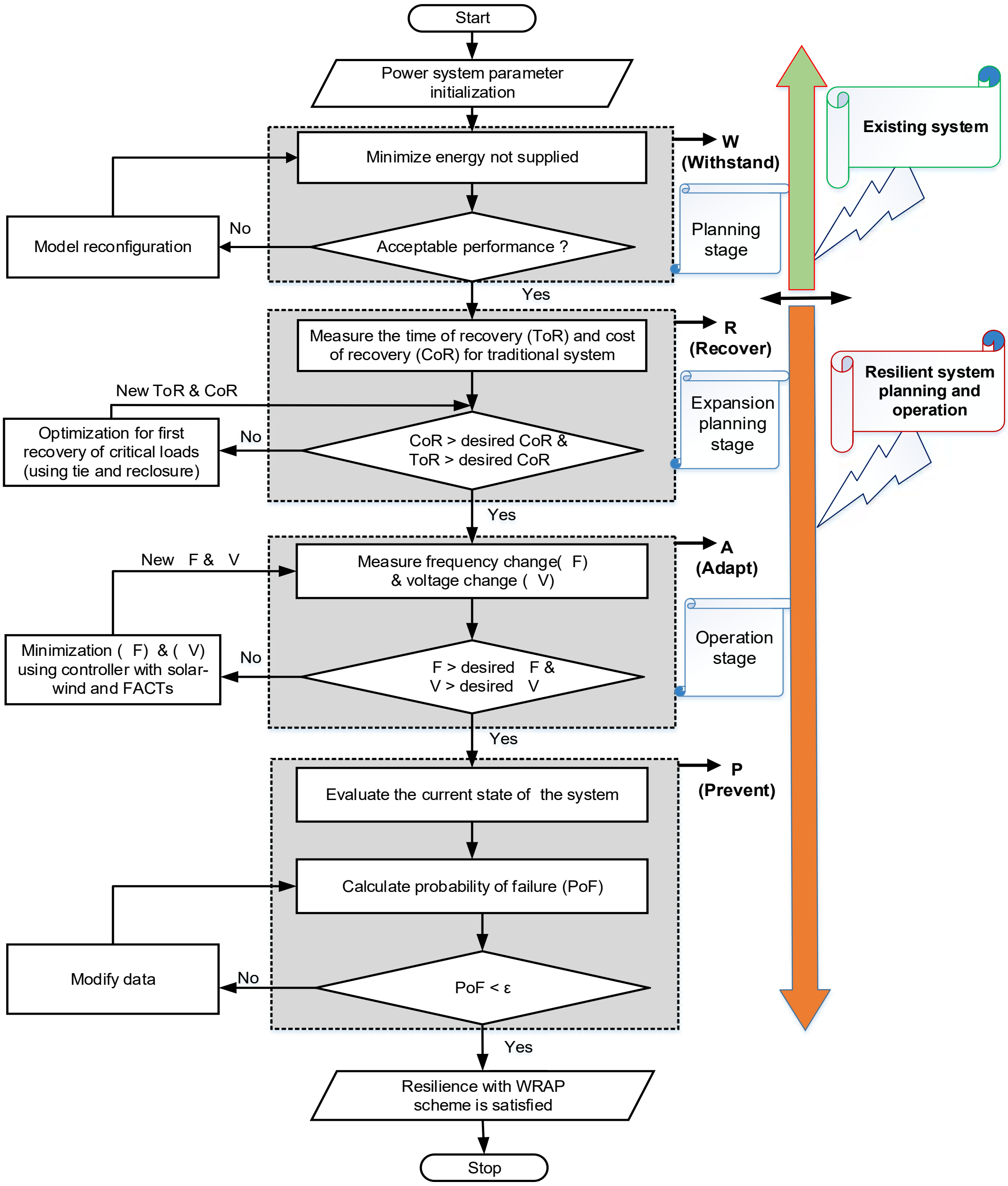

Fig. 2.13 WRAP flowchart

A detailed disaster study has greatly influenced the assessment of attributes [193]. Considering the previous data, the upcoming catastrophe can be predicted, and the system should be prepared according to these scenarios. Thus, crew member deployment, on-site generation facilities, disconnection of less vulnerable components, and easy access to emergency loads must be planned properly. Several studies that investigate the pre-event strategies against disaster in the power system context have been carried out [85, 113, 194].

Based on the discussions mentioned earlier, the response of the power systems to inevitable attacks in terms of resilience is a great concern. Therefore, power systems should be prepared for all kinds of unfavorable events through anticipation and decision models [195]. Hence, WRAP must be considered to form a resilient MMG. These four elements can enhance MMG resilience, lessen vulnerability, and maintain power system stability. The detailed concepts of WRAP, along with the resilience evaluation index and major attributes, are shown in Fig. 2.12.

In this framework, the four elements are used to measure the robustness, rapidity, and probability of response against disruptive events. Moreover, the pre, during, and post-event planning and operational activities of power systems in the WRAP framework have been speculated, as shown in Fig. 2.13.

The parameters in the initial attempt include the number of buses, loads, generations, and zones. To start with withstand phase of the WRAP scheme, the minimization technique can be used to minimize the energy that is not supplied as a resilience evaluation index. This approach signifies the robustness of the system after the events. If its performance is poor, then the reconfiguration of the network is needed to improve the resilience characteristics.

Furthermore, the time and cost of recovery can be measured to show the optimal operation of the power system. Meanwhile, a multi-objective optimization method, which can automatically tune the gains of the controller and DER allocation parameters, can be adapted to improve the optimal operation and stabilize the system throughout the events.

Thereafter, a prediction model can be used to predict upcoming events to prepare for and respond to catastrophes. Notwithstanding, this framework aims to provide a conceptual framework to measure the resiliency of the power system. In addition, the use of the WRAP procedure in power systems minimizes the damages and restoration costs and improves its withstanding capabilities.

2.5. Summary

This chapter thoroughly reviews the resilience research of ADS in various perspectives. The literature clearly states that the ADS resilience study is essential in terms of planning and operational activities. ADS resilience is an emerging area of research for the short and long-term improvements of electric infrastructures. Building a resilient system can greatly reduce power outage costs, help to boost the global economy, and minimize life threats that can enhance customer satisfaction.

Moreover, this review study presents the various resilience approach of ADS, which are discussed as follows.

- First, various weather-related scenarios, hardening overviews, taxonomies, and plans are summarized.
- Second, planning, operational, and planning-operational studies of resiliency are reviewed.
- Third, the major contributions, models used, and objectives of the literature are also presented in tabular form.

With this review study, knowledge from the following perspectives may be obtained.

- How can special planning schemes be implemented to enhance the resilience of distribution systems?
- What are the actions required to obtain the optimal operation of resiliency?
- What planning-operation frameworks and measures are required for the immediate recovery and response during/after an event?

On the other hand, the research questions, challenges, and gaps are searched out from the literature. Further, to deal with the challenges and fill out the gaps, a novel resilience framework (such as WRAP) is presented, and the significance of its attributes is also discussed thoroughly.

References

[1] M. Panteli and P. Mancarella, "The grid: Stronger, bigger, smarter?: Presenting a conceptual framework of power system resilience," *IEEE Power and Energy Magazine,* vol. 13, no. 3, pp. 58-66, 2015.

[2] L. Che, M. Khodayar, and M. Shahidehpour, "Only connect: Microgrids for distribution system restoration," *IEEE power and energy magazine,* vol. 12, no. 1, pp. 70-81, 2013.

[3] Z. Bie, Y. Lin, G. Li, and F. Li, "Battling the extreme: A study on the power system resilience," *Proceedings of the IEEE,* vol. 105, no. 7, pp. 1253-1266, 2017.

[4] D. K. Mishra, M. J. Ghadi, L. Li, and J. Zhang, "Proposing a Framework for Resilient Active Distribution Systems using Withstand, Respond, Adapt, and Prevent Element," in *2019 29th Australasian Universities Power Engineering Conference (AUPEC)*, 2019, pp. 1-6: IEEE.

[5] X. Wu, Z. Wang, T. Ding, X. Wang, Z. Li, and F. Li, "Microgrid planning considering the resilience against contingencies," *IET Generation, Transmission & Distribution,* vol. 13, no. 16, pp. 3534-3548, 2019.

[6] Z. Li and M. Shahidehpour, "Role of microgrids in enhancing power system resilience," in *2017 IEEE Power & Energy Society General Meeting*, 2017, pp. 1-5: IEEE.

[7] F. Yang, X. Feng, and Z. Li, "Advanced microgrid energy management system for future sustainable and resilient power grid," *IEEE Transactions on Industry Applications,* vol. 55, no. 6, pp. 7251-7260, 2019.

[8] Å. Holmgren, "Vulnerability analysis of electric power delivery networks," Citeseer, 2004.

[9] J. Beyza and J. M. Yusta, "Characterising the security of power system topologies through a combined assessment of reliability, robustness, and resilience," *Energy Strategy Reviews,* vol. 43, p. 100944, 2022.

[10] M. Panteli, P. Mancarella, D. N. Trakas, E. Kyriakides, and N. D. Hatziargyriou, "Metrics and quantification of operational and infrastructure resilience in power systems," *IEEE Transactions on Power Systems,* vol. 32, no. 6, pp. 4732-4742, 2017.

[11] W. Kröger, "Achieving Resilience of Large-Scale Engineered Infrastructure Systems," in *Resilient Structures and Infrastructure*: Springer, 2019, pp. 289-313.

[12] Y. Liu, X. Li, and L. Xiao, "Service Oriented Resilience Strategy for Cloud Data Center," in *2018 IEEE International Conference on Software Quality, Reliability and Security Companion (QRS-C)*, 2018, pp. 269-274: IEEE.

[13] A. Hussain, V.-H. Bui, and H.-M. Kim, "Microgrids as a resilience resource and strategies used by microgrids for enhancing resilience," *Applied energy,* vol. 240, pp. 56-72, 2019.

[14] M. Panteli and P. Mancarella, "The grid: Stronger bigger smarter?: Presenting a conceptual framework of power system resilience," *IEEE Power Energy Mag,* vol. 13, no. 3, pp. 58-66, 2015.

[15] A. Kwasinski, "Quantitative model and metrics of electrical grids' resilience evaluated at a power distribution level," *Energies,* vol. 9, no. 2, p. 93, 2016.

[16] M. Panteli, C. Pickering, S. Wilkinson, R. Dawson, and P. Mancarella, "Power system resilience to extreme weather: fragility modeling, probabilistic impact assessment, and adaptation measures," *IEEE Transactions on Power Systems,* vol. 32, no. 5, pp. 3747-3757, 2016.

[17] R. Rocchetta, E. Zio, and E. Patelli, "A power-flow emulator approach for resilience assessment of repairable power grids subject to weather-induced failures and data deficiency," *Applied energy,* vol. 210, pp. 339-350, 2018.

[18] J.-P. Watson *et al.*, "Conceptual framework for developing resilience metrics for the electricity oil and gas sectors in the United States," *Sandia National Laboratories, Albuquerque, NM (United States), Tech. Rep,* 2014.
[19] S. Charoenkit and S. Kumar, "Environmental sustainability assessment tools for low carbon and climate resilient low income housing settlements," *Renewable and sustainable energy reviews,* vol. 38, pp. 509-525, 2014.
[20] S. Mousavizadeh, M.-R. Haghifam, and M.-H. Shariatkhah, "A linear two-stage method for resiliency analysis in distribution systems considering renewable energy and demand response resources," *Applied energy,* vol. 211, pp. 443-460, 2018.
[21] T. Münzberg, M. Wiens, and F. Schultmann, "A spatial-temporal vulnerability assessment to support the building of community resilience against power outage impacts," *Technological Forecasting and Social Change,* vol. 121, pp. 99-118, 2017.
[22] J. Mitra and S. J. Ranade, "Power System Hardening through Autonomous, Customer-driven Microgrids," in *2007 IEEE Power Engineering Society General Meeting*, 2007, pp. 1-4.
[23] P. Hoffman, W. Bryan, M. Farber-DeAnda, M. Cleaver, C. Lewandowski, and K. Young, "Hardening and Resiliency, US Energy Industry Response to Recent Hurricane Seasons," *Office of Electricity Delivery and Energy Reliability, US Department of Energy, OE/ISER Final Report,* 2010.
[24] A. Kenward and U. Raja, "Blackout: Extreme weather climate change and power outages," *Climate central,* vol. 10, 2014.
[25] M. Rollins, "The hardening of utilitiy lines-implications for utility pole design and use," ed: Technical report, North American Wood Pole Council, 2007.
[26] N. Abi-Samra and W. Henry, "Actions Before... and After a Flood," *IEEE Power and Energy Magazine,* vol. 9, no. 2, pp. 52-58, 2011.
[27] R. J. Campbell, "Weather-related power outages and electric system resiliency," 2012: Congressional Research Service, Library of Congress Washington, DC.
[28] N. Romero, L. K. Nozick, I. Dobson, N. Xu, and D. A. Jones, "Seismic retrofit for electric power systems," *Earthquake Spectra,* vol. 31, no. 2, pp. 1157-1176, 2015.
[29] D. T. Ton and W. P. Wang, "A More Resilient Grid: The U.S. Department of Energy Joins with Stakeholders in an R&D Plan," *IEEE Power and Energy Magazine,* vol. 13, no. 3, pp. 26-34, 2015.
[30] M. Panteli and P. Mancarella, "Influence of extreme weather and climate change on the resilience of power systems: Impacts and possible mitigation strategies," *Electric Power Systems Research,* Review vol. 127, pp. 259-270, 2015.
[31] R. Arghandeh, A. Von Meier, L. Mehrmanesh, and L. Mili, "On the definition of cyber-physical resilience in power systems," *Renewable and Sustainable Energy Reviews,* vol. 58, pp. 1060-1069, 2016.
[32] S. C. Madathil *et al.*, "Resilient off-grid microgrids: Capacity planning and N-1 security," *IEEE Transactions on Smart Grid,* vol. 9, no. 6, pp. 6511-6521, 2017.
[33] J. Wang, W. Zuo, L. Rhode-Barbarigos, X. Lu, J. Wang, and Y. Lin, "Literature review on modeling and simulation of energy infrastructures from a resilience perspective," *Reliability Engineering & System Safety,* 2018.
[34] A. Gholami, T. Shekari, M. H. Amirioun, F. Aminifar, M. H. Amini, and A. Sargolzaei, "Toward a consensus on the definition and taxonomy of power system resilience," *IEEE Access,* vol. 6, pp. 32035-32053, 2018.
[35] G. Davis, A. F. Snyder, and J. Mader, "The future of distribution system resiliency," in *2014 Clemson University Power Systems Conference*, 2014, pp. 1-8: IEEE.
[36] M. Panteli, D. N. Trakas, P. Mancarella, and N. D. Hatziargyriou, "Power systems resilience assessment: Hardening and smart operational enhancement strategies,"

Proceedings of the IEEE, vol. 105, no. 7, pp. 1202-1213, 2017.
[37] N. Xin, L. Chen, L. Ma, and Y. Si, "A Rolling Horizon Optimization Framework for Resilient Restoration of Active Distribution Systems," *Energies,* vol. 15, no. 9, p. 3096, 2022.
[38] C. Abbey and F. Pilo, "Active Distribution Networks: General features present status of implementation and operation practices," *Electra,* no. 246, pp. 1286-1146, 2009.
[39] C. Abbey *et al.*, *Planning and optimization methods for active distribution systems*. CIGRE, 2014.
[40] R. Hidalgo, C. Abbey, and G. Joós, "A review of active distribution networks enabling technologies," in *IEEE PES General Meeting*, 2010, pp. 1-9: IEEE.
[41] C. D'Adamo, S. Jupe, and C. Abbey, "Global survey on planning and operation of active distribution networks-Update of CIGRE C6. 11 working group activities," in *CIRED 2009-20th International Conference and Exhibition on Electricity Distribution-Part 1*, 2009, pp. 1-4: IET.
[42] T. L. Vandoorn, B. Meersman, L. Degroote, B. Renders, and L. Vandevelde, "A control strategy for islanded microgrids with dc-link voltage control," *IEEE Transactions on Power Delivery,* vol. 26, no. 2, pp. 703-713, 2011.
[43] M. Singh, V. Khadkikar, A. Chandra, and R. K. Varma, "Grid interconnection of renewable energy sources at the distribution level with power-quality improvement features," *IEEE transactions on power delivery,* vol. 26, no. 1, pp. 307-315, 2010.
[44] F. Shahnia, R. P. Chandrasena, S. Rajakaruna, and A. Ghosh, "Autonomous operation of multiple interconnected microgrids with self-healing capability," in *2013 IEEE Power & Energy Society General Meeting*, 2013, pp. 1-5: IEEE.
[45] R. H. Lasseter, "Smart distribution: Coupled microgrids," *Proceedings of the IEEE,* vol. 99, no. 6, pp. 1074-1082, 2011.
[46] M. J. Hossain, M. A. Mahmud, F. Milano, S. Bacha, and A. Hably, "Design of robust distributed control for interconnected microgrids," *IEEE Transactions on Smart Grid,* vol. 7, no. 6, pp. 2724-2735, 2015.
[47] X. Fang, Q. Yang, J. Wang, and W. Yan, "Coordinated dispatch in multiple cooperative autonomous islanded microgrids," *Applied energy,* vol. 162, pp. 40-48, 2016.
[48] J. Li, X.-Y. Ma, C.-C. Liu, and K. P. Schneider, "Distribution system restoration with microgrids using spanning tree search," *IEEE Transactions on Power Systems,* vol. 29, no. 6, pp. 3021-3029, 2014.
[49] Z. Wang, B. Chen, J. Wang, and C. Chen, "Networked microgrids for self-healing power systems," *IEEE Transactions on smart grid,* vol. 7, no. 1, pp. 310-319, 2015.
[50] C. Yuen, A. Oudalov, and A. Timbus, "The provision of frequency control reserves from multiple microgrids," *IEEE Transactions on Industrial Electronics,* vol. 58, no. 1, pp. 173-183, 2010.
[51] T. Lv and Q. Ai, "Interactive energy management of networked microgrids-based active distribution system considering large-scale integration of renewable energy resources," *Applied Energy,* vol. 163, pp. 408-422, 2016.
[52] P. Kou, D. Liang, and L. Gao, "Distributed EMPC of multiple microgrids for coordinated stochastic energy management," *Applied energy,* vol. 185, pp. 939-952, 2017.
[53] J. He, Y. Li, B. Liang, and C. Wang, "Inverse Power Factor Droop Control for Decentralized Power Sharing in Series-Connected-Microconverters-Based Islanding Microgrids," *IEEE Transactions on Industrial Electronics,* vol. 64, no. 9, pp. 7444-7454, 2017.
[54] C. Wang, Y. Li, K. Peng, B. Hong, Z. Wu, and C. Sun, "Coordinated optimal design of inverter controllers in a micro-grid with multiple distributed generation units," *IEEE*

Transactions on Power Systems, vol. 28, no. 3, pp. 2679-2687, 2013.
[55] V. N. Coelho, M. W. Cohen, I. M. Coelho, N. Liu, and F. G. Guimarães, "Multi-agent systems applied for energy systems integration: State-of-the-art applications and trends in microgrids," *Applied energy,* vol. 187, pp. 820-832, 2017.
[56] F. Dörfler, J. W. Simpson-Porco, and F. Bullo, "Breaking the hierarchy: Distributed control and economic optimality in microgrids," *IEEE Transactions on Control of Network Systems,* vol. 3, no. 3, pp. 241-253, 2015.
[57] A. M. Caunhye, X. Nie, and S. Pokharel, "Optimization models in emergency logistics: A literature review," *Socio-economic planning sciences,* vol. 46, no. 1, pp. 4-13, 2012.
[58] F. He and J. Zhuang, "Balancing pre-disaster preparedness and post-disaster relief," *European Journal of Operational Research,* vol. 252, no. 1, pp. 246-256, 2016.
[59] D. Faramarzi, H. Rastegar, G. H. Riahy, and H. Doagou-Mojarrad, "A risk-averse multiyear framework for resilience improvement planning of active distribution networks against hurricanes," *IET Renewable Power Generation,* 2022.
[60] A. M. Salman, Y. Li, and M. G. Stewart, "Evaluating system reliability and targeted hardening strategies of power distribution systems subjected to hurricanes," *Reliability Engineering & System Safety,* vol. 144, pp. 319-333, 2015.
[61] J. Salmeron, K. Wood, and R. Baldick, "Worst-case interdiction analysis of large-scale electric power grids," *IEEE Transactions on power systems,* vol. 24, no. 1, pp. 96-104, 2009.
[62] G. Brown, M. Carlyle, J. Salmerón, and K. Wood, "Defending critical infrastructure," *Interfaces,* vol. 36, no. 6, pp. 530-544, 2006.
[63] X. Wang, Z. Li, M. Shahidehpour, and C. Jiang, "Robust line hardening strategies for improving the resilience of distribution systems with variable renewable resources," *IEEE Transactions on Sustainable Energy,* 2017.
[64] Y. Lin and Z. Bie, "Tri-level optimal hardening plan for a resilient distribution system considering reconfiguration and DG islanding," *Applied Energy,* vol. 210, pp. 1266-1279, 2018.
[65] M. J. Ghadi, S. H. Gilani, H. Afrakhte, and A. Baghramian, "A novel heuristic method for wind farm power prediction: A case study," *International Journal of Electrical Power & Energy Systems,* vol. 63, pp. 962-970, 2014.
[66] A. Sharifian, M. J. Ghadi, S. Ghavidel, L. Li, and J. Zhang, "A new method based on Type-2 fuzzy neural network for accurate wind power forecasting under uncertain data," *Renewable energy,* vol. 120, pp. 220-230, 2018.
[67] M. J. Ghadi, L. Li, J. Zhan, L. Chen, Q. Huang, and C. Li, "A Review on the Development of Concentrated Solar Power and its Integration in Coal-Fired Power Plants," in *2019 IEEE Innovative Smart Grid Technologies-Asia (ISGT Asia)*, 2019, pp. 1106-1111: IEEE.
[68] W. Zhang *et al.*, "Transmission Defense Hardening Against Typhoon Disasters Under Decision-Dependent Uncertainty," *IEEE Transactions on Power Systems,* 2022.
[69] M. Simonov, "Dynamic Partitioning of DC Microgrid in Resilient Clusters Using Event-Driven Approach," *IEEE Transactions on Smart Grid,* vol. 5, no. 5, pp. 2618-2625, 2014.
[70] M. He and M. Giesselmann, "Reliability-constrained self-organization and energy management towards a resilient microgrid cluster," in *2015 IEEE Power & Energy Society Innovative Smart Grid Technologies Conference (ISGT)*, 2015, pp. 1-5.
[71] E. Pashajavid, F. Shahnia, and A. Ghosh, "Development of a self-healing strategy to enhance the overloading resilience of islanded microgrids," *IEEE Transactions on Smart Grid,* vol. 8, no. 2, pp. 868-880, 2015.
[72] M. E. Nassar and M. M. A. Salama, "Adaptive Self-Adequate Microgrids Using

Dynamic Boundaries," *IEEE Transactions on Smart Grid,* vol. 7, no. 1, pp. 105-113, 2016.
[73] D. Tan, D. Baxter, S. Foroozan, and S. Crane, "A First Resilient DC-Dominated Microgrid for Mission-Critical Space Applications," *IEEE Journal of Emerging and Selected Topics in Power Electronics,* vol. 4, no. 4, pp. 1147-1157, 2016.
[74] A. Hussain, V.-H. Bui, and H.-M. Kim, "A resilient and privacy-preserving energy management strategy for networked microgrids," *IEEE Transactions on Smart Grid,* vol. 9, no. 3, pp. 2127-2139, 2016.
[75] K. S. A. Sedzro, A. J. Lamadrid, and L. F. Zuluaga, "Allocation of resources using a microgrid formation approach for resilient electric grids," *IEEE Transactions on Power Systems,* vol. 33, no. 3, pp. 2633-2643, 2017.
[76] H. Lee *et al.*, "An energy management system with optimum reserve power procurement function for microgrid resilience improvement," *IEEE Access,* vol. 7, pp. 42577-42585, 2019.
[77] G. L. Doorman, K. Uhlen, G. Kjolle, and E. S. Huse, "Vulnerability analysis of the Nordic power system," *IEEE Transactions on Power Systems,* vol. 21, no. 1, pp. 402-410, 2006.
[78] Y. Zhou, A. Pahwa, and S.-S. Yang, "Modeling weather-related failures of overhead distribution lines," *IEEE Transactions on power systems,* vol. 21, no. 4, pp. 1683-1690, 2006.
[79] X. Yu and C. Singh, "A practical approach for integrated power system vulnerability analysis with protection failures," *IEEE Transactions on Power Systems,* vol. 19, no. 4, pp. 1811-1820, 2004.
[80] D. A. Reed, "Electric utility distribution analysis for extreme winds," *Journal of Wind Engineering and Industrial Aerodynamics,* vol. 96, no. 1, pp. 123-140, 2008.
[81] C. J. Wallnerstrom and P. Hilber, "Vulnerability Analysis of Power Distribution Systems for Cost-Effective Resource Allocation," *IEEE Transactions on Power Systems,* vol. 27, no. 1, pp. 224-232, 2012.
[82] Y. Zhu, J. Yan, Y. Tang, Y. L. Sun, and H. He, "Resilience analysis of power grids under the sequential attack," *IEEE Transactions on Information Forensics and Security,* vol. 9, no. 12, pp. 2340-2354, 2014.
[83] W. Yuan, L. Zhao, and B. Zeng, "Optimal power grid protection through a defender–attacker–defender model," *Reliability Engineering & System Safety,* vol. 121, pp. 83-89, 2014.
[84] J. Salmeron, K. Wood, and R. Baldick, "Analysis of electric grid security under terrorist threat," *IEEE Transactions on power systems,* vol. 19, no. 2, pp. 905-912, 2004.
[85] C. Zapata, S. Silva, H. Gonzalez, O. Burbano, and J. Hernandez, "Modeling the repair process of a power distribution system," in *2008 IEEE/PES Transmission and Distribution Conference and Exposition: Latin America*, 2008, pp. 1-7: IEEE.
[86] Y. Ming-Jong and K. J. Min, "Repair-unit location models for power failures," *IEEE Transactions on Engineering Management,* vol. 45, no. 1, pp. 57-65, 1998.
[87] Y. Chang, S. Wilkinson, E. Seville, and R. Potangaroa, "Resourcing for a resilient post-disaster reconstruction environment," *International Journal of Disaster Resilience in the Built Environment,* vol. 1, no. 1, pp. 65-83, 2010.
[88] N. Safaei, D. Banjevic, and A. K. S. Jardine, "Workforce Planning for Power Restoration: An Integrated Simulation-Optimization Approach," *IEEE Transactions on Power Systems,* vol. 27, no. 1, pp. 442-449, 2012.
[89] A. Alsubaie, J. Marti, K. Alutaibi, A. D. Pietro, and A. Tofani, "Resources allocation in disaster response using Ordinal Optimization based approach," in *2014 IEEE Canada International Humanitarian Technology Conference - (IHTC)*, 2014, pp. 1-5.

[90] A. Arab, A. Khodaei, S. K. Khator, K. Ding, V. A. Emesih, and Z. Han, "Stochastic Pre-hurricane Restoration Planning for Electric Power Systems Infrastructure," *IEEE Transactions on Smart Grid,* vol. 6, no. 2, pp. 1046-1054, 2015.

[91] M. H. Imani, K. Yousefpour, M. T. Andani, and M. J. Ghadi, "Effect of Changes in Incentives and Penalties on Interruptible/Curtailable Demand Response Program in Microgrid Operation," in *2019 IEEE Texas Power and Energy Conference (TPEC)*, 2019, pp. 1-6: IEEE.

[92] M. H. Abbasi *et al.*, "Risk-constrained offering strategies for a price-maker demand response aggregator," in *2017 20th International Conference on Electrical Machines and Systems (ICEMS)*, 2017, pp. 1-6: IEEE.

[93] S. Ghavidel, A. Rajabi, M. J. Ghadi, A. Azizivahed, L. Li, and J. Zhang, "Risk-constrained demand response and wind energy systems integration to handle stochastic nature and wind power outage," *IET Energy Systems Integration,* 2019.

[94] A. Rajabi *et al.*, "A pattern recognition methodology for analyzing residential customers load data and targeting demand response applications," *Energy and Buildings,* vol. 203, p. 109455, 2019.

[95] H. Gao, Y. Chen, Y. Xu, and C.-C. Liu, "Resilience-oriented critical load restoration using microgrids in distribution systems," *IEEE Transactions on Smart Grid,* vol. 7, no. 6, pp. 2837-2848, 2016.

[96] R. Pérez-Guerrero, G. T. Heydt, N. J. Jack, B. K. Keel, and A. R. Castelhano, "Optimal restoration of distribution systems using dynamic programming," *IEEE Transactions on Power Delivery,* vol. 23, no. 3, pp. 1589-1596, 2008.

[97] J. Jian *et al.*, "Multi-stage supply restoration of active distribution networks with SOP integration," *Sustainable Energy, Grids and Networks,* vol. 29, p. 100562, 2022.

[98] T. Wegner, "Discrete simulation modelling for corporate manpower planning," *Omega,* vol. 13, no. 3, pp. 201-210, 1985.

[99] J. Q. Tortós and V. Terzija, "Controlled islanding strategy considering power system restoration constraints," in *2012 IEEE Power and Energy Society General Meeting*, 2012, pp. 1-8: IEEE.

[100] T. Ding, Z. Wang, M. Qu, Z. Wang, and M. Shahidehpour, "A Sequential Black-Start Restoration Model for Resilient Active Distribution Networks," *IEEE Transactions on Power Systems,* 2022.

[101] H. Ahmadi, A. Alsubaie, and J. R. Martí, "Distribution system restoration considering critical infrastructures interdependencies," in *2014 IEEE PES General Meeting | Conference & Exposition*, 2014, pp. 1-5.

[102] S. Yao, P. Wang, and T. Zhao, "Transportable energy storage for more resilient distribution systems with multiple microgrids," *IEEE Transactions on Smart Grid,* 2018.

[103] K. Aoki, K. Nara, T. Satoh, M. Kitagawa, and K. Yamanaka, "New approximate optimization method for distribution system planning," *IEEE Transactions on power systems,* vol. 5, no. 1, pp. 126-132, 1990.

[104] P. Carvalho, L. Ferreira, F. Lobo, and L. Barruncho, "Optimal distribution network expansion planning under uncertainty by evolutionary decision convergence," *International Journal of Electrical Power & Energy Systems,* vol. 20, no. 2, pp. 125-129, 1998.

[105] B. Li, Y. Chen, W. Wei, Z. Wang, and S. Mei, "Online Coordination of LNG Tube Trailer Dispatch and Resilience Restoration of Integrated Power-Gas Distribution Systems," *IEEE Transactions on Smart Grid,* vol. 13, no. 3, pp. 1938-1951, 2022.

[106] D. K. Mishra, T. K. Panigrahi, A. Mohanty, and P. K. Ray, "Impact of wind/solar integration on frequency control in two-area power system," in *2018 19th International*

Carpathian Control Conference (ICCC), 2018, pp. 580-584: IEEE.
[107] M. Nick, R. Cherkaoui, and M. Paolone, "Optimal planning of distributed energy storage systems in active distribution networks embedding grid reconfiguration," *IEEE Transactions on Power Systems,* vol. 33, no. 2, pp. 1577-1590, 2017.
[108] S. Chanda and A. K. Srivastava, "Defining and Enabling Resiliency of Electric Distribution Systems With Multiple Microgrids," *IEEE Transactions on Smart Grid,* vol. 7, no. 6, pp. 2859-2868, 2016.
[109] T. Jin, N. Mai, Y. Ding, L. Vo, and R. Dawud, "Planning for Distribution Resilience under Variable Generation: Prevention, Surviving and Recovery," in *2018 IEEE Green Technologies Conference (GreenTech)*, 2018, pp. 49-56.
[110] R. E. Brown, "Electric Power Distribution Reliability, Marcel Decker," *Inc, New York,* 2002.
[111] K. G. Zografos, C. Douligeris, and P. Tsoumpas, "An integrated framework for managing emergency-response logistics: The case of the electric utility companies," *IEEE Transactions on Engineering Management,* vol. 45, no. 2, pp. 115-126, 1998.
[112] C. J. Zapata, S. C. Silva, H. I. Gonzalez, O. L. Burbano, and J. A. Hernandez, "Modeling the repair process of a power distribution system," in *2008 IEEE/PES Transmission and Distribution Conference and Exposition: Latin America*, 2008, pp. 1-7.
[113] B. Chen, Z. Ye, C. Chen, J. Wang, T. Ding, and Z. Bie, "Toward a Synthetic Model for Distribution System Restoration and Crew Dispatch," *IEEE Transactions on Power Systems,* vol. 34, no. 3, pp. 2228-2239, 2018.
[114] A. Hussain, V.-H. Bui, and H.-M. Kim, "Optimal operation of hybrid microgrids for enhancing resiliency considering feasible islanding and survivability," *IET Renewable Power Generation,* vol. 11, no. 6, pp. 846-857, 2017.
[115] M. H. Amirioun, F. Aminifar, and H. Lesani, "Towards Proactive Scheduling of Microgrids Against Extreme Floods," *IEEE Transactions on Smart Grid,* vol. 9, no. 4, pp. 3900-3902, 2018.
[116] A. Gholami, T. Shekari, F. Aminifar, and M. Shahidehpour, "Microgrid Scheduling With Uncertainty: The Quest for Resilience," *IEEE Transactions on Smart Grid,* vol. 7, no. 6, pp. 2849-2858, 2016.
[117] C. Wang, Y. Hou, F. Qiu, S. Lei, and K. Liu, "Resilience Enhancement With Sequentially Proactive Operation Strategies," *IEEE Transactions on Power Systems,* vol. 32, no. 4, pp. 2847-2857, 2017.
[118] L. Che and M. Shahidehpour, "DC Microgrids: Economic Operation and Enhancement of Resilience by Hierarchical Control," *IEEE Transactions on Smart Grid,* vol. 5, no. 5, pp. 2517-2526, 2014.
[119] M. Zadsar, M. R. Haghifam, and S. M. M. Larimi, "Approach for self-healing resilient operation of active distribution network with microgrid," *IET Generation, Transmission & Distribution,* vol. 11, no. 18, pp. 4633-4643, 2017.
[120] M. Tavakoli, F. Shokridehaki, M. F. Akorede, M. Marzband, I. Vechiu, and E. Pouresmaeil, "CVaR-based energy management scheme for optimal resilience and operational cost in commercial building microgrids," *International Journal of Electrical Power & Energy Systems,* vol. 100, pp. 1-9, 2018.
[121] A. Gholami, T. Shekari, and S. Grijalva, "Proactive management of microgrids for resiliency enhancement: An adaptive robust approach," *IEEE Transactions on Sustainable Energy,* 2017.
[122] L. Liang, Y. Hou, D. J. Hill, and S. Y. R. Hui, "Enhancing resilience of microgrids with electric springs," *IEEE Transactions on Smart Grid,* vol. 9, no. 3, pp. 2235-2247, 2016.
[123] A. Mohanty, M. Viswavandya, S. Mohanty, and D. K. Mishra, "Reactive power compensation in a stand-alone wind-diesel-tidal hybrid system by a fuzzy logic based

UPFC," *Procedia Computer Science,* vol. 57, pp. 1281-1288, 2015.
[124] A. Mohanty, M. Viswavandya, D. Mishra, P. Paramita, and S. P. Mohanty, "Intelligent voltage and reactive power management in a standalone PV based microgrid," *Procedia Technology,* vol. 21, pp. 443-451, 2015.
[125] Z. Wang, B. Chen, and J. Wang, "Decentralized energy management system for networked microgrids in grid-connected and islanded modes," *IEEE Transactions on Smart Grid,* vol. 7, no. 2, pp. 1097-1105, 2015.
[126] K. M. Kelly-Pitou, A. Ostroski, B. Contino, B. Grainger, A. Kwasinski, and G. Reed, "Microgrids and resilience: Using a systems approach to achieve climate adaptation and mitigation goals," *The Electricity Journal,* vol. 30, no. 10, pp. 23-31, 2017.
[127] M. J. Hossain, M. A. Mahmud, F. Milano, S. Bacha, and A. Hably, "Design of Robust Distributed Control for Interconnected Microgrids," *IEEE Transactions on Smart Grid,* vol. 7, no. 6, pp. 2724-2735, 2016.
[128] S. D. Manshadi and M. E. Khodayar, "Resilient Operation of Multiple Energy Carrier Microgrids," *IEEE Transactions on Smart Grid,* vol. 6, no. 5, pp. 2283-2292, 2015.
[129] C. Chen, J. Wang, F. Qiu, and D. Zhao, "Resilient Distribution System by Microgrids Formation After Natural Disasters," *IEEE Transactions on Smart Grid,* vol. 7, no. 2, pp. 958-966, 2016.
[130] H. Farzin, M. Fotuhi-Firuzabad, and M. Moeini-Aghtaie, "Enhancing Power System Resilience Through Hierarchical Outage Management in Multi-Microgrids," *IEEE Transactions on Smart Grid,* vol. 7, no. 6, pp. 2869-2879, 2016.
[131] A. Hussain, V.-H. Bui, and H.-M. Kim, "Resilience-oriented optimal operation of networked hybrid microgrids," *IEEE Transactions on Smart Grid,* 2017.
[132] A. Hussain, A. O. Rousis, I. Konstantelos, G. Strbac, J. Jeon, and H.-M. Kim, "Impact of Uncertainties on Resilient Operation of Microgrids: A Data-Driven Approach," *IEEE Access,* vol. 7, pp. 14924-14937, 2019.
[133] Z. Wang, B. Chen, J. Wang, and C. Chen, "Networked Microgrids for Self-Healing Power Systems," *IEEE Transactions on Smart Grid,* vol. 7, no. 1, pp. 310-319, 2016.
[134] C. Colson, M. Nehrir, and R. Gunderson, "Distributed multi-agent microgrids: a decentralized approach to resilient power system self-healing," in *2011 4th International Symposium on Resilient Control Systems*, 2011, pp. 83-88: IEEE.
[135] A. Arif and Z. Wang, "Networked microgrids for service restoration in resilient distribution systems," *IET Generation, Transmission & Distribution,* vol. 11, no. 14, pp. 3612-3619, 2017.
[136] M. Amirioun, F. Aminifar, and H. Lesani, "Resilience-oriented proactive management of microgrids against windstorms," *IEEE Transactions on Power Systems,* vol. 33, no. 4, pp. 4275-4284, 2017.
[137] X. Liu, M. Shahidehpour, Z. Li, X. Liu, Y. Cao, and Z. Bie, "Microgrids for Enhancing the Power Grid Resilience in Extreme Conditions," *IEEE Transactions on Smart Grid,* vol. 8, no. 2, pp. 589-597, 2017.
[138] A. Hussain, V.-H. Bui, and H.-M. Kim, "Fuzzy logic-based operation of battery energy storage systems (BESSs) for enhancing the resiliency of hybrid microgrids," *Energies,* vol. 10, no. 3, p. 271, 2017.
[139] Z. Wang, J. Wang, and C. Chen, "A three-phase microgrid restoration model considering unbalanced operation of distributed generation," *IEEE Transactions on Smart Grid,* vol. 9, no. 4, pp. 3594-3604, 2016.
[140] Y. Kwon, A. Kwasinski, and A. Kwasinski, "Coordinated Energy Management in Resilient Microgrids for Wireless Communication Networks," *IEEE Journal of Emerging and Selected Topics in Power Electronics,* vol. 4, no. 4, pp. 1158-1173, 2016.
[141] N. M. Dehkordi, H. R. Baghaee, N. Sadati, and J. M. Guerrero, "Distributed noise-

resilient secondary voltage and frequency control for islanded microgrids," *IEEE Transactions on Smart Grid,* 2018.
[142] H. Farzin, M. Fotuhi-Firuzabad, and M. Moeini-Aghtaie, "Role of outage management strategy in reliability performance of multi-microgrid distribution systems," *IEEE Transactions on Power Systems,* vol. 33, no. 3, pp. 2359-2369, 2017.
[143] R. Romero, J. F. Franco, F. B. Leão, M. J. Rider, and E. S. De Souza, "A new mathematical model for the restoration problem in balanced radial distribution systems," *IEEE Transactions on Power Systems,* vol. 31, no. 2, pp. 1259-1268, 2015.
[144] T. Ding, Y. Lin, Z. Bie, and C. Chen, "A resilient microgrid formation strategy for load restoration considering master-slave distributed generators and topology reconfiguration," *Applied energy,* vol. 199, pp. 205-216, 2017.
[145] C. Chen, J. Wang, F. Qiu, and D. Zhao, "Resilient distribution system by microgrids formation after natural disasters," *IEEE Transactions on smart grid,* vol. 7, no. 2, pp. 958-966, 2015.
[146] T. Ding, Y. Lin, G. Li, and Z. Bie, "A new model for resilient distribution systems by microgrids formation," *IEEE Transactions on Power Systems,* vol. 32, no. 5, pp. 4145-4147, 2017.
[147] C. Chen, J. Wang, and D. Ton, "Modernizing distribution system restoration to achieve grid resiliency against extreme weather events: an integrated solution," *Proceedings of the IEEE,* vol. 105, no. 7, pp. 1267-1288, 2017.
[148] Y. Xu, C.-C. Liu, K. P. Schneider, F. K. Tuffner, and D. T. Ton, "Microgrids for service restoration to critical load in a resilient distribution system," *IEEE Transactions on Smart Grid,* vol. 9, no. 1, pp. 426-437, 2016.
[149] B. Chen, C. Chen, J. Wang, and K. L. Butler-Purry, "Multi-time step service restoration for advanced distribution systems and microgrids," *IEEE Transactions on Smart Grid,* vol. 9, no. 6, pp. 6793-6805, 2017.
[150] B. Simon, C. Coffrin, and P. Van Hentenryck, "Randomized adaptive vehicle decomposition for large-scale power restoration," in *Lecture Notes in Computer Science (including subseries Lecture Notes in Artificial Intelligence and Lecture Notes in Bioinformatics)* vol. 7298 LNCS, ed, 2012, pp. 379-394.
[151] H. Gao, Y. Chen, Y. Xu, and C. Liu, "Resilience-Oriented Critical Load Restoration Using Microgrids in Distribution Systems," *IEEE Transactions on Smart Grid,* vol. 7, no. 6, pp. 2837-2848, 2016.
[152] Y. Liu, N. U. Hassan, S. Huang, and C. Yuen, "Electricity cost minimization for a residential smart grid with distributed generation and bidirectional power transactions," in *2013 IEEE PES Innovative Smart Grid Technologies Conference (ISGT)*, 2013, pp. 1-6: IEEE.
[153] R. Eskandarpour, A. Khodaei, and A. Arab, "Improving power grid resilience through predictive outage estimation," in *2017 North American Power Symposium (NAPS)*, 2017, pp. 1-5: IEEE.
[154] R. Eskandarpour and A. Khodaei, "Machine Learning Based Power Grid Outage Prediction in Response to Extreme Events," *IEEE Transactions on Power Systems,* vol. 32, no. 4, pp. 3315-3316, 2017.
[155] M. Ouyang, L. Zhao, Z. Pan, and L. Hong, "Comparisons of complex network based models and direct current power flow model to analyze power grid vulnerability under intentional attacks," *Physica A: Statistical Mechanics and its Applications,* vol. 403, pp. 45-53, 2014.
[156] J. Johansson and H. Hassel, "An approach for modelling interdependent infrastructures in the context of vulnerability analysis," *Reliability Engineering & System Safety,* vol. 95, no. 12, pp. 1335-1344, 2010.

[157] A. Abedi, L. Gaudard, and F. Romerio, "Review of major approaches to analyze vulnerability in power system," *Reliability Engineering & System Safety,* 2018.
[158] M. Panteli, P. A. Crossley, D. S. Kirschen, and D. J. Sobajic, "Assessing the impact of insufficient situation awareness on power system operation," *IEEE Transactions on power systems,* vol. 28, no. 3, pp. 2967-2977, 2013.
[159] M. Panteli, D. S. Kirschen, P. A. Crossley, and D. J. Sobajic, "Enhancing situation awareness in power system control centers," in *2013 IEEE International Multi-Disciplinary Conference on Cognitive Methods in Situation Awareness and Decision Support (CogSIMA)*, 2013, pp. 254-261.
[160] J. R. Agüero, J. Wang, and J. J. Burke, "Improving the reliability of power distribution systems through single-phase tripping," in *IEEE PES T&D 2010*, 2010, pp. 1-7: IEEE.
[161] L. Ren, Y. Qin, B. Wang, P. Zhang, P. B. Luh, and R. Jin, "Enabling resilient microgrid through programmable network," *IEEE Transactions on Smart Grid,* vol. 8, no. 6, pp. 2826-2836, 2016.
[162] D. Jin *et al.*, "Toward a cyber resilient and secure microgrid using software-defined networking," *IEEE Transactions on Smart Grid,* vol. 8, no. 5, pp. 2494-2504, 2017.
[163] L. Ren *et al.*, "Enabling resilient distributed power sharing in networked microgrids through software defined networking," *Applied Energy,* vol. 210, pp. 1251-1265, 2018.
[164] M. A. Azzouz, A. Hooshyar, and E. F. El-Saadany, "Resilience enhancement of microgrids with inverter-interfaced DGs by enabling faulty phase selection," *IEEE Transactions on Smart Grid,* vol. 9, no. 6, pp. 6578-6589, 2017.
[165] H. Mo, M. Xie, and G. Levitin, "Optimal resource distribution between protection and redundancy considering the time and uncertainties of attacks," *European Journal of Operational Research,* vol. 243, no. 1, pp. 200-210, 2015.
[166] S. Ma, L. Su, Z. Wang, F. Qiu, and G. Guo, "Resilience enhancement of distribution grids against extreme weather events," *IEEE Transactions on Power Systems,* vol. 33, no. 5, pp. 4842-4853, 2018.
[167] A. Hussain, V.-H. Bui, and H.-M. Kim, "A proactive and survivability-constrained operation strategy for enhancing resilience of microgrids using energy storage system," *IEEE Access,* vol. 6, pp. 75495-75507, 2018.
[168] Y. Wu, Y. Wu, H. Cimen, J. C. Vasquez, and J. M. Guerrero, "Towards collective energy Community: Potential roles of microgrid and blockchain to go beyond P2P energy trading," *Applied Energy,* vol. 314, p. 119003, 2022.
[169] M. Yan *et al.*, "Blockchain for transacting energy and carbon allowance in networked microgrids," *IEEE Transactions on Smart Grid,* vol. 12, no. 6, pp. 4702-4714, 2021.
[170] D. Bose, C. K. Chanda, and A. Chakrabarti, "Blockchain insisted resilience enhancement of power electricity markets using distributed energy trading," *International Journal of Emerging Electric Power Systems,* 2021.
[171] H. Shahinzadeh, J. Moradi, G. B. Gharehpetian, H. Nafisi, and M. Abedi, "Internet of Energy (IoE) in smart power systems," in *2019 5th Conference on Knowledge Based Engineering and Innovation (KBEI)*, 2019, pp. 627-636: IEEE.
[172] M. Panteli, D. N. Trakas, P. Mancarella, and N. D. Hatziargyriou, "Boosting the power grid resilience to extreme weather events using defensive islanding," *IEEE Transactions on Smart Grid,* vol. 7, no. 6, pp. 2913-2922, 2016.
[173] L. Che and M. Shahidehpour, "Adaptive formation of microgrids with mobile emergency resources for critical service restoration in extreme conditions," *IEEE Transactions on Power Systems,* vol. 34, no. 1, pp. 742-753, 2018.
[174] S. Lei, J. Wang, C. Chen, and Y. Hou, "Mobile Emergency Generator Pre-Positioning and Real-Time Allocation for Resilient Response to Natural Disasters," *IEEE Transactions on Smart Grid,* vol. 9, no. 3, pp. 2030-2041, 2018.

[175] M. H. Amirioun, F. Aminifar, and M. Shahidehpour, "Resilience-Promoting Proactive Scheduling against Hurricanes in Multiple Energy Carrier Microgrids," *IEEE Transactions on Power Systems,* 2018.
[176] A. Arif, Z. Wang, J. Wang, and C. Chen, "Power distribution system outage management with co-optimization of repairs, reconfiguration, and DG dispatch," *IEEE Transactions on Smart Grid,* vol. 9, no. 5, pp. 4109-4118, 2017.
[177] A. K. Erenoğlu and O. Erdinç, "Real-time Allocation of Multi-mobile Resources in Integrated Distribution and Transportation Systems for Resilient Electrical Grid," *IEEE Transactions on Power Delivery,* 2022.
[178] X. Cao, T. Cao, Z. Xu, B. Zeng, F. Gao, and X. Guan, "Resilience Constrained Scheduling of Mobile Emergency Resources in Electricity-Hydrogen Distribution Network," *IEEE Transactions on Sustainable Energy,* 2022.
[179] W. Wang, X. Xiong, Y. He, J. Hu, and H. Chen, "Scheduling of separable mobile energy storage systems with mobile generators and fuel tankers to boost distribution system resilience," *IEEE Transactions on Smart Grid,* vol. 13, no. 1, pp. 443-457, 2021.
[180] Z. Wang and J. Wang, "Self-healing resilient distribution systems based on sectionalization into microgrids," *IEEE Transactions on Power Systems,* vol. 30, no. 6, pp. 3139-3149, 2015.
[181] X. Zhang, S. Mahadevan, S. Sankararaman, and K. Goebel, "Resilience-based network design under uncertainty," *Reliability Engineering & System Safety,* vol. 169, pp. 364-379, 2018.
[182] B. Chen, C. Chen, J. Wang, and K. L. Butler-Purry, "Sequential service restoration for unbalanced distribution systems and microgrids," *IEEE Transactions on Power Systems,* vol. 33, no. 2, pp. 1507-1520, 2017.
[183] M. Aly, E. M. Ahmed, and M. Shoyama, "Thermal and reliability assessment for wind energy systems with DSTATCOM functionality in resilient microgrids," *IEEE Transactions on Sustainable Energy,* vol. 8, no. 3, pp. 953-965, 2016.
[184] W. Cao, J. Wu, N. Jenkins, C. Wang, and T. Green, "Benefits analysis of Soft Open Points for electrical distribution network operation," *Applied Energy,* vol. 165, pp. 36-47, 2016.
[185] B. Cai, M. Xie, Y. Liu, Y. Liu, and Q. Feng, "Availability-based engineering resilience metric and its corresponding evaluation methodology," *Reliability Engineering & System Safety,* vol. 172, pp. 216-224, 2018.
[186] P. Ghosh and M. De, "Probabilistic Quantification of Distribution System Resilience for an Extreme Event," *International Transactions on Electrical Energy Systems,* vol. 2022, 2022.
[187] M. Amirioun, F. Aminifar, H. Lesani, and M. Shahidehpour, "Metrics and quantitative framework for assessing microgrid resilience against windstorms," *International Journal of Electrical Power & Energy Systems,* vol. 104, pp. 716-723, 2019.
[188] J. E. Ramirez-Marquez, C. M. Rocco, K. Barker, and J. Moronta, "Quantifying the resilience of community structures in networks," *Reliability Engineering & System Safety,* vol. 169, pp. 466-474, 2018.
[189] R. Sarkar, A. Gusrialdi, and Z. Qu, "An adaptive restorative method for resilient power distribution networks," in *2016 IEEE Power and Energy Society General Meeting (PESGM)*, 2016, pp. 1-5: IEEE.
[190] A. Cárcamo-Gallardo, L. García-Santander, and J. E. Pezoa, "Greedy reconfiguration algorithms for medium-voltage distribution networks," *IEEE Transactions on Power Delivery,* vol. 24, no. 1, pp. 328-337, 2008.
[191] S. Espinoza, M. Panteli, P. Mancarella, and H. Rudnick, "Multi-phase assessment and adaptation of power systems resilience to natural hazards," *Electric Power Systems*

Research, vol. 136, pp. 352-361, 2016.
[192] D. N. Trakas, M. Panteli, N. D. Hatziargyriou, and P. Mancarella, "Spatial risk analysis of power systems resilience during extreme events," *Risk Analysis,* vol. 39, no. 1, pp. 195-211, 2019.
[193] H. Zhang, H. Yuan, G. Li, and Y. Lin, "Quantitative Resilience Assessment under a Tri-Stage Framework for Power Systems," *Energies,* vol. 11, no. 6, p. 1427, 2018.
[194] S. Yao, P. Wang, and T. Zhao, "Transportable energy storage for more resilient distribution systems with multiple microgrids," *IEEE Transactions on Smart Grid,* vol. 10, no. 3, pp. 3331-3341, 2018.
[195] C. Wang, Y. Hou, F. Qiu, S. Lei, and K. Liu, "Resilience enhancement with sequentially proactive operation strategies," *IEEE Transactions on Power Systems,* vol. 32, no. 4, pp. 2847-2857, 2016.

CHAPTER 3

SIGNIFICANCE OF DISTRIBUTED ENERGY RESOURCES ON ACTIVE DISTRIBUTION SYSTEM RESILIENCE

3.1. Introduction

Nowadays, the power system is experiencing frequent power outages across the globe due to increasing natural disasters and cyber-attacks and owing to the fact that the power system was designed with reliability principles, i.e., security and adequacy. With these principles, the power system can only cope with a high-probability and low-impact event, which mostly involves known failures. Moreover, it doesn't affect considerably on power system infrastructure, which means it can be restored within a reasonable time with lesser impacts on society and the economy. However, in the past few decades, catastrophic events have been increasing, which remarks on the concern of reliability principles [1]. The evidence can be seen with major catastrophic events such as Hurricane Sandy and Katrina, Japan earthquake, Ukraine cyber-physical attack, and other major events that are reported in [2-4]. With these events, millions of people are affected, and energy infrastructure is damaged, significantly impacting the economy and life threats. Thus, to ensure a reduced impact on the economy against power system damage and energy security, the distribution system should be resilient, which deals with four major attributes in a single framework: withstand, recover, adapt, and prevent [4].

In the power system context, resilience deals with low-probability and high-impact (HILP) events. Hence in order to minimize the consequence of HILP events, the migration or modernization of the power system is of utmost need [5]. Moreover, extreme events like natural disasters or cyber-attacks are mostly affecting the distribution system. Therefore, the power system planner should emphasize modernizing the distribution system; for that, integrating distributed energy resources (DERs) is vital. Over the past few decades, the utilization of DER has been increasing significantly, which is achieved as a milestone for microgrid (MG) and smart grid technology. With these technologies, the distribution system can quickly restore the load (according to the priority) after the HILP event, which enhances the distribution system's resiliency [6, 7].

The importance of MG technology is treated as a promising solution for load restoration in the face of extreme events, and their interconnection (multi-microgrid) to the distribution system is further pursued as a resilient-based design [8]. The addition of a microgrid into the distribution system can be called an active distribution system (ADS). Indeed, the primary objective of ADS is to minimize load fluctuation and to maximize the reliability of the system. However, the ADS also deals with the source of resilience, as the number of DERs are connected to it [9]. Further, to enhance the resiliency of the ADS, the MG with the optimal placement of tie-line (TL) and mobile storage unit is also the great importance for fast load recovery.

In recent decades, the reconfiguration of the distribution system is increasing to improve the resourcefulness of the system, which plays a significant role against HILP events. In doing so, the system can have the self-sufficient capability (e.g., with the use of more renewable penetrations) [10], creates an alternative path for restoration (e.g., installing TLs) [11], and emergency services (e.g., mobile energy storage and crew member) [12, 13]. Moreover, resourcefulness is not only important for the HILP event, but also it can help during emergency and maintenance services. Several attempts are made to show the better resilient characteristics of ADS through MG and multiple-microgrids (MMGs). In [14], the adaptive formation of MG with a mobile resource is used to meet the critical load demand in extreme events. Similarly, the interconnected MG is presented in [8], where the two important types of load are considered, such as an integrated gas and power distribution network. The main aim was to improve the preparedness of the MG to minimize the load curtailment in the face of hurricane-based disasters. In recent years, few other studies have introduced tremendous solutions for the enhancement of ADS resiliency through the MG/MMG approaches, which are reported in [15-19]. On the other hand, to increase the resourcefulness of the ADS further, several recent studies have investigated MG/MMG with energy storage (fixed and mobile) [12, 20], an optimal connection of tie-lines [11, 21], workforce deployment [13, 22], and robust control strategies [23, 24].

As discussed above, resourcefulness aims to have self-healing capability, which is also the main objective of the resilient-based design. With this objective, and concerning the catastrophic events, as high-impact and time-intensive, the ADS can restore the load in the shortest possible time to minimize social threats and the economy. More importantly, critical loads such as health institutions, IT offices, important headquarters, gas and water networks are the first responders, which must be restored promptly to minimize the risk. However, it is possible that the ADS should have better resilient planning and operational schemes. Thus, in the planning stage, such as before the event, DERs are to be installed optimally where the power loss is taken as an objective function. Besides, the number of TLs can be connected optimally to recover the critical load as an alternative path. It can be called a planning and expansion planning strategy. Further, in the operation stage, such as after the event, according to the fault location, TL can be used to restore the critical load with minimum time and cost. This phase is otherwise called reconfiguration planning and operation. These objectives measure resilience performance through energy not supplied (ENS) and energy loss. Note that in this chapter, resilience is only focused on power grid restoration.

3.2. Mathematical modelling

The distribution system is considered an important section of the power system, which must be well-planned and have a flexible structure. Generally, the power generating stations are located far from the distribution systems (DSs). DSs are mostly of the radial type of network, where several small generation units can be installed to improve system reliability and resiliency. Notwithstanding, during disruptive events, the upstream grid might not be able to supply power to the end-users. Therefore, small generating units are needed to be installed to significantly contribute to the critical and non-critical loads. A DER unit can form an island, which can take a challenge to meet the load demand per the DER power availability. Noteworthy, during the events, the distribution network has to be transferred from a centralized control mode to a decentralized control mode through tie-switches, sectionalizers, and circuit breakers, to provide isolation from the upstream grid and form an islanding mode. In this study, four photovoltaics (PVs) units are installed along with four distinct islanding modes, and each unit has a specific capacity.

The ENS can be formulated with two main categories of consumers: first, consumers should consider the switching time (i.e., the time taken to form the islanding mode), and second, consumers experience the rate of failure and repair time.

The ENS can be expressed by (3.1) while considering each state of generation and load [25]:

$$ENS = \sum_{i=1}^{N_{br}} \lambda_i \, L_i \left(t_{rpr} + t_{swc}\right) \sum_{j\in\Omega_i} P_j \tag{3.1}$$

where

N_{br} : Number of branches

λ_i: Failure rate of branch i (f /km yr)

L_i : Length of a branch i (km)

P_j : Demand power of the j^{th} load

t_{rpr} : Fault repair time (hours)

t_{swc} : Switching time (hours)

Ω_i: The set of buses located at upstream of branch i

In this case study, four PV units are installed along with four distinct islanding modes, and each unit has a specific capacity. In the estimation method of ENS, the output of the DER power can be formulated as (3.2), which is the prerequisite to forming an island. In addition, it is assumed that the power loss of the grid equals 5% of the hourly total load demand of the network.

$$P_{DG} \geq P_{load} + P_{loss} \tag{3.2}$$

where $P_{DG}, P_{load},$ and P_{loss} are the DER power, active power load (exist in the island mode), and network power loss.

There are many indices that can be used to measure resilience, but ENS measurement has some consequential meaning, which is explained as follows. The significance of the ENS index is: it reflects the number of customers affected due to the event, which should be minimized; it needs prompt action to reduce the impact on life threats. Thus, in this study, the system has been reconfigured, and restoration is done by using the ENS index.

On the other hand, the resilience of the system on account of a catastrophic event can be estimated as the reciprocal of the system's loss performance [26], which can be defined as (3.3). In this case, a loss means the amount of generated power is not available to the test system. Hence, the loss can be estimated as (3.4)

$$\text{Resilience} = \frac{1}{\text{Loss}} \tag{3.3}$$

$$\text{Loss} = \frac{P_0 - P_{min}}{P_{min}} \tag{3.4}$$

where, P_0 and P_{min} are the total load and active load in the system after the event, respectively.

3.3. Results and discussion

In this section, a resilience study is carried out and applied to an IEEE 33-bus system. The findings from this study provide two contributions to the current literature, *i.e.*, firstly without assuming the emergency load in Study 1; and secondly with the consideration of emergency loads in Study 2. On the other hand, in Study 3, the resilience of the system on account of a catastrophic event is estimated, which is the reciprocal of the system's loss performance.

In Study 1, four different scenarios (such as no PV, with PV, considering PV power increase, and optimal allocation of PV units) are discussed. However, in Study 2, three different scenarios (i.e., no PV, with PV, and optimal allocation of PV units) are presented. The incorporation of DERs like PV and wind can migrate the system infrastructure from a conventional to a resilient system. Thus, a conventional system is taken as the base case, and three more cases of study are conducted in the course of a resilient system as follows. In this study, ENS of DS is considered as a resilience index after an extreme event. The presence of PV units can extensively reduce this index because of the proximity of generation sites and load centers. The formulation of the ENS is discussed and estimated as follows.

3.3.1. Study-1

In this study, the four types of scenarios are portrayed. Scenario-2 considers a base case where no DER unit is considered, and then four PV units are installed in scenario-2. In scenario-3, PV power is increased, and finally, the optimal allocation of the PV unit is addressed in scenario-4. Moreover, the single fault and double phase to ground fault are applied to the test system, and ENS is calculated. However, this test system does not consider an emergency load.

A. Scenario-1: Base case

In this scenario, the conventional operation of the grid is considered as the base case where no DER is incorporated, as illustrated in Fig. 3.1. Moreover, the single fault and double phase to ground fault events are applied to the system, and then the ENS is calculated as a performance index. During the single fault, the ENS is a constant value during the operational horizon because no backup unit (e.g., DERs) is incorporated into the system, and the ENS profile is shown in Fig. 3.2. Similarly, the performance of ENS by the application of double fault is shown in Fig. 3.3.

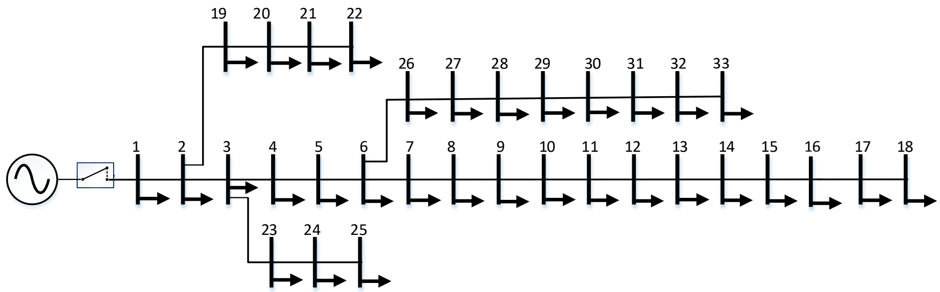

Fig. 3.1 Single-line diagram of IEEE 33-bus distribution network

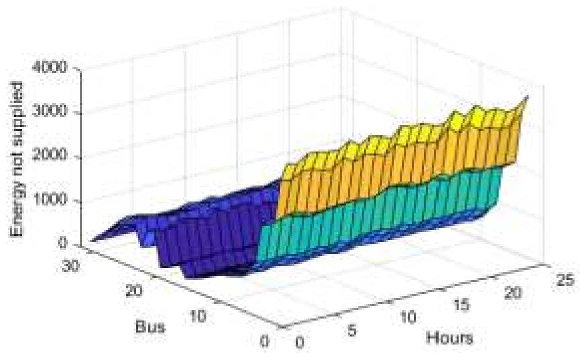

Fig. 3.2 Single fault without PV unit

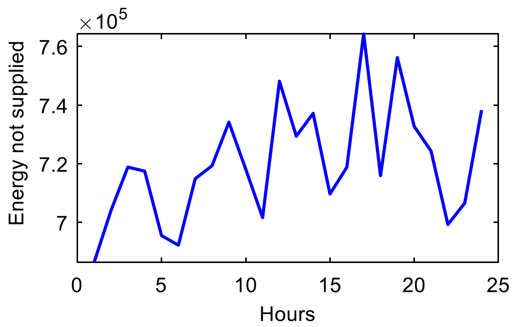

Fig. 3.3 Double fault without PV unit

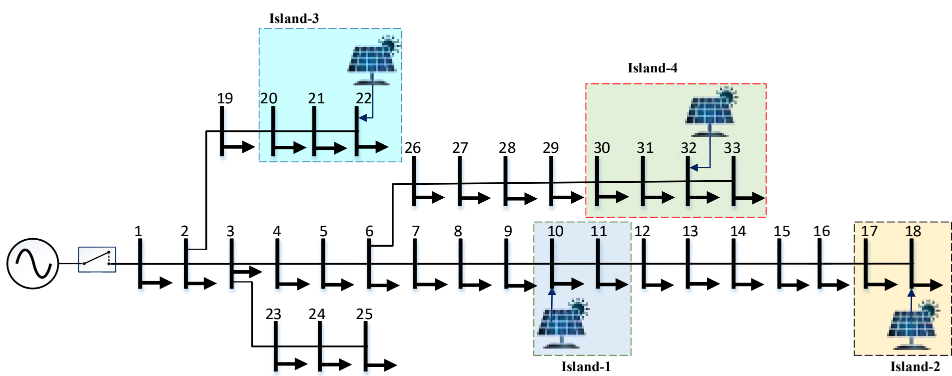

Fig. 3.4 Single-line diagram of IEEE 33-bus distribution network with four PVs

B. Scenario-2: PV unit set-up

In this scenario, four solar units with a capacity of 100 kW, 200 kW, 500 kW, and 1 MW are installed at buses 10, 18, 22, and 32, respectively, to make the system resilient, as shown in Fig. 3.4. Further, it is observed that after applying the DERs to the 33-bus system, the ENS of the proposed system is reduced in comparison with the conventional network, can be seen in Fig. 3.5. As noted, such a decrease gives a better situation to the end-users during the contingency period. Notwithstanding, during the peak hours of load demand, the ENS value is also minimum because solar power has its highest generation and is able to meet the major part of the load demand. Further, the performance of the ENS is depicted in Fig. 3.6 in response to the double fault.

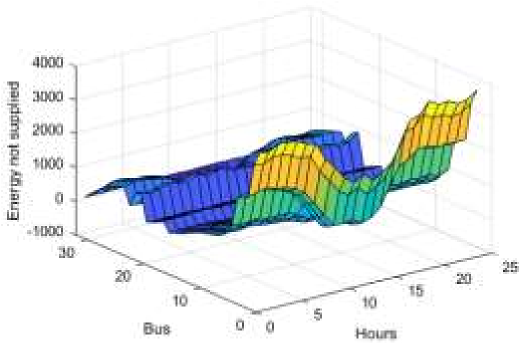

Fig. 3.5 Single fault with PV units

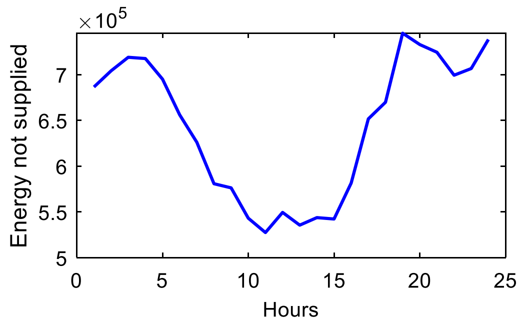

Fig. 3.6 Double fault with PV unit

C. Scenario-3: PV power enhance

Considering the four PVs in the 33-bus system, let us increase the output power of four PV units to 200 kW, 400 kW, 1 MW, and 2 MW, respectively, at the bus locations shown in Fig. 3.7 the ENS performance is assessed.

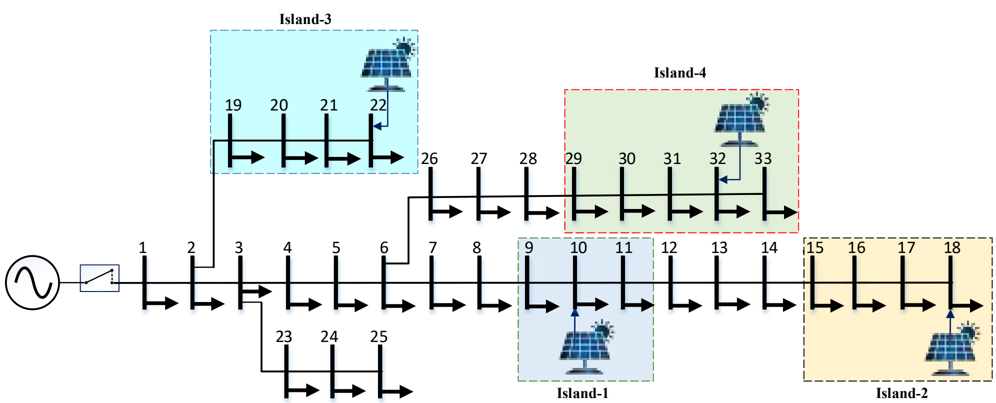

Fig. 3.7 Single-line diagram of IEEE 33-bus distribution network with PV power enhance

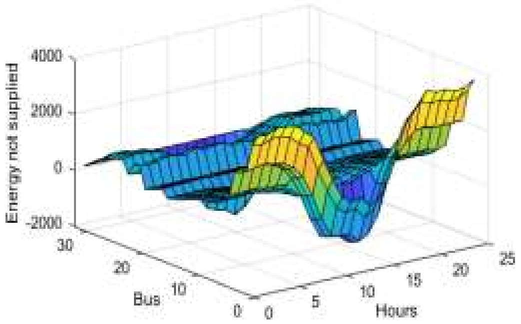

Fig. 3.8 Single fault with increasing PV power

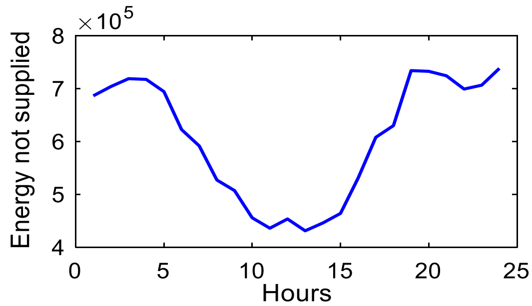

Fig. 3.9 Double fault increasing PV power

It is clear that using the proposed approach, the ENS value is reduced, which means that the system is more resilient than the above scenarios with the single fault inclusion, as shown in Fig. 3.8. In addition, the double fault is applied to the system, and the ENS performance is measured, as shown in Fig. 3.9. A comparison of the findings with those of other scenarios above confirms the better result, which means it can supply more power during the faults. It is clear that from Scenario-3, the DER capacity also plays a key role in minimizing the ENS of the system.

D. Scenario-4: PV optimal allocation

It is more important to note that the proper DER allocation can achieve increased system reliability and resiliency as well as reduced operating costs during the contingencies. Let us study the optimum location of DERs, which shows the optimal value of ENS in this scenario. The Swarm Robotics Search & Rescue (SRSR) [27] optimization method is applied here to optimize the location of PVs. In an initial attempt, the single fault is applied, and the optimum location of the PVs is shown in Fig. 3.10, and the ENS performance is shown in Fig. 3.11.

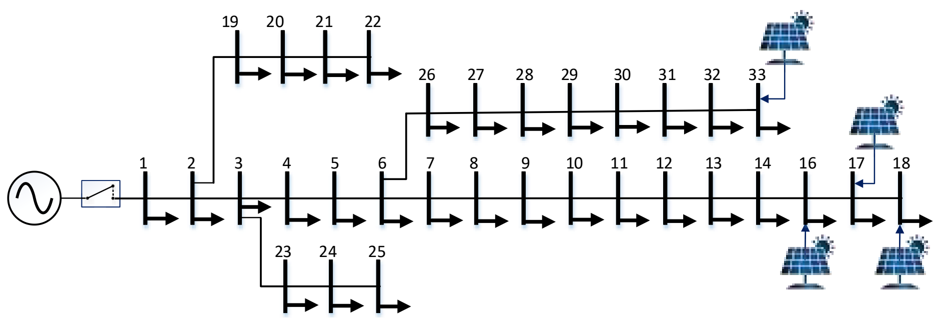

Fig. 3.10 Optimal location of PVs considering the single fault

Further, the double fault is applied, and the ENS performance is shown in Fig. 3.12, and the optimum location of the PVs is depicted in Fig. 3.13. Finally, the comparison characteristics of ENS in the case of double fault is shown in Fig. 3.14, which reveals that there is a significant performance improvement compared with Scenario-1 to Scenario-3.

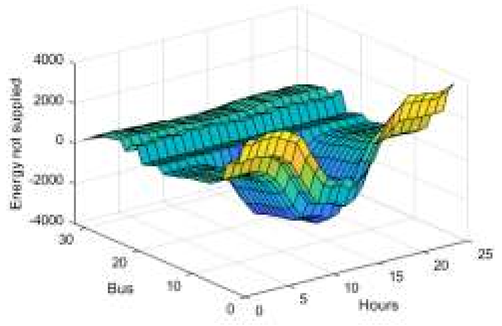

Fig. 3.11 Single fault with optimal PV allocation

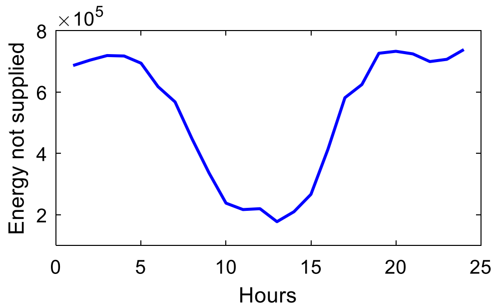

Fig. 3.12 Double fault with optimal PV allocation

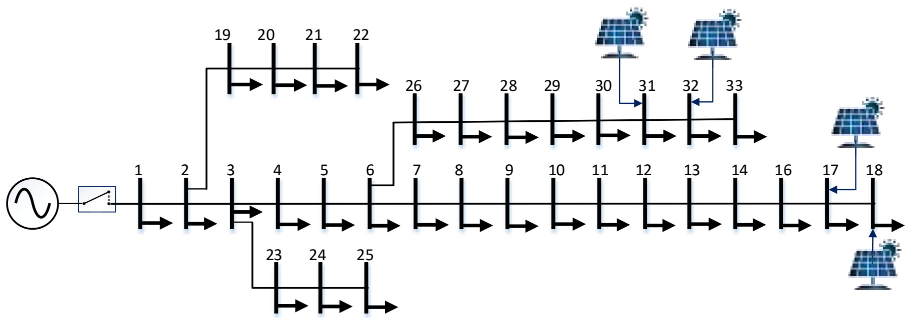

Fig. 3.13 Optimal location of PVs considering the double fault

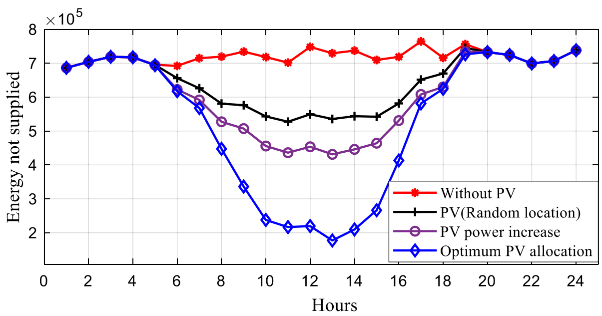

Fig. 3.14 Comparison characteristics of ENS for a double fault

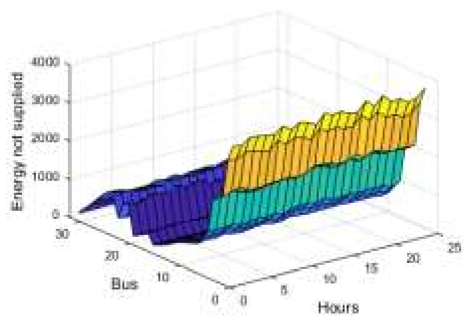

Fig. 3.15 Single fault without PV unit

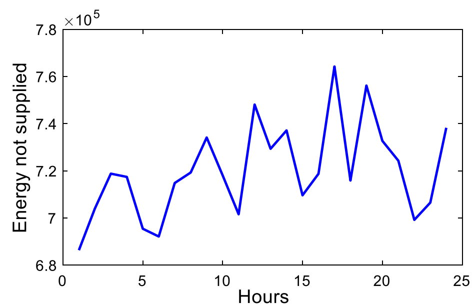

Fig. 3.16 Double fault without PV unit

3.3.2. Study-2

In response to unfavourable events, the consideration of emergency loads (e.g., first responders) is also a part of resiliency to minimize the life at risk. For that, there is a need for DERs to maintain the power supply to critical loads such as health institutions, financial institutions, process industries, communication centers, etc. Hence, in order to make a priority level, this case study includes four emergency loads in a 33-bus system. The emergency loads are considered on buses 16, 20, 24, and 31. In this test system, three scenarios are considered, including the base case, with PV units and the optimal allocation of PV units.

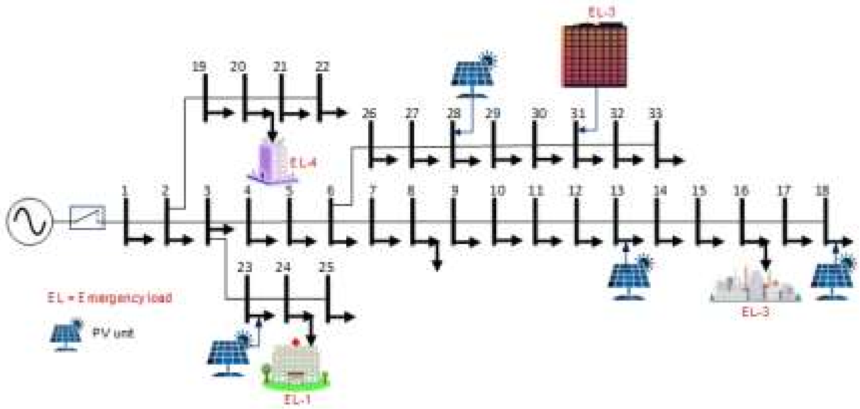

Fig. 3.17 Single-line diagram of IEEE 33-bus test system considering the emergency load

A. Scenario-1: Base case

In this scenario, the base case refers to the conventional operation of the system, where no DER is incorporated. Moreover, the single fault and double fault are applied to the system, and then the ENS value is calculated as a performance index. The ENS for a single fault is shown in Fig. 3.15, while Fig. 3.16 shows the ENS for a double fault event.

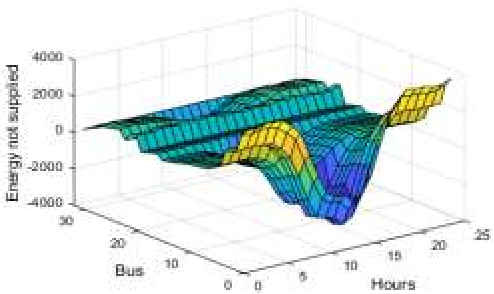

Fig. 3.18 Single fault with PV unit

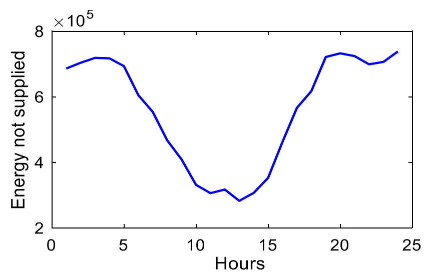

Fig. 3.19 Double fault with PV unit

B. Scenario-2: DER set-up

This scenario considers the four solar units (1MW, 1MW, 1.5 MW, and 2MW) incorporated into the 33-bus test system at bus locations 13, 18, 23, and 28, respectively, respectively as shown in Fig. 3.17. The ENS of the proposed system is reduced compared to the conventional system. As can be seen, the DERs could help to reduce the load curtailment of the system. Further, the performance of the ENS is depicted in Figs. 3.18 and 3.19 in response to the single fault and double fault, respectively.

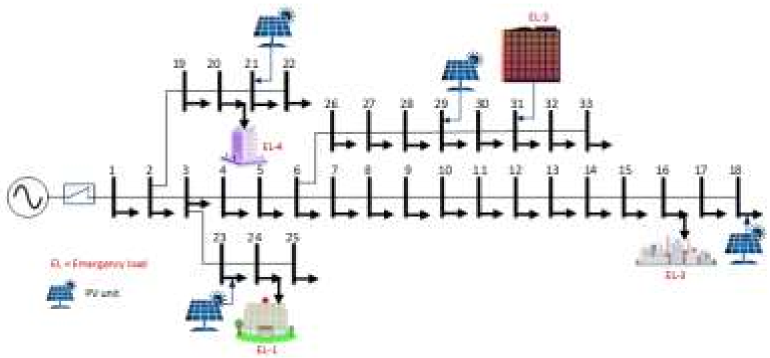

Fig. 3.20 Optimal location of PVs considering the emergency loads

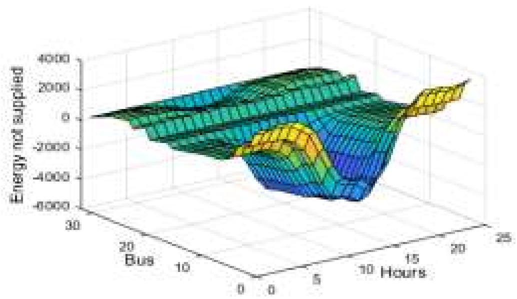

Fig. 3.21 Single fault with optimal PV allocation

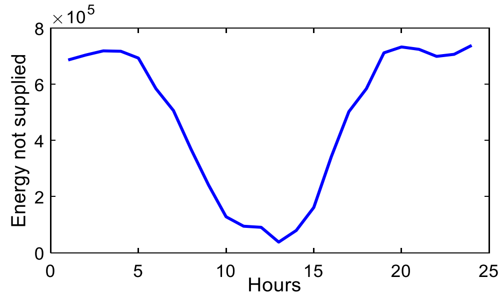

Fig. 3.22 Double fault with optimal PV allocation

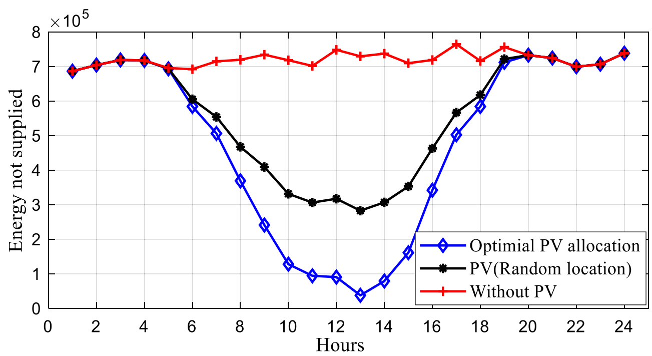

Fig. 3.23 Comparison characteristics of ENS for a double fault

C. Scenario-3: PV optimal allocation

The objective of this scenario is to minimize the ENS considering the emergency loads; hence, the optimal allocation of the PV unit is presented, where the result shows a lower value of ENS and better management of the PV unit to the emergency loads. The swarm robotics search & resecue (SRSR) optimization method is applied here to optimize the location of PVs. In an initial attempt, the single fault is applied, and the optimum location of the PVs are shown in Fig. 3.20, and the ENS performance is shown in Figs. 3.21 and 3.22 in case of a single fault and double fault. It is noted that the ENS is greatly reduced as compared to the other two scenarios, which means that the system reliability and resiliency is enhanced. Finally, the comparison characteristics of ENS in the response of the double fault of Test Network 2 is presented in Fig. 3.23. This study sets out the aim of assessing the importance of PV in a conventional system on account of resiliency, indicating the transformation from the traditional to the modern power system through the integration of DER units. More importantly, the ENS is directly related to the load curtailment, with the lower ENS value meaning that less load curtailment is needed.

3.3.3. Study-3

The catastrophic events that hit a network could inevitably need a prolonged period of recovery time and high recovery costs. In addition, the system generation loss increases, which further decreases the resiliency. Therefore, the system should be planned to have low loss and high resilience. To this end, installing DERs and their placement can play a crucial role in reducing generation loss and increasing the system's resiliency. With these objectives, Study-3 presents four different scenarios, as follows.

A. Resilience and loss measure

The resilience can be estimated in the range of zero (no resilience) to infinity (maximum resilience). Zero resilience refers to a system that does not have the coping capacity to recover the load after the events, which means the system is completely collapsed. On the other hand, infinity resilience refers to the system that can recover all the loads after the event [26].

In this study, PV units are taken as DER sources to show the resiliency of the system in the face of a double phase to ground fault. Moreover, the limitation of the PV unit is that it can only supply power when there is solar insolation available, e.g., from 8 am to 5 pm. With this assumption, if a fault happens during this time, the system can meet the load demand partially or fully according to the available capacity. As shown in Fig. 3.24 (a), the resilience is increased by PV installation, power increase, and optimal PV allocation. The resilience and loss can be measured by assuming that the maximum PV capacity is reached at 1 pm. Accordingly, loss and resilience values are estimated and presented in Figs. 3.24 (b), and (c), respectively.

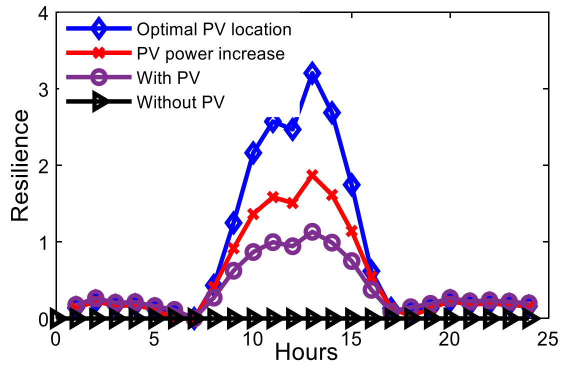

(a) Comparison characteristics of resilience

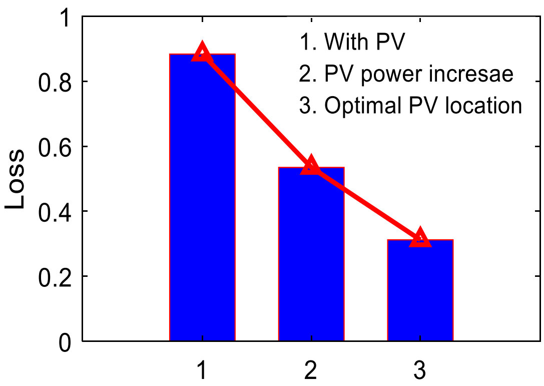

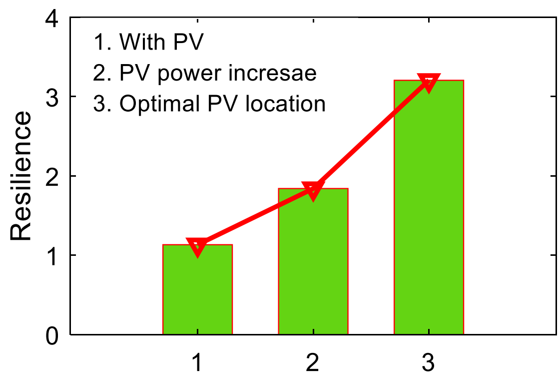

(b) Loss at peak hour

(c) Resilience at peak hour

Fig. 3.24. Resilience and loss characteristics of the proposed system

3.4. Summary

This chapter contributes to enhancing active distribution system resilience by properly allocating energy sources and increasing the generation capacity. Further, the system's resilience has been compared by measuring the indices, such as ENS and energy loss, with and without optimal allocation and power increment. It is noted that the optimal location of resources has greatly enhanced the resilience characteristics. The case study demonstrates the importance of DERs and their optimal placement in ADS. It has been tested through the IEEE 33-bus system with and without the incorporation of PV units. This study is presented with the following conclusion and limitations.

- Initially, the incorporation of PV units into the distribution system is presented, which shows that the value of ENS is decreased. Indeed, the reduced value of ENS demonstrates better resilience characteristics. Given this objective, study-1 and study-2 are simulated separately through a Matlab environment, without and with considering the emergency loads.
- Secondly, energy loss and resiliency are formulated, which states an inverse relationship between them. In fact, it is demonstrated that the energy loss is decreasing while the resilience factor is conversely increasing. The study reveals that adding DERs like PV units becomes crucial for making the system resilient and, accordingly, load restoration can be enhanced.
- This case study is based on the PV units but is not limited to PV only; other DERs like wind, fuel cell, microturbine, and storage units can be added to enhance the system resiliency. On the other hand, solar power during peak hours is considered here; however, extreme event can happen at any time of the day, when only solar energy might not be feasible to restore the load. Thus, from a practical perspective, considering the uncertainties is vital, which can be addressed in the future.

References

[1] M. Panteli and P. Mancarella, "The grid: Stronger, bigger, smarter?: Presenting a conceptual framework of power system resilience," *IEEE Power and Energy Magazine,* vol. 13, no. 3, pp. 58-66, 2015.

[2] L. Che, M. Khodayar, and M. Shahidehpour, "Only connect: Microgrids for distribution system restoration," *IEEE power and energy magazine,* vol. 12, no. 1, pp. 70-81, 2013.

[3] Z. Bie, Y. Lin, G. Li, and F. Li, "Battling the extreme: A study on the power system resilience," *Proceedings of the IEEE,* vol. 105, no. 7, pp. 1253-1266, 2017.

[4] D. K. Mishra, M. J. Ghadi, L. Li, and J. Zhang, "Proposing a Framework for Resilient Active Distribution Systems using Withstand, Respond, Adapt, and Prevent Element," in *2019 29th Australasian Universities Power Engineering Conference (AUPEC)*, 2019, pp. 1-6: IEEE.

[5] X. Wu, Z. Wang, T. Ding, X. Wang, Z. Li, and F. Li, "Microgrid planning considering the resilience against contingencies," *IET Generation, Transmission & Distribution,* vol. 13, no. 16, pp. 3534-3548, 2019.

[6] Z. Li and M. Shahidehpour, "Role of microgrids in enhancing power system resilience," in *2017 IEEE Power & Energy Society General Meeting*, 2017, pp. 1-5: IEEE.

[7] F. Yang, X. Feng, and Z. Li, "Advanced microgrid energy management system for future sustainable and resilient power grid," *IEEE Transactions on Industry Applications,* vol. 55, no. 6, pp. 7251-7260, 2019.

[8] M. H. Amirioun, F. Aminifar, and M. Shahidehpour, "Resilience-promoting proactive scheduling against hurricanes in multiple energy carrier microgrids," *IEEE Transactions on*

Power Systems, vol. 34, no. 3, pp. 2160-2168, 2018.
[9] R. R. Nejad and W. Sun, "Distributed load restoration in unbalanced active distribution systems," *IEEE Transactions on Smart Grid,* vol. 10, no. 5, pp. 5759-5769, 2019.
[10] Q. Gao, J. Zhu, and Y. Yuan, "Renewable generation capacity and reliability assessments for resilient active distribution networks based on time-sequence production simulation," *CSEE Journal of Power and Energy Systems,* 2020.
[11] Y. Liu, Y. Li, H. Xin, H. B. Gooi, and J. Pan, "Distributed optimal tie-line power flow control for multiple interconnected AC microgrids," *IEEE Transactions on Power Systems,* vol. 34, no. 3, pp. 1869-1880, 2018.
[12] S. Yao, P. Wang, X. Liu, H. Zhang, and T. Zhao, "Rolling optimization of mobile energy storage fleets for resilient service restoration," *IEEE Transactions on Smart Grid,* vol. 11, no. 2, pp. 1030-1043, 2019.
[13] S. Lei, C. Chen, Y. Li, and Y. Hou, "Resilient disaster recovery logistics of distribution systems: Co-optimize service restoration with repair crew and mobile power source dispatch," *IEEE Transactions on Smart Grid,* vol. 10, no. 6, pp. 6187-6202, 2019.
[14] L. Che and M. Shahidehpour, "Adaptive formation of microgrids with mobile emergency resources for critical service restoration in extreme conditions," *IEEE Transactions on Power Systems,* vol. 34, no. 1, pp. 742-753, 2018.
[15] F. Moghateli, S. A. Taher, A. Karimi, and M. Shahidehpour, "Multi-objective design method for construction of multi-microgrid systems in active distribution networks," *IET Smart Grid,* vol. 3, no. 3, pp. 331-341, 2020.
[16] R. Razi, C. Pham, A. Hably, S. Bacha, Q. T. Tran, and H. Iman-Eini, "A Novel Graph-based Routing Algorithm in Residential Multi-Microgrid Systems," *IEEE Transactions on Industrial Informatics,* 2020.
[17] F. Li, J. Qin, Y. Wan, and T. Yang, "Decentralized Cooperative Optimal Power Flow of Multiple Interconnected Microgrids via Negotiation," *IEEE Transactions on Smart Grid,* 2020.
[18] Q. Zhou, M. Shahidehpour, A. Alabdulwahab, and A. Abusorrah, "A cyber-attack resilient distributed control strategy in islanded microgrids," *IEEE Transactions on Smart Grid,* 2020.
[19] S. Zuo, O. A. Beg, F. L. Lewis, and A. Davoudi, "Resilient Networked AC Microgrids Under Unbounded Cyber Attacks," *IEEE Transactions on Smart Grid,* 2020.
[20] M. Nazemi, M. Moeini-Aghtaie, M. Fotuhi-Firuzabad, and P. Dehghanian, "Energy storage planning for enhanced resilience of power distribution networks against earthquakes," *IEEE Transactions on Sustainable Energy,* vol. 11, no. 2, pp. 795-806, 2019.
[21] R. Sarkar, A. Gusrialdi, and Z. Qu, "An adaptive restorative method for resilient power distribution networks," in *2016 IEEE Power and Energy Society General Meeting (PESGM)*, 2016, pp. 1-5: IEEE.
[22] T. Ding, Z. Wang, W. Jia, B. Chen, C. Chen, and M. Shahidehpour, "Multiperiod Distribution System Restoration with Routing Repair Crews, Mobile Electric Vehicles, and Soft-Open-Point Networked Microgrids," *IEEE Transactions on Smart Grid,* 2020.
[23] M. Mohiti, H. Monsef, A. Anvari-Moghaddam, and H. Lesani, "Two-stage robust optimization for resilient operation of microgrids considering hierarchical frequency control structure," *IEEE Transactions on Industrial Electronics,* 2019.
[24] M. Davari, M. P. Aghababa, F. Blaabjerg, and M. Saif, "A Modular Adaptive Robust Nonlinear Control for Resilient Integration of VSIs into Emerging Modernized Microgrids," *IEEE Journal of Emerging and Selected Topics in Power Electronics,* 2020.
[25] S. H. Gilani, M. J. Ghadi, and H. Afrakhte, "Optimal allocation of wind turbines considering different costs for interruption aiming at power loss reduction and reliability improvement using imperialistic competitive algorithm," *International Review of Electrical Engineering,* vol. 8, no. 1, pp. 284-296, 2013.
[26] Z. Li, M. Shahidehpour, F. Aminifar, A. Alabdulwahab, and Y. Al-Turki, "Networked microgrids for enhancing the power system resilience," *Proceedings of the IEEE,* vol. 105, no. 7, pp. 1289-1310, 2017.
[27] M. Bakhshipour, M. J. Ghadi, and F. Namdari, "Swarm robotics search & rescue: A novel artificial intelligence-inspired optimization approach," *Applied Soft Computing,* vol. 57, pp. 708-726, 2017.

CHAPTER 4

ACTIVE DISTRIBUTION SYSTEM RESILIENCE QUANTIFICATION AND ENHANCEMENT THROUGH MULTI-MICROGRID AND MOBILE ENERGY STORAGE

The functional capability of the active distribution network is continually challenged by extreme weather and unforeseen events. A complete resilience quantification framework is required to test the resilience of a distribution system. With this objective, a framework for demonstrating resilience enhancement through the utilization of multiple microgrids (MMGs) and mobile energy storage in extreme operating conditions is developed in this chapter. In the proposed framework, four resilience indices, such as withstand, recovery, adapt, and prevent (WRAP), are introduced. Withstand index signifies the coping capability after the event, where the microgrid (MG) plays a vital role. The recovery index measures the restoration after the event ends through the system reconfiguration using MG, tie-line, and mobile energy storage. The adapt index shows the stability of the system before and during the events. Finally, the prevent index suggests how different resources are important and responsible for fast recovery and minimizing consequences. A WRAP framework, as a resilience quantification framework, is formulated in this study, and the corresponding indices are quantified and enhanced through the MMG and mobile energy storage. The IEEE 33-bus system is considered for this study, and simulation is performed with different scenarios and measured resilience indices. It is found that appropriate reconfiguration through the use of MMG, tie-line, and mobile storage can remarkably enhance the distribution system's resilience.

4.1. Introduction

Current power distribution systems experience frequent power outages across the globe due to increasing natural disasters and cyber-attacks. In addition, the power systems are designed following reliability principles, i.e., security and adequacy. With these principles, the power system can only cope with a high-probability and low-impact event, mostly the known failures, where it is unremarkably affected and can be restored within a reasonable time with lesser impacts on energy end-users. However, in the past few decades, catastrophic events increased, significantly impacting end-users where the reliability-based design can not ensure stable operation [1]. The evidence includes major catastrophic events, such as Hurricane Sandy and Katrina, Japan earthquake, Ukraine cyber-physical attack, and other major events reported in [2-4]. These events affected millions of people and caused energy infrastructure damages, significantly impacting lives and the economy. Thus, to ensure a reduced impact on the economy against the power system damage and energy security, the distribution system should be resilient in dealing with four major attributes: withstand, recover, adapt, and prevent (WRAP).

In the power system context, resilience deals with low-probability and high-impact (HILP) events. Hence, power system decentralization is necessary to minimize the consequence against HILP events, particularly in the distribution system [5]. In order to obtain a decentralized system, the microgrid (MG) and smart grid technology are vital, where the integration of distributed energy resources (DERs) plays a key role. Subsequently, the interconnection of microgrids termed as MMG is further pursued as a resilient-based design [6]. With the help of such technology, the distribution system is termed an active distribution system (ADS). In addition, optimal reconfiguration and mobile services are greatly important for fast load recovery as well as resilience enhancement of the ADS.

In recent decades, extensive studies have been conducted to improve the power system's resilience, including the ADS. On the other hand, various resilience index has been proposed to quantify the system performance. As noted, four factors are extremely important for resilience studies such as WRAP. The detailed discussion can be seen in Section 4.3.3, where each factor and its relevance have been explained. Moreover, each factor of WRAP has significant value, and to enhance it, several methods have been used, as reported in [6-16].

In [6, 7], the importance of renewable energy penetrations in ADS has been discussed in terms of MG and MMG technology. The main aim was to increase the self-healing capability that refers to the withstand of the system. Secondly, Refs. [8-10] addresses the restoration techniques and their enhancement strategies through optimal reconfiguration of resources such as tie-lines and mobility services (mobile energy storage and crew member [11, 12]). Further, to enhance the adaptability of the system, a graph theory approach has been developed using algebraic connectivity and betweenness centrality, as reported in [13, 14]. Finally, preventive planning is a major concern, which can reduce the future power outage by assessing past experiences through probability measures, as discussed in [15, 16]. All four factors are combined in this study to introduce a resilience quantification framework such as WRAP.

Notably, various resilience quantification frameworks have been developed, such as RRRA (resourcefulness, recovery, robustness, and adaptability) by Abbasi et al. [13], where the authors have proposed 4 indices and considered only the black start unit using a large battery to restore the load. However, sometimes the disaster magnitude is very high, and a number of lines can be disconnected; thus, the same operation might be affected. Considering the above issue, we have presented the resilience quantification framework as well as the enhancement technique through reconfiguration and mobile storage units in the wake of single and multi-fault analysis. In Ref. [20], Panteil et al. developed FLEP (fast, low, extensive, promptly), and this study has focused on transmission networks using fragility modelling. According to the tower condition, the FLEP can be measrured. In [14], Srivastava et al., have developed the resilience indices through the graph theory approach, and the enhancement of resilience is ensured by switching operation.

However, in this study, the resilience enhancement is achieved by using reconfiguration and mobile storage units. Apart from the above indices, a few others studies has been carried out to quantify the resilience indices such as degradation, restoration efficiency, and MG resilience index [21], resilience achievement worth [22], expected energy curtailment [23], grid recovery index [24], sub resilience index [25], grid resilience metric [26], severity risk index [27], and a few more are reported in [28, 29]. Due to increasedcyber-attacks from the last few decades [30], authors in [31, 32] presented the cyber-physical power system to monitor the microgrid resiliency. However, those indices do not reflect the whole process of the event (pre, during, and post). Although a few studies have contributed to the resilience indices, all do not have the same test case and scenarios, e.g., studies are considered on high wind storm, ice storm, cyber-attacks, single line or multi-line failure, and on the other hand, either the indices are considered for transmission or distribution systems. However, our model is for expansion planning and operation in an active distribution system using reconfiguration and mobility services to enhance the system resilience. In addition, we have applied the multi-fault scenarios where the grid outage is taken into consideration, and then the critical load has been restored through the multi-microgrid and mobility service approach. In a nutshell, this chapter has significant value in terms of resilience quantification framework, enhancement techniques, and load recovery in an expansion planning and operation stage while considering the grid-connected and grid outage conditions.The main contributions of this study are as follows.

- A two-stage programming model is proposed on account of resiliency in ADS. In stage I, a normal operational scheme is implemented to minimize operating costs. In stage II, an unforeseen event is applied, and the critical loads are restored to normal operation, where maximizing the critical load restoration is considered an objective function.
- Furthermore, the resilience quantification framework, such as WRAP, is developed to measure the system's resiliency.
- The proposed strategy considers the optimal allocation of MG and tie-line (TL) to minimize the load curtailment. In addition, mobile storage units (MSU) is allocated optimally as an emergency source to enhance the resiliency of the system.
- This proposed approach is a complete solution for planning and operational scheme through the WRAP framework, where all four attributes, such as withstand, recover, adapt, and prevent stages, are well defined and measured to show the resiliency of the ADS.
- The prominent feature of the proposed WRAP framework is tested through the IEEE 33-bus test system with different scenarios.

4.2. Proposed resilience quantification framework

As noted earlier, the WRAP framework, where four significant factors are used to show the resiliency of the ADS in terms of coping capacity after the HILP event, rapid recovery through available resources, measured stability during and after the event, and preventive measurement. The short description of the WRAP framework with its objective and proposed index is presented in Fig. 4.1. The four major attributes of resilience are shown in Fig. 4.2, representing how the resources are responsible for the system performance level. The detailed discussions of the characteristics of the WRAP framework are as follows.

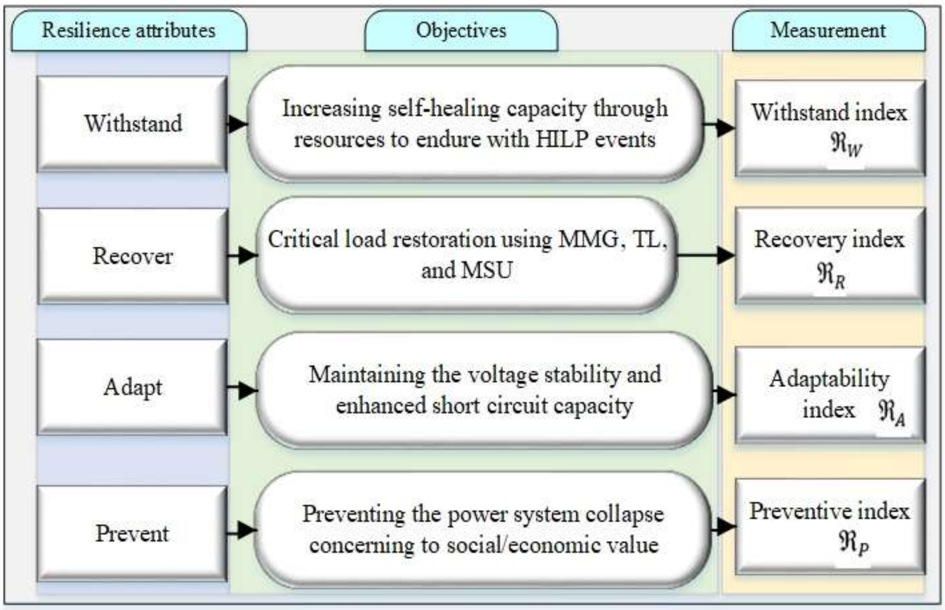

Fig. 4.1 WRAP framework and measurement indices (*Source: Author*)

Fig. 4.2 shows the system performance according to the event period, such as pre, during, and post. The pre-event is the normal operation, i.e., before t_{ds}; from t_{ds} to t_{de} is the during-event; from t_{de} to t_{re} is the post-event, and then comes the normal operation. From t_{ds} to t_{re}, the system operator should consider the four main factors concerning the system's resilience within the event period. Moreover, these factors can show the resiliency of the system by utilizing a number of resources. For instance, the contribution of MG can enhance the system resiliency and serve more loads after the event, which is considered a withstand phase.

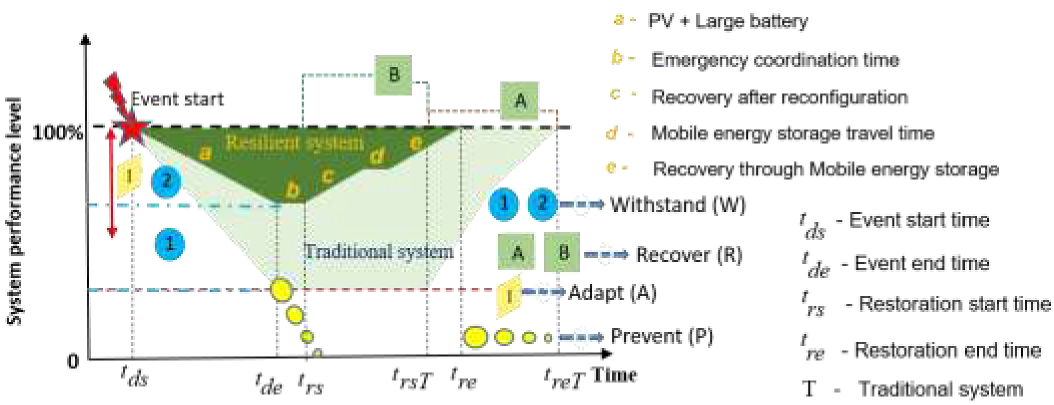

Fig. 4.2. System performance curve with four major attributes to resilience (*Source: Author*)

The fault occurs at t_{ds} and can continue for a few minutes or hours. During that time, if the system does not have any other resources except grid supply, it might fail to supply all the critical loads (CLs), resulting in system collapse. However, if the resources, such as MGs, are available, then they can supply the CLs, which are connected inside the MG. On the contrary, the CLs, which are outside the MG, cannot be supplied if the grid fails. Moreover, the system can withstand some of the CLs during the events to minimize the impact of an event, represented as 1 and 2 (in the blue circle) in Fig. 4.2. After t_{de}, the restoration process begins. However, switching the topology or DERs into operation requires considerable time. Thus, it can be started from t_{rs} and end up to t_{re}. Moreover, the restoration can be performed when alternative resources or paths are sufficient because the same path may not have the grid supply to satisfy the load if a fault occurs between the lines. Thus, during that period, the DERs with TLs can partially or fully satisfy the load demand. With this objective, less restoration time is required than usual, as shown in Fig. 4.2 (A and B). Here, B considers the traditional system, which requires a longer time to restore the loads. Moreover, the recovery is divided into three phases: c, d, and e. During the c-phase, the restoration is conducted through the reconfiguration technique. However, sometimes, due to multiple events, it cannot restore all the CLs. Thus, MSU is added, and it requires a few minutes to reach the load center presented as d-phase. Then, the remaining CLs can be recovered through MSU, presented as e-phase.

Furthermore, as far as adaptability is concerned, sufficient resources, including DERs, storage, and alternative paths, such as TLs, can increase the flexibility of the system. This finding implies that the system can quickly switch from one point to another towards load recovery, indicating that the system could follow better resilient characteristics, presented as I in Fig. 4.2. Finally, the system operator should always consider the assessment of impact after the event; it helps to minimize the total system collapse in the forthcoming event, which is the prevent phase.

To prevent future events, the system should be hardened, a decentralized network should be designed, and a better prediction strategy should be used. In addition, to reduce the outage duration, the recovery time should be fast. This condition can be obtained by system reconfiguration using TL and DERs, as well as the adaptive formation of MG and mobile services, such as MSU, mobile substations, crews, and mobile de-icing devices. Considering this design, the system can eventually be robust, and the power loss and outages can be reduced. A detailed discussion of introduced WRAP indices is presented in the following section.

4.3. Resilient system formulation

4.3.1. Objective function

This section deals with problem formulation, such as objective functions, system constraints, and resilience indices. The objective is to minimize operational costs and maximize critical load restoration while satisfying operational constraints and ensuring radial operation. Equations (4.1) and (4.2) present the objective function of operational cost and maximization of critical load pickup, respectively.

$$\min_{t \in T} \left| \left(\sum_{r \in R} C_r P_{r,t} \right) + \left(\sum_{d \in D} C_d P_{d,t} \right) + \left(\sum_{b \in B} C_b \, P_{b,t} \right) + \left(\sum_{l \in L} C_l \, P_{l,t} \right) + \left(\sum_{h \in H} C_h D_{h,t} \right) \right| \tag{4.1}$$

$$max \sum_{j=1}^{N} . \sum_{k=1}^{M_j} P_{CL,k}^{j} \tag{4.2}$$

4.3.2. System constraints

For each MG and at each timeslot, the sum of the total generated power by DER and diesel generator (DG) units, charging/discharging power of battery energy storages (BESs), and curtailed load must be equal to the total load expressed in (4.3). The ramping up and down of the DG unit limits is expressed in (4.4), (4.5), and (4.6). The curtailment of load demand must not increase the total load, as expressed in (4.7). In storage unit constraints, the permissible charging/discharging limits of power are expressed in (4.8) and (4.9) with state-of-charge (SOC) limits in (4.10), and simultaneous charging/discharging of the storage unit should be avoided; the constraint can be written as (4.11). Eq. (4.12) represents the relationship between SOC and charging/discharging power.

$$\sum_{r \in R_i} P_{r,t}^{i} + \sum_{d \in D_i} P_{d,t}^{i} + \sum_{b \in B_i} (P_{b,t}^{i,dis} - P_{b,t}^{i,ch}) = \sum_{l \in L_i} (P_{LD,l,t}^{i} - P_{l,t}^{i}) \qquad \forall i, t. \tag{4.3}$$

$$P_d^{min} \leq P_{d,t}^{i} \leq P_d^{max} \qquad \forall_g, t, i \tag{4.4}$$

$$P_{d,t}^{i} - P_{d,t-1}^{i} \leq R_{U,d} \qquad \forall_{g}, t, i \tag{4.5}$$

$$P_{d,t-1}^{i} - P_{d,t}^{i} \leq R_{D,d} \qquad \forall_{g}, t, i \tag{4.6}$$

$$0 \leq P_{l,i}^{t} \leq P_{TL,t}^{i} \qquad \forall_{g}, t, i \tag{4.7}$$

$$0 \leq P_{b,t}^{i,ch} \leq \delta_{b,t}^{i,ch} P_{b,t}^{ch,max}, \delta_{b,t}^{i,ch} \in \{0,1\} \qquad \forall_{b}, t, i \tag{4.8}$$

$$0 \leq P_{b,t}^{i,dis} \leq \delta_{b,t}^{i,dis} P_{b,t}^{dis,max}, \delta_{b,t}^{i,dis} \in \{0,1\} \ \forall_{g}, t, i \tag{4.9}$$

$$E_{b}^{min} \leq E_{b,t}^{i} \leq E_{b}^{max} \qquad \forall_{g}, t, i \tag{4.10}$$

$$\delta_{b,t}^{i,ch} + \delta_{b,t}^{i,dis} = 1 \qquad \forall_{g}, t, i \tag{4.11}$$

$$E_{b,t+1}^{i} = E_{b,t}^{i} + \left(P_{b,t}^{i,ch} \eta_{b,t}^{ch} \Delta t - P_{b,t}^{i,dis} \eta_{b,t}^{dis} \Delta t \Big/ \eta_{b}^{dis} \right) \qquad \forall_{b}, t, i \tag{4.12}$$

where

B = Index of energy storage units

D = index of DG units

H = Index of MSU units

L = Index of loads

N = Index of disaster scenario considered

M = Index of number of loads pick up by DGs for each scenario

R = Index of renewable DG units

C_b = Operation cost of battery, b

C_d = Unit generation cost of DG d

C_h = Transportation cost of MSU m per kM

C_l= Load shedding cost of load l

C_r = Unit generation cost of renewable generation unit r

D_h= Distance traveled by MSU h in kMs

E_b^{min}, E_b^{max} = Minimum/maximum energy stored in battery b

$E_{b,t}$ = Battery SOC at time instant t

P_b = Active power generation by battery b

$P_{CL,k}^{j}$ = Critical load of k^{th} load point restored after j^{th} extreme event

P_d = Active power generation by DG d

P_d^{min}/P_d^{max} = Minimum/maximum active power by DG d

P_g = Power output of cost of the generator, g after the event

P_l = Load curtailment, l after the event

$P_{LD,l}$ = Total load demand at load point l

P_r= Active power generation by PV

Δt = Timeslot duration

$P_{b,t}^{ch}(P_{b,t}^{ch,max})/P_{b,t}^{dis}(P_{b,t}^{dis,max})$= Charging/discharging power (limit)

4.3.3. Resilience index

The performance of the ADS is evaluated by the proposed resilience quantification framework, such as WRAP. Withstand and recovery indices have the same unit, such as kilo-watt-hour (kWh), and the other two indices, such as the adapt and prevent index, have no unit. The value of these indices depends on the capacity of the system and restoration time (how fast restoration takes place). There is no particular range in these indices except the adaptability index, which ranges from 0 to 1.

A. Withstand

Withstand refers to the coping capacity of the system after the event. It indicates whether the system is completely collapsed or partially collapsed. The system can be a total outage when the grid supply is unavailable and no additional generation unit is available in the system. However, the system with DERs can cope with extreme events and minimize outages. The withstand index ($\Re_W$) can be measured by Eq. (4.13) as follows:

$$\Re_{Wi} = (P_{CLi} - P_{CL0}) \times (t_{de} - t_{ds}) \tag{4.13}$$

where

P_{CLi} = Critical power available after the addition of MG in kW

P_{CL0} = Critical active power available at the end of the event as a reference in kW

t_{de} = Disturbance end time in hour

t_{ds} = Disturbance start time in hour

This index measures the withstanding capability, sometimes called survivability, which can be shown after the events. If the system is able to survive extreme events, then the system can have better-withstanding ability, and critical service interruption can be minimized. With this consideration, this index shows the withstanding capacity in kWh. If it affects the system's survivability in the wake of extreme events, then the system reconfiguration can be done, and load recovery takes place. The fast recovery can enhance resiliency.

B. Recover

The recovery index ($\Re_{\mathrm{R}}$) measures the restored energy after the event, as expressed in Eq. (4.14). Different resources, such as PV, BES, TL, and DG, are used to restore the critical load in the recovery process. In addition, if it still fails to recover all the critical load, then MSU can be used.

$$\Re_{Rj} = \left(P_{CL,j}^{R} - P_{CL,0}\right) \times \left(t_{rs,j+1} - t_{rsj}\right) \tag{4.14}$$

where

$P_{CL,j}^{R}$ = Critical active power available after restoration step j

$P_{CL,0}$ = Critical active power available at the end of the event as reference (without any resource)

$j =$ Steps for critical load recovery

$t_{rs} =$ Restoration start time

$t_{rs,j} =$ Restoration end time after j^{th} step

This index refers to the recovery phase of the resilience framework. Once the event hits the network, the immediate action is the recovery through tile-line arrangement, mobile energy storage service, diesel generator, and island connection. In fact, priority-based restoration is always preferred to avoid a large impact on critical services and the economy. Each step of the recovery process is switched from one service to another, such as til-line, MMG arrangement using island connection, mobile energy storage, etc.

C. Adapt

The stability of the system can be measured through its short circuit capacity (SCC), followed by voltage stability index (VSI), called adaptability index ($\Re_{\mathrm{A}}$), expressed in (4.17). The incorporation of DER is vital to increase the resiliency of the system; however, it affects the SCC of the distribution network. Moreover, the SCC is highly dependent on the voltage magnitudes of the distribution network buses [31]. Thus, the SCC can be considered a VSI for the system, which represents the capacity of loads that can be served by the network [32, 33]. The significance of the SCC, *i.e.*, a high value of short-circuit capacity, indicates that the network can serve more loads. Conversely, low short-circuit capacity indicates that the network is weak to support loads.

As a matter of resilience, the main aim is to serve more loads within a stability limit. Therefore, this index can show the system's stability before, during, and after the HILP event.

The short circuit capacity S_{sc}^{t} is obtained by (4.15), followed by (4.16).

$$S_{sc,j}^{t} = \frac{E_{th,j}^{t}}{Z_{th,j}^{t}} \tag{4.15}$$

$$S_{sc,min,j}^{i} = \frac{2S_{L,j}^{i}\left(1 + \sin \emptyset_{j}^{i}\right)}{E_{th,j}^{t}} \tag{4.16}$$

$$\Re_{A,j} = VSI_{j} = \frac{1}{N_{bus}^{i}} \sum_{1=1}^{N_{bus}^{t}} \left(\frac{S_{sc,min,j}^{i}}{S_{sc,j}^{i}}\right) \tag{4.17}$$

where

$E_{th,j}^{i}$ and $Z_{th,j}^{i}$ are Thevenin voltage and impedance of bus j at the t^{th} stage, respectively.

$S_{L,j}^{i}$ and $\emptyset_{j}^{i}$ are the apparent power magnitude and power factor angle of bus i at the j^{th} stage, respectively.

VSI_{ij} is the VSI at the j^{th} stage.

$S_{sc,min,j}^{i}$ is the minimal short circuit capacity.

The adaptability index defines by the voltage stability index and short circuit capacity. The adaptable system can operate in any scenario, and the voltage deviation should be within the limit. If it deviates from the large value, then the system can be treated as less stable or collapse.

D. Prevent

Finally, the preventive measure can be considered from a few outage histories. Two parameters are crucial to prevent future power outages, such as failure rate and outage duration; these parameters should be reduced. Thus, the system's robustness and responsiveness should be improved by MMG, reconfiguration, and mobile services. The consequence of power outages in terms of life threats, outage cost, and loss of load can be minimized. The preventive index is expressed in (4.18). The lower value of $\Re_{\text{P}}$ can signify that the system follows better resilient characteristics.

$$\Re_{\mathrm{Pi}} = \sum_{i=1}^{N_i} \left(\Psi_i \times P_{lost_i}\right) \tag{4.18}$$

where

Ψ_i = Total outage duration in i^{th} failure

$P_{lost,i}$ = Total power lost in i^{th} failure

N = Number of failures

Prevent index is crucial for future studies, where the total outage time and the number of failures are taken to measure. By reducing the number of failures or outage duration can significantly enhance resiliency. On the other hand, preventive measures can remarkably save costs, which is discussed in section 4.4.

4.4. Case study and results

To assess the proposed resilience framework, the developed model is applied to the IEEE 33-bus ADS, which comprises four MGs, four TLs, and three MSUs. The total load of the test system is 3715 kW+ j2300 kVAR. Among 33 buses, 10 buses are considered critical load connected buses, as shown in Fig. 4.3. The MG includes the PV, DG, BES units, and load; the available capacity is presented in Table 4.1. The power required for critical load restoration is 1560 kW+ j1285 kVAR. Furthermore, the critical bus data are shown in Table 4.2. In the planning stage, four TLs are placed optimally as $B_8 - B_{21}(T_1)$, $B_9 - B_{15}(T_2)$, $B_{25} - B_{29}(T_3)$, and $B_{18} - B_{33}(T_4)$. In addition, the MSUs are placed optimally as B_{10}, B_{22}, and B_{23} and can travel in accordance with the restoration requirement. Two different studies, such as single and multiple fault analyses, are conducted. Each study has three scenarios with different combinations, such as without resources (WR), DERs, and reconfiguration (REC). In WR, only grid power denoted as G, is used to satisfy the load demand, and in DERs, PV, DG, and BES are used. Finally, in REC, TL and MSU in addition to DER resources, are used to satisfy the CL demand.

Table 4.1 System data

MG	PV (MW)	BES (MW)	DG (MW)	MSU (MW)
1	0.5	0.4	0.2	0.25×3 = 0.75
2	0.5	0.25	0.2	

3	1	0.5×2 = 1	0.25×2 = 0.5	
4	1	0.35×2 = 0.7	0.2×2 = 0.4	

Table 4.2: Critical load data

	Bus	Bus data (kW +j kVAR)	MG
1	4	120 + j80	-
2	7	200 + j100	-
3	8	200 + j100	-
4	10	60+ j20	-
5	14	120 + j80	1
6	18	90 + j40	1
7	21	90 + j40	2
8	24	420 + j200	3
9	27	60+ j25	-
10	30	200 + j600	4
	Total	*1560+ j1285*	

4.4.1. Study 1: Single-fault scenario

If an extreme event occurs and line L_5 is out (as shown in Fig. 4.3), the restoration is performed according to different scenarios, as follows.

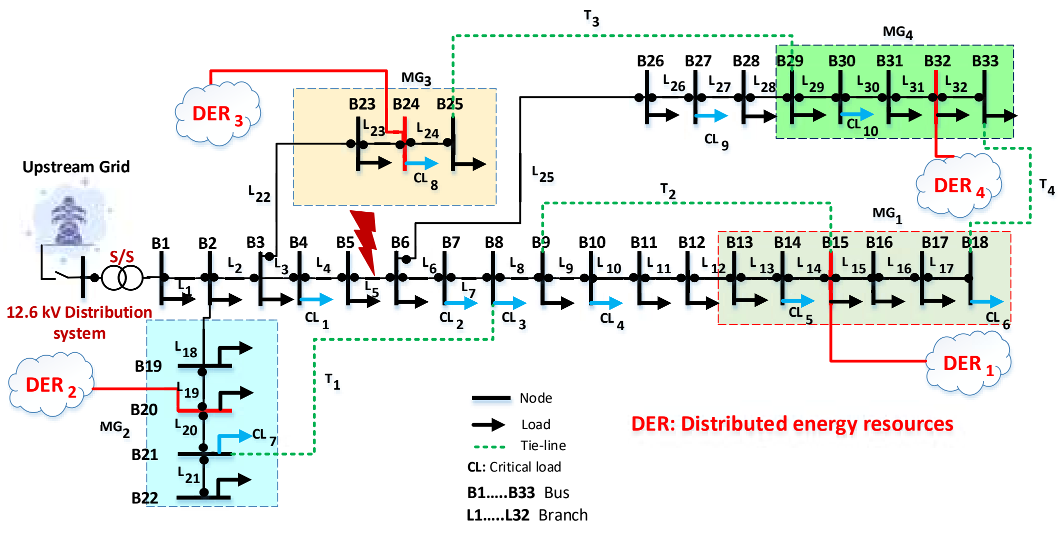

Fig. 4.3 IEEE 33-bus active distribution system

A. Scenario I: Disaster occurs at time 2.00 (PV power = 0 and SOC = 0.9)

Although the grid is available after the event, it can only restore the critical loads such as CL_1, CL_7, and CL_8, but other CLs cannot be restored because the remaining system is outage after L_5. However, with the installation of DERs and formation as MG, they can switch to islanding mode when necessary.

All MGs are in islanding mode after the events, and the critical loads inside the MG can easily be restored. However, the PV is unavailable in this scenario, and some CLs can be restored through BES, as presented in Table 4.3. On the contrary, using REC, the grid supply can be fed directly to CLs through TL and restore all the CLs. Tables 4.3 and 4.4 present the participation of available resources and restoration paths, respectively.

Table 4.3: Available resources corresponding to CL recovery

	G	PV	BES	DG	CL recovered	Open switch
WR	✓	×	×	×	CL_1, CL_7, CL_8,	L_5
DERs	✓	×	✓	×	CL_1, CL_5, CL_6, CL_7, CL_8, CL_{10}	L_5, L_{12}, L_{28}
REC	✓	×	×	×	All	L_5, T_2, T_3, T_4

Table 4.4: Participation

	PV (MW)	DG (MW)	BES (MW)	MSU (MW)	Total load served (MW)	CL served (MW)
DERs	×	0.2	1.95	×	2.79	0.98
REC	×	0	0	×	3.715	1.56

Table 4.5: Resources and restoration path for CL recovery

CL	G	MG	TL	MSU	Recovery path
CL_1	✓	×	×	×	B_1- L_1- L_2 - L_3 - B_4
CL_2	✓	×	✓	×	B_1- L_1- L_{18} -- L_{20} - T_1-L_7-B_7
CL_3	✓	×	✓	×	B_1- L_1- L_{18} -- L_{20} - T_1 – B_8
CL_4	✓	×	✓	×	B_1- L_1- L_{18}-- L_{20} -T_1–L_8 - L_9- B_{10}
CL_5	×	MG_1	×	×	B_{15} - L_{14} - B_{14}
CL_6	×	MG_1	×	×	B_{15} - L_{15} - L_{16} - L_{17}- B_{18}
CL_7	×	MG_2	×	×	B_{20} - L_{20} – B_{21}
CL_8	×	MG_3	×	×	B_{24}
CL_9	✓	×	×	×	B_1- L_1- L_{18} -- L_{20} -T_1–L_7- L_6- L_{25}– L_{26}- B_{27}
CL_{10}	×	MG_4	×	×	B_{32} - L_{31} - L_{30} – B_{30}

B. Scenario-II: Disaster occurs at time 14.00 (PV = available and SOC = 0.2)

In this scenario, the PV power and grid are available to restore the CL after the event. The WR case is the same as scenario 1. In the DER case, all MGs are switched to islanding mode, and the loads connected to MGs are restored. However, the CLs outside the MG, such as CL_2, CL_3, CL_4, and CL_9, cannot be restored. Although the CL_1 is outside the MG, it has been restored due to the available grid power.

Table 4.6: Available resources corresponding to CL recovery

	G	PV	BES	DG	CL recovered	Open switch
WR	✓	×	×	×	CL_1, CL_7, CL_8,	L_5
DERs	✓	✓	×	×	CL_1, CL_5, CL_6, CL_7, CL_8, CL_{10}	L_5, L_{12}, L_{28}
REC	✓	✓	×	×	All	L_5, L_{12}, L_{28}, T_2, T_3, T_4

Furthermore, using REC mode, the MG-connected CL is able to restore itself, and the grid power through TL restores CL outside the MG. Tables 4.6, 4.7, and 4.8 present the resource availability, participation of different resources, and restoration paths, respectively.

Table 4.7: Participation

	PV (MW)	DG (MW)	BES (MW)	MSU (kW)	Total load served (MW)	CL served (MW)
DERs	2.6	×	×	×	2.79	1.04
REC	2.6	×	×	×	3.715	1.56

Table 4.8: Resources and restoration path for CL recovery

CL	G	MG	TL	MSU	Recovery path
CL_1	✓	×	×	×	B_1- L_1- L_2 - L_3 – B_4
CL_2	✓	×	✓	×	B_1- L_1- L_{18} -- L_{20} - T_1–L_7– B_7
CL_3	✓	×	✓	×	B_1- L_1- L_{18} -- L_{20} - T_1 – B_8
CL_4	✓	×	✓	×	B_1- L_1- L_{18} -- L_{20} - T_1–L_8 – L_9 – B_{10}
CL_5	×	MG_1	×	×	B_{15} - L_{14} - B_{14}
CL_6	×	MG_1	×	×	B_{15} - L_{15} - L_{16} - L_{17}- B_{18}
CL_7	×	MG_2	×	×	B_{20} - L_{20} – B_{21}
CL_8	×	MG_3	×	×	B_{24}
CL_9	✓	×	×	×	B_1- L_1- L_{18} -- L_{20} - T_1–L_7– L_6– L_{25}– L_{26}– B_{27}
CL_{10}	×	MG_4	×	×	B_{32} - L_{31} - L_{30} – B_{30}

C. Scenario III: Disaster occurs at time 14.00 (PV = available, and SOC = 0.9)

This scenario is relatively similar to scenario II. If the grid and PV power are available, then the other resources are not required. The MG-connected CL can restore itself, and other CLs can be restored through grid power using TL. Tables 4.9, 4.10, and 4.11 present the detailed analysis of scenario III.

Table 4.9: Available resources corresponding to CL recovery

	G	PV	BES	DG	CL recovered	Open switch
WR	✓	×	×	×	CL_1, CL_7, CL_8,	L_5
DERs	✓	✓	×	×	CL_1, CL_5, CL_6, CL_7, CL_8, CL_{10}	L_5, L_{12}, L_{28}
REC	✓	✓	×	×	All	L_5, L_{12}, L_{28}, T_2, T_3,T_4

Table 4.10: Participation

	PV (MW)	DG (MW)	BES (MW)	MSU (MW)	Total load served (MW)	CL served (MW)
DERs	2.6	×	×	×	2.79	1.04
REC	2.6	×	×	×	3.715	1.56

Table 4.11: Resources and restoration path for CL recovery

CL	G	MG	TL	MSU	Recovery path
CL_1	✓	×	×	×	B_1- L_1- L_2 - L_3 – B_4
CL_2	✓	×	✓	×	B_1- L_1- L_{18} – L_{19} – L_{20} - T_1–L_7– B_7
CL_3	✓	×	✓	×	B_1- L_1- L_{18} – L_{19} – L_{20} - T_1 – B_8
CL_4	✓	×	✓	×	B_1- L_1- L_{18} – L_{19} – L_{20} - T_1–L_8 – L_9 – B_{10}
CL_5	×	MG_1	×	×	B_{15} - L_{14} - B_{14}
CL_6	×	MG_1	×	×	B_{15} - L_{15} - L_{16} - L_{17}- B_{18}
CL_7	×	MG_2	×	×	B_{20} - L_{20}– B_{21}
CL_8	×	MG_3	×	×	B_{24}
CL_9	✓	×	×	×	B_1- L_1- L_{18} – L_{19} – L_{20} - T_1–L_7– L_6– L_{25}– L_{26}– B_{27}
CL_{10}	×	MG_4	×	×	B_{32} - L_{31} - L_{30} – B_{30}

Remark: If the grid is less vulnerable and is a single-fault event, then the grid can supply the CL through TL. Moreover, the capacity of BES can sometimes be insufficient to satisfy the demand, and MG can use the grid power to restore the load. If the grid power and PV generations are available, then the storage power shouldn't be used to be kept for an emergency purpose. Thus, the MG's operation cost can be reduced. DG can also be used when necessary. Usually, it is not preferred due to the high operating cost. Moreover, the MSU is not required to travel in such type of event as long as the CL cannot be restored through any combinations (G, TL, BES, and PV). The final restored network is shown in Fig. 4.4. After the fault happens at L_5, a number of loads can be disconnected; therefore, network reconfiguration is required. Firstly, tie-lines are used to recover the load; the restored network can be seen in Fig. 4.4. (a). Further, if MGs are used with tie-lines, the total load can be restored, and the final restored network is shown in Fig. 4.4. (b).

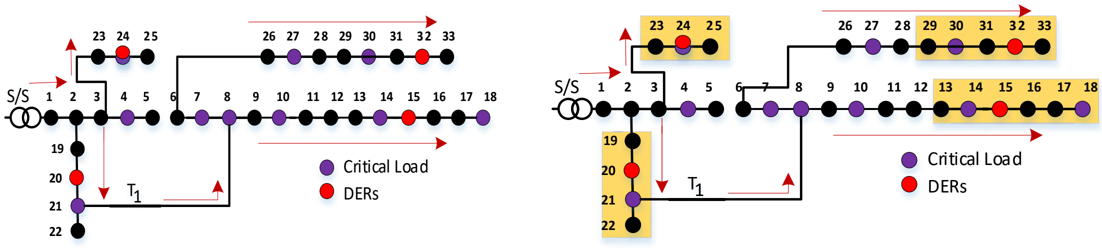

Fig. 4.4. Final restored network (Study-1) (a) Grid with TL (b) Grid, MG, and TL

4.4.2. Study 2: Multiple faults scenario

If a high disruptive event occurs and three lines, such as L_1, L_5, and L_7, are out (shown in Fig. 4.5), then the restoration can be performed according to different scenarios.

A. Scenario I: Disaster occurs at time 2.00 (PV = 0 and SOC = 0.9)

During multiple faults, the grid power to the network is zero because the fault occurs at L_1. Therefore, in the case of WR, the restored CL is zero. In case 2, with the incorporation of DERs, the PV power is zero according to the scenario. However, some critical loads are restored using BES and DG, *i.e.*, 920 kW. Furthermore, reconfiguration techniques are applied with four TLs placed optimally, as shown in Fig. 4.5, and the optimal placements of MSUs are 10, 22, and 23. The remaining critical loads (CL_1, CL_2, CL_3, CL_4, and CL_9) are restored through MGs and MSUs. The MG_3 and MG_4 have increased the capacity through DG and restored critical loads, such as $CL_1$and CL_9, respectively.

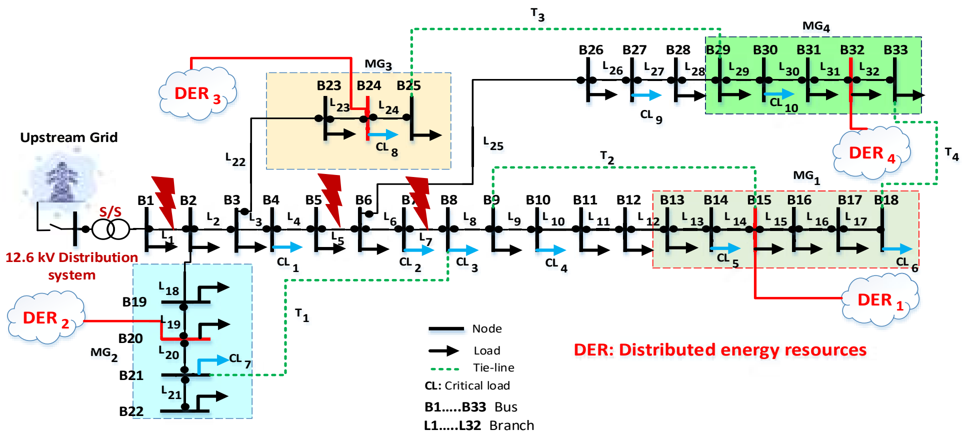

Fig. 4.5. IEEE 33-bus active distribution system with multiple faults

In addition, the MSUs are then moved to locations B_7, B_8, and B_{10}, for the restoration of CL_2, CL_3, and CL_4. For CL_2, a MSU can travel from B_{23} to B_7 and then recover CL_2; for CL_3, other MSUs can stravel from B_{22} to B_8 and recover CL_2; for CL_4, an MSU is in the same place as per the optimal location. The restored network of scenario-I is shown in Fig. 4.6 (a). Besides, the open switch location, participation, and recovery paths are presented in Tables 4.12, 4.13, and 4.14, respectively.

Table 4.12: Available resources corresponding to CL recovery

	PV	BES	DG	MSU	CL recovered	Open switch
WR	×	×	×	×	-	L_1, L_5, L_7
DERs	✓	✓	✓	×	CL_5, CL_6, CL_7, CL_8, CL_{10}	L_1, L_5, L_7, L_{12}, L_{28}
REC	✓	✓	✓	✓	All	L_1, L_4,, L_5, L_7, L_8, L_9, L_{10}, L_{12}, L_{26}, T_2, T_3, T_4

Table 4.13: Participation

	PV (MW)	DG (MW)	BES (MW)	MSU (MW)	Total load served (MW)	CL served (MW)
DERs	×	0.85	1.95	×	2.48	0.92
REC	×	1.3	1.95	0.75	3.175	1.56

Table 4.14: Resources and restoration path for CL recovery

CL	MG	TL	MSU	Recovery path
CL_1	MG_3	×	×	B_{24}- L_{23}- L_{22} - L_3 – B_4
CL_2	×	×	✓	MSU_2 – B_4
CL_3	×	×	✓	MSU_3- B_7
CL_4	×	×	✓	MSU_1 – B_8
CL_5	MG_1	×	×	B_{15} - L_{14} - B_{14}
CL_6	MG_1	×	×	B_{15} - L_{15} - L_{16} - L_{17}- B_{18}
CL_7	MG_2	×	×	B_{20} - L_{20}– B_{21}
CL_8	MG_3	×	×	B_{24}
CL_9	MG_4	×	×	B_{32} - L_{31} ….- L_{27} – B_{27}
CL_{10}	MG_4	×	×	B_{32} - L_{31} - L_{30} – B_{30}

B. Scenario II: Disaster occurs at time 14.00 (PV = available and SOC = 0.2)

As shown in Tables 4.15 and 4.16, considering WR, the entire system is blackout as the grid fails. In addition, no resources are used to restore the loads after the events. By using DERs, and according to the scenario, the PV power is available, but SOC is 0.2. The maximum critical load can be restored using PV and DG.

Table 4.15: Available resources corresponding to CL recovery

	G	PV	BES	DG	MSU	CL recovered	Open switch
WR	×	×	×	×	×	-	L_1, L_5, L_7
DERs	×	✓	×	✓	×	CL_5, CL_6, CL_7, CL_8, CL_{10}	L_1, L_5, L_7, L_{12}, L_{28}
REC	×	✓	×	✓	✓	All	L_1, L_2, L_4, L_5, L_7, L_8, L_9, L_{10}, L_{12},T_2, T_3, T_4

Table 4.16: Participation

	PV (MW)	DG (MW)	BES MW)	MSU (MW)	Total load served (MW)	CL served (MW)
DERs	2.4	0.45	0	×	2.48	0.92
REC	2.4	0.65	0	0.5	3.36	1.56

Table 4.17: Resources and restoration path for CL recovery

CL	MG	TL	MSU	Recovery path
CL_1	MG_3	×	×	B_{24}- L_{23}- L_{22} - L_3 – B_4
CL_2	-	×	✓	MSU_2 – B_7
CL_3	MG_2	T_1	×	B_{20}- L_{20} - T_1 – B_8
CL_4	MG_1	×	✓	MSU_1 – B_{10}
CL_5	MG_1	×	×	B_{15} - L_{14} – B_{14}
CL_6	MG_1	×	×	B_{15} - L_{15} - L_{16} - L_{17} – B_{18}
CL_7	MG_2	×	×	B_{20} - L_{20} - B_{21}
CL_8	MG_3	×	×	B_{24}
CL_9	MG_4	×	×	B_{32} - L_{31} ….- L_{27} - B_{27}
CL_{10}	MG_4	×	×	B_{32} - L_{31} - L_{30}- B_{30}

Furthermore, in the REC case, the capacity of MG_3 is increased through DG, and critical loads, such as CL_1, are restored. Similarly, with the increased capacity of MG_4, the critical loads CL_2 and CL_9 can be restored. In addition, the MSU is then moved to the locations, such as B_{10}, for the restoration of CL_4. For CL_4, no travel is required because an MSU is in the same place as the optimal location. For CL_2, the MSU at bus B_{22} can travel to B_7. CL_3 can be restored through T_1 using MG_2. The final restored network can be seen in Fig. 4.6 (b), and Table 4.17 shows the responsible resources and path for restoration.

C. Scenario III: Disaster occurs at time 14.00 (PV = available and SOC = 0.9)

As reported in Tables 4.18 and 4.19, considering WR, the entire system is blackout as the grid fails. In addition, no resources are used to restore the loads after the events. In case 2, and according to the scenario, the PV power is available, and SOC is 0.9. The critical load, i.e., 920 kW, can be restored using PV and BES restoration operation, as shown in Table 4.20, and the restored network is shown in Fig. 4.6 (c). Furthermore, the RECON technique increases MG capacities through BES, and restoration operation is performed, as discussed in Table 4.20.

Table 4.18: Available resources corresponding to CL recovery

	PV	BES	DG	MSU	CL recovered	Open switch
WR	×	×	×	×	-	L_1, L_5, L_7
DERs	✓	✓	×	×	CL_5, CL_6, CL_7, CL_8, CL_{10}	L_1, L_5, L_7, L_{12}, L_{18}, L_{22}, L_{28}
REC	✓	✓	×	×	All	L_1, L_2, L_4, L_5, L_7, L_8, L_{10}, L_{18}, L_{12},T_3, T_4

Tables 4.19: Participation

	PV (MW)	DG (MW)	BES (MW)	MSU (MW)	Total load served (MW)	CL served (MW)
DERs	2.4	×	0.7	×	2.48	0.92
REC	2.4	×	1.4	×	3.55	1.56

Table 4.20: Resources and restoration path for CL recovery

CL	MG	TL	MSU	Recovery path
CL_1	MG_3	×	×	B_{24}- L_{23}- L_{22} - L_3 - B_4
CL_2	MG_4	×	×	B_{32} - L_{29} .... L_{25} - L_6- B_7
CL_3	MG_3	T_1	×	B_{20}- L_{20} - T_1 – B_8
CL_4	MG_1	T_2	×	B_{15} - T_2 – L_9- B_{10}
CL_5	MG_1	×	×	B_{15} – L_{14}- B_{14}
CL_6	MG_1	×	×	B_{15} - L_{15} - L_{16} - L_{17}- B_{18}
CL_7	MG_2	×	×	B_{20} - L_{20} – B_{21}
CL_8	MG_3	×	×	B_{24}
CL_9	MG_4	×	×	B_{32} - L_{31} ….- L_{27}- B_{27}
CL_{10}	MG_4	×	×	B_{32} - L_{31} - L_{30}- B_{30}

Remark: In the event of multiple faults, DG and MSU's participation is vital for restoration. The emergency resources are integrated because DG is highly expensive, and the recovery time becomes higher using MSU because the grid supply fails and the load point cannot be reached through TL. However, life threats and critical services should be considered. On that premise, resourcefulness is extremely important during multiple event scenarios. All the CLs can be restored using reconfiguration techniques. On the contrary, as reported in Tables 4.12, 4.15, and 4.18, the number of open switches is more in multiple fault scenarios than in a single fault. Thus, line switching is also important to manage priority-based restoration.

After multiple faults, a maximum number of loads are disconnected; therefore, critical load restoration is extremely urgent, and so network reconfiguration is required. Firstly, MGs with three mobile energy storage units are used, but still, a number of loads are disconnected (Fig. 4.6. (a)). Secondly, tie-line, MGs, and mobile energy storage are used to restore the load. Here, all the loads can be restored; however, mobile energy storage can increase the cost and recovery time (Fig. 4.6. (b)). Finally, the capacity of the energy sources is increased, and with tie-line, all the load can be restored in a short span of time (Fig. 4.6.(c)).

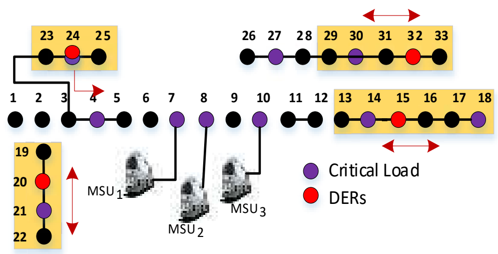

(a)

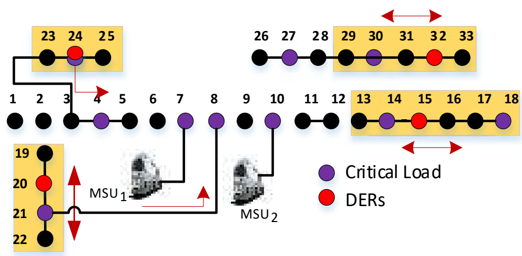

(b)

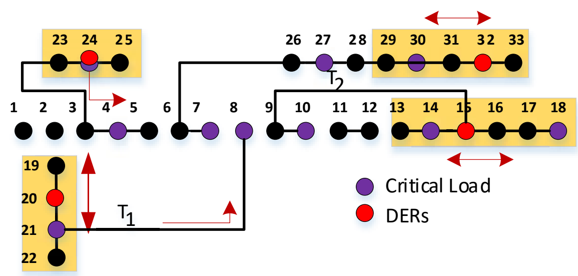

(c)

Fig. 4.6. Final restored network (Study-2) (a) Scenario I, (b) Scenario II, (c) Scenario III

4.4.3. Performance comparison with resilience index

This section evaluates four resilience indices corresponding to three scenarios. Each index has its own significance, reported in a tabular form, along with the improvement values.

During the event, the contribution of DERs is pivotal because the grid might fail to supply the CLs. Thus, the CLs should be restored as quickly as possible. Table 4.21 shows the $\Re_W$ value, which indicates that the CL is available after the event. According to scenarios I, II, and III, the availability of resources can withstand the system in the wake of extreme events.

Table 4.21: Withstand capacity and its improvement

Case-1- Single fault		
Scenario	$\Re_W$ (MWh)	Coping capacity increased (MW)
I	0.35	0.98
II	0.41	1.04
III	0.41	1.04
Case-2- Multiple faults		
I	0.83	0.83
II	0.92	0.92
III	0.92	0.92

Further, it has been compared with WR and DERs; the coping capacity is increased using DERs. Scenarios II and III have the same value because the PV power is available in both cases; thus, sufficient energy can restore the CL as per the feasibility. In this case, TL and MSU are not considered. The grid is unavailable under multiple faults; thus, with DERs, the system can restore the maximum loads inside the MGs.

Tables 4.22: Recovery and its improvement

Case-1- Single fault			
Scenario	Resource	$\Re_R$(MWh)	CL restoration improvement (MW)
I	G+MG	0.01603	0.98
	G+MG+TL	0.03348	1.56
II	G+MG	0.017056	1.04
	G+MG+TL	0.06417	1.56
III	G+MG	0.017056	1.04
	G+MG+TL	0.06417	15.6
Case-2- Multiple faults			
I	G+MG	0.0382	0.92
	G+MG+TL	0.069	1.38
	G+MG+TL+MSU	3.96	1.56
II	G+MG	0.05038	1.1
	G+MG+TL	0.06318	1.30
	G+MG+TL+MSU	3.30	1.56
III	G+MG	0.0115	0.92
	G+MG+TL	0.02896	1.56
	G+MG+TL+MSU	-	-

Recovery phase starts from t_{rs}. In an initial attempt, the grid and MG can restore the CLs. However, these resources cannot restore all the CLs, and then TL is used with grid and MG. In the single-fault analysis, MSUs are not required because, through TL, all CLs can be restored, as shown in Table 4.22. On the contrary, in the multiple faults, the reconfiguration of the system is crucial, and MSUs are used, as reported in Table 4.22. Moreover, the restoration improved using a combination of resources. In Scenario III, MSUs do not participate because the available PV power and BES can restore all the CLs through TL.

As far as adaptability is concerned, the system should be stable irrespective of the event that could happen in the network. On the other hand, the voltage should be in the limiting range to avoid system collapse. Thus, the voltage stability index is measured in this study, presented in Table 4.23, corresponding to various scenarios.

Table 4.23: VSI, and its improvement

Case-1- Single fault		
Scenario	$\Re_A$ (pu)	Stability improvement (pu)
I	0.7764	0.1159
II	0.7653	0.127
III	0.6148	0.2775
Case-2- Multiple faults		
I	0.8745	0.8745
II	0.7597	0.1148
III	0.6012	0.2504

Table 4.23 presents the VSI and its improvement using different resource combinations. It can be seen that the worst value of VSI is 0.8923, which is taken as the reference, and the best value of VSI in this study is 0.6012, considering the critical load recovery. Accordingly, the stability improvement has shown in percentage. As noted in scenario III considering multiple faults, the stability is reached maximum because all the CL has been restored through MG and TL, where MSU is not required.

Tables 4.24: Prevent and reduced impact

Case-1- Single fault			
Scenario	Resource	$\Re_P$(MWh)	Reduced impact
I	WR	1.86	-
	G+MG+TL	0.6	67.75 %
II	WR	1.86	-
	G+MG+TL	0.522	71.94 %
III	WR	1.86	-
	G+MG+TL	0.522	71.94 %
Case-2- Multiple faults			
I	WR	9.36	-
	G+MG+TL	0.66	93.58%
	G+MG+TL+MSU	0.189	97.98 %
II	WR	9.36	
	G+MG+TL	0.4810	94.86 %
	G+MG+TL+MSU	0.2764	97.04 %
III	WR	9.36	
	G+MG+TL	0.647	93.08 %
	G+MG+TL+MSU	-	-

To prevent future power outages, past experience and outage data are critically important. The system operator should analyze the outage data to prepare for future events. The impact of the power outage mainly depends on the failure rate (α_i) and outage duration (Ψ_i). To minimize the failure rate, the system should be hardened; that is, a decentralized network and better prediction strategy should be formed. On the contrary, to reduce the outage duration, the recovery should be faster, and this condition is possible through system reconfiguration using TL and DERs, and the adaptive formation of MGs and mobile services, such as MSU, mobile substation, crews, and mobile de-icing devices.

In the proposed system, the outage duration is minimized using different resources. The minimization of the failure rate is out of the scope of this study. In this case, the line repair is 2 hours for each traditional system after the event ends, and after the reconfiguration, the system follows the exact recovery time from the simulation. Table 4.24 shows the preventive index and reduced impact in terms of percentage.

Table 4.25: Major power outages in 2020

Sl No.	Event Date	Duration (hours)	Loss (MW)	affected customer
1	01/17/2020	4.75	87	67864
2	02/17/2020	8.08	91	70000
3	03/16/2020	69	165	110800
4	08/14/2020	27.75	1680	> 500000
5	08/16/2020	34.56	1580	> 500000
6	08/18/2020	7	917	>200000
7	09/05/2020	3.28	986	> 200000
8	09/7/2020	42.73	610	172000
9	09/27/2020	20.83	337	102267
10	10/25/2020	51.46	1218	370000
11	12/17/2020	0.416	35	170000
Total		202.05	7706	

The measured data of the preventive index represent a single failure in 24 hours. However, to verify the importance of the preventive index, α and Ψ should be changed. Thus, outage history data are obtained from [34], representing the California power outage data. The state of California has one of the topmost frequent power outages in the united states. In 2020, the major power outage across California was 11, as shown in Table 4.25. The evaluation of $\Re_{\mathrm{P}}$ with different α and Ψ is discussed as follows. Tables 4.26 and 4.27 present the preventive index with constant and reduced failure rates, respectively.

- Total duration of power outages in 2020 (Ψ) = 202.05 hrs
- Total loss of power due to outages in 2020 = 7706 MW
- Total number of failures (N) = 11.
- As per Eq. (4.18), the value of $\Re_{\mathrm{Pi}} = \ 219189.3\ \mathrm{MWh}$

Table 4.26 presents the prevent index for constant failure rate (N =11) and different Ψ. The outage duration is reduced (assume recovery is faster). Furthermore, considering the reduced failure rate, the prevent index is reduced, as shown in Table 4.27. As far as the reduced preventive index is concerned, it directly impacts the outage cost. According to the United States Department of Energy, outages cost an average of about $18 billion to $53 billion per year in the United States. So, boosting the power system's resiliency is essential.

Tables 4.26: Constant failure rate

Sl No.	Ψ (hours)	$\Re_{\mathrm{P}}$(MWh)
1	1/4	109594.6
2	1/3	73063.1
3	1/2	54797.32

Table 4.27: Reduced failure rate

Sl No.	N	$\Re_{\mathrm{P}}$(MWh)
1	9	156496.4
2	6	120177.3
3	3	12533.53

The outage cost can be estimated by viewing the values from Tables 4.26 and 4.27. For example, the outage cost can be calculated as: loss of load (MWh) × value of loss of load ($/MWh)

Let us consider N =11, Ψ =202.05, loss of load = 219189.3

outage cost = $219189.3\ \times 4000 = \$876{,}757{,}200$ (Assumed value of loss of load (VOLL) = 4000)

By considering Table 4.26 and Table 4.27, the outage costs are $219,189,280 and $50,134,120 It is noted that a significant amount of cost can be saved by designing a resilient system.

4.5. Summary

This chapter presents a novel resilience quantification framework, WRAP, to design a resilient ADS in the wake of extreme events. With the WRAP framework, the coping capacity, fast recovery, system stability, and preventive measure are quantified during and after the event, and the enhancement of these indices is also discussed. Moreover, the resiliency of the system is measured with a different scenarios (in terms of event time and resource availability), where the available resources are utilized optimally. Furthermore, MSU is added, and its participation is vital for critical load restoration with multiple fault scenarios. The result of the applied test system has proven that resourcefulness is the prior requirement in the context of resilience; it can minimize the catastrophic consequences of an extreme unfolding event. This study is limited to a single renewable source, such as PV. However, in future research, the integration of more renewable, ancillary devices, and hardening plans can be considered to enhance the robustness and fast recovery of the system. Furthermore, better prediction techniques using machine learning can be applied to minimize future damages for preventive measures. The proposed framework can provide a better planning and operation scheme, which can be applied to the standard test system to quantify the resilience characteristics and compare them with existing studies.

References

[1] M. Panteli and P. Mancarella, "The grid: Stronger, bigger, smarter?: Presenting a conceptual framework of power system resilience," *IEEE Power and Energy Magazine,* vol. 13, no. 3, pp. 58-66, 2015.

[2] L. Che, M. Khodayar, and M. Shahidehpour, "Only connect: Microgrids for distribution system restoration," *IEEE power and energy magazine,* vol. 12, no. 1, pp. 70-81, 2013.

[3] Z. Bie, Y. Lin, G. Li, and F. Li, "Battling the extreme: A study on the power system resilience," *Proceedings of the IEEE,* vol. 105, no. 7, pp. 1253-1266, 2017.

[4] D. K. Mishra, M. J. Ghadi, L. Li, and J. Zhang, "Proposing a Framework for Resilient Active Distribution Systems using Withstand, Respond, Adapt, and Prevent Element," in *2019 29th Australasian Universities Power Engineering Conference (AUPEC)*, 2019, pp. 1-6: IEEE.

[5] X. Wu, Z. Wang, T. Ding, X. Wang, Z. Li, and F. Li, "Microgrid planning considering the resilience against contingencies," *IET Generation, Transmission & Distribution,* vol. 13, no. 16, pp. 3534-3548, 2019.

[6] M. H. Amirioun, F. Aminifar, and M. Shahidehpour, "Resilience-promoting proactive scheduling against hurricanes in multiple energy carrier microgrids," *IEEE Transactions on Power Systems,* vol. 34, no. 3, pp. 2160-2168, 2018.

[7] L. Che and M. Shahidehpour, "Adaptive formation of microgrids with mobile emergency resources for critical service restoration in extreme conditions," *IEEE Transactions on Power Systems,* vol. 34, no. 1, pp. 742-753, 2018.

[8] M. Nazemi, M. Moeini-Aghtaie, M. Fotuhi-Firuzabad, and P. Dehghanian, "Energy storage planning for enhanced resilience of power distribution networks against earthquakes," *IEEE Transactions on Sustainable Energy,* vol. 11, no. 2, pp. 795-806, 2019.

[9] S. Yao, P. Wang, X. Liu, H. Zhang, and T. Zhao, "Rolling optimization of mobile energy storage fleets for resilient service restoration," *IEEE Transactions on Smart Grid,* vol. 11, no. 2, pp. 1030-1043, 2019.

[10] Y. Liu, Y. Li, H. Xin, H. B. Gooi, and J. Pan, "Distributed optimal tie-line power flow control for multiple interconnected AC microgrids," *IEEE Transactions on Power Systems,* vol. 34, no. 3, pp. 1869-1880, 2018.

[11] S. Lei, C. Chen, Y. Li, and Y. Hou, "Resilient disaster recovery logistics of distribution systems: Co-optimize service restoration with repair crew and mobile power source dispatch," *IEEE*

Transactions on Smart Grid, vol. 10, no. 6, pp. 6187-6202, 2019.

[12] T. Ding, Z. Wang, W. Jia, B. Chen, C. Chen, and M. Shahidehpour, "Multiperiod Distribution System Restoration with Routing Repair Crews, Mobile Electric Vehicles, and Soft-Open-Point Networked Microgrids," *IEEE Transactions on Smart Grid,* 2020.

[13] S. Abbasi, M. Barati, and G. J. Lim, "A parallel sectionalized restoration scheme for resilient smart grid systems," *IEEE Transactions on Smart Grid,* vol. 10, no. 2, pp. 1660-1670, 2017.

[14] P. Bajpai, S. Chanda, and A. K. Srivastava, "A novel metric to quantify and enable resilient distribution system using graph theory and choquet integral," *IEEE Transactions on Smart Grid,* vol. 9, no. 4, pp. 2918-2929, 2016.

[15] G. Huang, J. Wang, C. Chen, J. Qi, and C. Guo, "Integration of preventive and emergency responses for power grid resilience enhancement," *IEEE Transactions on Power Systems,* vol. 32, no. 6, pp. 4451-4463, 2017.

[16] N. L. Dehghani, Y. M. Darestani, and A. Shafieezadeh, "Optimal life-cycle resilience enhancement of aging power distribution systems: A MINLP-based preventive maintenance planning," *IEEE Access,* vol. 8, pp. 22324-22334, 2020.

[17] M. Panteli, P. Mancarella, D. N. Trakas, E. Kyriakides, and N. D. Hatziargyriou, "Metrics and quantification of operational and infrastructure resilience in power systems," *IEEE Transactions on Power Systems,* vol. 32, no. 6, pp. 4732-4742, 2017.

[18] H. Sabouhi, A. Doroudi, M. Fotuhi-Firuzabad, and M. Bashiri, "Electrical power system resilience assessment: a comprehensive approach," *IEEE Systems Journal,* vol. 14, no. 2, pp. 2643-2652, 2019.

[19] M. Amirioun, F. Aminifar, H. Lesani, and M. Shahidehpour, "Metrics and quantitative framework for assessing microgrid resilience against windstorms," *International Journal of Electrical Power & Energy Systems,* vol. 104, pp. 716-723, 2019.

[20] M. Panteli, C. Pickering, S. Wilkinson, R. Dawson, and P. Mancarella, "Power system resilience to extreme weather: fragility modeling, probabilistic impact assessment, and adaptation measures," *IEEE Transactions on Power Systems,* vol. 32, no. 5, pp. 3747-3757, 2016.

[21] H. Farzin, M. Fotuhi-Firuzabad, and M. Moeini-Aghtaie, "Enhancing power system resilience through hierarchical outage management in multi-microgrids," *IEEE Transactions on Smart Grid,* vol. 7, no. 6, pp. 2869-2879, 2016.

[22] X. Liu, M. Shahidehpour, Z. Li, X. Liu, Y. Cao, and Z. Bie, "Microgrids for enhancing the power grid resilience in extreme conditions," *IEEE Transactions on Smart Grid,* vol. 8, no. 2, pp. 589-597, 2016.

[23] J. Najafi, A. Peiravi, and J. M. Guerrero, "Power distribution system improvement planning under hurricanes based on a new resilience index," *Sustainable cities and society,* vol. 39, pp. 592-604, 2018.

[24] C. Shao, M. Shahidehpour, X. Wang, X. Wang, and B. Wang, "Integrated planning of electricity and natural gas transportation systems for enhancing the power grid resilience," *IEEE Transactions on Power Systems,* vol. 32, no. 6, pp. 4418-4429, 2017.

[25] D. N. Trakas, M. Panteli, N. D. Hatziargyriou, and P. Mancarella, "Spatial risk analysis of power systems resilience during extreme events," *Risk Analysis,* vol. 39, no. 1, pp. 195-211, 2019.

[26] Z. Li, M. Shahidehpour, F. Aminifar, A. Alabdulwahab, and Y. Al-Turki, "Networked microgrids for enhancing the power system resilience," *Proceedings of the IEEE,* vol. 105, no. 7, pp. 1289-1310, 2017.

[27] P. Jamborsalamati, M. Hossain, S. Taghizadeh, G. Konstantinou, M. Manbachi, and P. Dehghanian, "Enhancing power grid resilience through an IEC61850-based ev-assisted load restoration," *IEEE Transactions on Industrial Informatics,* vol. 16, no. 3, pp. 1799-1810, 2019.

[28] V. Krishnamurthy and A. Kwasinski, "Effects of power electronics, energy storage, power distribution architecture, and lifeline dependencies on microgrid resiliency during extreme events," *IEEE Journal of Emerging and selected topics in Power Electronics,* vol. 4, no. 4, pp. 1310-1323, 2016.

[29] B. L. Preston *et al.*, "Resilience of the US electricity system: a multi-hazard perspective," *US Department of Energy Office of Policy. Washington, DC,* 2016.

[30] D. K. Mishra, M. J. Ghadi, A. Azizivahed, L. Li, and J. Zhang, "A review on resilience studies in active distribution systems," *Renewable and Sustainable Energy Reviews,* vol. 135, p. 110201, 2021.

[31] Y. Qin, J. Xu, Y. Sun, L. Huang, T. Cui, and H. Xu, "Application analysis on voltage stability index based on the short-circuit capacity in Hubei Power Grid," in *2012 Asia-Pacific Power and Energy Engineering Conference*, 2012, pp. 1-4: IEEE.

[32] S. Li, Z. Zhu, and Y. Li, "Optimal tripping transmission lines scheme based on SCC level and voltage stability," *IET Generation, Transmission & Distribution,* vol. 11, no. 7, pp. 1709-1715, 2017.

[33] G. Deng, S. Fu, K. Shu, and J. Chen, "Local voltage-stability margin based on short-circuit capacity," in *2010 Asia-Pacific Power and Energy Engineering Conference*, 2010, pp. 1-4: IEEE.

[34] Major Disturbances and Unusual Occurrences, Year-to-Date 2020 [Online]. Available: https://www.eia.gov/electricity/monthly/epm_table_grapher.php?t=epmt_b_1

[35] S. Baik, A. L. Davis, J. W. Park, S. Sirinterlikci, and M. G. Morgan, "Estimating what US residential customers are willing to pay for resilience to large electricity outages of long duration," *Nature Energy,* vol. 5, no. 3, pp. 250-258, 2020.

CHAPTER 5

RESILIENT CONTROL-BASED FREQUENCY REGULATION SCHEME OF ISOLATED MICROGRIDS CONSIDERING CYBER ATTACK AND PARAMETER UNCERTAINTIES

Cyber-physical attacks and parameter uncertainties are becoming a compelling issue on load frequency control, directly affecting the resilience (i.e., reliability plus security) of the microgrid and multi-microgrid systems enabled by the internet of things and the 5G communication system. A resilient system aims to endure and quickly restore system transients in the face of extreme events. Therefore, it is critically important to have a resilient system to evade total system failure or blackout to make them attack-resilient. With this objective, this chapter presents a resilience-based frequency regulation scheme in a microgrid under different operating conditions like step and random load changes and wind speed patterns. Furthermore, a cyber-attack model is considered in the problem formulation. To protect against the cyber-attack and parameter uncertainties in the system, different control schemes such as conventional proportional-integral-derivative (PID), type-1 fuzzy PID, and type-2 fuzzy PID are employed, and their robustness characteristics are compared through various performance indices. Besides, the proposed control schemes are validated through a real-time simulation environment, i.e., OPAL-RT. As noted, the proposed type-2 fuzzy PID-based controller provides the most significant improvement in the dynamic performance for frequency regulation compared to that of the others under cyber-attack and uncertainties.

5.1. Introduction

Over the past few decades, extreme events like natural disasters and cyber-attacks have been increasing, eventually impacting the power distribution system infrastructure [1]. Consequently, the power system blackout occurs, which affects social and economic activities. As traditional power networks are largely interconnected systems, they are also affected by cyberattacks [2]. The past decade has seen the rapid development of power system reconfiguration, where the main aim was to convert them from bulk power networks to small-scale networks like microgrids (MGs), and smart grids [3]. Further, MGs can be changed to the islanded mode under fault/attack conditions, supplying the local loads through MG connection [4]. Thus, the deployment of MGs as isolated systems can enhance system resiliency in response to extreme operating conditions such as natural disasters, cyber-attacks, etc. As cyber-attacks have been increasing in the past decades, the power system reconfiguration is also migrating rapidly, like MG, multiple-microgrids (MMGs), and smart grid structure. Thus, a cyber-resilient power system is increasingly important to evade the power system failure which is addressed in this chapter.

In the modern power distribution system, the concept of MG is crucial where distributed energy resources are the key players. However, the integration of intermittent sources like solar and wind could inevitably impact system stability and, in certain instances, it leads to power failure. Moreover, due to intermittencies, such as solar insolation and wind speed, and in addition to the incorporation of power electronic devices into the MGs, the frequency profile can be significantly changed, which is the leading cause of power failure. Thus to ensure a reliable power supply, the participation of electric vehicles (EVs) and energy storage devices could be the solution for meeting the load demand requirements and help in frequency stabilization [5].

As far as the MG and smart grid technology are concerned, they become more reliable and secure by employing information, communication, and control technologies (e.g., internet-of-things, 5G communication systems, etc.) that enable data-exchange information. However, due to the open wireless intrusion interface, hackers can easily falsify the signals transmitted via vulnerable units (e.g., remote terminal units); consequently, the system's stability disrupts, resulting in cyber threats [6]. Moreover, the hacker can inject malicious data at the load point, generation point, breaker, or controller point. This leads to a mismatch in the generation and load demand, resulting in frequency instabilities and power outages [7]. In the past two decades, there have been continuously increasing hacking attacks across the globe. Examples of cyber-attack are in Iran's nuclear power station due to the StuxNet virus and in Ukraine due to KillDisk malware, as presented in [8] and [9], respectively. Thus, serious security challenges need to be adopted in the energy sector. Concerning these challenges, more recent attention has focused on the provision of cyber-resilient through different control schemes, and robust design approaches are discussed as follows. In [10], the cyber-physical resiliency metric is proposed, where the Ukraine cyber-attack is taken as the case study. The work in [11] emphasizes the detection and mitigation scheme of cyber-physical attacks on load frequency control (LFC) with area control error (ACE) as an objective function. Further, the denial-of-service attack models are presented in [12, 13], where the event-triggering approach is considered to defeat the attack on the LFC system. Cheng *et al.* [14] introduced an additional secondary control loop for LFC, considering the denial-of-service attack model.

Furthermore, to ensure a reliable and stable grid, LFC's contribution is momentous, where generator collaboration and a multi-area system through tie-line are established. However, on the verge of cyberattacks, they might fail to control the frequency [15]. Many secure control strategies are introduced to ensure the cyber-resilient-based LFC. However, the existing models have not considered the parameter uncertainties along with a cyber-attack model, which is addressed in this chapter.

This study aims to elucidate a type-2 fuzzy logic control-based resilient frequency regulation scheme of isolated MGs under parameter uncertainties and cyber-attack. It can help power system engineers to understand the scenarios intuitively and the importance of proper control actions according to the available information (such as frequency, load data, generation data, etc.) to ensure resiliency. The key contributions of this chapter are as follows.

- Presenting a cyber-resilient frequency regulation scheme for isolated MGs considering cyber-attack, variation of solar insolation, and wind speed patterns.
- Quantifying the cyber-attack model's impact with different uncertainties on the frequency deviation of isolated MGs using three control methods.
- Studying the stability of the proposed system through the frequency domain approach and statistical analysis.
- Finally, validating the proposed system through the real-time simulation platform using OPAL-RT to show the effectiveness of the proposed controller with regard to resiliency.

The remainder of the chapter comprises five sections. This chapter begins with the introduction section, followed by the system modeling in Section-5.2. Thereafter, the simulation results are discussed in Section-5.3. Further, the extension of simulation work is validated through a real-time platform, presented in Section-5.4. Finally, Section-5.5 gives a brief summary of this chapter.

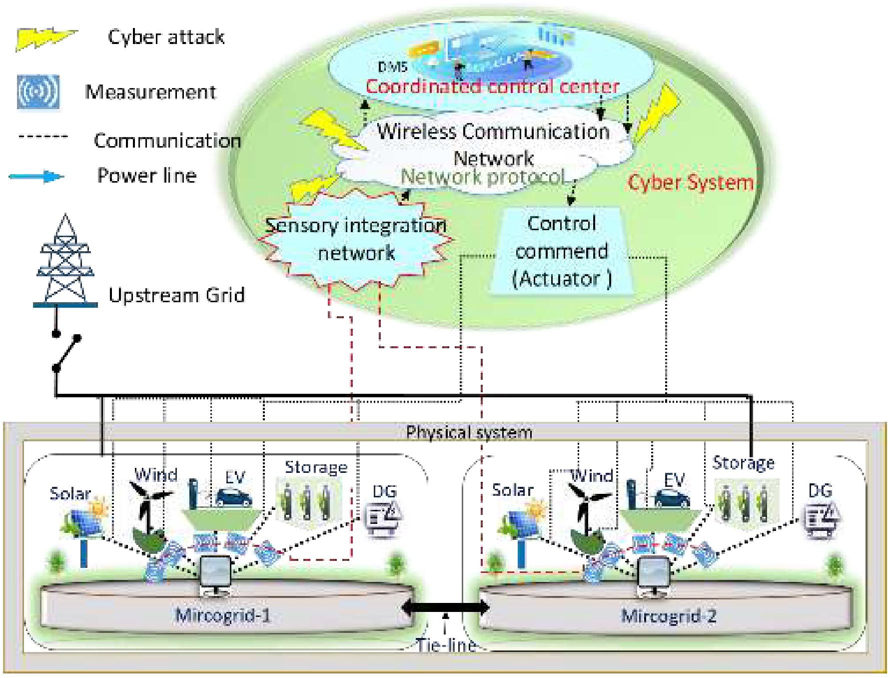

Fig. 5.1. Cyber-physical system (*Source: Author*)

5.2. System configuration and modeling

5.2.1. Microgrid model

In this work, an interconnected microgrid is considered a physical system, and the sensory network is termed a cyber system, as shown in Fig. 5.1. This study aims to show the microgrid's robustness as a means of the cyber-resilient system to evade the power system blackout and provide a stabilized frequency deviation profile considering the uncertainties and cyber-attack. With this objective, the proposed system is designed with two renewable sources such as PV and wind, two storage units (flywheel energy storage devices (FESS) and battery energy storage systems (BESS)), an aggregated electric vehicle, along with a diesel generator (i^{th} control area LFC scheme can be seen in Fig. 5.2). Besides, the distributed management system is employed in the control center to coordinate the MG data and communicate the state information. Further, the sensory network is used to receive the signals from the output (*i.e.*, frequency signal), and then it gives a command to the actuator to change the generation accordingly to minimize the load demand-generation imbalance through set points, which can be done by the controller with tuned values. An attack model is considered in this work, which can change the area control error that could significantly lead to a change in the frequency deviation. Consequently, the system goes into an unstable zone. However, the countermeasure is taken to evade the system failure, and the frequency deviation is forced to zero or a negligible value through different control actions.

The detailed modeling of the proposed system is as follows.

The wind power is modeled with (5.1) and (5.2) [16]. Eq. (5.1) represents the electric power output ($\mathcal{P}_W$) from the mechanical power, and Eq. (5.2) signifies the power output according to the wind speed ($\mathbb{w}_s$) in relation to the rated ($\mathbb{w}_{rated}$), cut-in ($\mathbb{w}_{cut-in}$), and cut-out wind speed ($\mathbb{w}_{cut-out}$), where ρ, $\mathcal{A}_s$, $\mathcal{C}_p$, $\mathbb{w}_s$, and $\mathcal{P}_{rated}$ are the air density in kg/m^3, blade swept-area in m^2, power coefficient, wind speed in m/s, and rated wind power in kW, respectively.

$$\mathcal{P}_W = \frac{1}{2} \times \rho \times \mathcal{A}_s \times \mathcal{C}_p \times \mathbb{w}_s^3 \tag{5.1}$$

$$\mathcal{P}_W = \begin{cases} 0, & \mathbb{w}_s < \mathbb{w}_{cut-in} \text{ or } \mathbb{w}_s > \mathbb{w}_{cut-out} \\ \mathcal{P}_{rated}, & \mathbb{w}_{rated} \le \mathbb{w}_s \le \mathbb{w}_{cut-out} \\ 0.01312\mathbb{w}_s^6 - 0.04603\mathbb{w}_s^5 + 0.3314\mathbb{w}_s^4 + & \\ \quad 3.687\mathbb{w}_s^3 - 51.1\mathbb{w}_s^2 + 2.33\mathbb{w}_s + 366 & \text{else} \end{cases} \tag{5.2}$$

The PV system comprises a combination of series and parallel cells to provide the required voltage and current. The PV panel output depends on the solar insolation, which is a non-linear relationship with the PV current. Accordingly, the PV output ($\mathcal{P}_{PV}$) can be presented in (5.3), where $\eta, \emptyset, \mathcal{A}_m$, θ_A, $\mathcal{P}_{PV}$ are the PV array conversion efficiency, solar insolation in kW/m^2, area of measurement in m^2, and ambient temperature in ℃, and PV output in kW, respectively.

$$\mathcal{P}_{PV} = [1 - 0.005\ (\theta_A + 25)]\eta \times \emptyset \times \mathcal{A}_m \tag{5.3}$$

The equivalent EV model [17] is considered in this study, where a number of EVs are charged at an EV fast-charging station, *i.e.,* vehicle-to-grid is not considered. The total capacity of the aggregated EVs can be estimated in (5.4) and expanded in (5.5), where the control time period is sampled by $\Delta\, t$, t represents a sampled time period, $\mathcal{P}_{EV}(t)$ denotes the total charging power at the station, $\mathcal{N}_{con}(t)$ is the number of connected EVs charging at this station at time t; $\mathcal{P}_{EV\_inv}$ is the average charging power at each charging point of this station (e.g., 50~150kW), initial numbers of charging EVs at time t_0 is represented as $\mathcal{N}_{ini}(t_0)$; newly connected EVs at time *t* are as $\mathcal{N}_{con\_in}(t)$, and the number of disconnected EVs is symbolized as $\mathcal{N}_{plug\_out}(t)$.

$$\mathcal{P}_{EV}(t) = \mathcal{N}_{con}(t) \times \mathcal{P}_{EV\_inv} \tag{5.4}$$

$$\mathcal{N}_{con}(t) = \mathcal{N}_{con}(t-1) + \mathcal{N}_{con\_in}(t) - \mathcal{N}_{plu\_out}(t)$$

$$= \mathcal{N}_{ini}(t_0) + \sum_{j=t_0+1}^{t} (\mathcal{N}_{con\_in}(j) - \mathcal{N}_{plu_{out}}(j)) \tag{5.5}$$

Assume that each EV is charged roughly the same time duration at this station with the same charging power $\mathcal{P}_{EV\_inv}$, and denote this averaged charging time as $k\Delta t$ (*e.g.,* 30 minutes). Then the amount of energy charged at time interval t is calculated as follows.

$$E_{EV}(t) = \mathcal{N}_{con}(t) \times \mathcal{P}_{EV\_inv} \times k\Delta t$$

Further, a storage device such as FESS stores the kinetic energy and the energy density, *i.e.*, $\mathcal{W}_{vol}$ is given in (5.6), where $\sigma_r = \varrho_m\ (l \times \omega_m^2\ )$. This design concept was modeled through a rotating flywheel rotor, which stores mechanical energy and then converts it into electrical energy. Eq. (5.7) gives the flywheel's kinetic energy, followed by (5.8) representing the maximum stored energy value. In (5.6)-(5.8), the parameters are the radial tensile stress (σ_r), material density (ϱ_m), circular path radium (*l*), spinning angular speed (ω_m), flywheel shape ($\mathcal{K}_F$), flywheel volume ($\mathcal{V}$), angular velocity (ω_{FH}), inertia ($\mathcal{I}$), and maximum tensile stress (σ_{r_Max}). Besides, the BESS and diesel generator are also incorporated into the system for load balancing, nullification of harmonics, and further improving the emergency voltage/frequency profile.

$$\mathcal{W}_{vol} = \frac{1}{2} \times \mathcal{K}_F \times \sigma_r \tag{5.6}$$

$$\mathcal{W}_{FESS} = \frac{1}{2} \times \mathcal{I} \times \omega_{FH}^2 \tag{5.7}$$

$$\mathcal{W}_{FESS\_Max} = \frac{1}{2} \times \mathcal{K}_F \times \mathcal{V} \times \sigma_{r\_Max} \tag{5.8}$$

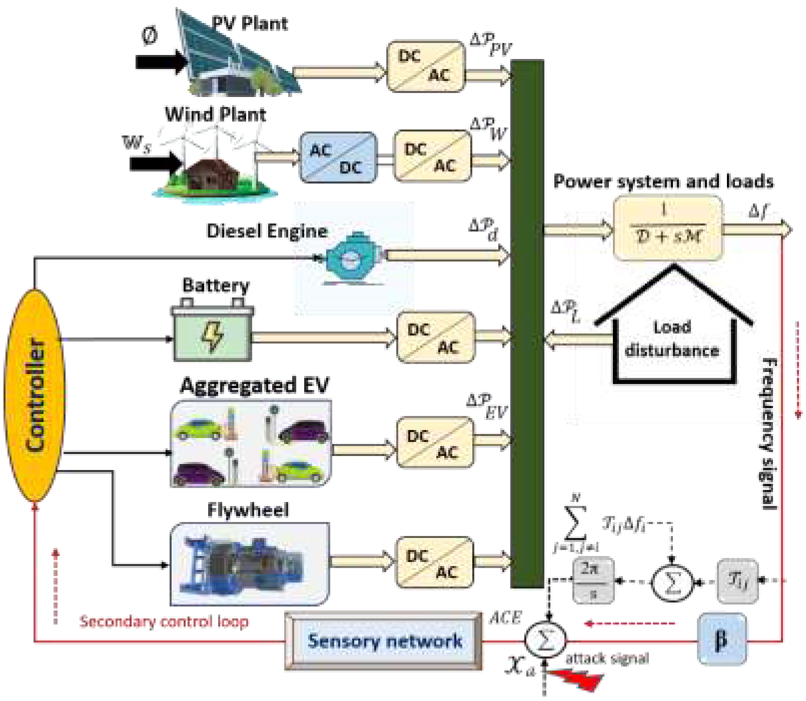

Fig. 5.2. i^{th} control area LFC scheme (*Source: Author*)

The self-healing microgrid system is modeled in this section by implementing the wind, PV, EV, BESS, FESS, and the load unit as shown in Fig. 5.2. It is represented in (5.9)-(5.13) as the linear state-space model in (5.9)-(5.10), followed by (5.11)-(5.13).

$$\dot{x}(t) = Ax(t) + Bu(t) + \mathcal{W}(t) \quad (5.9)$$

$$y\,(t) = Cx(t) + Du(t) \quad (5.10)$$

$$x^T(t) = [\Delta\mathcal{P}_{PV}\ \ \Delta\mathcal{P}_d\ \ \Delta\mathcal{P}_W\ \ \Delta\mathcal{P}_{EV}\ \ \Delta\mathcal{P}_{BESS}\ \ \Delta\mathcal{P}_{FESS}\ \ \Delta f] \quad (5.11)$$

$$\mathcal{W}^T(t) = [\,\Delta\mathcal{P}_L\ \mathfrak{P}_C] \quad (5.12)$$

$$y(t) = \Delta f \text{ and } u(t) = [\Delta u_d\ \ \Delta u_{EV}]^T \quad (5.13)$$

where $x, u, y, \mathcal{W}$ are the state, control input, output and disturbance variables; A, B, C, D are the state, input, output and feedthrough matrices; $\mathcal{P}_d$, $\mathcal{P}_{PV}$, $\mathcal{P}_W$, $\mathcal{P}_{EV}$, $\mathcal{P}_{BESS}$, $\mathcal{P}_{FESS}$, and $\mathcal{P}_L$ represent the diesel generator, solar, wind, electric vehicle, FESS, BESS, and load dynamics, respectively; $\mathfrak{P}_C$ denotes the cyber-attack signal, regarded as the disturbance to the system, which can be $\mathcal{X}_a$ in Fig. 5.2 or a random cyber-attack pattern; Δu_d and Δu_{EV} represent the control input to the diesel generator and EV, respectively; The symbol Δ denotes the change of variable from its nominal value; f is the frequency.

The total generation of the system ($\mathcal{P}_G$) can be presented as in (5.14), and then the balance between generation and load demand ($\Delta\mathcal{P}_e$) can be expressed in (5.15). In (5.14), $\mathcal{P}_{FESS}$ and $\mathcal{P}_{FESS}$ can be positive or negative, indicating storing or releasing the energy, respectively. The power balance equation of the LFC system can be presented as (5.16), followed by the system transfer function in (5.17). Then, the tie-line power change is represented in (5.18) [18, 19]. Finally, the objective function (obj) of the proposed system as an error function, *i.e.*, $ACE_i\ (t)$, is represented in (5.19).

$$\mathcal{P}_G = \mathcal{P}_W + \mathcal{P}_{PV} + \mathcal{P}_{EV} + \mathcal{P}_d + \mathcal{P}_{FESS} + \mathcal{P}_{BESS} \tag{5.14}$$

$$\Delta\mathcal{P}_e = \mathcal{P}_G - \mathcal{P}_L \tag{5.15}$$

$$\Delta f = \frac{\Delta\mathcal{P}_e}{Ms + D} \tag{5.16}$$

$$\mathcal{G}_{Sys} = \frac{\Delta f}{\Delta\mathcal{P}_e} = \frac{1}{Ms + D} \tag{5.17}$$

$$\Delta\mathcal{P}_{tie}^{i} = \sum_{\substack{j=1,\\ j\neq i}}^{\mathcal{N}} \Delta\mathcal{P}_{tie}^{ij} = \frac{2\pi}{s}\left[\sum_{j=1,j\neq i}^{\mathcal{N}} \Delta\mathcal{T}_{ij}\Delta f_i - \sum_{j=1,j\neq i}^{\mathcal{N}} \Delta\mathcal{T}_{ij}\Delta f_{ij}\right] \tag{5.18}$$

where $\mathcal{T}_{ij}$, D, and M signifies the synchronizing coefficient, equivalent damping constant, and equivalent inertia constant of the system; $\Delta\mathcal{P}_{tie}^{i}$ and $\mathcal{N}$ are the tie-line power flow exchange and the number of areas that are interconnected in the system, respectively.

$$ACE_i\ (t) = \beta_i \Delta f_i(t) + \sum_{j=1,j\neq i}^{\mathcal{N}} ⅆ_{ij}\Delta\mathcal{P}_{tie}^{ij}(t) \tag{5.19}$$

where $ⅆ_{ij} = \mathcal{P}_{ri}/\mathcal{P}_{rj}$ denotes the area capacity factor, $\mathcal{P}_{ri}$ and $\mathcal{P}_{rj}$ are the power capacities of the i-th and j-th areas, correspondingly, and ACE is the area control error.

The first term of (5.19) denotes per unit (p.u.) values in terms of frequency bias parameter (β in pu/Hz) and area frequency (Δf_i in Hz), where i is the index of the area. The second term denotes the p.u. values of exchange power in terms of the area capacity factor (p.u.) and tie-line power (p.u.). Further, the dynamic model of an individual system can be expressed as follows in (5.20 - 5.24) [20].

$$\Delta\dot{f_\imath}(t) = \frac{1}{\mathcal{M}_i}\Delta\mathcal{P}_{di}(t) + \frac{1}{\mathcal{M}_i}\Delta\mathcal{P}_{PVi}(t) + \frac{1}{\mathcal{M}_i}\Delta\mathcal{P}_{Wi}(t) + \frac{1}{\mathcal{M}_i}\Delta\mathcal{P}_{EVi}(t) - \frac{1}{\mathcal{M}_i}\Delta\mathcal{P}_{Li}(t) - \frac{\mathcal{D}_i}{\mathcal{M}_i}\Delta f_i(t) \tag{5.20}$$

$$\Delta\dot{\mathcal{P}_{d\imath}}(t) = \frac{1}{\mathcal{T}_{di}}\Delta u_{di}(t) - \frac{1}{\mathcal{T}_{di}}\Delta\mathcal{P}_{di}(t) \tag{5.21}$$

$$\Delta\dot{\mathcal{P}}_{PVi}(t) = \frac{1}{\mathcal{T}_{PVi}}\Delta\phi_i(t) - \frac{1}{\mathcal{T}_{PVi}}\Delta\mathcal{P}_{PVi}(t) \tag{5.22}$$

$$\Delta\dot{\mathcal{P}}_{Wi}(t) = \frac{1}{\mathcal{T}_{Wi}}\Delta\mathbb{W}_{si}(t) - \frac{1}{\mathcal{T}_{Wi}}\Delta\mathcal{P}_{Wi}(t) \tag{5.23}$$

$$\Delta\dot{\mathcal{P}}_{EVi}(t) = \frac{1}{\mathcal{T}_{EVi}}\Delta u_{EVi}(t) - \frac{1}{\mathcal{T}_{EVi}}\Delta\mathcal{P}_{EVi}(t) \tag{5.24}$$

5.2.2. Cyber-attack

In the last few decades, the risk and severity of cyber-threat phenomena have considerably increased in the power system sector [21]. Moreover, in an LFC system, two critical parameters, *i.e.*, frequency and tie-line power, are significantly important and potentially targeted by hackers. Through communication channels, the hacker can falsify these parameter values to make the system more vulnerable. Moreover, the attack can be made through the cyber layer or the physical layer (system or plant), where data-exchange information or other communications are being handled. Considering the cyber layer attack can be a data integrity attack or denial of service attack [13, 22]. On the other hand, considering the physical layer's attack, the load can be changed to make the frequency unstable via an internet-based or direct approach termed a resonance attack [7]. Under the data integrity attack, the hacker can

- replace the measurement value termed as replay attack;
- falsify the actual signal, known as a false data injection attack;
- cancel the effect of attack by estimating the system's output, and then subtract it from estimation reading known as a covert attack.

Further, a false data injection attack is classified into two types: extraneous attack and scaling attack, as discussed below.

i. *Extraneous attack*: In this type of attack, the measured value ($\mathcal{M}_{mea}$) is the addition of actual value ($\mathcal{M}_{actual}$) and disturbance signal ($\mathcal{X}_a$), as given in (5.25). The disturbance can be signum, sinusoidal, ramp, step, or random signal.

$$\mathcal{M}_{mea} = \mathcal{M}_{actual} + \mathcal{X}_a \tag{5.25}$$

ii. *Scaling attack*: The actual value of measurement can be multiplied by the attack parameter, as in (5.26).

$$\mathcal{M}_{mea} = \mathcal{K}_a \times \mathcal{M}_{actual} \tag{5.26}$$

where, $\mathcal{K}_a$ is the scaling attack constant.

In this chapter, the extraneous attack is considered in two forms; one is the cyber-attack pattern-1 ($\mathcal{X}_a$), as expressed in (5.27) and shown in Fig. 5.3(b), and the other one is cyber-attack pattern-2 as a random signal presented in Fig. 5.3(c), which can be placed before the actuator. These two attacks are considered in this work, and for counterbalance, a secondary controller is employed, designed through the fuzzy logic approach. The attack input of pattern-1 is given as $\mathcal{X}_a$, where the y_i is the system output as a function of frequency (Δf). The given cyber-attack model ($\mathcal{X}_a(t)$) is taken from [7], where it was applied at the load point; however, it is applied at the sensor point in this study.

For instance, let the output signal generated from a signal generator be a sine wave with a delay component of 0.25. Further, a simple Matlab program can be embedded in the system to make a new signal referred to as a cyber-attack in this study, as shown in Fig. 5.3 (a-b). With the cyber-attack signal, Eq. (5.19) can be modified as (5.28).

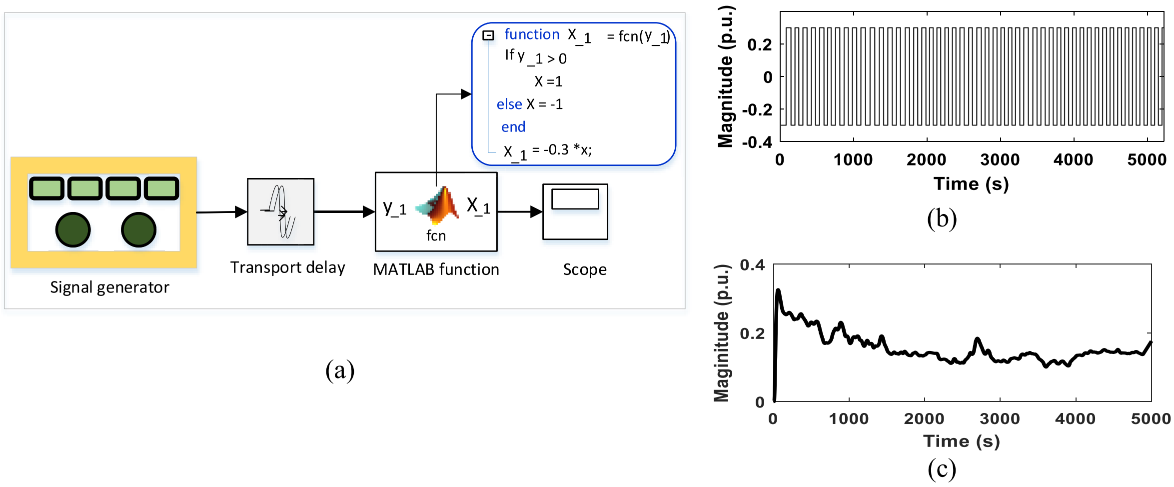

Fig. 5.3. Cyber-attack signal generation (a) Simulink model of signal generation, (b) Cyber-attack signal pattern-1 generated from Simulink model, (c) Cyber-attack signal pattern-2 as a random signal

$$\mathcal{X}_a(t) = -0.3 \times sign\left(y_i(t - 0.25)\right) \tag{5.27}$$

$$sign\ (p) = \begin{cases} 1, & p > 0; \\ -1, & p \leq 0; \end{cases}$$

$$ACE_{i\_m}(t) = \beta_i \Delta f_i(t) + \sum_{j=1, j\neq i}^{N} a_{ij} \Delta \mathcal{P}_{tie}^{ij}(t) + \mathcal{X}_a(t) \tag{5.28}$$

where $\mathcal{X}_a(t)$ is the cyber attack signal in (5.28).

Generally, the LFC system has been studied with the presumption of load deviation, which is very frequent. However, far too little attention has been paid to the cyber-attack on the LFC system. The issue has grown in importance in light of major power outages due to cyber-attack such as Ukraine and Iran power plant attacks. Therefore, this study considers the cyber-attack as well as the load disturbance on the LFC system. To distinguish the level of fault, whether the system is affected by load change or due to a cyber-attack, the cumulative-sum (CUSUM) based detection scheme is applied in this study. The CUSUM checks the threshold value, either it is greater or lower, through the routine calculation of the difference between the current sample and the preceding sample. During steady-state, the sample difference is presumed to be zero or fixed [23]. However, in the wake of events, either load deviation or cyber-attack, the deviation in frequency and the corresponding CUSUM will be dramatically high, which is discussed as follows. Eqs. (5.29) and (5.30) denote two complementary signals as current samples required for disturbance detection.

$$\mathcal{D}_{k} = \mathcal{S}_{k} \tag{5.29}$$

$$\mathcal{D}_{k-1} = -\mathcal{S}_{k} \tag{5.30}$$

where $\mathcal{S}_{k}$ denotes the sample value of the signal at k^{th} time.

Using the signals mentioned above, the two-sided CUSUM assessment is estimated as in (5.31) and (5.32).

$$\mathcal{G}_{k\_current} = max(\mathcal{G}_{k\_1\_current} + \mathcal{D}_{k} - \mathfrak{D}, 0) \tag{5.31}$$

$$\mathcal{G}_{k\_preceding} = max(\mathcal{G}_{k\_1\_preceding} + \mathcal{D}_{k-1} - \mathfrak{D}, 0) \tag{5.32}$$

where $\mathcal{G}_{k}$ and $\mathfrak{D}$ signifies the test statistics and drift parameter, respectively; $\mathcal{G}_{k\_current}$ and $\mathcal{G}_{k\_preceding}$ are the CUSUM test value of the current and preceding signal with and without the inception of fault.

In this case, if the cyber-attack happens, the $\mathcal{G}_{k}$ value will exceed the threshold value ($\mathcal{H}$), as given in (5.33). It is noted that the value of $\mathcal{H}$ ought to be ideally zero.

$$\mathcal{G}_{k\_current} > \mathcal{H} \text{ or } \mathcal{G}_{k_{preceding}} > \mathcal{H} \tag{5.32}$$

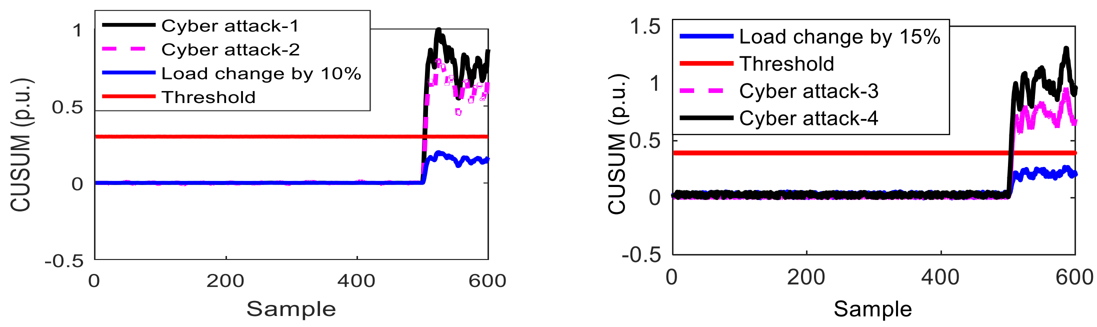

(a) Load change by 10% (b) Load change by 15%

Fig. 5.4. CUSUM for cyber-attack detection

As shown in Fig. 5.4, the output signal is sampled, where both steady-state and disruptive events are taken. It is revealed that when the load changes by 10% or 15%, the CUSUM value is lower than the threshold. However, with cyber-attack, it increases significantly and exceeds the threshold value that is selected based on the comparison of estimated CUSUM in different scenarios.

5.2.3. Control methods

As noted, frequency stabilization is vital to evade grid failure, and the regulation can be made through primary and secondary control. The primary control is the local control with a faster timescale through automatic feedback action, e.g., the governor and the secondary controller can be used to a wider network with a slower timescale through quasistatic control action. However, on the verge of a cyber-attack, the hacker can falsify the signal to mismatch the load demand-generation value, leading to an unstable grid or blackout. To this end, the secondary controller is vital and a promising solution to avoid grid outages. The following sub-section discusses the secondary controllers, such as PID, type-1 fuzzy PID, and type-2 fuzzy PID, which are modeled and tested through the proposed system.

A. Method-1: PID controller

PID controller is a simple and effective control scheme that has made a milestone and is best suited for industrial use [24]. The output of the PID controller in the time-domain can be expressed as (5.34), where $u(t)$ is the control signal, and correspondingly, *e(t)* is the error signal.

$$u(t) = \mathcal{K}_p e(t) + \mathcal{K}_i \int_0^t e(\tau) d\tau + \mathcal{K}_d \frac{de(t)}{dt} \tag{5.34}$$

The role of the PID gains are: proportional gain ($\mathcal{K}_p$) responds to error response to disruption; integral gain ($\mathcal{K}_i$) minimizes the steady-state error, and derivative gain ($\mathcal{K}_d$) responds to transient behavior. However, this simple PID controller could not meet the frequency stabilization in the wake of extreme events. Therefore the, advanced control methods are needed, discussed as follows.

B. Method-2: Type-1 Fuzzy

The type-1 fuzzy-PID (T1FPID) controllers are widely used in control methods since traditional controllers are less efficient and more sluggish. Unlike the traditional controllers, which are premised on the basis of a linearized mathematical model, the fuzzy logic approach attempts to determine the control outputs directly from the measurements by the operators or users. Several studies have been attempted in LFC; for example, *Bevrani et al.* applied the fuzzy logic control scheme in LFC considering the wind power fluctuation and successfully minimized the system frequency and tie-line deviation [25]. In [26], the Fuzzy PI controller is used and compared with the traditional PI controller, showing better frequency regulation characteristics.

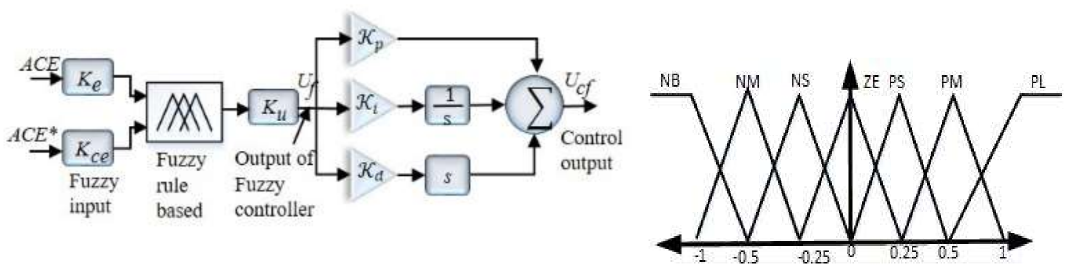

(a) (b)

Fig. 5.5. T1FIPD structure (a) Block diagram, (b) Membership function

The structure of T1FPID is presented in Fig. 5.5 (a), where three main stages are included: fuzzification, rule base, and defuzzification. Further, the proposed fuzzy logic membership function (MF) of input and output is shown in Fig. 5.5 (b). The input of FIPID is ACE and $ACE*$ (which is a derivative function of ACE), and out of fuzzy is U_f. Further, the control output of fuzzy is the input of the PID controller, and then the output of the T1FPID controller is U_{cf} and the output of fuzzy control (U_f) is the function of K_e, and K_{ce}, such as $U_f = f_{flc}(K_e\, ACE, K_{ce}\, ACE^*)$, where K_e and K_{ce} are the scaling parameters, and f_{flc} is the function of the fuzzy logic system.

C. Method-3: Type-2 Fuzzy-PID controller

Although the type-1 fuzzy has an excellent control characteristic, it is less significant in an unstructured environment because it cannot control linguistic uncertainties. Thus, to overcome the T1FPID limitation, the type-2 fuzzy PID controller (T2FPID) is adopted in this chapter, which offers higher-degree-of freedom accomplished by the footprint of uncertainty. Indeed, the type-2 fuzzy controller is designed with two inputs, which are mostly used; however, some authors have developed a single input type-2 fuzzy controller (SIT2FC), which gives enhanced control performance and simple design [27]. This controller's main objective is to minimize system frequency fluctuation, and consequently, the error can also be decreased.

$$u_m = \mathcal{K}_u \left(\mathcal{K}_{p,IT2} v_0 + \mathcal{K}_{i,IT2} \int_0^t v_0 \, dt + \mathcal{K}_{d,IT2} \frac{dv_0}{dt} \right) \tag{5.35}$$

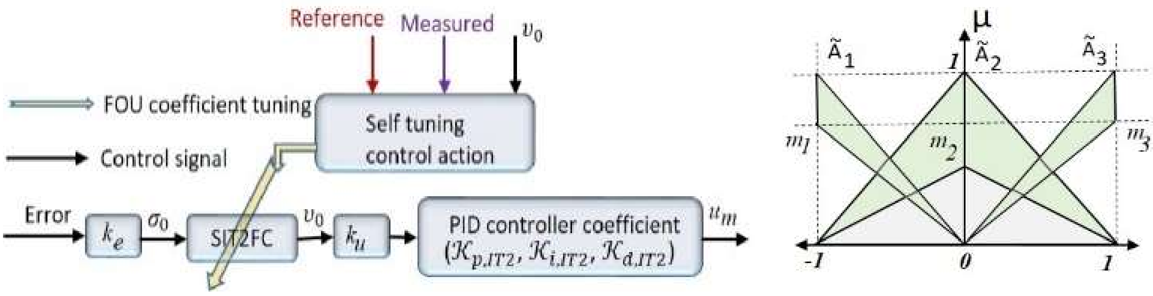

(a) SIT2FC structure (b) Triangular MFs of SIT2FC

Fig. 5.6. Type-2 Fuzzy system

A traditional PID controller is cascaded to the T2FPID, shown in Fig. 5.6 (a), and Fig. 5.6 (b) represents the membership function. The input scaling factor k_e normalizes the input and is defined as $k_e = \frac{1}{e_{max}}$, where e_{max} denotes the maximum error. Since the error is the frequency deviation, which will go through the scaling factor, it is converted into another factor as the input to a SIT2FC, *i.e.*, σ_0. Further, the control action is denoted as u_m is regulated through the output of the controller, symbolized as v_0. Thus, the control action can be expressed as in (5.35), where $k_u = k_e^{-1}$ is the output of the scaling factor and $\mathcal{K}_p$, $\mathcal{K}_i$ and $\mathcal{K}_d$ are the gain of the PID controller.

5.3. Case study and results

5.3.1. Simulation results

This section presents the transient analysis of the interconnected microgrid considering the step load, random load, and considering uncertainties like solar insolation, wind speed, and cyber-attack. In addition, three control methods are employed, such as conventional PID (CPID), T1FPID, and T2FPID controllers, and finally, the comparison characteristics are analyzed to identify the better controller. The interconnected MG system is simulated through the MATLAB/ Simulink environment, and the parameters of the system are presented in Appendix 5.A.

This study aims to show the system's resiliency based on various operating scenarios and malicious data injection, which can be seen by frequency deviation. As far as the frequency deviation is concerned, the frequency range limitation is ± 0.5 Hz (49.5 to 50.5) for 50 Hz; beyond this value, the system can collapse. Hence, the frequency fluctuation should be in the range in which the system's objective function can be minimized, as given in (5.34). On the other hand, cyber-attacks are increasing, which must be taken into account to design a resilient system. With this objective, this chapter gives a resilient system solution of a microgrid for minimizing the frequency deviation as a consequence of cyber-attack and uncertainties. In this study, the parameters are taken as per unit (p.u.) values except for wind speed ($\mathbb{W}_s$), which is in the range from 3 to 20 m/s. During normal operation, the total power of each MG is 1.0 p.u. Moreover, the proposed system is simulated through different control methods, and the gains of the controller are presented in Table 5.1. By doing so, the frequency change characteristics are shown with different scenarios, illustrated as follows.

Table 5.1: Controller gains

Controller	K_P	K_I	K_D
CPID	1.464	0.575	0.123
T1FPID	1.673	1.402	0.481
T2FPID	0.974	0.946	0.784

A. Scenario-1: Step load change and cyber-attack

In this scenario, the continuous step load change with a cyberattack such as an extraneous attack is considered. During the simulation, the wind speed is allowed to ± 5 % in continuous steps of the rated value of 12 m/s. The load, solar, and cyber-attack patterns are presented in Fig. 5.7 (a), (b), (c), respectively. In response to the aforementioned signal, the frequency deviation response is presented in Fig. 5.7 (d). It is noted that the proposed T2FPID controller provides better performance as compared to the other controllers, with a cyberattack and variations in solar insolation, wind speed as well as load. Consequently, the system's objective function, *i.e.*, ACE_{i_m} (t) in addition to peak overshoot, settling time, and the statistical indices such as variance and standard deviations, are reduced, and frequency change within the reasonable limit is achieved, as presented in Table 5.2.

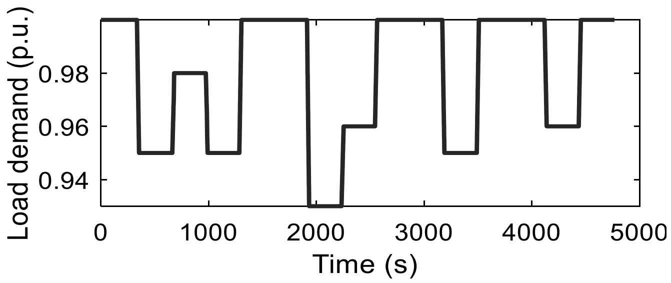

(a) Step load change

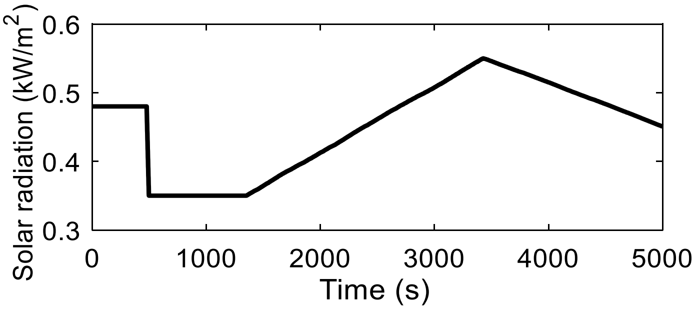

(b) Solar pattern

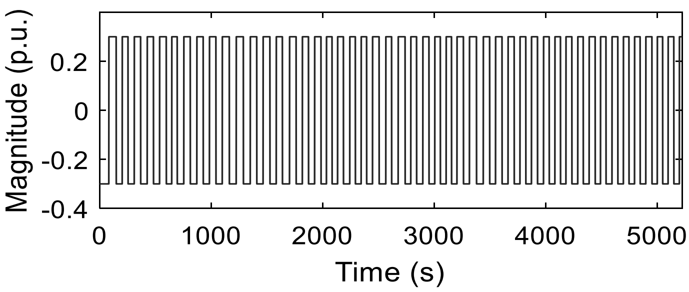

(c) Cyber-attack signal

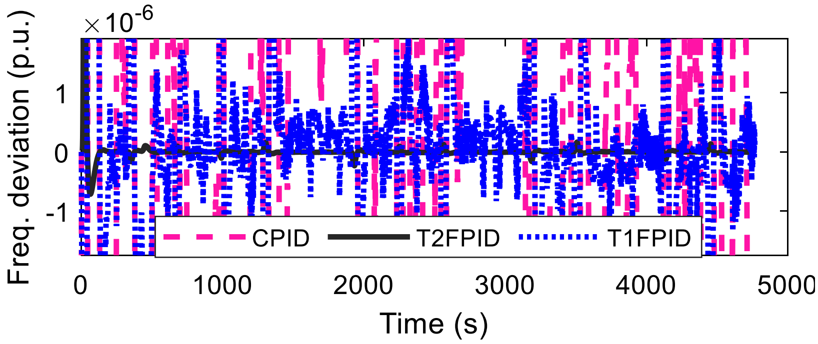

(d) Frequency deviation of an isolated MG (IMG)

Fig. 5.7. Pattern and performance of scenario-1

B. Scenario-2: Continuous step change in wind speed and cyber-attack

This scenario holds the same solar profile, and the cyber-attack pattern is followed (as in scenario-1) with continuous (Fig. 5.8 (a)) step change in wind speed, as well as load, is allowed to change in step with ± 5 % of the rated value of 1 p.u. The system is then simulated, and the frequency deviation characteristics and performance index are presented in Fig. 5.8 (b) and Table 5.2, respectively.

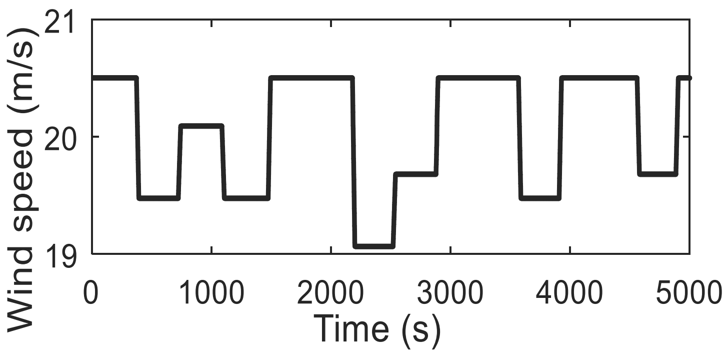

(a) Step change in wind speed

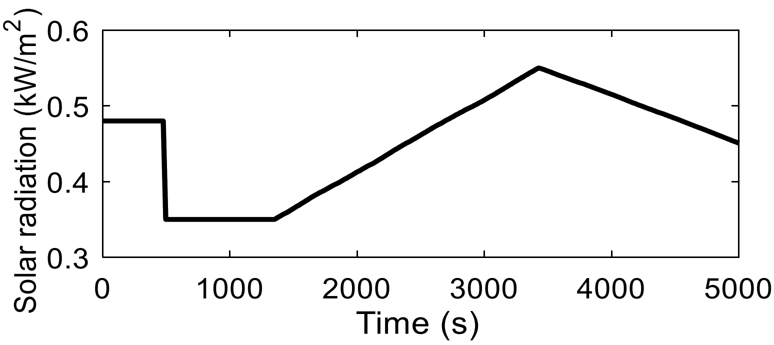

(b) Solar pattern

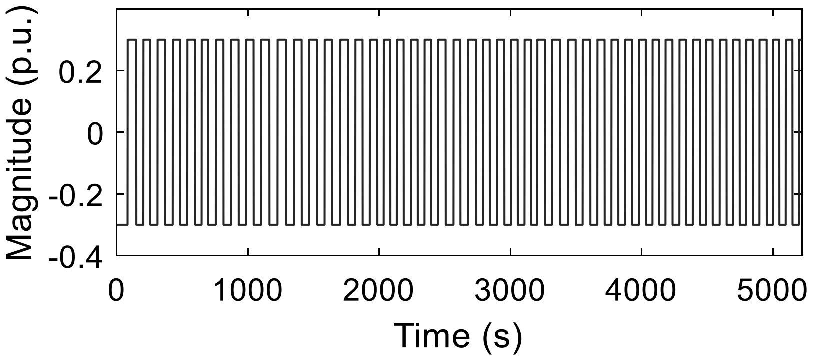

(c) Cyber-attack signal

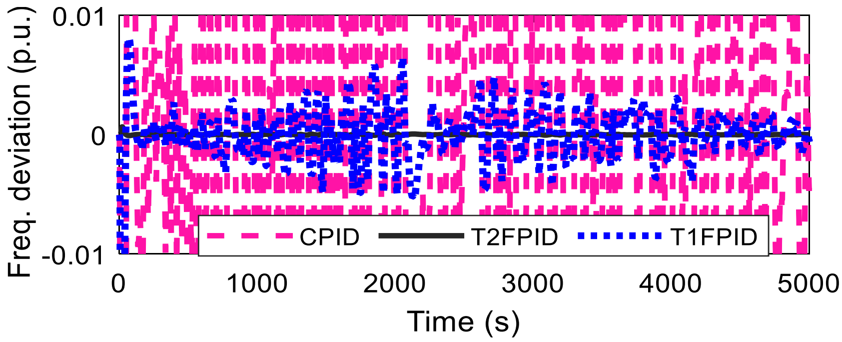

(d) Frequency deviation of an IMG

Fig. 5.8. Pattern and performance of scenario-2

It is noticed that the frequency deviation of the system is minimized with continuous step load change and cyber-attack through the control actions. However, the T2FPID controller shows a better response than other controllers, as noticed from the indices given in Table 5.2.

C. Scenario-3: Random change in load and cyber-attack

Further, the load (pattern-1 and pattern-2) and cyber-attack patterns are changed as random functions, as shown in Fig. 5.9 (a-b) and (c), respectively. The solar insolation and wind speed patterns are varied in steps within ± 5 % of the rated values of 1000 W/m^2 and 12 m/s. Here, the main aim is to show how the frequency is affected in response to a random change in load and malicious data injection with uncertainties.

With reference to Fig. 5.9 (a-b) and (c), the corresponding frequency change characteristics are illustrated in Fig. 5.9 (d) and (e), respectively, and the performance indices are given in Table 5.2. It is observed that the proposed T2FPID controller provides robust performance with lower performance indices like peak overshoot, settling time, integral square error (ISE), variance, and standard deviation.

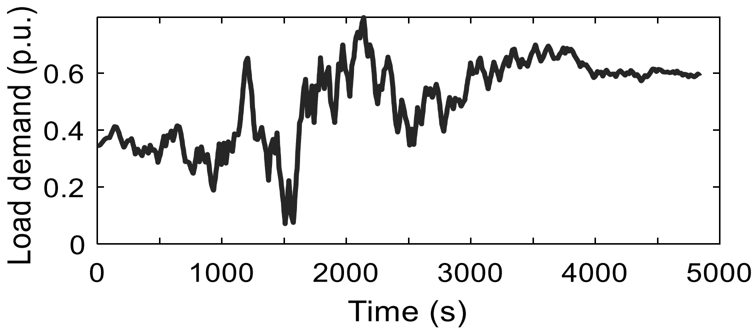

(a) Random load pattern-1

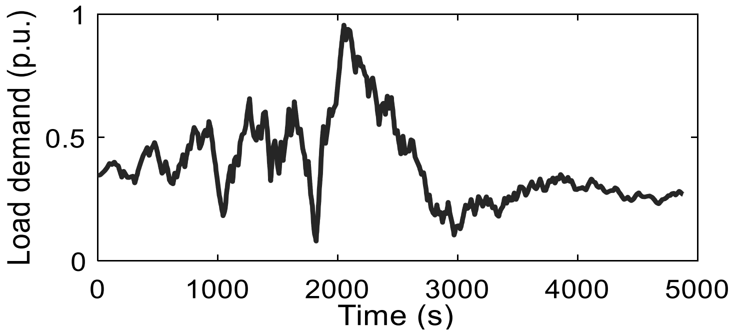

(b) Random load pattern- 2

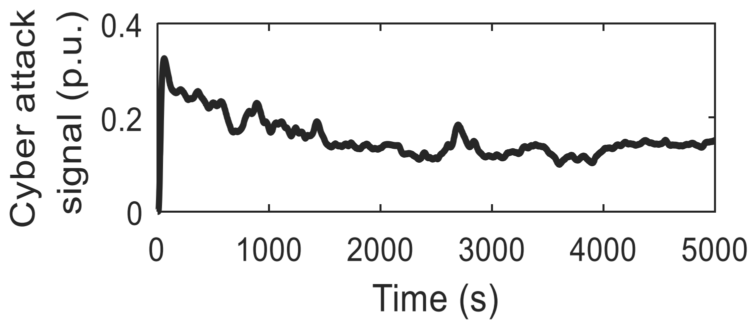

(c) Cyber-attack pattern

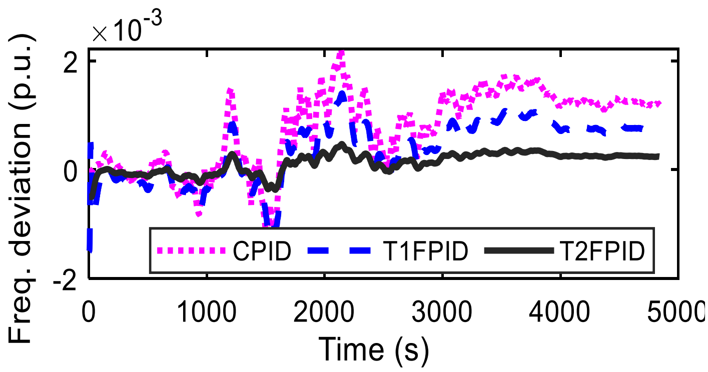

(d) Frequency deviation of an IMG

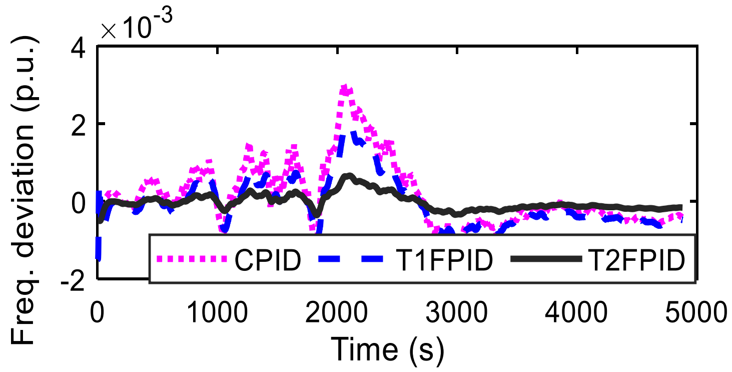

(e) Frequency deviation of an IMG

Fig. 5.9. Pattern and performance of scenario-3

D. Scenario-4: Random change in wind speed and cyber-attack

Finally, the wind speed pattern-1 and pattern-2 given in Fig. 5.10 (a, b), and cyber-attack patterns same as Fig. 5.9 (c) are changed in random, correspondingly. The solar insolation and load patterns are varied in steps within ± 5 % of the rated values of 1000 W/m^2 and 1 p.u., respectively.

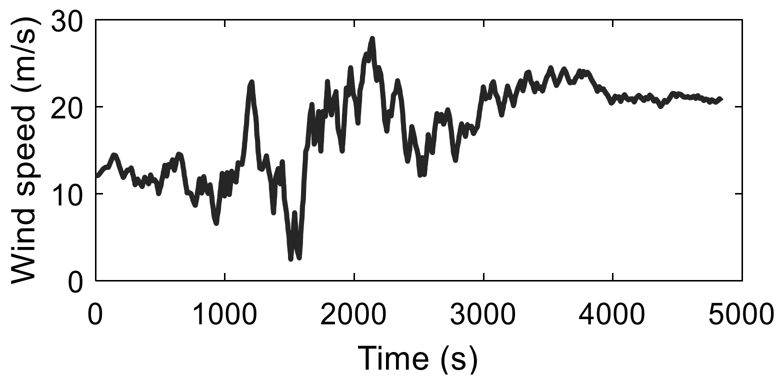

(a) Wind speed pattern-1

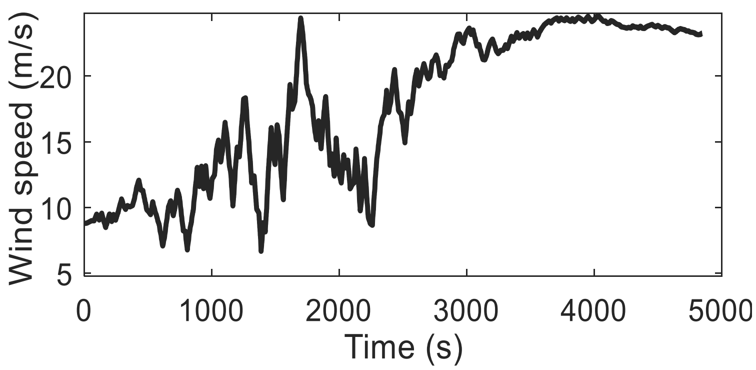

(b) Wind speed pattern-2

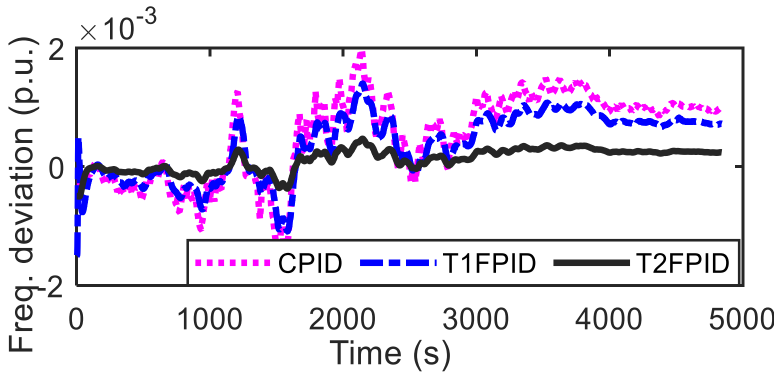

(c) Frequency deviation of IMG

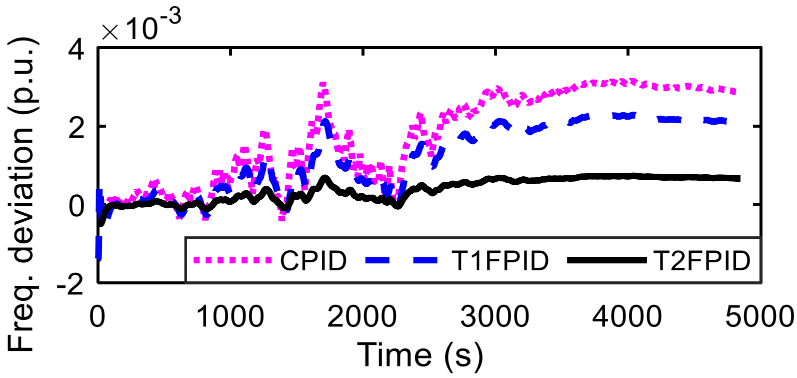

(d) Frequency deviation of an IMG

Fig. 5.10. Pattern and performance of scenario-4

Furthermore, two types of wind patterns are considered, as shown in Fig. 5.10 (a) and (b), and the respective frequency performances are depicted in Fig. 5.10 (d) and (e). Here, the frequency deviation is affected in response to a random change in wind speed and malicious data injection due to cyber-attacks. It indicates that the T2FPID controller can efficiently handle the frequency instabilities, showing robustness in reducing the indices such as peak overshoot, settling time, ISE, variance, and standard deviation, as reported in Table 5.2. Besides that, each generation's sources share the load efficiently according to the availability to stabilize the system frequency.

E. Scenario-5: Change in cyber-attack magnitude

The aim of this study is to show the system's resiliency against cyber-attack. As noted, the magnitude of a cyber-attack is significant because it can lead to the system collapse either fully or partially. The large cyber-attack could severely impact a system's performance, resulting in obliterating a system’s stability. Considering the different magnitude of cyber-attack, this study has revealed the degree of tolerance of the proposed controller and its effectiveness in terms of transient responses. With reference to (5.27), the magnitude of the cyber-attack signal has been increased to 0.4 and 0.5, and the simulation is carried out. The variation of the magnitude of cyber-attack has substantially affected the optimal frequency regulation characteristics, as can be seen in Fig. 5.11. It is observed that with the magnitude of 0.3 and 0.4, the system can cope with the event; however, beyond this value, the system could not have better performance. Fig. 5.11(a) represents the simulation results, whereas Fig. 5.11(b) validates the result through a real-time environment.

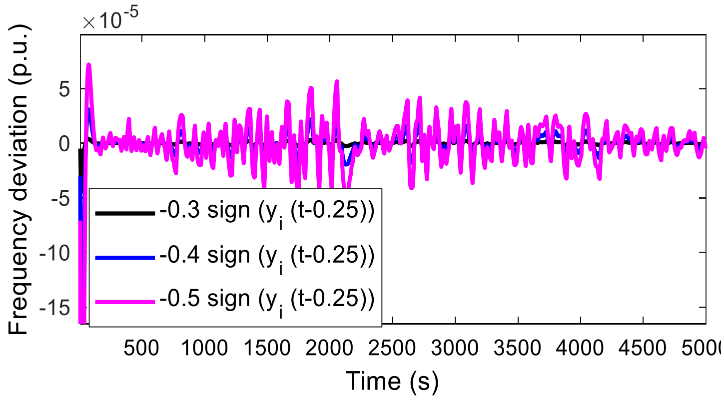

(a) Simulation result

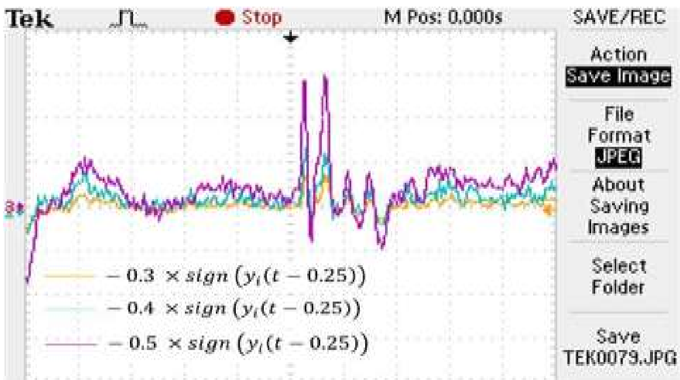

(b) Real-time validation

Fig. 5.11. Impact of the variation of the cyber-attack magnitude on frequency deviation in IMG

5.3.2. Real-time validation using OPAL-RT

The real-time hardware-in-the-loop (HIL) environment study is presented in this sub-section through the OPAL-RT simulator to validate the simulation results, as discussed above. The OAPL-RT and RT-Lab system architecture is shown in Fig. 5.12 (a), and the flow of validation starting from the Matlab model to HIL validation is also demonstrated in Fig. 5.12 (b). The real-time simulator, which is used for this study, is OPAL-RT 5142. The host PC specification is Windows 7, 32-bit, Xilinx v10.1, and Matlab 2016b version. In addition, OPAL-RT's adapter board supports distributed processing, which operates faster with inbuilt FPGA. It delivers 2.6 GBits full duplex rates.

The OP 5142 board's main task is to infer the Simulink model into the target that integrates the FPGA in RT-Lab. With this, the real-time simulation can be done through a cluster to make it faster and more distributed execution.

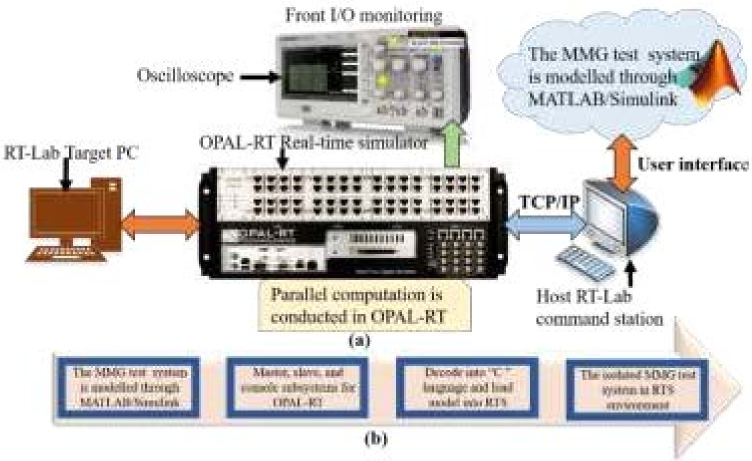

(a) OAPL-RT and RT-Lab system architecture, (b) Real-time validation flow

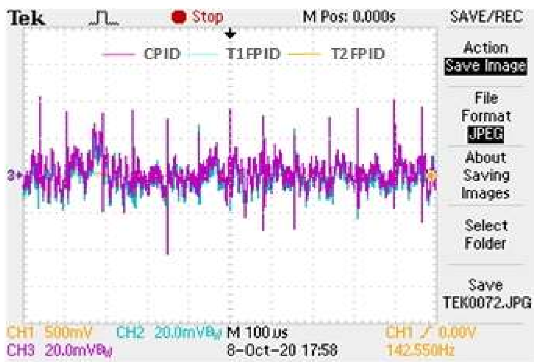

(c) Frequency deviation for scenario-1

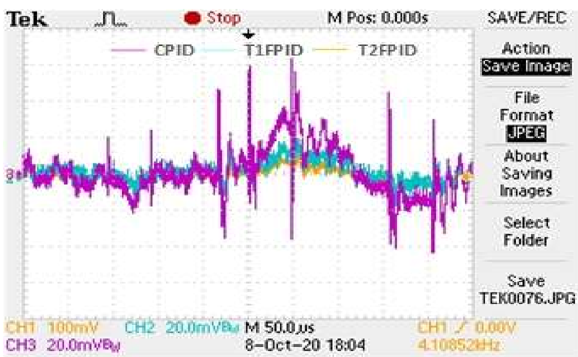

(d) Frequency deviation for scenario-2

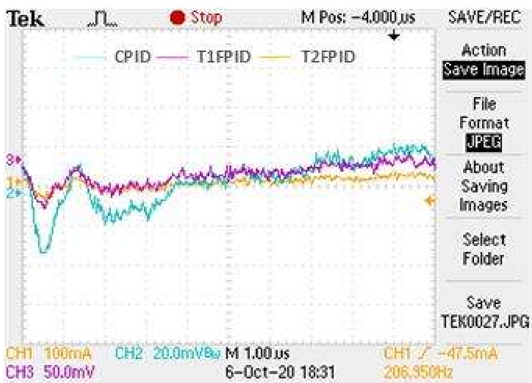

(e) Frequency deviation for scenario-3 with load pattern-1

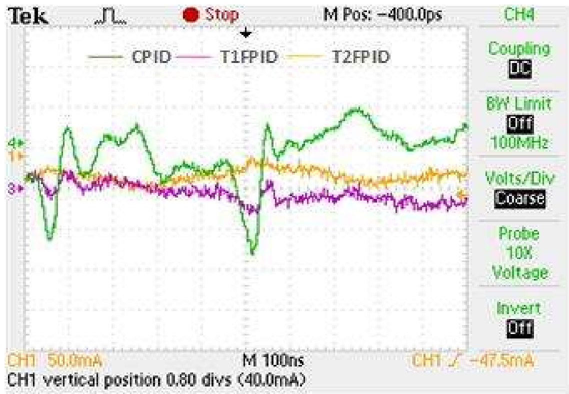

(f) Frequency deviation for scenario-3 with load pattern-2

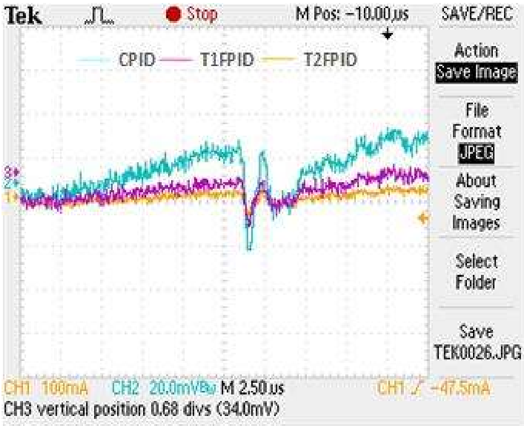

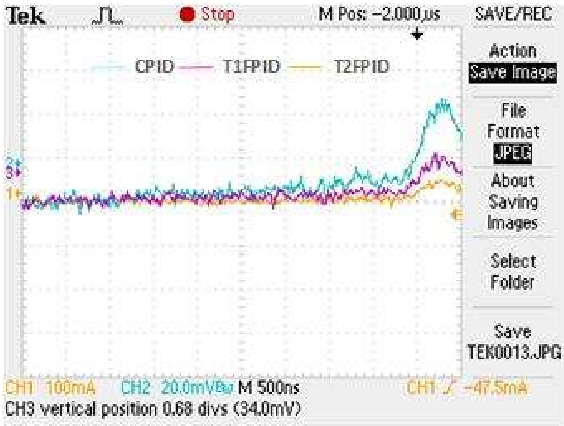

(g) Frequency deviation for scenario-4 with wind speed pattern-1 (h) Frequency deviation for scenario-4 with wind speed pattern-2

Fig. 5.12. Real-time study using OPAL-RT

The deviation in frequency for scenarios 1, 2, 3, and 4 are displayed in Fig. 5.12 (c), (d), (e), (f), (g), and (h), respectively. In Fig. 5.12 (c-h), the aqua color represents the PID control-based characteristics, while the purple and coral color characterizes the optimized-based PID control characteristics. It is observed that the frequency deviation is minimum using the proposed T2FPID controller compared to the other two under scenarios 1, 2, 3, and 4, respectively.

5.3.3. Performance analysis using statistical parameters

In this subsection, the performance of the T2FPID, T1FPID, and CPID is tested in terms of the eigenvalue and damping factor. The eigenvalue analysis between the above controllers is done using mathematical modeling under different operating scenarios and is presented in Table 5.3. The system state matrix (A) is obtained from the state-space modeling of the power system, and then the eigenvalues and damping ratios are evaluated. To augment the validation, a comparison of different techniques is plotted in Box and whisker plot, as shown in Fig. 5.13 (a). The Nyquist and Bode plots are displayed in Fig. 5.13 (b) and (c) represent different controller's stability performances. As noted, eigenvalue analysis and stability plots justify that the proposed T2FPID shows better frequency stabilization characteristics as compared to the FPID and PID controllers under different operating scenarios. In addition, the controller's performances are illustrated in Fig. 5.14 in terms of peak overshoot, variance, standard deviation, and ISE, which are the reflection from Table 5.2. It is noted that the proposed T2FPID controller offers reduced overshoots, deviation, and error, as can be seen in Table 5.2. In addition to checking the system's stability, eigenvalue and damping ratio are measured in different scenarios, and it is observed that the proposed T2FPID controller provides a more negative value of eigenvalues and higher damping ratios, reported in Table 5.3. By measuring various performance indices in this study in the face of cyber-attacks and uncertainties, the proposed T2FPID provides a better and faster response. As far as the resilience concept is concerned, if the system responds quickly with reduced overshoot, deviation and error, the system can be treated as robust and resilient, which has been done by the T2FPID controller. Thus, this study states the resilience-control-based frequency regulation scheme using an adaptive fuzzy controller approach.

Table 5.2: Performance indices using different techniques

Controller	% peak overshoot	Variance	Standard deviation	ISE
Scenario-1:				
PID	2.04e-03	3.27e-03	3.52e-03	4.38e-03
T1FPID	1.27e-03	2.18e-03	2.56e-03	3.33e-03
T2FPID	0.32e-03	1.49e-03	1.71e-03	2.84e-03
Scenario-2:				
PID	1.24e-02	3.11e-03	3.18e-03	5.56e-03
T1FPID	0.87e-02	2.04e-03	2.56e-03	3.33e-03
T2FPID	0.22e-02	1.25e-03	1.48e-03	1.37e-03
Scenario-3:				
PID	2.15-03	3.11e-03	4.58e-03	4.78e-03
T1FPID	1.07e-03	2.20e-03	2.56e-03	2.34e-03
T2FPID	0.38e-03	1.49e-03	1.16e-03	0.98e-03
Scenario-4:				
PID	4.47e-03	5.51e-03	3.18e-03	5.38e-03
T1FPID	2.69e-03	3.38e-03	2.60e-03	3.51e-03
T2FPID	0.92e-03	1.21e-03	1.08e-03	1.13e-03

Table 5.3 Eigenvalue and damping ratio analysis

Operating conditions	Methodology	Eigenvalues	Damping ratios
Scenario-1:	PID	$-3.4532 \pm j6.3217$	0.4527
	T1FPID	$-5.1463 \pm j\,7.3554$	0.4836
	T2FPID	$\mathbf{-6.4858 \pm j\,8.5791}$	**0.6395**
Scenario-2:	PID	$-4.2674 \pm j\,5.6725$	0.3021
	T1FPID	$-6.6738 \pm j\,6.9681$	0.4581

	T2FPID	**-7.1258±*j* 7.8249**	**0.6042**
Scenario-3:	PID	-4.2261±*j*5.6465	0.3869
	T1FPID	-5.8782±*j* 6.7586	0.5821
	T2FPID	**-7.1168±*j* 8.5883**	**0.7839**
Scenario-4:	PID	-5.2369±*j*6.6786	0.3869
	T1FPID	-7.3508±*j* 8.8286	0.5470
	T2FPID	**-8.0842±*j* 8.5704**	**0.7149**

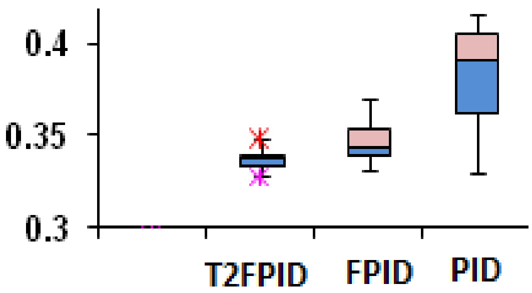

(a) Box plot

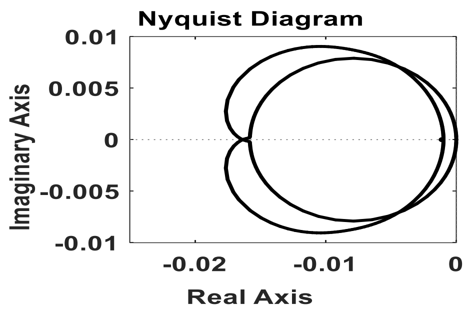

(b) Nyquist plot

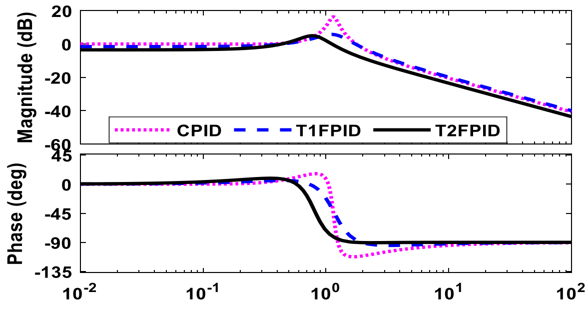

(c) Bode plot

Fig. 5.13. Performance analysis

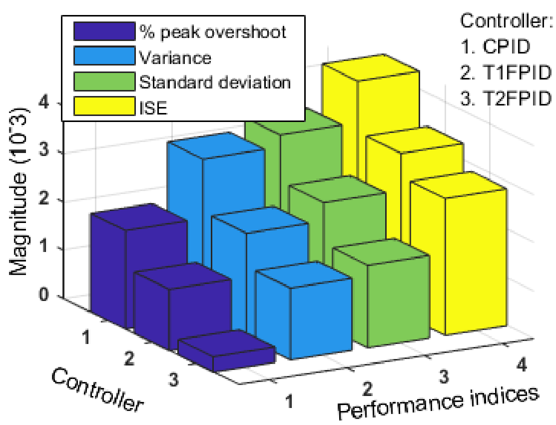

(a) Performance indices of scenario-1

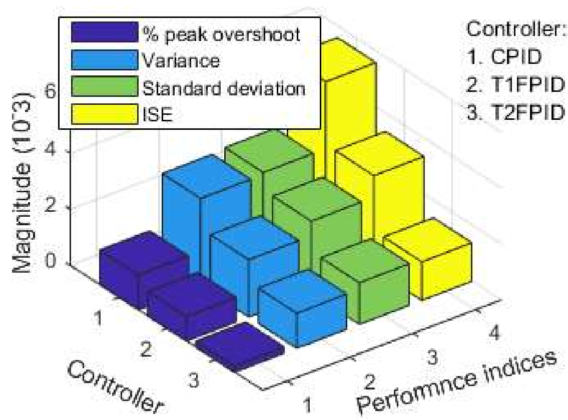

(b) Performance indices of scenario-2

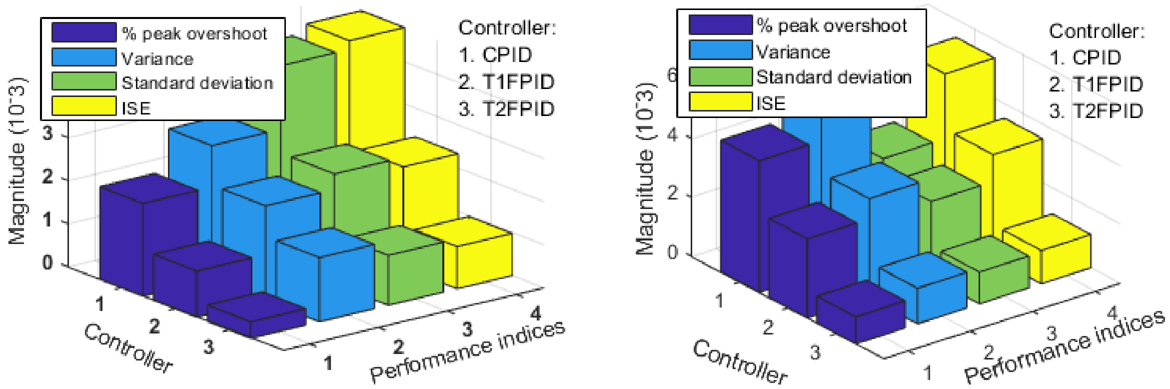

(c) Performance indices of scenario-3 (d) Performance indices of scenario-4

Fig. 5.14. Controller comparison and performance indices bar chart

5.4. Summary

This chapter focuses on modeling and validating resilience-based frequency regulation schemes for isolated microgrids under different operating scenarios. The following key conclusions are drawn by comprehensive simulation and real-time HIL testing. Firstly, the model is simulated with step load change, step wind speed, and solar pattern. Secondly, random changes in load, random wind speed, and solar patterns are considered and simulated. Thirdly, the cyber-attack model is incorporated and tested through three different control methods, where T2FPID shows better regulation and holds improved resiliency characteristics with reduced error. Further, real-time HIL testing is performed through the OPAL-RT simulator, and it is revealed that the HIL results follow the simulation results, and the proposed controller (i.e., T2FPID) played a significant role in showing the robustness of the system. Finally, various performance indices and system's stability are characterized by the percentage of peak overshoot, variance, standard deviation, ISE, eigenvalues, and stability curves, such as Nyquist and Bode plots.

This study is limited to sensor attacks only, and isolation/disconnection of the system after the attack is not considered. In addition, if a false data injection attack can strike the entire communication system of MG, the whole system can be collapsed; as such, there is a need for an advanced method of control mechanism which can cope against false data injection attacks on the communication system. These will be studied further.

Appendix 5.A: System data

Rating:

PV = 30 kW;

Wind = 100 kW;

EV = 70 kW;

DG = 100 kW;

FESS = 45 kW;

BESS = 45 kW

$P_{L1} = P_{L2}$ = 200 kW

Other parameters:

$\mathcal{T}_W$ = 1.5 s; $\mathcal{T}_{PV}$= 1.8 s; $\mathcal{T}_d$= 8 s; $\mathcal{T}_g$= 0.1 s; $\mathcal{T}_{BESS}$ = 0.1 s; $\mathcal{T}_{FESS}$ = 0.1 s

δ_{dg} = 0.001 puMW/s; μ_{dg} = 0.04 puMW

K_{BESS} = -0.003; K_{FESS} = -0.01; $\mathcal{M}$ = 0.4; $\mathcal{D}$ = 0.003

References

[1] Z. Bie, Y. Lin, G. Li, and F. Li, "Battling the extreme: A study on the power system resilience," *Proceedings of the IEEE,* vol. 105, no. 7, pp. 1253-1266, 2017.

[2] E. D. Vugrin, M. J. Baca, M. D. Mitchell, and K. L. Stamber, "Evaluating the effect of resource constraints on resilience of bulk power system with an electric power restoration model," *International Journal of System of Systems Engineering,* vol. 5, no. 1, pp. 68-91, 2014.

[3] M. Panteli and P. Mancarella, "The grid: Stronger, bigger, smarter?: Presenting a conceptual framework of power system resilience," *IEEE Power and Energy Magazine,* vol. 13, no. 3, pp. 58-66, 2015.

[4] X. Wu, Z. Wang, T. Ding, X. Wang, Z. Li, and F. Li, "Microgrid planning considering the resilience against contingencies," *IET Generation, Transmission & Distribution,* vol. 13, no. 16, pp. 3534-3548, 2019.

[5] K. S. Ko and D. K. Sung, "The effect of EV aggregators with time-varying delays on the stability of a load frequency control system," *IEEE Transactions on Power Systems,* vol. 33, no. 1, pp. 669-680, 2017.

[6] C. Chen, K. Zhang, K. Yuan, L. Zhu, and M. Qian, "Novel detection scheme design considering cyber attacks on load frequency control," *IEEE Transactions on Industrial Informatics,* vol. 14, no. 5, pp. 1932-1941, 2017.

[7] Y. Wu, Z. Wei, J. Weng, X. Li, and R. H. Deng, "Resonance attacks on load frequency control of smart grids," *IEEE Transactions on Smart Grid,* vol. 9, no. 5, pp. 4490-4502, 2017.

[8] M. Kenney, "Cyber-terrorism in a post-stuxnet world," *Orbis,* vol. 59, no. 1, pp. 111-128, 2015.

[9] G. Liang, S. R. Weller, J. Zhao, F. Luo, and Z. Y. Dong, "The 2015 ukraine blackout: Implications for false data injection attacks," *IEEE Transactions on Power Systems,* vol. 32, no. 4, pp. 3317-3318, 2016.

[10] V. Venkataramanan, A. K. Srivastava, A. Hahn, and S. Zonouz, "Measuring and Enhancing Microgrid Resiliency Against Cyber Threats," *IEEE Transactions on Industry Applications,* vol. 55, no. 6, pp. 6303-6312, 2019.

[11] W. Bi, K. Zhang, Y. Li, K. Yuan, and Y. Wang, "Detection scheme against cyber-physical attacks on load frequency control based on dynamic characteristics analysis," *IEEE Systems Journal,* vol. 13, no. 3, pp. 2859-2868, 2019.

[12] J. Liu, Y. Gu, L. Zha, Y. Liu, and J. Cao, "Event-Triggered $ H_\infty $ Load Frequency Control for Multiarea Power Systems Under Hybrid Cyber Attacks," *IEEE Transactions on Systems, Man, and Cybernetics: Systems,* vol. 49, no. 8, pp. 1665-1678, 2019.

[13] K.-D. Lu, G.-Q. Zeng, X. Luo, J. Weng, Y. Zhang, and M. Li, "An Adaptive Resilient Load Frequency Controller for Smart Grids With DoS Attacks," *IEEE Transactions on Vehicular Technology,* vol. 69, no. 5, pp. 4689-4699, 2020.

[14] Z. Cheng, D. Yue, S. Hu, C. Huang, C. Dou, and L. Chen, "Resilient load frequency control design: DoS attacks against additional control loop," *International Journal of Electrical Power & Energy Systems,* vol. 115, p. 105496, 2020.

[15] M. R. Khalghani, J. Solanki, S. Solanki, M. H. Khooban, and A. Sargolzaei, "Resilient Frequency Control Design for Microgrids Under False Data Injection," *IEEE Transactions on Industrial Electronics,* 2020.

[16] A. A. El-Fergany and M. A. El-Hameed, "Efficient frequency controllers for autonomous two-area hybrid microgrid system using social-spider optimiser," *IET Generation, Transmission & Distribution,* vol. 11, no. 3, pp. 637-648, 2017.

[17] T. Masuta and A. Yokoyama, "Supplementary load frequency control by use of a number of both electric vehicles and heat pump water heaters," *IEEE Transactions on smart grid,* vol. 3, no. 3, pp. 1253-1262, 2012.

[18] S. A. Hosseini, M. Toulabi, A. S. Dobakhshari, A. Ashouri-Zadeh, and A. M. Ranjbar, "Delay compensation of demand response and adaptive disturbance rejection applied to power system frequency control," *IEEE Transactions on Power Systems,* vol. 35, no. 3, pp. 2037-2046, 2019.

[19] S. F. Aliabadi, S. A. Taher, and M. Shahidehpour, "Smart deregulated grid frequency control in presence of renewable energy resources by EVs charging control," *IEEE Transactions on*

Smart Grid, vol. 9, no. 2, pp. 1073-1085, 2016.

[20] M. H. Khooban, "An Optimal Non-Integer MPC-based Load Frequency Control for Modern AC Power Grids with V2G Technology," *IEEE Transactions on Energy Conversion,* 2020.

[21] B. C. Ervural and B. Ervural, "Overview of cyber security in the industry 4.0 era," in *Industry 4.0: managing the digital transformation*: Springer, 2018, pp. 267-284.

[22] A. M. Mohan, N. Meskin, and H. Mehrjerdi, "A Comprehensive Review of the Cyber-Attacks and Cyber-Security on Load Frequency Control of Power Systems," *Energies,* vol. 13, no. 15, p. 3860, 2020.

[23] S. Mohanty, A. Pradhan, and A. Routray, "A cumulative sum-based fault detector for power system relaying application," *IEEE transactions on power delivery,* vol. 23, no. 1, pp. 79-86, 2007.

[24] M. Farahani, S. Ganjefar, and M. Alizadeh, "PID controller adjustment using chaotic optimisation algorithm for multi-area load frequency control," *IET Control Theory & Applications,* vol. 6, no. 13, pp. 1984-1992, 2012.

[25] H. Bevrani and P. R. Daneshmand, "Fuzzy logic-based load-frequency control concerning high penetration of wind turbines," *IEEE systems journal,* vol. 6, no. 1, pp. 173-180, 2011.

[26] I. Kocaarslan and E. Çam, "Fuzzy logic controller in interconnected electrical power systems for load-frequency control," *International Journal of Electrical Power & Energy Systems,* vol. 27, no. 8, pp. 542-549, 2005.

[27] A. Sarabakha, C. Fu, E. Kayacan, and T. Kumbasar, "Type-2 fuzzy logic controllers made even simpler: From design to deployment for UAVs," *IEEE Transactions on Industrial Electronics,* vol. 65, no. 6, pp. 5069-5077, 2017.

CHAPTER 6

RESILIENCE-DRIVEN SCHEME IN MULTIPLE MICROGRIDS WITH TRANSACTIVE ENERGY SYSTEM USING BLOCKCHAIN TECHNOLOGY

In concern of energy trilemma such as energy security, energy equity, and environmental sustainability, the electric infrastructures are significantly developing the manifold avenues for decentralization, decarbonization, and digitalization. Over the years, the growth of decentralized power systems using distributed energy resources is increasing rapidly, bringing new prospects for local energy trading concerning economic and control operations in a single framework called transactive energy (TE). However, considering the uncertainties due to renewable energy sources has remained a potential challenge for the energy market operator. Thus, to triumph over the challenges, this chapter proposes a novel TE framework with resiliency consideration. On the other hand, cyber-attacks are an increasing concern, which impacts digital platforms, such as energy digitization. Considering this, homomorphic Blockchain technology is applied to secure the TE platform against cyber-attacks. To show the leveraging capabilities, this chapter considers various case studies in the wake of high-disruptive events such as microgrid outage conditions and cyber-attack. The result shows that the proposed TE framework enhances the microgrid benefit and guarantees optimal trading performance. In addition, empowering Blockchain realizes that the security of the system is vital for the TE system when it faces data tampering or any external attacks. The effectiveness and feasibility of the proposed system are evaluated by cost, benefit, and probability of success.

6.1. Introduction

Over the past few decades, power distribution systems are undergoing a significant change due to the increase in renewable energy penetrations and energy storage. This change has played a key role in distribution system modernization and remarkably switched the mindset of customer choices from consumer to prosumer. Prosumers are the end-users who also have their own generations; thus, the surplus power can be fed to the upstream grid. Nowadays, the smart grid evolved as an emerging technology in the power system in which the energy trading services can take place, and the prosumer plays a major role in buying and selling the power. This technology is called transactive energy (TE), where prosumers trade energy economically [1].

Several studies on the TE scheme have focused on different pricing mechanism strategies to achieve economical operation and customer benefits. For example, a TE control mechanism with the double-auction market is introduced in [2], which coordinates the internal electrical equipment of commercial buildings. A day-ahead TE model is proposed in [3] to manage the operation and participation of the distribution system operator in the wholesale market. The active participation of distributed energy resources through residential consumers is modeled via a multi-agent-based TE scheme [4]. The cost-benefit studies of the TE scheme through various scenarios are reported in [5, 6]. In addition, a few other studies cover the TE market based on bidding mechanisms according to consumer priorities [7, 8]. Indeed, the developed TE schemes have great potential to provide better opportunities for the future energy market, but the pricing mechanism and incentive schemes still need attention. On the other hand, the function of the TE system could suffer from a higher degree of complexity in fostering the stakeholder objectives of the market [9]. Notwithstanding, the TE system needs to take care of stakeholder's malicious and inattentive trading action, which would obstruct the trustworthiness of market operations and, subsequently, cause instability in the active distribution system. In addition, privacy leakage is another challenge in the TE system that stakeholders should avoid. A Blockchain-based TE system has recently shed new light on overcoming the abovementioned issues [10].

Furthermore, in the TE scheme, a large amount of information, including bids, offers, and energy availability, are exchanged, and it could face huge challenges in the face of a cyber-attack. Thus, the Blockchain-enabled TE scheme is vital to secure the transaction and critical information. Considering the above challenges and issues, power system researchers have initiated Blockchain applications in the TE system in the last few years, which are discussed in [10-12]. Moreover, these studies are only early-stage designs and frameworks, which still need to be explored more.

In today's world, Blockchain is one of the emerging technologies and has great potential to drive comprehensibility and profitability through a high level of security concern. It has far-reaching appeals in financial services, public sectors, and media industries, but now it is also the emergence of technology in the energy sector to transform the ongoing energy market operation. Blockchain is a growing list of files, classed as blocks that are connected to each other through cryptographic signature, and each block includes a hash function, timestamp, and transaction data [13]. Recently, the application of Blockchain through Ethereum has reached a milestone in terms of transactions due to its faster operation [14]. It enables a definitive and trusty computation using smart contracts. In reference to this operation, the application of Blockchain sheds light on energy system security, as evidenced through executing multiple data verification and secure market-based transaction for the peer-to-peer energy markets [15]. It creates a decentralized database where data are stored chronologically with a crypto signatory as an individual secret key, which cannot be tampered. A recent study in [16] elucidates the significance of a secret key, otherwise called a data authentication key, through homomorphic encryption-based Blockchain technology. As far as the data authentication key is concerned, it is explicitly used for securing transaction data through ciphertext. The ciphertext is a text which has two forms, encryption cipher, and decryption cipher. The plaintext is encrypted initially, and data can be transferred from one node to another, and then it transforms the ciphertext to plaintext through decryption using secret keys.

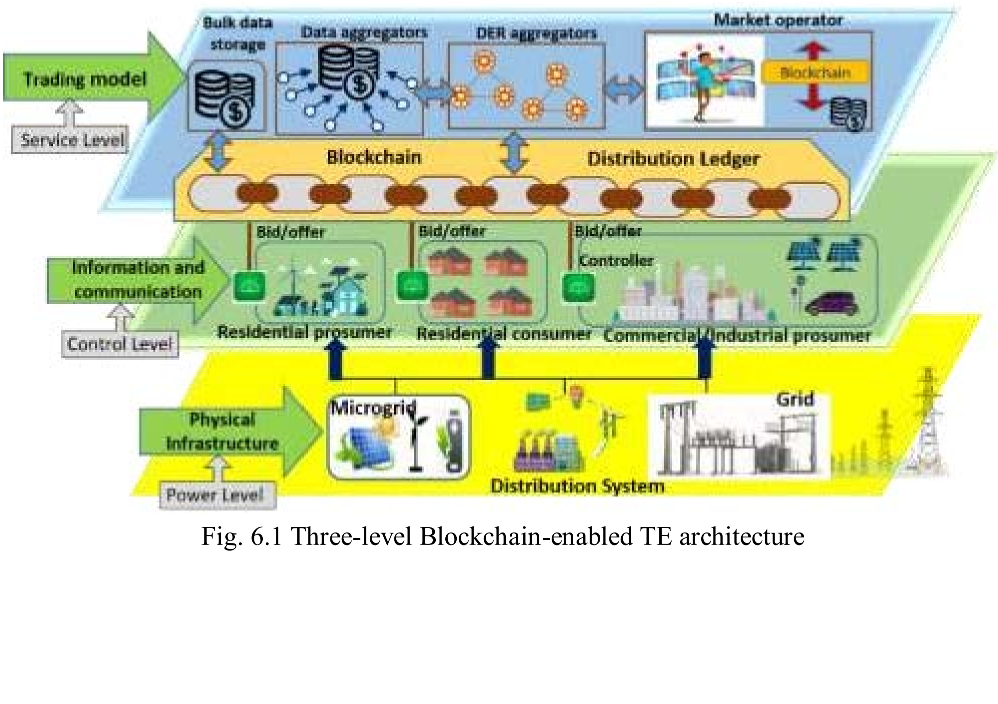

Fig. 6.1 Three-level Blockchain-enabled TE architecture

On the other hand, the cyber-physical power system has already marked a breakthrough in the energy sector, and further implementation of Blockchain can be a remarkable change [17]. Thus, three layers of energy market structure have begun, such as power level, control level, and service level, which are considered in this study, as shown in Fig. 6.1. The physical infrastructure, such as grid supply and multi-microgrids, is considered in the power level. Each microgrid (MG) comprises energy storage units and renewable generation (including PV and wind). Greater divergence of the load profiles of MGs is assumed, and the energy exchange is made through MG to MG and MG to grid. All the information and communication devices are put into practice at the control level to regulate the bids, offers, and supply-demand profiles. This level enables the TE mechanism to ensure the operator benefits. To enable the TE scheme, the decision of pricing mechanism is not only the key but also needs a secured data exchange platform. Thus, a trading model through Blockchain is implemented at the service level to secure the platform.

The proposed TE framework considers three factors: economical operation with a better pricing mechanism scheme, resiliency, and security concerns. In the TE framework, multiple MGs are considered with high penetration of renewables, such as PV and wind, and to support the load during an emergency, battery storage is used in each MG. Further, the extreme event is considered to show the resiliency of the system and restore the critical load through MG sharing and grid supply, where MG outage condition is assumed. Moving further, homomorphic Blockchain technology is applied to secure the transaction against cyber attacks. To sum up, the main contributions of this chapter are as follows:

- A novel TE framework is presented in this study to address two critical issues of the energy market, *i.e.*, energy optimality and privacy assurance.
- For energy optimality, this study considers a new pricing mechanism using the TE framework. To this end, different operating scenarios are discussed, and the energy costs and benefits are analyzed.
- Further, secure energy trading is done by Blockchain-empowered technology to ensure privacy assurance.

- Regarding resilience facts, the proposed framework developed a defensive mechanism against high-disruptive events, such as MG outage conditions and false data injection (FDI) attacks.
- Finally, an extensive evaluation of the attack-defensive capability of Blockchain technology is illustrated in terms of success probability.

6.2. System model

This section presents the proposed system model for a TE system, which can be applied to any multi-MG system. Each MG comprises a combination of PV, wind, and battery storage systems as a clean energy generation. In the proposed TE system, energy trading occurs between MGs and the power grid, as shown in Fig. 6.2 (a). The generation from PV and wind can be used in the TE scheme and storage requirement or sent back to the upstream grid. Indeed, there are two ways to trade the energy within the TE system, such as MG to MG and MG to grid. This condition will arise when the generation is not sufficient to meet its own load demand, and the required energy can be received from other MGs or the upstream grid, as shown in Fig. 6.2(b). Notably, the main aim of the TE scheme is to reduce the dependence on the upstream grid, and optimal trading can be made among neighbor MGs. On the other hand, it is a great platform for dynamic energy balancing, and subsequently, through market interaction, the overall energy cost of MG can be minimized. Moreover, the main focus of the TE scheme exhibits two major factors: economic and environmental. From the economic point of view, the TE system has a low energy cost provider platform, whereas the environmental aspect denotes energy generation through renewable-based sources [18]. Thus, the TE framework is becoming more popular as it realizes the economic and environmental goals through the TE scheme.

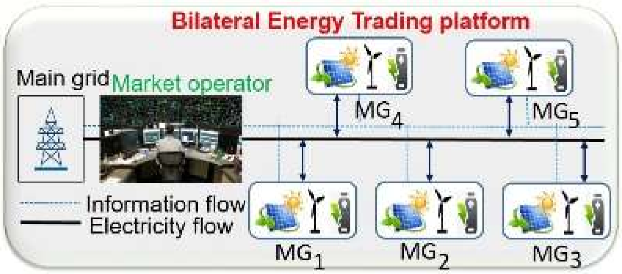

(a) Operational framework

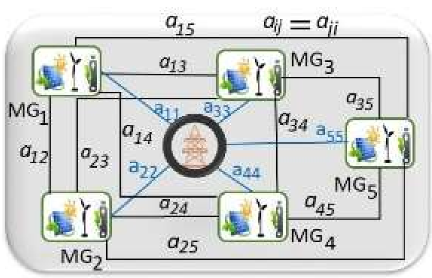

(b) Multi-Microgrid TE topology

Fig. 6.2 TE structure

6.2.1. Objective function

The objective of the proposed TE system is to minimize the total energy cost of each MG, which is expressed in (6.1), while satisfying the operational constraints (6.2-6.15).

$$Min\ (\mathcal{C}_1, \mathcal{C}_2, \dots \dots \mathcal{C}_i) \tag{6.1}$$

$$\mathcal{C}_i = \sum_{t \in \mathcal{T}} \sum_{j \in N} (\mathcal{C}_{ij}^t) \qquad i \in N$$

where $\mathcal{C}_{ij}^t$ (\$) is the energy cost at time t, with $\mathcal{C}_{ij}^t > 0$ indicating the obtained energy cost and $\mathcal{C}_{ij}^t < 0$ the delivered energy cost.

6.2.2. Constraints

A. Generation-load balance

At every time t, the amount of generation should be equal to the consumption expressed in (6.2) to maintain the electricity balance.

$$\mathbb{P}_{\mathcal{W},i,t} + \mathbb{P}_{\mathcal{PV},i,t} + \mathbb{P}_{E,i,t} = \mathbb{P}_{LD,i,t} + \mathbb{P}_{\mathcal{B},i,t} \qquad \forall i, \forall t \tag{6.2}$$

where $\mathbb{P}_{\mathcal{W},i,t}$ is the wind power generation in i^{th} MG at time t

$\mathbb{P}_{\mathcal{PV},i,t}$ is the PV power generation in i^{th} MG at time t

$\mathbb{P}_{E,i,t}$ is the net power injection in i MG from other MGs/grid through TE market at time t

$\mathbb{P}_{\mathcal{B},i,t}$ is the charging /discharging rates for battery storage in i^{th} MG at time t (positive is charging, negative is discharging);

$\mathbb{P}_{LD,i,t}$ is the load demand in i^{th} MG at time t.

B. PV constraints

$$\mathbb{P}_{\mathcal{PV},i,t} \le \mathcal{A}_{\mathcal{PV},i} \cdot \eta_{\mathcal{PV}} \cdot \mathfrak{S}_{\mathcal{PV},t} \tag{6.3}$$

where

$\mathcal{A}_{\mathcal{PV},i}$ = size of the PV panel in i^{th} MG

$\eta_{\mathcal{PV}}$ = efficiency of the PV panel

$\mathfrak{S}_{\mathcal{PV},t}$ = solar radiation at time t

C. Wind turbine constraints

$$\mathbb{P}_{\mathcal{W},i,t} = \begin{cases} 0, & \mathcal{W}_{s,t} < \mathcal{W}_{\mathfrak{C}\mathbb{I}_i} \text{ or } \mathcal{W}_{s,t} > \mathcal{W}_{\mathfrak{C}\mathbb{O},i} \\ \mathbb{P}_{\mathcal{W}\mathbb{R},t,max} \cdot \left(\frac{\mathcal{W}_{s,t} - \mathcal{W}_{\mathfrak{C}\mathbb{I}_i}}{\mathcal{W}_{\mathbb{R},i} - \mathcal{W}_{\mathfrak{C}\mathbb{I}_i}}\right)^3, & \mathcal{W}_{\mathfrak{C}\mathbb{I}_i} \le \mathcal{W}_{s,t} \le \mathcal{W}_{\mathbb{R},i} \\ \mathbb{P}_{\mathcal{W}\mathbb{R},t,max} & \mathcal{W}_{\mathbb{R},i} \le \mathcal{W}_{s,t} \le \mathcal{W}_{\mathfrak{C}\mathbb{O},i} \end{cases} \quad (6.4)$$

where

$\mathbb{P}_{\mathcal{W},i,t}$ = wind turbine output in i^{th} MG at time t

$\mathbb{P}_{\mathcal{W}\mathbb{R},i,max}$ = rated wind power in i^{th} MG at time t

$\mathcal{W}_{s,t}$,$\mathcal{W}_{\mathbb{R},i}$ $\mathcal{W}_{\mathfrak{C}\mathbb{I}_i}$, and $\mathcal{W}_{\mathfrak{C}\mathbb{O},i}$ = predicated, rated, cut-in, and cut-out wind speeds in i^{th} MG at time t, respectively.

D. Battery storage constraints

$$SOC_{i,t+1} = SOC_{i,t} + \frac{\mathbb{E}_{\mathcal{B},i,t}}{\mathbb{E}^{c}_{\mathcal{B},i}} \qquad \forall_t \in \mathcal{T}, i \in N \quad (6.5)$$

$$SOC_i^{min} \le SOC_{i,t+1} \le SOC_i^{max} \quad \forall_t \in \mathcal{T}, i \in N \quad (6.6)$$

$$\mathbb{E}_{\mathcal{B},i,t} = \begin{cases} \eta_{\mathcal{B},c}\mathbb{P}_{\mathcal{B},i,t}\Delta t & if\ \mathbb{P}_{\mathcal{B},i,t} > 0 \\ \mathbb{P}_{\mathcal{B},i,t}\ \Delta t / \eta_{\mathcal{B},d} & if\ \mathbb{P}_{\mathcal{B},i,t} \le 0 \end{cases} \quad (6.7)$$

$$\mathbb{P}_{\mathcal{B},i,t} \in [-\overline{\mathbb{P}}_{\mathcal{B}}, \overline{\mathbb{P}}_{\mathcal{B}}] \qquad \forall_t \in \mathcal{T}, i \in N \quad (6.8)$$

where $SOC_{i,t}$ is the battery state-of-charge for MG i at time t

SOC_j^{min} and SOC_j^{max} are respectively battery minimum and maximum SOC for MG i

$\mathbb{E}^{c}_{\mathcal{B},i}$ is the battery capacity for MG i

$\overline{\mathbb{P}}_{\mathcal{B},i}$ is the maximum battery charging/discharging power of MG i which is positive

Δt is the time interval

$\eta_{\mathcal{B},c}$ and $\eta_{\mathcal{B},d}$ are charging and discharging efficiency, respectively.

$\mathcal{T}$ = [1,2,…T] and N =[1,2 .. ℕ].

E. Power grid constraints

Eq. (6.9) defines active power generation and Eqs. (6.10-6.12) represent the apparent power, voltage, and angle limit.

$$\mathcal{P}_{i,t}^{inj}(\mathcal{V}_{i,t}, \emptyset_{i,t}) + \mathbb{P}_{LD,i,t} = \mathcal{P}_{i,t}^{gen} \qquad \forall i, \forall t \tag{6.9}$$

$$\mathbb{S}_{i,m,t}^{inj}(\mathcal{V}_{i,t}, \emptyset_{i,t}) \leq \mathbb{S}_{i,j}^{max} \qquad \forall i, \forall j, \forall t \tag{6.10}$$

$$\mathcal{V}_{t}^{min} \leq \mathcal{V}_{i,t} \leq \mathcal{V}_{t}^{max} \qquad \forall i, \forall t \tag{6.11}$$

$$-\pi \leq \emptyset_{i,t} \leq \pi \qquad \forall i, \forall t \tag{6.12}$$

where

$\mathcal{P}_{i,t}^{inj}(\mathcal{V}_{i,t}, \emptyset_{i,t})/\mathcal{P}_{i,t}^{gen}$ = active power injection/production at i^{th} node at time t

$\mathbb{S}_{i,j,t}^{inj}(\mathcal{V}_{i,t}, \emptyset_{i,t})$ = apparent power between nodes i & j at time t

$\mathbb{S}_{i,j}^{max}$ = maximum apparent power

$\mathcal{V}_{i,t}/\emptyset_{i,t}$ = voltage/phase angle at i^{th} node at time t

$\mathcal{V}_{t}^{min}/\mathcal{V}_{t}^{max}$ = minimum/maximum voltage magnitude

F. Load demand profile

In this proposed system, each MG has a different load profile, and 30% of its load is considered as the critical load. Accordingly, the minimum level of resilience should be 0.3. Hence, considering the resiliency, the load constraint should be $\mathbb{P}_{LD,i} \geq (1-\mathfrak{B})\mathbb{P}_{LD,i}^{rated}$, where $\mathbb{P}_{LD,i}^{rated}$ is the rated load demand profile of MG is; $\mathfrak{B}$ is the percentage of non-critical load. This means the minimum load can be served if an extreme event happens. In this study, $\mathfrak{B}$ is taken as 70% or 0.7. Assume that the demand profile in i^{th} MG is expressed as (6.13), and the actual demand is expressed as (6.14).

$$\mathbb{P}_{LD} = [\mathbb{P}_{LD,1}\ \mathbb{P}_{LD,2} \dots \mathbb{P}_{LD,\mathbb{N}}] \tag{6.13}$$

$$\mathbb{P}_{LD,i}^{nc} = \mathfrak{B}\mathbb{P}_{LD,i} \tag{6.14}$$

where

$\mathbb{P}_{LD}$ is the demand profile of MG

$\mathbb{P}_{LD,i}$ and $\mathbb{P}_{LD,i}^{nc}$ are the actual demand and non-critical load of MG i, respectively

$\mathfrak{B}$ is the percentage of non-critical load

G. Resilience measure

As per the load demand profile expressed in (6.14), the critical load must be met irrespective of extreme event conditions. So the resiliency ($\Re$) of the system can be measured as (6.15)

$$\Re = \frac{P_{Rec}}{P_{TL}} \tag{6.15}$$

$\Re$ can be the $0.3 < \Re < 1$; P_{Rec} & P_{TL} are the recovered load and total load of outage MGs.

6.3. Transactive energy framework

This section presents the TE modeling and pricing mechanism. In the proposed TE model, five MGs and the main grid have been considered for energy trading. Moreover, the market operator is operating all the trading actions optimally as per the load demand and time (on-peak, mid-peak, and off-peak). The energy exchange ($M_{ij,t}$) of multi-MG system can be defined as (6.16).

$$M_t = \begin{vmatrix} M_{11,t} & M_{12,t} & M_{13,t} & M_{14,t} & M_{15,t} \\ M_{21,t} & M_{22,t} & M_{23,t} & M_{24,t} & M_{25,t} \\ M_{31,t} & M_{32,t} & M_{33,t} & M_{34,t} & M_{35,t} \\ M_{41,t} & M_{42,t} & M_{43,t} & M_{44,t} & M_{45,t} \\ M_{51,t} & M_{52,t} & M_{53,t} & M_{54,t} & M_{55,t} \end{vmatrix} \tag{6.16}$$

where M_{ij} is the energy trading amount between MG i and MG j ($i \neq j$) or between MG i and upstream grid ($i = j$), with a positive sign indicating MG i buying energy and a negative sign indicating MG i selling energy. The net power injection in i^{th} MG from other MGs/grid through TE market at time t is defined in (6.16),

$$\mathbb{P}_{E,i,t} = \sum_{j=1}^{\mathbb{N}} \widehat{M}_{ij,t}/\Delta t \tag{6.17}$$

where $\widehat{M}_{ij,t} = \begin{cases} M_{ij,t}, & M_{ij,t} \geq 0 \\ \frac{M_{ij,t}}{1-a_{ij}}, & M_{ij,t} < 0 \end{cases}$ and a_{ij} is the power loss percentage.

Assume $\mathcal{B}$ is a physical transfer contract specifying that the customer receives energy from TE market at a price $\mathfrak{C}_t^{\mathcal{B}}$. This price is calculated as the average value of a reference price related to the contract, denoted by $\mathfrak{C}_{ij}^{\mathfrak{S}}$, and the pool price $\mathfrak{C}_t^{P}$. Indeed, the pool prices depend on the time interval t, and the final price of the trading energy through the bilateral contact is defined by $\mathfrak{C}_{ij,t}^{\mathcal{B}}$, expressed in (6.18). Further, the cost can be calculated using the bilateral price, and energy quantity is presented in (6.19).

$$\mathfrak{C}_{ij,t}^{\mathcal{B}} = \begin{cases} \frac{\mathfrak{C}_{ij}^{\mathfrak{S}} + \mathfrak{C}_{ij,t}^{P}}{2} & i \neq j, \\ \mathfrak{C}_{G,t}^{pur} & i = j,\ M_{ij} \geq 0 \\ \mathfrak{C}_{G,t}^{sell} & i = j,\ M_{ij} < 0 \end{cases} \tag{6.18}$$

$$C_{i,t}^{\mathcal{B}} = \sum_{j=1}^{\mathbb{N}} \mathfrak{C}_{ij,t}^{\mathcal{B}} M_{ij}^{\mathcal{B}}\, \Delta t\,, \qquad t \in T \tag{6.19}$$

where $\mathfrak{C}_{ij,t}^{\mathcal{B}}$ (\$/kWh) is the transaction price of MG at time *t*; $\mathfrak{C}_{G,t}^{pur}$ (\$/kWh) is the buying price from the upstream grid at time *t*; $\mathfrak{C}_{G}^{sell}$ (\$/kWh) is the selling price to the upstream grid.

The cost is stated in (6.20), which depends on the trading hours, such as on-peak, mid-peak, and off-peak time, and the relation is expressed in (6.21).

$$\mathfrak{C}_{t}^{\mathcal{B}} = \left[\mathfrak{C}_{ij,t}^{\mathcal{B}}\right]_{\mathbb{N}\times\mathbb{N}}, t \in T^{on} \cup T^{mid} \cup T^{off} \tag{6.20}$$

$$\mathfrak{C}_{t^{on}}^{\mathcal{B},} > \mathfrak{C}_{t^{mid}}^{\mathcal{B},} > \mathfrak{C}_{t^{off}}^{\mathcal{B},}, t^{on} \in T^{on}, t^{mid} \in T^{mid}, t^{off} \in T^{off} \tag{6.21}$$

where T^{on}, T^{mid}, T^{off} are the sets of the on-, mid-, and off-peak time.

Further, the energy cost is calculated in a different form, either obtained or delivered, and from MG to MG and MG to the main grid, as discussed in (6.22).

$$C_{ij}^{t} = \begin{cases} M_{ii} \times \mathfrak{C}_{G,t}^{pur} & i = j,\ M_{ij} \geq 0 \\ M_{ii} \times \mathfrak{C}_{G,t}^{sell} & i = j,\ M_{ij} < 0 \\ M_{ij} \times \left(\mathfrak{C}_{ij,t}^{B} + \frac{\mathfrak{C}_{O}}{2}\right), & M_{ij} \geq 0\,, i \neq j\ (obtained) \\ -\frac{M_{ij}}{1 - a_{ij}} \mathfrak{C}_{gc} + M_{ij}\mathfrak{C}_{ij,t}^{B} - M_{ij}\frac{\mathfrak{C}_{O}}{2} & M_{ij} < 0, i \neq j\ (delivered) \end{cases} \tag{6.22}$$

where $\mathfrak{C}_{gc}$ (\$/kWh) is the generation cost coefficient; $\mathfrak{C}_{O}$ (\$/kWh) is the utilization cost coefficient of each transaction, which is the benefit of market operator paid by the seller and buyer evenly; a_{ij} is the power loss percentage.

In this calculation, the following assumptions have been taken.

- The trading can be done through MG to MG or MG to Grid;
- The trading price ($/kWh) is dynamic according to time (on-peak, mid-peak, and off-peak);
- The purchasing price from the grid is greater than the TE trading price ($\mathfrak{C}_{G,t}^{pur} > \mathfrak{C}_{ij,t}^{\mathcal{B}}$);
- The selling price to the grid is less than the TE trading price ($\mathfrak{C}_{G,t}^{sell} < \mathfrak{C}_{ij,t}^{\mathcal{B}}$);
- The seller will pay the extra cost due to power loss; The market operator benefit will be calculated as per the amount of energy transactions. The price will be paid by the receiver and delivery side (half-half), as they are using the network, such as network utilization fees.

Further, the benefit of the market operator is calculated as (6.23). It uses the power network to trade the energy, in which the utilization fee is considered for each transaction.

$$\mathcal{C}_{\mathbb{B}_{MO},t} = \sum_{i=1}^{\mathbb{N}} \sum_{j=1, i\neq j}^{\mathbb{N}} |M_{ij,t}| \times \frac{\mathfrak{C}_O}{2} \tag{6.23}$$

where $\mathcal{C}_{\mathbb{B}_{MO},t}$ is the market operator benefit at time *t*.

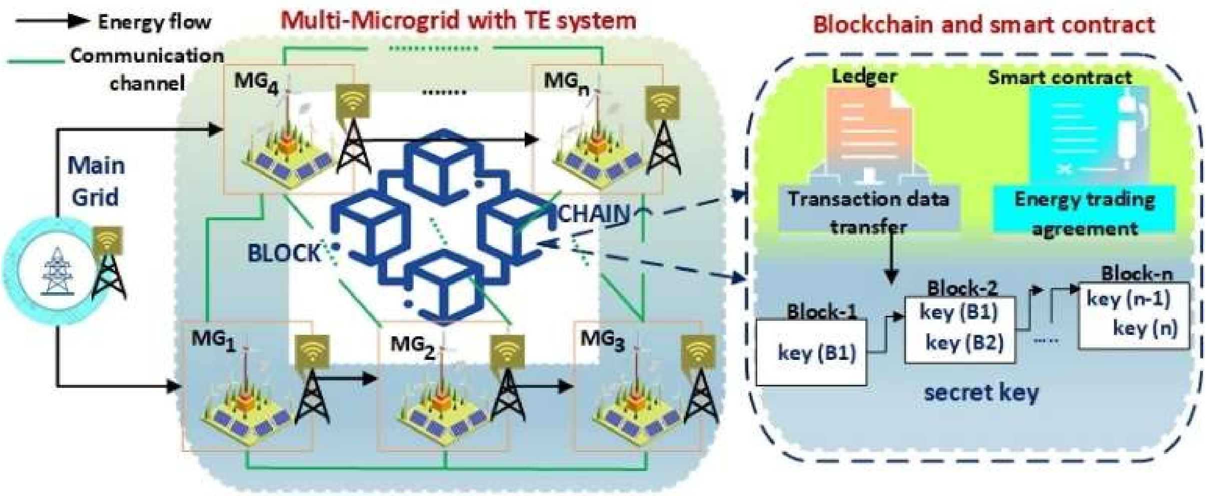

Fig. 6.3 Energy trading approach on Blockchain-enabled TE platform (*Source: Author*)

Algorithm 6.1: Blockchain-enabled TE trading algorithm

1: **Initialization**

2: **for** MG i=1, $\mathbb{N}$ **do**

3: With a homomorphic encryption algorithm, MG i generates a public key $\mathbb{K}_{pu}$ as the digital signature receipts and private key $\mathbb{K}_{pr}$ as the digital signature to confirm the transaction. Then, they are stored in the Blockchain ledger.

4: **end for**

5: **for** MG i=1, $\mathbb{N}$ **do**

6: MG i solves an optimization problem to minimize the total cost ($min\ C_i$). MG i obtains the optimal energy trading quantity $M_{ij}(t)$ with MG j ($j \neq i$) and the Grid ($j = i$).

7: **end for**

8: **for** time step $t = 1, T$ **do**

9: **for** MG i=1, $\mathbb{N}$ **do**

MG i generates the proposed optimal trading quantity $M_{ij}(t)$ with MG j using public-key $\mathbb{K}_{pu}$. The information is sent to the Blockchain.

10: **end for**

11: The Blockchain miner is responsible for verifying the transactions that are delivered by each MG.

$$\begin{cases} if\ M_{ij} = -M_{ji}, \text{verification passes, process the transaction} \\ else,\ \text{verification fails, ignore the transaction} \end{cases}$$

The verified transaction will generate a new block and enter the Blockchain. The balance transfer will be automatically triggered for verified transaction.

12: **end for**

6.4. Blockchain implementation

Blockchain defines that the data or transactions are structured in blocks, and then it links with each other like chains stored in cryptologic hash keys from one block to another, followed by the consensus protocol among the Blockchain network. It brings up a top-notch technological solution for data security in terms of transparency, verifiability, and immutability. Notably, in the Blockchain, consensus protocol and smart contracts are the great players who drive the technology into a resilient system, which are described below.

Blockchain technology is an emerging trend nowadays and picked considerable attention in the TE market. A few authors have introduced this concept into the energy sector and mentioned as the internet of energy (IoE), which facilitates the decentralized network where all the energy trading can take place [19, 20]. With the rapid growth of smart devices in the power system, it is argued that the energy sectors are getting ready for the digital revolution [21]. However, this revolution cannot be fulfilled with the centralized TE market scheme, which needs a better arrangement for data exchange solutions. On the other hand, prosumers are showing a keen interest in participating in the TE market. However, they are unwilling to participate due to complex structures, poor pricing mechanisms, and reduced incentive schemes. Further, moving towards a decentralized energy system is the main aim of the energy transition, which can increase the penetration of renewable energy sources to enhance sustainability. With all the considerations mentioned above, blockchain technology can help the energy sector through a decentralized platform with digital technology. With this technology, peer-to-peer energy trading can be done quickly, smartly, and securely [22]. In addition, using this technology, several applications have successfully emerged, such as electric e-mobility, energy democratization, demand-response schemes, smart metering, smart grid management, automation of green certificate issuance and carbon trading, etc. [23, 24]. In this chapter, blockchain technology is applied in the TE energy market to secure the platform in the face of cyber-attack.

6.4.1. Consensus protocol

The consensus protocol plays a critical role in establishing the trusted path through transaction verification. Moreover, the consensus protocol deals with verification and validation followed by the linking from an old to a new block in the distributed ledger, shown in Fig. 6.3. This mechanism expels the role of central authorities in dealing with data authentication, and, eventually, it manages peer-to-peer without any intermediatory. The implementation of the consensus protocol is to verify and validate the transaction in each stage; however, it is critically important in the final stage as the authentication of the private key is required to start the trading process. The procedure is discussed in Algorithm 6.1.

6.4.2. Smart contract

A smart contract defines a handshake between seller and buyer established by a digitally signed computer. According to the energy requirements, the operator is responsible for automatically performing the trading action in each period. The seller and buyer could respond to the bids and offers generated by the market operator regarding energy quantity and price. Then, the parties will validate the contract, which is the price and quantity of energy exchanged by all the peers in the TE market. Once it achieves the optimal pricing, the energy exchange can be done. In a smart contract, three components will be written in the agreement: energy quantity, trading price, and trading time (on-peak, mid-peak, or off-peak time). The trading price is not constant, and it depends on the time of transfer. There will be two ways of action: for example, MG_i receives M_{ij} quantity of energy from MG_j, thereafter, the MG_i will transfer the C_{ij} dollars to MG_j as per the quantity of energy received. Indeed, the payment will be automatically executed and updated through ciphertext.

6.4.3. Homomorphic encryption scheme

In this scheme, the plaintext and ciphertext are denoted as Q and $\mathbb{X}$, encryption and decryption functions are stated as $\mathcal{E}$ and $\mathcal{D}$, and public and private keys are specified as $\mathbb{K}_{pu,M_1}$ and $\mathbb{K}_{pr,M_1}$, respectively.

Plaintext = $Q = \{\mathcal{U}_1, \mathcal{U}_2, \mathcal{U}_3 \ldots\ldots \mathcal{U}_n\}$

Ciphertext = $\mathbb{X} = \{\mathfrak{x}_1, \mathfrak{x}_2, \mathfrak{x}_3 \ldots\ldots \mathfrak{x}_n\}$

Key = $\mathbb{K}$ = $\{\mathscr{k}_1, \mathscr{k}_2, \mathscr{k}_3 \ldots\ldots \mathscr{k}_n\}$

The function f is called a homomorphic when it follows (6.24).

$$\mathcal{E}(f(u_1, u_2, \ldots\ldots u_n)) = f(\mathcal{E}(u_1), \mathcal{E}(u_2), \ldots \mathcal{E}(u_n)) \tag{6.24}$$

The implementation of the homomorphic encryption method is to verify and validate the transaction in each stage. This method is categorized into four steps: key generation, data authentication (encryption and decryption function) and transaction confirmation.

Firstly, it starts with the key generation, formed according to the number of nodes (sender as a source node and receiver as destination), which are different from each other. Secondly, node identification means identifying the parties who wish to trade with each other. Then the nodes of the parties must go through the authentication (homomorphic encryption/ decryption) stage. Further, the TE nodes use the secret keys to get the authentic response. If the authentication fails, the trading can't be done, and it will be assumed that there is a privacy leakage or any form of attack. Once the authentication is passed, trading (both energy and payment) can be executed automatically based on the smart contract. After the confirmation of the transaction, a new block will be created in the Blockchain, and the same process will go on.

Let us assume each MG has its own beneficiary account with a balance of $\{\mathbb{b}_1, \mathbb{b}_2, \mathbb{b}_3 \ldots\ldots \mathbb{b}_n\}$. With this account balance, the ciphertext can be defined as $\left(\mathbb{X}(\mathbb{b}_1), \mathbb{X}(\mathbb{b}_2), \ldots \mathbb{X}(\mathbb{b}_n)\right)$, and then the miner can easily estimate $\mathcal{E}\left(f(\mathcal{u}_1, \mathcal{u}_2, \ldots\ldots \mathcal{u}_n)\right)$ by $f\left(\mathcal{E}(\mathcal{u}_1), \mathcal{E}(\mathcal{u}_2), \ldots \mathcal{E}(\mathcal{u}_n)\right)$, where n is the number of blocks.

When the energy supplier M_1 intends to transfer energy as per the need by M_2, M_1 commences the transaction to the Blockchain. Assume that the energy available in M_1 is $\mathbb{R}_1$ and the energy trading that M_1 wants to transfer to M_2 is $\mathcal{U}_1$. Then the secured energy trading actions can be performed through the homomorphic encryption scheme in three steps are discussed as follows [16].

Step-1: Key generation: Assume that there are two random prime numbers chosen by M_1 and M_2, such as $\mathfrak{z}_{\mathbb{i}}$ and $\mathfrak{y}_{\mathbb{i}}$, $\mathbb{i} = 1,2 \ldots$ and compute $\mathbb{Z}_{\mathbb{i}}$ and $\mathbb{K}_{\mathbb{i}}$, defined in (6.25), and (6.26), respectively.

$$\mathbb{Z}_{\mathbb{i}} = \mathfrak{z}_{\mathbb{i}} . \mathfrak{y}_{\mathbb{i}} \tag{6.25}$$

$$\mathbb{K}_{\mathbb{i}} = \mathbb{L}(\mathfrak{z}_{\mathbb{i}} - 1, \mathfrak{y}_{\mathbb{i}} - 1), \mathbb{i} = 1,2 \ldots \tag{6.26}$$

Again, M_1 and M_2 choose another integer randomly as $\mathfrak{g}_{\mathbb{i}} = \mathcal{R}^*_{\mathbb{Z}^2}$, $\mathbb{i} = 1,2.\ldots$, which must satisfy (6.27).

$$\mathbb{G}\left(\frac{\mathfrak{g}_{\mathbb{i}}{}^{\mathfrak{T}_{\mathbb{i}}} \bmod \mathbb{Z}_{\mathbb{i}}^2 - 1}{\mathbb{Z}_{\mathbb{i}}}, \mathbb{Z}_{\mathbb{i}}\right) = 1 \tag{6.27}$$

where $\mathbb{Z}$ is the modulus, $\mathbb{K}$ is the key, $\mathbb{L}$ and $\mathbb{G}$ are the lowest common multiple and greatest common factor, respectively, $\mathcal{R}_{\mathbb{Z}^2}$ is the set of integers that is lower than $\mathbb{Z}^2$ and $\mathcal{R}^*_{\mathbb{Z}^2}$ is the set of integers co-prime with $\mathbb{Z}^2$. Let the public and private keys of M_1 and M_2 be stated as (6.28) and (6.29).

$$\mathbb{K}_{pu,M_1} = (\mathbb{Z}_1, \mathfrak{g}_1), \text{ and } \mathbb{K}_{pr,M_1} = \mathbb{K}_1 \tag{6.28}$$

$$\mathbb{K}_{pu,M_2} = (\mathbb{Z}_2, \mathfrak{g}_2), \text{ and } \mathbb{K}_{pr,M_2} = \mathbb{K}_2 \tag{6.29}$$

Step-2: Encryption phase:

In this stage, data encryption is done through ciphertext. The sender (M_1) randomly chooses the encryption parameter such as $\mathfrak{P}_{1\mathcal{U}} \in \mathcal{R}^*_{\mathbb{Z}}$. Then it encrypts $\mathcal{U}_1$ by $\mathbb{K}_{pu,M_1} = \left(\mathbb{Z}_1, \mathfrak{g}_1\right)$ to derive the ciphertext, expressed in (6.30). Further M_1 selects another encryption parameter randomly as $\mathfrak{P}_{2\mathcal{U}} \in \mathcal{R}_{\mathbb{Z}}^*$, and then it encrypts $\mathcal{U}_2$ by $\mathbb{K}_{pu,M_2} = (\mathbb{Z}_2, \mathfrak{g}_2)$ to derive the ciphertext, expressed in (6.31).

$$\mathbb{X}_{1\mathcal{U}} = \mathcal{E}_1(\mathcal{U}_1) = \mathfrak{g}_1{}^{\mathcal{U}_1} . \mathfrak{g}_{1\mathcal{U}}{}^{\mathbb{Z}_1} \mod \mathbb{Z}_1^2 \tag{6.30}$$

$$\mathbb{X}_{2\mathcal{U}} = \mathcal{E}_2(\mathcal{U}_2) = \mathfrak{g}_2{}^{\mathcal{U}_2} . \mathfrak{g}_{2\mathcal{U}}{}^{\mathbb{Z}_2} \mod \mathbb{Z}_2^2 \tag{6.31}$$

The above two ciphertexts are derived from the randomness of $\mathfrak{P}$ with the same energy transaction $\mathcal{U}$, and then it can be decrypted with the same $\mathcal{U}$. Thus, M_1 needs to prove to the miner that the plaintext data of the ciphertext $\mathbb{X}_{1\mathcal{U}}$, $\mathbb{X}_{2\mathcal{U}}$ are equal.

Step-3: Decryption phase

The ciphertext is the encrypted text that needs to be decrypted using a private key to validate the transaction and energy transfer. Suppose that $\mathbb{Z}_1 = \mathbb{Z}_2$ and private keys for M_1 and M_2 are $\mathbb{K}_1$ and $\mathbb{K}_2$, and the decryption can be done using (6.34).

$$\mathcal{U}_{\mathbb{i}} = \mathcal{D}(\mathbb{X}_{\mathbb{i}\mathcal{U}}) = \frac{F(\mathbb{X}_{\mathbb{i}\mathcal{U}}{}^{\mathbb{K}_{\mathbb{i}}}) \mod \mathbb{Z}^2}{F(\mathfrak{g}_{\mathbb{i}}{}^{\mathbb{K}_{\mathbb{i}}}) \mod \mathbb{Z}^2} \mod \mathbb{Z} \tag{6.32}$$

where $F(\mathbb{a}) = \frac{\mathbb{a}-1}{\mathbb{Z}}$, $\mathcal{U}_1 = \mathcal{U}_2 = \mathcal{U}$. In this case, the below properties are to be followed [25].

Property-1: $\forall \mathcal{U}_1, \mathcal{U}_2 \in \mathcal{R}_{\mathbb{Z}}$

$$\mathcal{D}\,(\mathcal{E}(\mathcal{U}_1) . \mathcal{E}(\mathcal{U}_2) \mod \mathbb{Z}^2) = (\mathcal{U}_1 + \mathcal{U}_2) \mod \mathbb{Z} \tag{6.33}$$

Property-2: $\forall \mathcal{U} \in \mathcal{R}_{\mathbb{Z}}$

$$\mathcal{D}\left(\mathcal{E}(\mathcal{U})^{k} \mod \mathbb{Z}^2\right) = k\mathcal{U} \mod \mathbb{Z} \tag{6.34}$$

Step-4: Transaction confirmation

As per the aforementioned process, the homomorphism of the cryptographic system is used to certify the miner that the ciphertexts $\mathbb{X}_{1\mathcal{U}}$ and $\mathbb{X}_{2\mathcal{U}}$ comprise the identical plaintext records, and then it validates the authority of the transaction, which ensures trading security. The detailed discussion of the authentication process is summarized as follows.

Authentication process	
1.	*Initialization:*
1.1	Take $\mathcal{J}$ as the safety parameter
1.2	M_1 generates random number $\rho_{\ddot{\imath}}$
1.3	Estimate $\mathcal{U}_1 + \rho_{\ddot{\imath}}$, where $1 \le \ddot{\imath} \le \mathcal{J}$
1.4	Assume $\mathcal{Q}_{1\ddot{\imath}} = \mathcal{E}_1(\rho_{\ddot{\imath}})$, $\mathcal{Q}_{2\ddot{\imath}} = \mathcal{E}_2(\rho_{\ddot{\imath}})$ where $1 \le \ddot{\imath} \le \mathcal{J}$
1.5	Addition of homomorphic by the public key (M_1). $\mathcal{U}_{1\ddot{\imath}} = \mathbb{X}_{1\mathcal{U}} + \mathcal{Q}_{1\ddot{\imath}}$, $1 \le \ddot{\imath} \le \mathcal{J}$
1.6	Addition of homomorphic by the public key (M_2). $\mathcal{U}_{2\ddot{\imath}} = \mathbb{X}_{2\mathcal{U}} + \mathcal{Q}_{2\ddot{\imath}}$, $1 \le \ddot{\imath} \le \mathcal{J}$
2.	*Process:*
2.1	M_1 sends the required parameters to Blockchain,
2.2	Miner sends a string Ξ to M_1, $\Xi_{\ddot{\imath}} \in \{0,1\}$
2.3	When M_1 receives Ξ, if $\Xi_{\ddot{\imath}} = 0$, M_1 sends $\rho_{\ddot{\imath}}$ of $\mathcal{Q}_{1\ddot{\imath}}$,$\mathcal{Q}_{2\ddot{\imath}}$, and $\mathfrak{P}_{1\ddot{\imath}}$, $\mathfrak{P}_{2\ddot{\imath}}$ to miners. if $\Xi_{\ddot{\imath}} = 1$, M_1 sends $\mathcal{U}_1 + \rho_{\ddot{\imath}}$ of $\mathcal{U}_{1\ddot{\imath}}$, $\mathcal{U}_{2\ddot{\imath}}$ and $\mathfrak{P}_{1\mathcal{U}} + \mathfrak{P}_{1\ddot{\imath}}$,$\mathfrak{P}_{2\mathcal{U}} + \mathfrak{P}_{2\ddot{\imath}}$ to miners.
3.	When verification is passed, miners accept the transaction; otherwise, decline the transaction.

6.5. Results and discussion

In this section, the verification of the proposed TE framework is presented with four different scenarios: such as, Case-1 is the base case where no TE framework is considered; in Case-2, the proposed TE framework is implemented; in Case-3, the TE framework with MG outage condition is investigated; and finally, in Case-4, the Blockchain technology is applied to show the effectiveness of the system through the premise of success probability using various FDI attack.

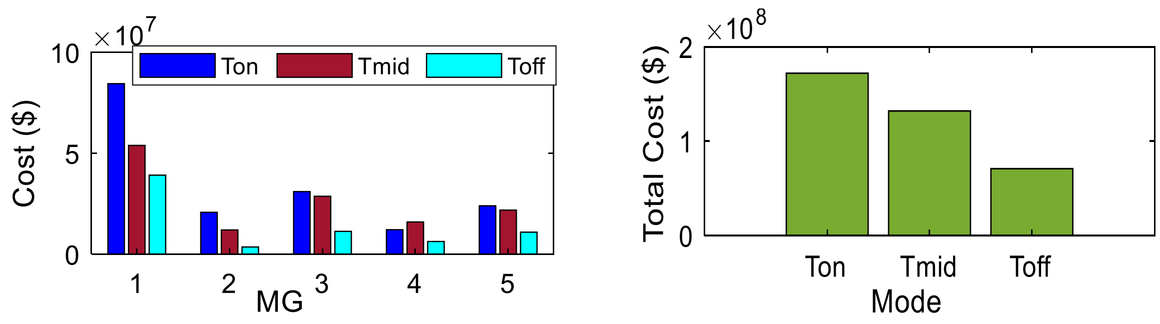

(a) Cost of each MG w.r.t time period (b) Total cost

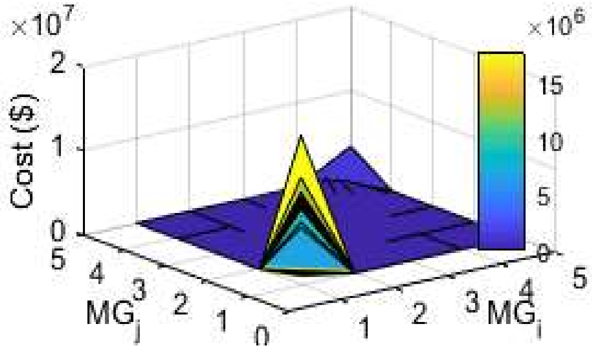

(c) Energy trading cost

Fig. 6.4. Cost comparison in Case-1

In the proposed model, the market operator maintains the energy balance of the whole system through optimal energy trading between MGs and grid supply. The main objective of this framework is to minimize the overall energy cost and helps to benefit each MG in terms of selling surplus energy to other MGs or Grid, which are illustrated in Figs. 6.4 - 6.6. Three time-of-use periods are considered in this simulation, on-peak (6-9 hrs, and 18-21hrs), mid-peak (10-17hrs), and off-peak time (22-5 hrs), and prices are also varied accordingly.

6.5.1. Case-1: Base case (without TE framework)

In this case, the load demand has been met through the MG's own generation and grid supply. The interconnection of MGs is not taken into consideration here. As can be seen from Fig. 6.4, the cost of most MGs (MG_1, MG_3, MG_4) is high (Fig. 6.4 (a)) at the on-peak compared to mid-peak and off-peak time, and subsequently, the overall cost is also high at the on-peak time (see Fig. 6.4 (b)). In this case, the MGs only trade the energy with the grid, and the cost of trading energy can be seen in Fig. 6.4 (c).

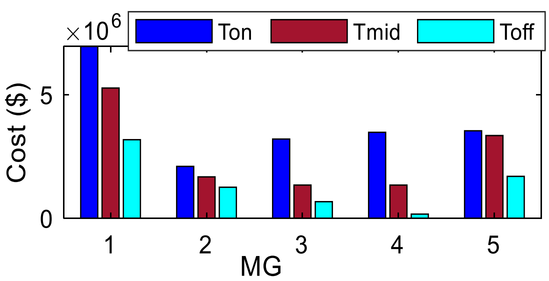

(a) Cost of each MG w.r.t time period

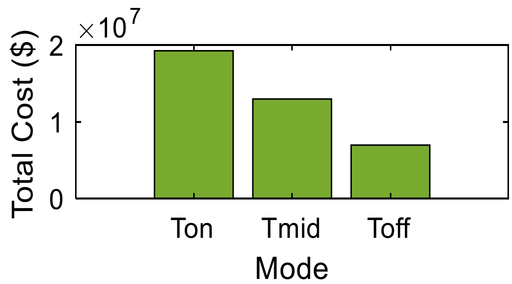

(b) Total cost

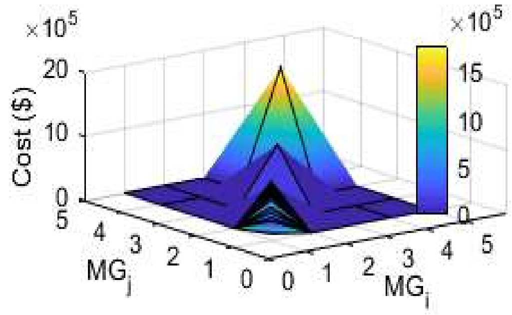

(c) Energy trading cost

Fig. 6.5. Cost comparison in Case-2

6.5.2. Case-2: With TE framework

In this case, the proposed TE framework has been implemented, and the overall energy cost as well as each MG's benefits is optimized. As can be seen from Fig. 6.5, the cost of each MG is high (Fig. 6.5 (a)) at the on-peak compared to mid and off-peak time, and subsequently, the overall cost is also high at the on-peak time (see Fig. 6.5 (b)). The trading energy cost between the MGs can be seen in Fig. 6.5.(c). It is noted that, compared to Case-1, the energy cost is reduced significantly in Case-2, as illustrated in Fig. 6.5.

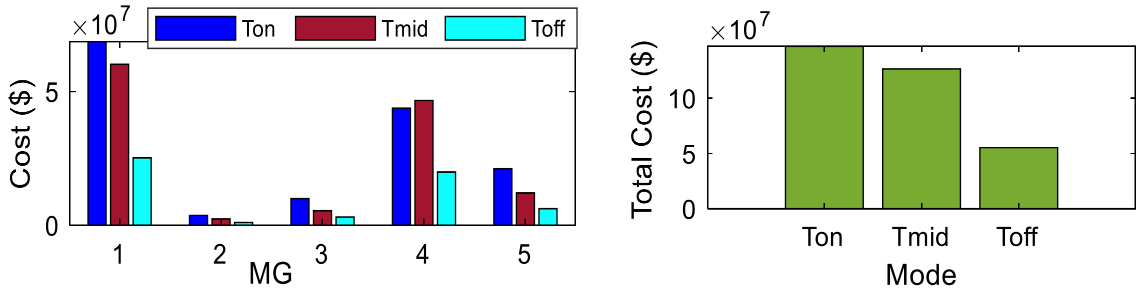

(a) Cost of each MG w.r.t time period (b) Total cost

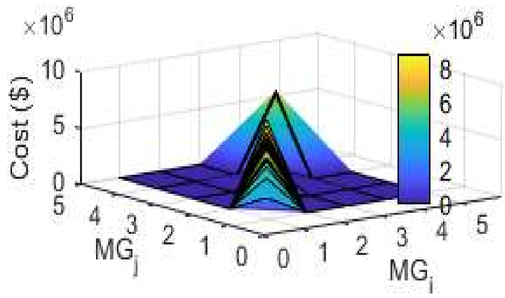

(c) Energy trading cost

Fig. 6.6. Cost comparison in Case-3

6.5.3. Case-3: With TE framework and resiliency consideration

This study considers the resilience-based approach where two MGs are taken as outage conditions. As per the load demand profile based on (6.14), a minimum of 30% of the load needs to be served, as it is considered a critical load, and then the minimum level of resilience (0.3) can be maintained. With this objective, energy trading has been done with the healthy MGs and the main grid.

It can be observed that the proposed TE framework achieves the minimum resilience level and restores the critical load optimally. As shown in Fig. 6.6, the overall cost of the TE system cost is considerably higher than Case-2, but it is smaller than Case-1, even considering the extreme events.

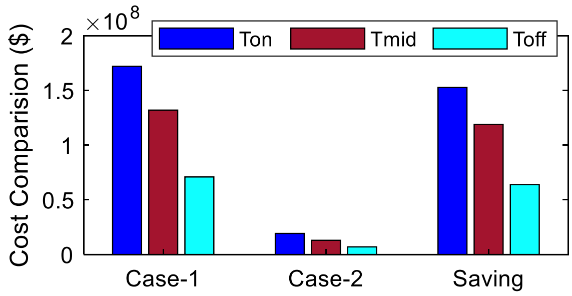

(a) Case-1 vs Case-2

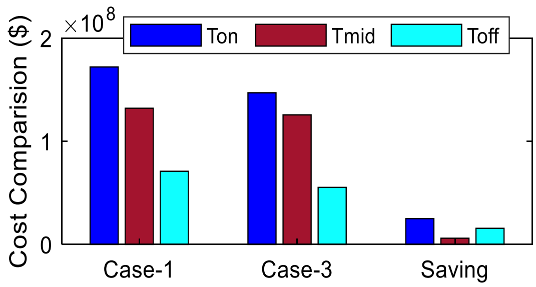

(b) Case-1 vs Case-3

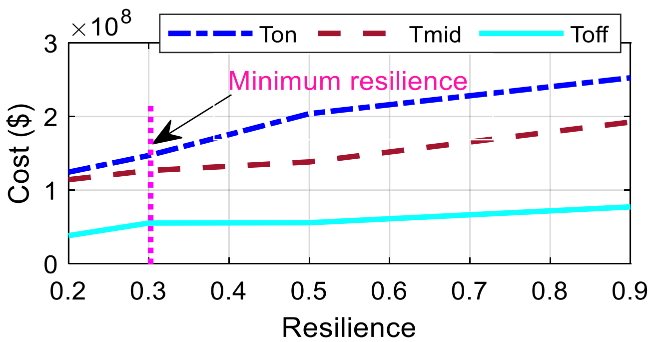

(c) Cost vs resilience

Fig. 6.7. Cost comparison and resilience characteristics

In addition to the above analysis, the cost comparison with Case -1 & 2 and Case-1 & 3 are depicted in Fig. 6.7 (a) and (b), respectively. It is observed that using TE technology in the existing system can save \$325.6M. While considering the resiliency in the TE system, it saves \$46.69M. Fig. 6.7 (c) demonstrates the cost versus resilience, which needs to be a tradeoff. The minimum resilience 30% is considered here as it is assumed as the critical load. The resiliency can be improved, but the cost would be very high due to MG outage conditions. During the event, the available MG has no sufficient capacity to meet all the load demand; eventually, the unmet demand can be bought from the grid, which increases the cost significantly, as can be seen in Fig. 6.7 (c).

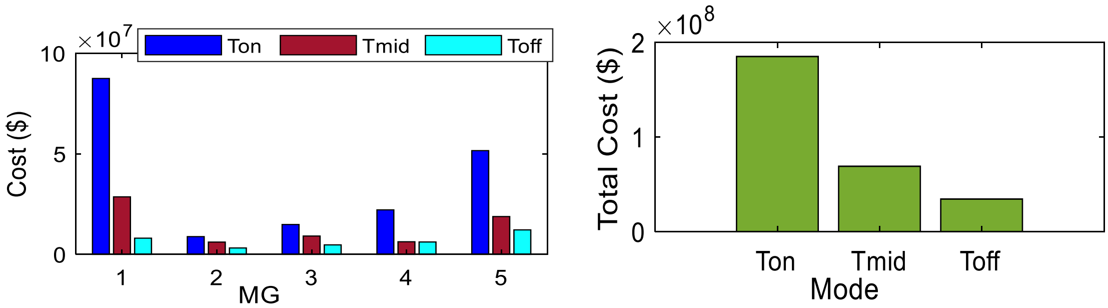

(a) Cost of each MG (b) Total cost

Fig. 6.8. Cost comparison in Case-4

6.5.4. Case-4: With TE framework and Blockchain

There are many types of attacks possible in the TE system by cyberpunk; however, the FDI attack is well known. The FDI attack can be shoot into the system by three ways of data falsification, such as at the sender side (prior to data transfer), the transmission path (data in transmission), and the receiver side (after the data are received) [26]. This can be done using the meters used in the network or falsifying the control center's data. All the FDI attacks are considered in this study with and without the application of Blockchain as scenario-1 and scenario-2, respectively. Indeed, to show the effectiveness of security operations using the homomorphic-based Blockchain technique against FDI, the success probability of an attack is estimated. In scenario-1, the FDI attack is applied to the TE system, and it is observed that the cost of each MG and the overall cost is exceptionally high, which can be seen in Fig. 6.8. Since the energy cost is remarkably high, which does not meet the objective of the proposed TE framework, it needs to be revamped through advanced technology. With this concern, state-of-the-art technology such as Blockchain is applied and studied in scenario-2. While considering the security operation against the attack, the probability of success illustration is vital, showing the attack-defensive mechanism of the proposed system, which is discussed as follows.

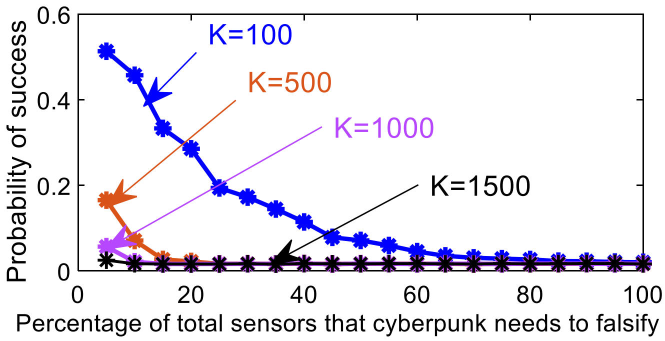

(a) Scenario-1

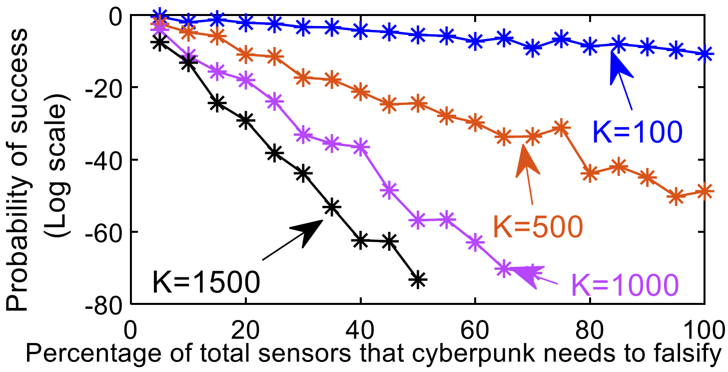

(b) Scenario-2

Fig. 6.9. Probability of successful attacks comparison

Let us assume there are 105 sensors used in the TE system to collect the data, such as voltage, current, frequency, power, etc. With these 105 sensors, there are $105 \times (105-1)/2 = 5460$ communication channels established, as derived in [27]. The cyberpunk can hack the sensor data and try to steal critical information to launch a fruitful attack. Therefore, the probability of a successful attack is measured in this study with and without Blockchain technology. The same concept of successful attack probability is used in [27]. In scenario-1, it is assumed that the TE system has no private key for each node, and then the cyberpunk has made the attack on K communication channels. In scenario-2, it is assumed that each transaction has a secret key with encryption and decryption techniques, and then the FDI attack is applied. Further, a Monte Carlo method is used to generate random draws to show the best comparison in terms of short to long variation (in this study, increasing the number of communication channels is considered). The success probability of scenarios 1 and 2 with various K (attacked communication channels) values in [1, 1500] is presented in Fig. 6.9.

Moreover, in Fig. 6.9 (a), it is reported that the probability of success decreases as the number of sensors that need to be hacked increases. The data manipulation has been done through communication channels with steps such as 5% to 100% of K value, where K has been set to 100, 500, 1000, and 1500, respectively, for comparative analysis. On the other hand, Fig. 6.9 (b) reveals the attack-defensive capability using Blockchain, reducing the probability of success. In this graph, the natural logarithm is taken on the y-axis, only to show the better comparison characteristics, as the probability of success is very low (< 0.1).

Further, the overall probability is measured by considering the scenario where the system is assumed to be very weak with the successful attacking probability for the attacker in the range of [0.9, 0.99], and the probabilities of all three ways of data falsification (sender side, transmission path, receiver side) are assumed to be equal. In addition, uncertainty is considered here, which is the combination of the probability of cyberpunk in three ways of attack. As shown in Fig. 6.10, the number of sensors that need to be hacked (h) and uncertainty are considered variables, and it is observed that when a cyberpunk has a definite proportion of falsification data with fewer sensors, the overall probability of success is high, as can be seen in Fig. 6.10 (a), whereas, with the Blockchain in scenario-2, the overall probability of success is low, as shown in Fig. 6.10 (b). Moreover, with fewer sensors, the probability of successful attacks is higher, as it is easy to duplicate the data in the sensors and channels. It is noticed that a Blockchain-enabled TE system provides a highly secure platform for trading energy as well as payment operations.

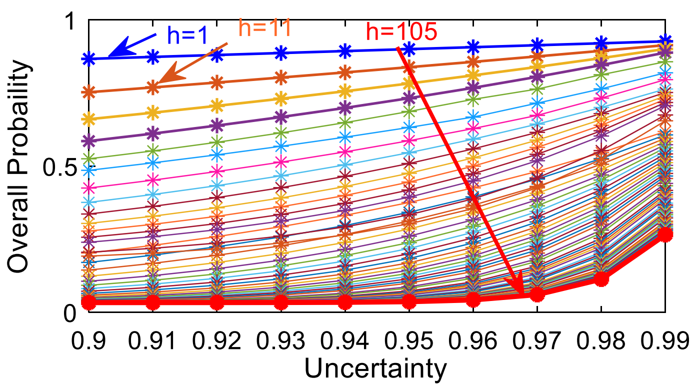

(a) Scenario-1

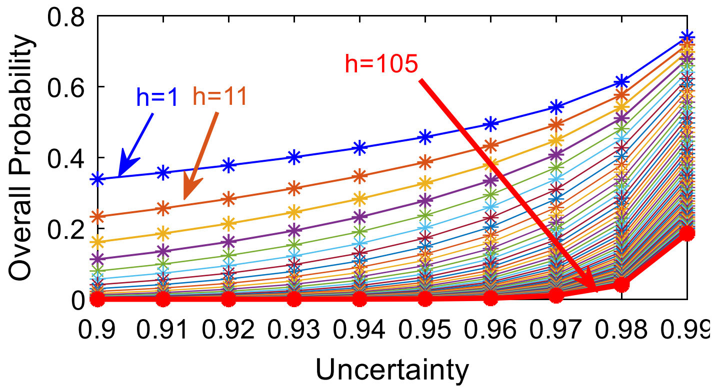

(b) Scenario-2

Fig. 6.10. Overall probability of successful attacks and its defensive capability

As noted, Blockchain technology prevents several malicious attacks and reduces many associated risks. Besides, it has the desirable features of decentralization, autonomy, immutability, verification, fault tolerance, auditability, and transparency. These features are possible as they deal with smart contract and cryptographic methods such as public and private key generation. It helps to create a proof-of-work mechanism where all authentication can be trusted to finalize the trading process. Trading activity fails if the attacker tries to steal the information or change some signal/data. Therefore, the probability of success of the attack from the attacker's point of view is low. With this technology, the whole transaction of the system can be secure and resilient.

6.6. Summary

This chapter presents a Blockchain-empowered TE framework for improving privacy preservation and energy security against cyber threats. The proposed scheme greatly enhances the overall energy cost-saving, and each MG benefits from using the bilateral trading pricing mechanism. In addition, implementing Blockchain into the TE system shows a remarkable achievement when it faces cyber-attacks. Various operational case studies are demonstrated with the inclusion of extreme events such as MG outage conditions and FDI attacks, and in both cases, the proposed system has shown its defensive capabilities. The effectiveness of the proposed system is verified with resiliency versus cost trade-off in Case-3 and probability of successful attacks in Case-4.

In a nutshell, the Blockchain-enabled TE framework has a renowned interest in this chapter, where the various distinguishing characteristics appealing to the current needs of the energy market have been shown. The results outlined that the proposed TE platform provides better economical operation to the operator and energy providers. In addition, with the Blockchain, the whole system can be regarded as a promising solution for economic and secure operations for the TE scheme.

An efficient decentralized-based TE scheme with a large-scale system in future work will be studied. In addition, the breakthrough of Blockchain with more favorable features is to be implemented in the TE scheme, such that it could follow the industrial revolution in the energy sector. On the other hand, under extreme events, Blockchain-related cyberinfrastructure has a risk of being damaged. The willingness of the MG operators in damaged areas to participate in the TE market will be studied further.

References

[1] Y. Cao *et al.*, "Optimal Energy Management for Multi-Microgrid Under a Transactive Energy Framework With Distributionally Robust Optimization," *IEEE Transactions on Smart Grid,* vol. 13, no. 1, pp. 599-612, 2021.

[2] H. Hao, C. D. Corbin, K. Kalsi, and R. G. Pratt, "Transactive control of commercial buildings for demand response," *IEEE Transactions on Power Systems,* vol. 32, no. 1, pp. 774-783, 2016.

[3] Y. K. Renani, M. Ehsan, and M. Shahidehpour, "Optimal transactive market operations with distribution system operators," *IEEE Transactions on Smart Grid,* vol. 9, no. 6, pp. 6692-6701, 2017.

[4] M. S. H. Nizami, M. J. Hossain, and E. Fernandez, "Multiagent-based transactive energy management systems for residential buildings with distributed energy resources," *IEEE Transactions on Industrial Informatics,* vol. 16, no. 3, pp. 1836-1847, 2019.

[5] M. N. Akter, M. A. Mahmud, and A. M. Oo, "A hierarchical transactive energy management system for microgrids," in *2016 IEEE Power and Energy Society General Meeting (PESGM)*, 2016, pp. 1-5: IEEE.

[6] S. M. Sajjadi, P. Mandal, T.-L. B. Tseng, and M. Velez-Reyes, "Transactive energy market in distribution systems: A case study of energy trading between transactive nodes," in *2016 North American Power Symposium (NAPS)*, 2016, pp. 1-6: IEEE.

[7] G. Prinsloo, A. Mammoli, and R. Dobson, "Customer domain supply and load coordination: A case for smart villages and transactive control in rural off-grid microgrids," *Energy,* vol. 135, pp. 430-441, 2017.

[8] C. Zhang, J. Wu, Y. Zhou, M. Cheng, and C. Long, "Peer-to-Peer energy trading in a Microgrid," *Applied Energy,* vol. 220, pp. 1-12, 2018.

[9] H. Hui *et al.*, "A transactive energy framework for inverter-based HVAC loads in a real-time local electricity market considering distributed energy resources," *IEEE Transactions on Industrial Informatics,* 2022.

[10] Q. Yang and H. Wang, "Blockchain-empowered socially optimal transactive energy system: Framework and implementation," *IEEE Transactions on Industrial Informatics,* vol. 17, no. 5, pp. 3122-3132, 2020.

[11] U. Cali, C. Lima, X. Li, and Y. Ogushi, "DLT/blockchain in transactive energy use cases segmentation and standardization framework," in *2019 IEEE PES Transactive Energy Systems Conference (TESC)*, 2019, pp. 1-5: IEEE.

[12] S. Saha, N. Ravi, K. Hreinsson, J. Baek, A. Scaglione, and N. G. Johnson, "A secure distributed ledger for transactive energy: The Electron Volt Exchange (EVE) blockchain," *Applied Energy,* vol. 282, p. 116208, 2021.

[13] S. Farshidi, S. Jansen, S. España, and J. Verkleij, "Decision support for blockchain platform selection: Three industry case studies," *IEEE transactions on Engineering management,* vol. 67, no. 4, pp. 1109-1128, 2020.

[14] G. Wood, "Ethereum: A secure decentralised generalised transaction ledger," *Ethereum project yellow paper,* vol. 151, no. 2014, pp. 1-32, 2014.

[15] E. Münsing, J. Mather, and S. Moura, "Blockchains for decentralized optimization of energy resources in microgrid networks," in *2017 IEEE conference on control technology and applications (CCTA)*, 2017, pp. 2164-2171: IEEE.

[16] W. Liang, D. Zhang, X. Lei, M. Tang, K.-C. Li, and A. Y. Zomaya, "Circuit copyright blockchain: blockchain-based homomorphic encryption for IP circuit protection," *IEEE Transactions on Emerging Topics in Computing,* vol. 9, no. 3, pp. 1410-1420, 2020.

[17] K. Kaur, G. Kaddoum, and S. Zeadally, "Blockchain-based cyber-physical security for electrical vehicle aided smart grid ecosystem," *IEEE Transactions on Intelligent Transportation Systems,* vol. 22, no. 8, pp. 5178-5189, 2021.

[18] R. Ambrosio, "Transactive energy systems," *IEEE Electrification Magazine,* vol. 4, no. 4, pp. 4-7, 2016.

[19] A. Miglani, N. Kumar, V. Chamola, and S. Zeadally, "Blockchain for Internet of Energy management: Review, solutions, and challenges," *Computer Communications,* vol. 151, pp. 395-418, 2020.

[20] S. Ding, J. Zeng, Z. Hu, and Y. Yang, "A peer-2-peer management and secure policy of the energy internet in smart microgrids," *IEEE Transactions on Industrial Informatics,* vol. 18, no. 8, pp. 5689-5697, 2021.

[21] R. L. Kumar, F. Khan, S. Kadry, and S. Rho, "A survey on blockchain for industrial internet of things," *Alexandria Engineering Journal,* vol. 61, no. 8, pp. 6001-6022, 2022.

[22] M. B. Mollah *et al.*, "Blockchain for future smart grid: A comprehensive survey," *IEEE Internet of Things Journal,* vol. 8, no. 1, pp. 18-43, 2020.

[23] M. Andoni *et al.*, "Blockchain technology in the energy sector: A systematic review of challenges and opportunities," *Renewable and sustainable energy reviews,* vol. 100, pp. 143-174, 2019.

[24] B. Teufel, A. Sentic, and M. Barmet, "Blockchain energy: Blockchain in future energy systems," *Journal of Electronic Science and Technology,* vol. 17, no. 4, p. 100011, 2019.

[25] Z. Brakerski and V. Vaikuntanathan, "Efficient fully homomorphic encryption from (standard) LWE," *SIAM Journal on computing,* vol. 43, no. 2, pp. 831-871, 2014.

[26] G. Liang, S. R. Weller, J. Zhao, F. Luo, and Z. Y. Dong, "The 2015 ukraine blackout: Implications for false data injection attacks," *IEEE Transactions on Power Systems,* vol. 32, no. 4, pp. 3317-3318, 2016.

[27] G. Liang, S. R. Weller, F. Luo, J. Zhao, and Z. Y. Dong, "Distributed blockchain-based data protection framework for modern power systems against cyber attacks," *IEEE Transactions on Smart Grid,* vol. 10, no. 3, pp. 3162-3173, 2018.

CHAPTER 7

CONCLUSIONS AND FUTURE WORKS

7.1. Conclusions

This thesis is concerned with the resilience framework for ADS with various enhancement techniques. In spite of the fact that the resilience consideration is widely adopted in the energy sector, the robust design of ADS still suffers some issues with reference to the quantification framework, enhancement methods, cyber-security, and energy market participation. To address the aforementioned issues, various resilient strategies should be studied subject to extreme event conditions, including transmission line outages, microgrid outages, and cyber-attack. Along with this, today's energy markets are undergoing a significant transformation where digitalization is crucial. However, it creates a vulnerable path for the attacker that needs to be taken care of. Motivated by this concern, a novel TE framework should be developed where security will be the primary concern using emerging technology. The following are the concluding remarks of each chapter.

In Chapter 2, a comprehensive literature review is presented on various planning and operational scheme of ADS on account of resiliency. It also outlines several frameworks for resilience quantification and enhancement approach with their respective conditions. From the state-of-the-art literature, it has been found that four factors, such as withstand, recover, adapt, and respond, are significantly important and considered major attributes of resilience, which are discussed in detail.

In Chapter 3, the importance of distributed energy resources in ADS on account of resiliency is presented. The resilience study in this chapter is validated by measuring an index as 'energy-not-supplied' in the presence of renewables and storage units and their optimal location. This index signifies the number of customers affected due to the supply shortage, and to reduce it, proper allocation of the DER is vital. On the other hand, the case study verifies the performance with various approaches, where the appropriate resource allocation method has remarkably enhanced the resilience characteristics.

In Chapter 4, the study has contributed to two manifolds: (a) introducing a resilience quantification framework; (b) a resilience enhancement approach through MMG arrangements and mobile energy storage placements. This study concludes that the quantification of resilience is vital, and thereafter, various approaches can be attempted to show the resiliency of the system. Fostering the development, the optimal reconfiguration technique using MMG and mobile energy storage has been applied, where the resilience indices are measured and compared with the enhancement value. In addition, the value of resilience is also illustrated in terms of failure rate, outage time, and economy, which have been examined through real-time data. With this examination, the outage cost will be exceptionally high if the failure rate is not reduced. Moreover, due to high-disruptive events, some towers and/or transmission lines get abolished, where power flow is not possible even though the system has ample resources. In such a case, the role of the mobile storage unit is significant since it is movable and can go to the desired location to meet the load demand, which can greatly enhance the resilience characteristics, save lives, and saves the economy.

In Chapter 5, the role of isolated MG by considering the parameter uncertainties and cyber-attack is presented. As noted, the decentralized power system plays a key role in remote area power supply, where the grid connection would not be possible, and an isolated MG can be the best way. Indeed, frequency is a sensitive parameter of the power system, which needs to be within rigid limits ($\pm$ 2.5 % deviation); otherwise, the system can face a blackout. On the other hand, there are many mediums that compel the frequency change, which can be a sudden load change and parameter uncertainties due to intermittent energy sources. Nowadays, external attacks, such as hackers, can inject false signals, which can largely affect the system's performance and frequency, and it's not easy to defend with a traditional control method. With this concern, a resilient control strategy is implemented through an adaptive fuzzy PID controller, which can deal with non-linearities and cyber-attacks. Evidently, the proposed control method upholds the frequency support to evade the power system failure and offers better dynamic response. Further, the proposed model with different control methods has been tested through a real-time simulation platform, such as OPAL-RT. It also gives a satisfactory performance, and finally, it shows the system validation.

In Chapter 6, a novel concept of the TE framework is introduced where two factors are considered important: resiliency and security. The empirical finding in this study offers a realization of the energy market in a better approaching way through a competitive pricing scheme. In an initial attempt, the TE framework is compared with a traditional system, and it is observed that the energy cost is saved significantly. Secondly, the proposed system is simulated under two MG outage conditions, showing that the minimum level of resilience has been achieved and the overall energy cost is lower than the traditional system, which means the TE system can cope with extreme events. The investigation has moved further to cyber-attack-related issues, as the number of transactions and information are in a public forum, which makes the system vulnerable to cyber attacks. In such an instance, the hacker can easily falsify the transaction data that needs to be secured, which can be mitigated by using an authentication key through Blockchain technology. Through Blockchain, encryption and decryption methods are employed where two keys are essential to initiate and finalize the transaction, such as public and private keys. To show the performance of the Blockchain against attack, the probability of success is measured, and surprisingly, it has an implausible effect on the TE system, as it defends against the cyber-attack signal. The interesting fact of this study is that the proposed TE framework can be assured of a paradigm shift in the energy market scheme, which can cope with extreme events and deal with security issues. More importantly, it can lead to a far more cost-effective system, which verifies the main aim of the TE platform.

7.2. Future works

This thesis develops and validates various resilience frameworks with their respective scenarios. Further, this research can be put forward in several directions as follows:

- **Incorporating communication system into resilience framework:** The proposed resilience framework incorporates only the electrical sources in the assessment; however, the telecommunication system needs to be integrated into the framework, as it is extremely important to the smart electric infrastructure.
- **Technological advancement:** With the advancement of technology in the energy sector, the proposed models can be extended to assess the impact of smart/micro-grids, EV integrations,

static/mobile energy storage devices, variable generations, etc., on resilience performances.

- **Test with a large-scale system:** The developed frameworks in this thesis used small-scale networks, *i.e.*, 5-bus and IEEE 33-bus test systems. However, a large-scale system will be preferred for further studies to show the functionalities and capabilities of the proposed framework.
- **Integrating different types of cyber-attack models into the proposed system:** The cyber-attack model used in this thesis is only the false data injection attack; however, a more complicated attack model can be employed to show the robustness of the proposed frameworks.
- **Behavioral science strategy for the energy market:** The proposed TE framework only considers the customer benefit in terms of price and security. However, consumer decisions and behavior potentially contribute to energy efficiency, which should be added to the framework to enhance the resilience of the smart distribution system.

APPENDIX

I. Resources and funding authority

MATLAB is a design and programming tool, which is a licensed package toolbox provided by University of Technology Sydney (UTS) with an updated version (2021), which is used to perform simulation through Simulink design from the control system and sim power system toolbox and coding from the main MATLAB window. Besides, microsoft visio is a licensed tool provided by UTS, which is used to draw the diagrams in the thesis. Furthermore, one of the most powerful devices, such as OPAL-RT, is provided by the UTS to do the real-time simulation, and finally, it has been used to validate the model for the betterment of publication.

Further, this work is truly supported by the UTS through scholarship and the HDR research fund.

II. Research ethics and integrity statement

The proposed research project is purely computational. This project does not involve physical contact, environmental clearance, or machinery testing. Hence, ethical clearance is not required for this research.